Concept Development and Implementation of Online Monitoring Methods in the Transfer Molding Process for Electronic Packages

vorgelegt von
M.Sc.
Burcu Kaya
geb. in Izmir, Türkei

von der Fakultät IV- Elektrotechnik und Informatik
der Technischen Universität Berlin
zur Erlangung des akademischen Grades

Doktor der Ingenieurwissenschaften
- Dr.-Ing -

genehmigte Dissertation

Promotionausschuss:

Vorsitzender:	Prof. Dr.-Ing. Rolf Schuhmann
Gutachter:	Prof. Dr.-Ing. Dr. sc. techn. Klaus-Dieter Lang
Gutachter:	Prof. Dr.-Ing. Martin Schneider-Ramelow
Gutachter:	Prof. Dr.-Ing. André Zimmermann

Tag der wissenschaftlichen Aussprache: 23. Mai 2018

Berlin 2018

Abstract

The transfer molding process is one of the major processes for the encapsulation of electronic packages. To provide a structural support and to protect the electronic components from the environment, epoxy molding compounds (EMCs) are mainly used as encapsulation material. The quality of the molded packages depends strongly on the process parameters of the transfer molding process and also the characteristics of EMC. Despite the fact that the transfer molding process has many advantages such as cost-effectiveness and high volume applicability, there are some challenges regarding process optimization. Parameter settings in transfer molding process are usually done in a trial and error manner and defining optimum parameters is mostly laborious. Moreover, the defined machine process parameters are deviating from the conditions in the tool cavity e.g. pressure measured in the cavity differs from the parameter settings in the machine. In addition to process parameters, the EMC characteristics also have great influence on the package quality. The reactive nature of the epoxy resins can be influenced by prolonged storage duration and moisture content, and the possible variations from batch to batch may cause alterations in the characteristics of the EMC, i.e. moldability, change in the flow behavior of the material in the cavity and excessive void formation. Yet, some common defects can occur in the package such as wire sweep, delamination, void formation and warpage, which may ultimately lead to a total package failure.

This work aims to support a more comprehensive understanding of the influence of process parameters and the variations in the material characteristics of EMC on the package quality, to reduce the possible defects in the electronic packages and to ensure a stable transfer molding process. Systematic approaches are evaluated to generate models which describe the correlations between process parameters, material characteristics and package quality. Detailed process analysis is conducted to correlate significant process parameters of the transfer molding process with quality features such as void formation, wire sweep and warpage. To determine the relationship between the process parameters and the quality characteristics mathematically, process models are generated. An approach to generate and calibrate the models is presented. The optimum process parameters of the transfer molding process are determined with the generated model to achieve the optimal package quality concerning the selected quality features and to reduce the failure costs. Moreover, with the generated models it is also possible to predict the package quality of the electronic packages. Thus, the estimation quality and the limitations of the process model are evaluated with validation experiments. In addition to that, the influence of variations of the material characteristics of the EMC due to prolonged storage duration, humidity and batch variations on the package quality is investigated. The online monitoring method, Dielectric Analysis (DEA) is implemented in the transfer molding process to observe the variations in the characteristics of the EMC. Suitability of the DEA to monitor the alterations in the material characteristics of the EMC in-situ in transfer molding process is assessed. In addition to DEA, additional temperature and pressure sensors are implemented in the cavity of the transfer molding process for process control. Material models are introduced to define the correlation between the variations in the material characteristics of EMC and the package quality and to determine the processing limitations of the preconditioned EMC in order to achieve predefined package quality. The validation of the material model is performed with another EMC to generalize the observed impact of material characteristics of the EMC on package quality.

Kurzzusammenfassung

Das Transfer Molding Verfahren ist einer der wichtigsten Prozesse für die Verkapselung von elektronischen Komponenten. Um eine strukturelle Unterstützung zu gewährleisten und die elektronischen Komponenten vor Umwelteinflüssen zu schützen, werden häufig Epoxidformmassen als Verkapselungsmaterial verwendet. Die Qualität der gemoldeten Bauteile hängt stark von den Prozessparametern des Transfer Molding Verfahrens und von den Eigenschaften der Epoxidformmassen ab. Obwohl der Transfer Molding Prozess viele Vorteile, wie z.B. geringe Kosten und große Volumenanwendbarkeit, aufweist, gibt es einige Herausforderungen hinsichtlich der Prozessoptimierung. Die Parametereinstellungen beim Transfer Molding Prozess werden in der Regel auf Basis von Trial-and-Error Verfahren ermittelt, und die Definition der optimalen Parameter ist sehr aufwändig. Darüber hinaus weichen die definierten Prozessparameter der Maschine von den gemessenen Zuständen in der Werkzeugkavität ab, z. B. stimmt der in der Kavität gemessene Druck nicht mit den Parametereinstellungen in der Maschine überein. Neben den Prozessparametern haben auch die Eigenschaften von Epoxidformmassen großen Einfluss auf die Bauteilqualität. Die reaktive Natur der Epoxidharze kann durch eine verlängerte Lagerdauer und den Feuchtigkeitsgehalt beeinflusst werden. Zusätzlich können die möglichen Variationen von Charge zu Charge Veränderungen in den Eigenschaften der Epoxidharze insbesondere hinsichtlich der Formbarkeit, Veränderung des Fließverhaltens des Materials in der Kavität und übermäßiger Lunkerbildung verursachen. Dennoch können einige charakteristische Defekte in den verkapselten Bauteilen auftreten, wie z. B. Drahtverwehung, Delamination, Lunker und Verzug, was letztendlich zu einem Gesamtversagen der verkapselten Bauteile führen kann.

Diese Arbeit zielt darauf ab, ein umfassenderes Verständnis über den Einfluss von Prozessparametern und die Variationen in den Materialeigenschaften von Epoxidformmassen auf die Bauteilqualität zu erarbeiten. Weiterhin ist es das Ziel, mögliche Defekte in den verkapselten Bauteilen zu reduzieren und einen stabilen Transfer Molding Prozess sicherzustellen. Systematische Ansätze werden evaluiert, um Modelle zu generieren, die die Zusammenhänge zwischen Prozessparametern, Materialeigenschaften und Bauteilqualität beschreiben. Zur Verknüpfung signifikanter Prozessparameter des Transfer Molding Verfahrens mit Qualitätsmerkmalen wie Lunkerbildung, Drahtverwehung und Verzug, wird eine detaillierte Prozessanalyse durchgeführt. Um den Zusammenhang zwischen den Prozessparametern und den Qualitätsmerkmalen mathematisch zu ermitteln, werden Prozessmodelle generiert. Ein Ansatz zum Generieren und Kalibrieren der Modelle wird vorgestellt. Mit dem generierten Modell werden die optimalen Prozessparameter des Transfer Molding Prozesses ermittelt, damit eine optimale Bauteilqualität hinsichtlich der ausgewählten Qualitätsmerkmale sichergestellt und somit mögliche Fehlerkosten reduziert werden können. Darüber hinaus ist es mit den generierten Modellen auch möglich, die Bauteilqualität vorherzusagen. Daher werden die Prognosequalität und die Grenzen des Prozessmodells mit Validierungsversuchen evaluiert. Weiterhin wird der Einfluss von Veränderungen der Materialeigenschaften der Epoxidformmassen aufgrund der Lagerdauer, Feuchte und Chargenschwankungen auf die Bauteilqualität untersucht. Die Online-Überwachungsmethode Dielektrische Analyse (DEA) wird im Transfer Molding Prozess implementiert, um die Veränderungen in den Eigenschaften der Epoxidharze zu beobachten. Die Eignung der DEA zur in-situ Überwachung der Veränderungen der Materialeigenschaften der Epoxidharze im Transfer Molding Prozess wird bewertet. Zusätzlich zu der DEA sind Temperatur- und Drucksensoren in der Kavität des Transfer Molding Werkzeuges zur Prozesssteuerung implementiert. Um die Korrelation zwischen den Veränderungen in den Materialeigenschaften von Epoxidformasse und der Bauteilqualität zu definieren, werden Materialmodelle eingeführt. Weiterhin werden so die Verarbeitungsbeschränkungen der vorkonditionierten Epoxidformmasse zum Erreichen einer vordefinierten Baueilqualität bestimmt. Zur Überprüfung einer allgemeinen Gültigkeit des Materialmodells wird eine Validierung des Modells mit einer zweiten Epoxidformmasse durchgeführt.

Acknowledgements

I would like to use the opportunity and thank all the people who supported me during the completion of this thesis. First of all, I would like to thank Prof. Klaus-Dieter Lang from TU Berlin and institute leader of Fraunhofer IZM for accepting the supervision of this thesis, for the valuable discussions and for his mentoring. In addition, I would like to sincerely thank to Prof. Martin Schneider-Ramelow and Prof. André Zimmermann for reviewing of thesis and Prof. Rolf Schuhmann as the chairman of the doctoral admission committee.
Moreover, I would like to express my gratitude to Dr. Jan-Martin Kaiser from Robert Bosch GmbH for accepting the co-supervision of this thesis. His continuous support and deep discussions have guided me through the intense journey of this thesis and gave me the motivation for the completion of the thesis. I am grateful to have the opportunity to work under his supervision. I would like to also sincerely thank Karl-Friedrich Becker and Dr. Tanja Braun from Fraunhofer IZM for valuable discussions, for sharing their knowledge about material science and processing and their constant support. Last but not least, I would like to thank my colleagues at CR/APP at Robert Bosch GmbH for the good collaboration, for continuous support and for helping me to realize this thesis. It was pleasure for me to get to know them and have a chance working with them. I would like to also thank the master students and interns who supported me during this thesis. Without their help, it would not be possible to complete the thesis in this form.
Finally and most importantly, I would like to thank my family for their endless support and giving me a constant motivation, and always being there for me. I am so grateful to have them.

Contents

Symbols and Abbreviations

A	Electrode plate area
C_p	Parallel capacitance
C_{sub}	Substrate capacitance
d	Distance between the electrodes
E''	Loss modulus
E'	Storage modulus
ε''	Dielectric loss factor
$\acute{\varepsilon}$	Dielectric permittivity
ε_0	Permittivity of vacuum (dielectric constant)
e	Error
f	Frequency
T_g	Glass transition temperature
P	Pressure
R_p	AC parallel resistance
R^2	Coefficient of determination
R^2_{adj}	Adjusted coefficient of determination
T	Temperature
t	(Preheat) time
$tan\ \delta$	Tangent delta
v	Transfer speed
σ	Ionic conductivity
$\boldsymbol{\rho}$	Ion viscosity
α	Degree of cure
$\Delta H(t)$	Enthalpy at time t
ΔH_{total}	Total reaction enthalpy

BC	Boundary conditions
CTE	Coefficient of thermal expansion
DEA	Dielectric analysis
DoE	Design of experiments
DSC	Dynamic scanning calorimetry
DMA	Dynamic mechanical analysis
EMC	Epoxy molding compound
FTIR	Fourier-transform infrared spectroscopy
IC	Integrated circuit
OFAT	One factor at a time
LIC	Logarithmic of ion viscosity
RH	Relative humidity
PMC	Post mold cure
SAM	Scanning acoustic microscope
TIM	Thermal interface material

1 Introduction

Semiconductor packages are widely used in many areas such as automotive, military, aerospace, communication and computing applications [1], [2]. The market for semiconductor packages has experienced an enormous development in recent years. Accordingly, a trend to decrease the package size by increasing integration density on the lead frame significantly raises the requirements for the packaging. Thus, the demand for reliable robust packages has become even more pronounced. To yield long-term reliability of the packages, i.e. to protect them from environmental effects such as heat, temperature, pressure, mechanical stress and humidity, the electronic packages are encapsulated. Transfer molding is one of the major processes for encapsulation of semiconductor devices due to its high productivity, cost effectiveness, ability to mold complex features and resulting robust packages. As an encapsulation material for the electronic packages, mostly polymeric materials are used. Non-hermetic packages, which are encapsulated with polymeric materials, offer some advantages over hermetic packages such as light-weight, cost and flexibility. Hence, over 90 % of the electronic packages are encapsulated with polymeric materials [1], [3]. Among polymeric materials, epoxy molding compounds (EMCs) are mainly used as an encapsulation material. EMCs possess superior properties such as high mechanical strength, thermal stability and good thermo-mechanical matching to the materials typically used in packaging.

The quality of the molded packages heavily depends on the material properties of EMC and the process parameters of the transfer molding process. Although transfer molding is a common process for producing electronic packages and billions of electronic packages are manufactured with this process every year, process optimization is still challenging. Parameter settings of the transfer molding process are mostly developed in a trial and error manner and optimal settings are often not obtained [4]–[6]. Additionally, the machine settings in the molding process do not usually reflect the real condition in the cavity, e.g. the machine pressure is often not equivalent to the pressure in the cavity. In the case of power electronics, process control is even more challenging due to the large volume of the modules. Direct information from the cavity of the mold tool cannot be obtained and the temperature and pressure in the cavity can only be monitored via machine settings.

In addition to process parameters, the EMC characteristics also have a large influence on the package quality. The reactive nature of the epoxy resins can be influenced by the variations in the characteristics of the EMC such as the moldability and change in the flow behavior of the material, which can be especially critical for large complex power modules. Therefore, acquiring information about the cure behavior of the EMC in-situ in the transfer molding process is very determining for an ultimate package quality. Due to this limited process knowledge and the alterations in the material characteristics of the EMC, during the encapsulation of the electronic packages, some common defects can occur in the package such as wire sweep, delamination, void formation and warpage, which may lead to total package failure at the end. When the failure mechanisms arise in the package during one of the last steps in the assembly process, namely in the transfer molding process, it can cause high failure costs, particularly for complex power modules. On that account, understanding the impacts of the material characteristics of the EMC and the process parameters on the package quality is essential. An established correlation between process parameters, material characteristics and the package quality can improve process understanding, yet diminish the failure mechanisms in the molded packages.

The aim of this work is to provide a conceptual understanding of the influence of the process parameters of the transfer molding process and the variations in the material characteristics of EMC on the package quality. Extensive process analysis is conducted for improved process understanding of transfer molding process. As an electronic package, a test vehicle having similar geometrical dimensions as a power module is used in this work. Systematic approaches are evaluated to generate models, which describe the relationship between the process parameters, the variations in the material characteristics of EMC and the package quality. Additionally, the represented approach also allows definition of the optimum

process parameters of the transfer molding process to achieve the best package quality. Online monitoring methods are implemented in the transfer molding process to gain more insight into the cavity of the transfer molding process and to obtain a stable process. Detailed material investigations are conducted to increase the knowledge on the influence of alterations in the material properties of the EMC prior to the molding process on the cure behavior of the EMC and on the package quality. Online monitoring method, DEA, is employed to monitor the variations in the material properties of EMC in-situ during transfer molding process.

2 State of the Art

In this chapter an overview of the state of the art on the encapsulation of the electronic packages, as well as the technologies and the materials employed to produce the electronic packaging is given. In Section 2.1 the components and the main functions of the electronic packaging as well as the manufacturing process of an electronic packaging are introduced. Different defects can occur in an electronic package, which can cause a total package failure. Thus, in Section 2.2 possible failure mechanisms of an electronic package are summarized. The transfer molding process, which is the most established encapsulation process of semiconductor devices is explained in detail in Section 2.3. The process steps, the significance of the process parameters, and their influences on the package quality are discussed. In Section 2.4 an overview on the commonly used encapsulation materials, namely epoxy molding compounds (EMCs) is provided. The properties of the EMC, and their impact on the package performance are explained in detail. Recently, online monitoring techniques gained significant attention in terms of observing the cure reaction of the EMC in-situ in process. Various monitoring techniques are introduced in Section 2.5. Their potentials and limitations are discussed. More focus is given to dielectric analysis (DEA) as an online monitoring technique, hence the measurement principle and some important features of the method are expressed in Section 2.5 in detail. To understand the influences of the material characteristics and the process parameters on the package quality and to describe the correlations in a best possible way, statistical analysis is used in this work. Thus, in Section 2.6 the statistical analysis and the important terms regarding the Design of Experiments (DoE) are highlighted. Finally, in Section 2.7, a brief summary of the state of the art is done, and the unresolved issues in terms of influence of material characteristics and of process parameters on the package quality are discussed. Additionally, the outline of the thesis is introduced in Section 2.7.

2.1 Electronic Packaging

Semiconductor packages have been used in many electronic products and equipment such as personal computers, consumer electronics, and automotive electronics.

Electronic packages include transistors assembled in integrated circuit (IC) chips, resistors, diodes, capacitors as well as housing [7]. In Figure 2.1 an electronic package, consisting of electronic components such as chips, and wire bonds as well as adhesives and lead frame plus the molding compound is depicted schematically.

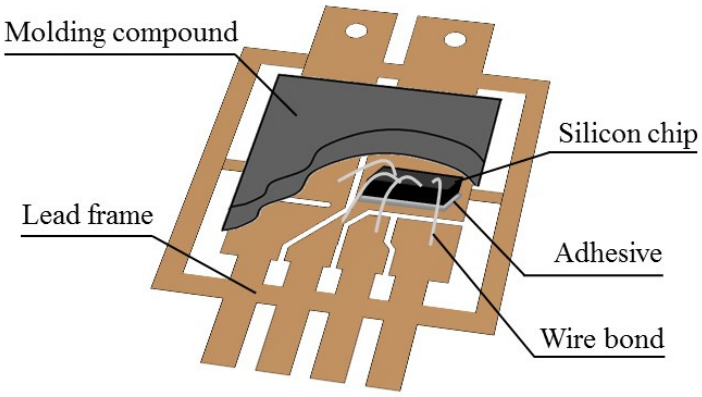

Figure 2.1: Schematic illustration of structure of an electronic package

The main functions and the requirements of the electronic packages are:

- Protection of the chip from harsh environment
- Protection of the components from heat, temperature, humidity, moisture and radiation

- Providing resistance to ionic contaminations
- Protection from mechanical stress such as pressure
- Reducing the thermo-mechanical stresses
- Isolation of the electrical contacts
- Providing mechanical support [1].

Packaging material plays a very critical role in an electronic system so that the package can perform the desired functions and meet the aforementioned requirements. Depending on the employed encapsulation material, two different types of packages can be produced: hermetic or non-hermetic packages. In hermetic packaging, a ceramic or metallic material is used as a package material, whereas in non-hermetic packages, a polymeric material is utilized as an encapsulant. In comparison to hermetic packaging, non-hermetic packaging offers some advantages such as weight, costs, handling, flexibility in design and availability [3], [8], [9]. Thus, over 90 % of the microelectronic components are encapsulated with plastic materials [1], [3]. Among plastic materials, EMCs are typically used in semiconductor devices due to their superior properties, which will be addressed in Section 2.4 in more detail.

Electronic packaging, described here for a lead frame based package, starts with a chip on wafer level. After the fabrication of a wafer, the chip preparation steps start which involve grinding and dicing processes. After the singulation of the chips, the assembly process for the electronic package starts with an attachment of a chip onto the lead frame (die attach pad). The chips are attached onto the lead frame using typically a polymeric adhesive, which is subsequently sent to an oven for complete adhesive curing [10]. To achieve a smooth clean surface for the following wire bonding process, usually the lead frame is dispatched to a cleaning process. For an electrical connection, wire bond process is applied, where the chip is connected with wire bonds to the lead frame fingers. Following the wire bond process, the interconnected chip assembly is encapsulated. To achieve the mechanical stability and high network density of molding compound, a post mold cure (PMC) is performed after the molding process. Finally, the leads are trimmed and formed to various shapes [1]. The schematic illustration of the assembly steps for a lead frame based electronic package is depicted in Figure 2.2.

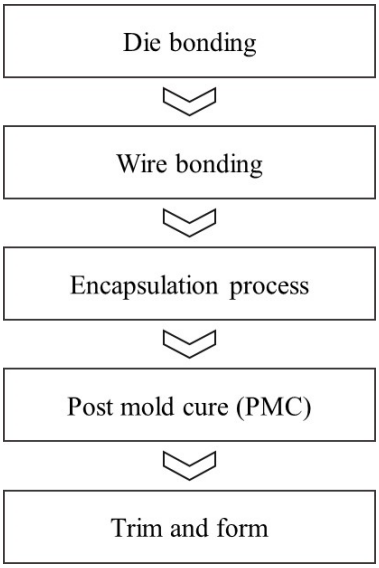

Figure 2.2: Assembly steps for electronic packages [11], [12]

The encapsulation process is one of the last steps in the process configuration for manufacturing of electronic packages, so it has a major importance to satisfy the desired package quality. When defects are introduced into the package in one of the last process steps, namely during the encapsulation process, it can cause high failure costs due to the yield loss. Hence, the encapsulation step is very critical to yield

the stable package quality. Various encapsulation methods are available such as molding, potting, glop-top and underfill [1]. Among all methods, transfer molding is widely used for an encapsulation of semiconductor devices [5], [13], [14]. As mentioned above, some severe defects can arise in an electronic package during transfer molding process, which may ultimately cause a complete package failure. Thus, some of the essential quality criteria for the electronic packages are summarized in following section.

2.2 Quality Criteria of Electronic Packages

Different defects can occur in an electronic package due to various reasons such as selection and the properties of the EMC, process parameters of transfer molding or the transfer mold design. Some of the most common defects in the molded packages are wire sweep, delamination, void formation, cracks, warpage, incomplete cure, bleed and flash. Such defects can become very critical in terms of the package quality since they may cause a total package failure. For instance, warpage can occur in the package, which is defined as the bending and deformation of the package [1]. Different warpage types can happen in a package such as convex or concave [15], [16]. The warpage can not only induce stresses to the package and cause die cracking and interface delamination, but it can also lead to assembly problems in the following process steps due to the dimensional instability and non-coplanarity of the package [17], [18]. Particularly, the warpage in large power modules can be very critical due to thermal management issues [16]. In the power modules large amount of heat is generated due to the high voltage and large currents applied in the package. Thus, to remove the heat from the package, the power module is contacted with heat sink, and between power module and the heat sink a thermal interface material (TIM) is applied to improve the thermal behavior. Possible warpage issue in power modules can cause poor connection to TIM, which may lead to insufficient thermal connection. Hence, the heat generated in the power module cannot be effectively dissipated which may threaten long-term reliability and cause a device failure. Another common problem is the existence of gas or air voids in the package. Voids can arise in the package due to the volatile materials or organic vapors present in resin encapsulant, which are likely released by polymerization reaction or outgassing of the air trapped in the pressed pellet of EMC [19]–[22]. Alternatively the voids can arise due to air that enters from the runners during the transfer molding process or due to improper molding conditions [21]–[23]. The voids in the package can cause corrosion on the electronic components such as aluminum wires or on the lead frame [22], [24]. In addition, they can lead to stress concentration and hence, induce cracks and threaten package reliability. Moreover, the voids connecting two leads of different voltage level cause insulation problems and might lead to a short circuit. Even small voids between two leads of different voltage level might cause to partial discharge. The detachment of the molding compound from a contiguous material at the interface is defined as delamination [1]. Delamination causes structural disintegrity, and usually initiates an electrical failure [25]. Resin bleed happens when the encapsulant flows onto the leads. So-called flash is also excess material that runs through the molding part but flash is usually thicker than the bleed. When this material remains on the leads, some problems may occur in the subsequent operations such as lead trimming and forming [1], [24]. Another important defect is the wire sweep. Wire sweep is defined as the deformation and lateral displacement of the wire loop inside the cavity of mold tool [1], [20], [26], [27]. Different criteria are defined as a wire sweep tolerance depending on the package design. Some authors suggest 10 % of the wire sweep as a maximum lateral displacement, some additionally try to reduce the wire sweeping less than 2 wire diameters and less than 10 % of the lateral displacement [28], [29]. Some authors have defined wire displacement exceeding half of the pad-to-pad distance as unacceptable [20]. When excessive wire sweep occurs, this can lead to short circuit and/or current leakage and can even cause to package failure [1], [3], [13], [30]. Some of the mentioned defects occurring in an electronic package are exemplarily shown in Figure 2.3.

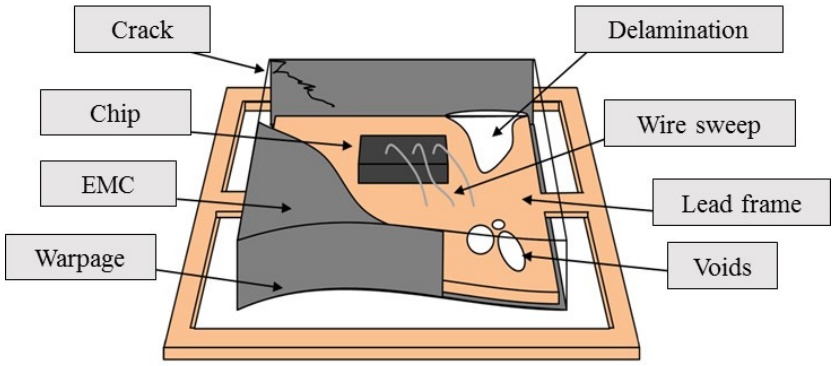

Figure 2.3: Exemplary illustration of possible defects in plastic encapsulated package [31]

2.3 Transfer Molding Process

Transfer molding is an established process to encapsulate the microelectronic components of semiconductor devices. Transfer molding process has many advantages such as ability to mold complex features, high production volume, and cost-effective manufacturing and to produce high quality and robust packages [32]–[35]. The equipment for the molding process consists of cavities, a pot in which the EMC is placed, and the plungers that help to transfer the viscous material into the cavities. There are two types of transfer molding process: the conventional method and the multi-plunger method. In a conventional method, there is one pot, where one large-size pellet is placed and injected into multiple cavities. In the multi-plunger method, there are several pots, where small pellets of EMC are injected to one or more cavities of the mold tool [2]. Transfer molding process includes several process steps. Firstly, the lead frame, which is assembled with electronic components and bonded with wires, is placed in the cavity. The lead frame is preheated in the cavity to improve the adhesion between the thermoset material and lead frame. The pellets of the EMC are placed in the pot, and then the tool is closed, the lead frame is clamped. Before the plungers move with a defined transfer speed, the required clamping pressure is applied to ensure the complete closure of the tool halves and the pellets are preheated in the pot and reach its melting temperature. The molten material is injected with the help of the plungers through the channels (called runners) and enters through the gate into the cavity. The plungers apply the required pressure to fill the viscous molding compound into the cavity and the pressure is maintained until the cavity is filled to assist the curing reaction of the molding compound as well as to compress any remaining voids to yield a void-free package [1]. The molding compound undergoes an irreversible chemical reaction in the cavity and forms a 3D cross-linked network. During the curing reaction, the molecular weight of the material increases and material becomes solidified. Usually the cycle time of 1-3 min at molding temperature of 175 °C is required for material to solidify so that the encapsulated module can be removed with the help of ejectors without damaging the molded package [1]. Figure 2.4 illustrates the steps of the transfer molding process for encapsulation of the semiconductor packages.

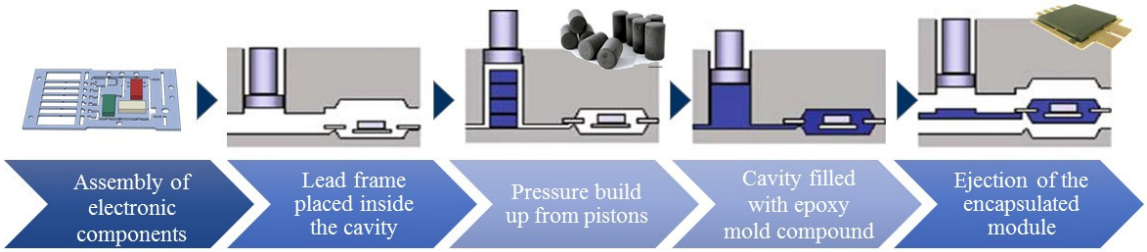

Figure 2.4: Process steps of the transfer molding for encapsulation of the semiconductor packages; lead frame is placed in the cavities of heated mold, the EMC pellets are brought to the pots, EMC is injected, ejection of the encapsulated lead frames after cycle time is over, encapsulated electronic packages after the molding process. Adopted from [2]

After the cycle time is completed, the thermoset material achieves a certain degree of cure. However, to complete curing reaction of the molding compound for obtaining a desired mechanical stability, the post mold cure (PMC) is required [24], [36]. Depending on the properties of the molding compound, the conditions of the required PMC can vary, nonetheless, PMC is generally done at 170 °C - 180 °C for 2-4 hours in an oven depending on the material selected [2], [33], [37].
The molding compound, which has a reactive nature, undergoes different chemical reactions in the cavity. The moldability duration of the EMC depends on the gel time of the material [3], [12], [33]. Gel time is defined as a point, where the molding compound changes its state from a liquid into a gel [1]. Thus, the time for filling the cavity is restricted and should not exceed the gel time of the material. On the other hand, the process parameters should be selected in a way that the sensitive components such as wire bonds are not damaged due to set process parameters. Yet, the combination of the process parameters plays a significant role on the curing reaction of the molding compound and on the quality of the final molded package. Some of the important process parameters of the transfer molding are molding temperature, transfer speed, clamping pressure, preheat time, holding pressure, cure time, and transfer time, which is the time to fill the cavities in the tool. Higher molding temperatures can be selected to diminish the curing time, which induce faster curing rate of the thermoset material (molding compound). However, at very high temperatures, the material cures very quickly, and the viscosity increases so fast that the cavity cannot be filled completely which leads to an incomplete filling of package. Hence, the window for processing time of the molding compound is restricted. Figure 2.5 depicts the limited processing window of the transfer molding process.

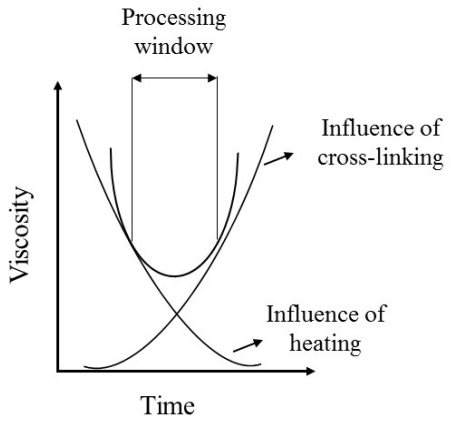

Figure 2.5: Viscosity behavior of a molding material [38]

According to Figure 2.5, the viscosity of the molding compound drops drastically at the beginning due to the high temperature. As the cycle time propagates, the cure reaction takes place and the bigger

molecules are formed, which raises the viscosity of the material. The time to fill the cavity should not exceed the indicated processing window to achieve good molded package quality.
During transfer molding, the clamping force is crucial for keeping the tool halves together. If the clamping pressure is too low, the material can flow between two halves of the tool and causes flash on the package. The transfer pressure, which is applied via plungers, assists the molding material into the cavity. During the chemical reaction of the molding compound, chemical shrinkage of the material occurs. The packing pressure is applied through plungers to bring more material into the cavity to compensate the shrinkage and fill the cavity completely. This process is also-called packing [1]. Higher transfer speed can help to fill the cavity faster and provide a complete filling, however, it can also lead to severe wire sweep and even lift-off of the wire bonds in extreme situations [39]. Decreasing the transfer speed can help improve the wire sweep, but it may also cause an incomplete filling particularly for large mold tools [5]. This aspect is especially important for the power modules, where the large cavity volume for the modules has to be filled within the gel time of the material. When the wire bonds possibly attached at the cavity end are subjected to highly viscous molding compound, this may lead to wire sweep. Thus, by the selection of the process parameters many different mechanisms should be taken into account since achieving a good quality of the molding packages in transfer molding process is a multi-objective optimization problem [4]. Therefore, understanding the influence of the process parameters as well as the interactions between the process parameters and the material characteristics are very important to yield a defined package quality.
Great efforts have been done by many authors to apprehend the effects of process parameters on failure mechanisms and to define the optimum process parameters of transfer molding process [4], [14], [40]. Among other defects void formation is one important concern in the molded packages. To remove volatile materials and air during the molding and to achieve homogenously filled packages, using the air vents in the molding tool such as vacuum molding is favorable [21], [41]. Nevertheless, there may be still some voids within the package or some bubbles on the surface area of the package. M. M. Prasad investigated the impacts of the transfer time and preheat time on the void formation of package [34]. In particular, the same batch of the EMC pellets was used to prevent any possible variations in the EMC properties. DoE was conducted, regression analysis was carried out and the interactions between the significant parameters were discussed. They found that an increase in transfer time and preheat time led to an overall decrease in void occurrence in the package. Regression analysis indicates that there is an interaction between the transfer time and the preheat time in which reducing the transfer time and increasing the preheat time cause less void formation. S. L. Liu et al. studied the influence of molding temperature, preheat time, transfer time, curing time and holding pressure of transfer molding process on short molding and on the void formation with novolac-type EMC [42]. They conducted a two-level DoE matrix consisting of 32 experiments. The scanning acoustic microscopy images showed that the voids were formed in low holding pressure and short transfer time, whereas the packages, which were molded with high holding pressure and longer transfer time showed no voids. In addition the holding pressure, the selection of higher transfer pressure, lower mold temperature and faster transfer speeds were also suggested in the literature in favor of attaining reduced number of voids in the molded packages [21], [22]. The suggested selection of process parameter settings to reduce the void formation, however, can increase viscosity of EMC, which can be unfavorable for other package qualities such as wire sweep. Among other process parameters, the transfer speed is found as a key process parameter on the wire sweep. Decreasing the transfer speed reduces the wire sweep by diminishing the viscous drag force exerted on the wire bond [13], [20]. However, injecting EMC with too slow transfer speed into the cavity can be critical since EMC already starts curing and the viscosity increases too much before the complete filling [13], [20], [39]. Therefore, the chemo-rheological properties and the curing reaction of EMC during molding must be considered in addition to the process parameters to improve the wire sweep.
One of the challenges in the transfer molding process is to define the optimum process parameters. Although transfer molding process is one of the most established processes for the encapsulation of the

semiconductor packages and billions of parts are produced every year with the process, the optimum process parameters are commonly unknown [5], [13]. Usually the optimum process parameters are identified in a trial and error manner by experienced molding personnel [6]. Moreover, the definition of the optimum process parameters is considered as a multi-objective optimization, since several quality characteristics of the transfer molding process are required to be analyzed at the same time [4], [43]. Thus, obtaining the optimum process parameters is very laborious. At present, most of the work presented above, consider only one quality characteristic, which involves single-objective optimization. As the multi-objective optimization is challenging and very time consuming, some authors studied simulation methods to investigate the influence of process parameters on various quality characteristics at the same time and to define optimum process parameters [4], [6], [14], [44], [45]. Tong et al. used the process simulation combined with Taguchi experiments, which allow to determine the influence of significant parameters on the mold package quality and to determine the optimum process parameters [14]. They investigated the influence of fill time, mold temperature, clamping force, post-fill time on the wire sweep, incomplete fill, flash, voids and resin bleed. They conducted virtual experiments with the process simulation. The results showed that the quality results can be improved by adjusting the individual parameter, however, the interactions between the parameters are not involved in Taguchi experiments and their effects are not considered on the package quality. Thus, the authors stated that such kind approach cannot be helpful to deal with the multi-objective optimization problems [4]. The authors further studied the simulation methods to generate process models, which delivered the optimum process parameters of transfer molding process by implementing the methods such as artificial neural networks, the DoE and multiple regression analysis [4]. The results showed that the process models generated by using simulation methods could help to define the optimum process parameters, however no validation experiments have been conducted to verify the obtained results. In addition, the authors noted that the prediction accuracy of the generated process models was not sufficient for a precise prediction and needs to be improved further. Thus, at present the simulation methods are not sufficiently developed to solve the complicated phenomenon of transfer molding process.

Despite many efforts done in literature, complete understanding of the influence of the process parameters on the package quality and the definition of the optimum process parameters are still not achieved. No systematic approach has been introduced to understand the influence of the process parameters on the package quality and to obtain the optimum process parameters of the transfer molding process. Since the complex nature of the thermoset material, which undergoes chemical reaction during transfer molding process, plays a significant role on the package quality as well, it is important to consider the properties of the EMC to achieve a good package quality. Thus, to provide a conceptual understanding, the properties and the characteristics of the EMC and their impact on the package quality will be explained in the following section in detail.

2.4 Epoxy Molding Compounds

Epoxy molding compounds (EMCs) are mostly used as encapsulation materials due to their superior properties such as high mechanical strength, good thermo-mechanical matching and good electrical properties, small shrinkage as well as good moisture resistance. Moreover, they possess good thermal stability; hence, they can withstand operation at elevated temperatures. One of the important properties in terms of moldability is that EMC has low melt viscosity before curing and a short curing time [2]. To achieve aforementioned properties and to meet the desired requirements as a packaging material, various raw material ingredients are added to an EMC. Some of the ingredients are fillers, catalyst or accelerators, release agents, flame retardants, and coloring agents. The typical ingredients in EMC are depicted in Figure 2.6.

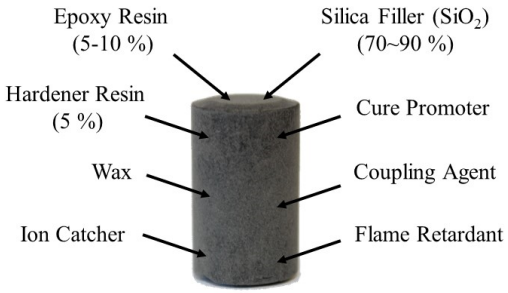

Figure 2.6: Typical ingredients in an epoxy molding compound with corresponding compositions [2]

EMCs are based on epoxy resins, which are thermoset materials and cured mostly with the polyaddition reaction. Epoxy resin is defined as any molecule having more than one epoxy group which has a capability to be conversed to useful thermoset form [46], [47]. The chemical structure of the epoxy resin is illustrated in Figure 2.7.

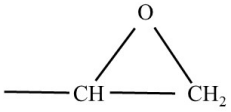

Figure 2.7: Chemical structure of an epoxy group

Some of the common epoxy resins systems are: novolac epoxy resins, multifunctional epoxy resin, biphenyl epoxy resin, multiaromatic epoxy resin, orthocresol novolac epoxy resin, and cycloaliphatic epoxy resins [1], [48]. Among all resin types, novolac resin is one of the most commonly used resin type due to their good moisture and chemical resistance, good adhesion to a substrate and high cross-linking density after curing [42]. For a cross-linking reaction of epoxy resin, a hardener is necessary. With the help of hardeners, functional epoxies form a solid, three-dimensional network. Aliphatic amines, aromatic amines and phenol novolac resins are some of the known hardeners. Phenol novolac resins are mostly used as a hardener type since they have a good performance in terms of heat and moisture resistance, storage stability as well as curing property [2]. Moreover, phenol novolac resins offer an advantage, where the number of the repeating units in novolac structure can be tailored to control the molecular weight distribution of EMC [2].

As illustrated in Figure 2.6, EMC contains high amount of fillers. High volume fraction of the filler particles is essential in EMC in order to reduce the water absorption and to improve the thermal conductivity [1], [2], [49], [50]. With the help of the filler particles, the coefficient of thermal expansion (CTE) of the EMC can be lowered, which is very crucial in terms of package integrity. The epoxy resins, which possess a high CTE and low thermal conductivity, can cause some significant dimensional change in the package without supplementation of the filler particles. Moreover, the filler particles increase the elastic modulus, and diminish EMC shrinkage during cure [51]. It has been shown that the package warpage decreases with increasing the amount of filler particles in the molding compound [52]. On the other hand, the amount of the particles in the EMC is very determining in terms of the flowability of EMC during encapsulation process as the viscosity of the EMC can increase with higher loading of filler particles [53]. Kiong et al. showed that by increasing the filler content from 87.5 % to 90 %, the wire sweep increased from an average of 2.5 % to 4.0 % [52]. Additionally, the shape and the particle size of filler as well as the type of filler can also influence flowability of the EMC, hence the performance of the electronic packages [50], [54], [55]. As filler particles usually silica, alumina or silicon nitride are used due to their high-thermal conductivity [2]. For higher volume fraction of filler particles in the epoxy resins, mostly silica particles are preferred since they decrease the warpage, yet enhance the package reliability [42], [52], [56]. Usually spherical particles are used for higher filler content to ensure good flowability of the EMC. To strengthen the interface between the epoxy resins and the filler particles, silane coupling agent is added to the epoxy resins. The organic functional groups in silane coupling

agent react with the epoxy resin and hardening agent and act as a bridge between the filler particles and the epoxy resin matrix [57]. Moreover, it promotes the adhesion between the EMC and lead frame [2], [12], [57]. To accelerate the curing speed of the reaction and to reduce the cycle time, catalysts such as accelerators are used. Nitrogen containing catalyst, amines and imidazoles are some of the important catalysts types. In addition, some other additives are added to the epoxy resin such as synthetic wax to facilitate the part removal from the tool surface, carbon black as colorant, ion getter to capture the ionic impurities such as Na^+ and Cl^-, and flame retardant to satisfy the molded product inflammability rating [2], [58].

After adding the additives to the epoxy resins, all raw materials are blended and subsequently kneaded by applying heat and cooled down into a sheet shape [2]. Subsequently, they are pulverized and pelletized into a pellet shape in desired dimensions, which is then used in the transfer molding process for the encapsulation of semiconductor devices. As the kneading process is conducted under heat, the cross-linking reaction already begins. However, as the degree of cure of EMC is only slightly influenced by the kneading process, it does not increase the viscosity of the EMC significantly. On the other hand, after the preparation of the EMC, the pellets must be stored in a cold environment such as freezer at around -20 °C prior to the molding process to prevent any possible reaction in EMC pellet, where the resin and hardener are pressed together.

Considering many ingredients included into the epoxy resins, any possible variations in the EMC properties might influence the package quality. For instance, since the electronic packages are built by composing of dissimilar materials, CTE mismatch between the components can cause some defects in the package such as warpage or delamination [16], [59]. In addition to that, as the power modules can operate at high temperatures especially in automotive applications, all the components in the package should withstand the operation temperature. Currently the limit for the EMC is around 175 °C and for the high temperature applications exceeding 180 °C new formulations of the EMC are necessary for the thermal stability at elevated temperatures [60], [61], [62]. Moreover, the viscosity of the EMC also plays a significant role on the package quality, especially for the large power modules where the process control is challenging. The variations in the viscosity of the EMC can cause some severe defects in the package such as wire sweep, voiding, which may lead to failure mechanisms. Thus, the characteristics of the EMC have a determining impact on the end package quality.

One of the crucial problems regarding the EMC, which is extensively studied in literature, is the impact of humidity content of cured EMC on the package quality [63]–[66]. Epoxy resins have a hydrophilic structure and they can absorb humidity easily from the environment. Water, which is a polar molecule, has a capability of hydrogen bonding with other polar species such as hydroxyls and amines in the epoxies [67], [68]. It is suggested that in polymeric materials the water molecules can be either present in free volume of the polymer or they can be bonded via hydrogen bonds to the polymer chains [1], [69], [70]. The water molecules can act as plasticizers or crazing agents in epoxides [67]. Moisture changes the thermo-mechanical properties of the EMC, reduces modulus, strength, decreases the glass transition temperature (T_g) and it can additionally cause the swelling [53], [63], [71], [72]. Thus, the absorbed humidity in the EMC can also lead to internal stresses in the electronic packages [73], [74]. Popcorn cracking due to the moisture absorption during board level assembly (assembly flow soldering process) is a well-known phenomenon [72], [75]–[78]. Therefore, moisture absorption becomes one of the major reliability issues in the electronic packages and the moisture mechanisms in the package as well as influence of moisture absorption during storage or the service are extensively studied by many researchers [63], [64], [69], [79], [80]. In addition to that, the humidity absorption of the mold compound preforms in uncured state before the molding process can be also very critical during encapsulation process for the manufacturers. Especially, in East Asian countries, which have a high atmospheric humidity level, the EMC pellets are subjected to a highly humid environment during manufacturing in case they are not stored under dry vacuum, which may induce variations in the EMC properties [81], [82]. The absorbed humidity can influence the rheological properties of EMC, the spiral flow length, which is a typical indication of the rheological behavior of the resin encapsulant, so it can affect the

moldability [5], [82]. Existing humidity in EMC can also affect the curing properties of the molding compound, and the thermo-mechanical properties of the cured material [72]. Absorbed moisture in the EMC pellets can introduce voids into the package, yet diminish the quality of the final package [5], [83]. Although humidity absorption into the EMC preforms is a critical issue for encapsulation process, only few studies have addressed the impact of humidity of EMC prior to the molding process. T.Y. Lin et al. investigated the influence of the moisture content on the warpage [84]. They stored the pellets of EMC for 0 h, 12 h, 24 h and 72 h in a clean room at room temperature with a relative humidity (RH) control between 35 % to 55 % RH and subsequently molded the packages with the preconditioned pellets in transfer molding process. They observed that increasing the moisture content causes an increment in the shrinkage and also influences the warpage. They concluded that the humidity control in clean room environment is crucial to maintain high yield in molding process as well as to prevent warpage rejects in the SMT process. Lin et al. emphasized the importance of the measurement of the moisture uptake in the EMC package prior to molding and compared the methods to measure the moisture content of the pellets [82]. Karl-Fischer Titration is given as a promising test method for measuring the moisture content in the EMC pellets, and they investigated dynamic scanning calorimetry (DSC) as an alternative method [82]. They found that with DSC the change in the EMC properties due to humidity uptake can be detected, where the area under the endothermic peak in DSC curve is decreased, and the T_g of uncured resin shifts to lower temperature with increasing moisture content. However, the impact of the absorbed humidity in the EMC on the package quality was not addressed in this work.

In addition to humidity absorption, extended storage duration or floor life can also influence the EMC characteristics. With the prolonged storage duration, the cross-linking degree before the molding process can increase and the gel time of EMC can decrease [85]. The increase in the cross-linking degree or the reduction in gel time can be critical during molding process by causing some severe defects such as wire sweep or incomplete filling. The influence of floor life of the EMC on its gel time, spiral flow and on the wire sweep were investigated by Penapunga et al. by varying the floor time from 0 to 60 hours with steps of 12 hours [85]. It was found that the wire sweep of wire bonds increases by prolonging the floor life of EMC in all packages. The gel time does not decrease significantly whereas the spiral flow length deteriorates with prolonged floor time. Spiral flow length is usually defined by measuring the distance of the flow of compound in a specific mold tool under specific mold process parameters [24], [86]. The correlation between the flow characteristics of EMC such as spiral flow length and the gel time on the failure mechanisms are assessed by some other authors [21], [22]. Tanaka et al. investigated the relationship between the spiral flow length and the inner void formation by producing eight different molding compounds, which had different filler contents, raw resin viscosities, catalyst concentrations and ratio of the spherical filler particles [21]. However, no clear relationship is observed between the molding compounds having different spiral flow lengths and the number of inner voids in the package [21]. This is explained by the non-Newtonian viscosity behavior of the thermoset material, where the material viscosity depends on the shear rate. Nonetheless, in general it is suggested that resin encapsulant with high viscosity offers some advantages in terms of reducing the voids in the package [21], [22]. On the other hand, it is important to consider that since the viscosity has a direct impact on the wire sweep, the EMC having higher viscosity can cause also more severe wire sweep [87].

In addition to the prolonged storage duration, another known problem in manufacturing is the variation in EMC properties between different batches [58], [86]. Studies emphasized that different batches of the EMC can have different T_g, different pre-cured levels, or different chemo-rheological characteristics [34], [88]. However, no systematic investigation has been reported so far to understand the influence of the possible batch differences on the package quality.

Another important issue is the transportation of the EMC from suppliers to the manufacturers. During shipping of the EMC additional dry ice is periodically added to the storage boxes, but the transport chain may not be always continuous, can be broken which can raise the temperature of EMC pellets during the shipping. This may increase cross-linking in EMC and thus the viscosity. When the EMC pellets arrive at the manufacturer, there is usually no quick way to detect this situation about the prior curing

before the molding process. The only possibility to examine possible changes in EMC is in the laboratories with analytical methods outside of the production line. Evidently, such problems during transport can cause variations in the properties of EMC such as reducing the shelf life in which the manufacturer may not be aware at first sight and have no possibilities to find out easily during transfer molding process.

Therefore, those aforementioned variations in the characteristics of EMC can yield poor package quality by inducing voids, causing warpage or wire sweep. Apart from that, such variations in the EMC characteristics can reduce the flexural strength of the package, which prepares a suitable basis further in service or in application for increasing moisture absorption in the package and endanger the reliability of the package as well [25], [58]. Therefore, the initial characteristics of the EMC not only play a significant role on the final package quality, but also in terms of reliability of the molded package. Yet, a systematic approach is required to understand the influence of the variations in the EMC characteristics prior to molding process on the final package quality. In addition to that, the best possible way to determine any possible variations in the material characteristics is seen in examining such changes directly during the molding process, before those variations cause severe problems during production. The information about the viscosity of the EMC and the temperature directly from the mold cavity can be very useful to analyze the cure behavior of the EMC and the interactions of process parameters with the material properties during the encapsulation process in order to decrease possible wire sweep issues and void formation. In that manner, the online process monitoring techniques can be helpful to highlight the complex phenomenon of the curing reaction of EMC during molding process and to understand their influence on the package quality. Hence, different online monitoring methods will be addressed in the following section.

2.5 Online Monitoring Methods and Process Optimization

In the previous sections, the influence of viscosity and cure behavior of the EMC on package quality during transfer molding process, as well as the dependency of EMC behavior on the process parameters are described in detail. It is emphasized that EMC, which undergoes different chemical reactions during molding has a vital influence on the performance of the package. Therefore, monitoring the cure state of the EMC during molding with defined set process parameters is a key issue to improve package quality. In that manner, many studies have been already carried out to study the curing mechanisms of EMC and to model the cure behavior of the EMC with different methods, such as rheometery [89]–[93], DSC [90], [94]–[96], Raman spectroscopy [97] and Fourier-transform infrared spectroscopy (FTIR) [98]–[101]. However, such methods can only deliver information under laboratory environment and not in-situ or, in other words, under real time process conditions. Real time implies that the measurements are performed on a time scale in which any change in the process conditions is possible before the measurements are completed [102]. Therefore, in process cure monitoring in real time is of utmost importance to gather more information from the process conditions in the cavity and to monitor the changes in physical state of material during the progress of the cure reaction. Additionally, the material characteristics can have variations such as viscosity, batch to batch difference which is already addressed in Section 2.3, thus in-situ real time monitoring not only helps to monitor the cure mechanisms of epoxy resins but also ensures the process stability in order to achieve stable package quality [103], [104].

Many different methods are investigated for monitoring the cure process such as fiber optic sensors [105]–[107], pressure and temperature sensors (thermocouples) [108], [109], ultrasonic methods [110], [111] and dielectric analysis (DEA) [103], [104], [112]–[116]. With fiber optic sensors, the monitoring of the resin is possible by refracting the infrared signal when the resin gets in contact with the sensor [117]. However, the sensitivity of the method for online monitoring of the cure reaction of polymers is not very high since the optical properties of the polymers do not vary much during the curing process [118]. Thermocouple sensors deliver information about the temperature of the media in the tool. The temperature drops when the resin, which is colder than the tool surface, arrives at the sensor and indicates the arrival of the resin flow front. As the reaction progresses, the temperature increases due to the heat

release during the exothermic curing reaction of the epoxy resins. These sensors are low-cost, durable and they do not influence the flow of the resin [108]. Thus, they are suitable to control and adjust the temperature in the process. Pressure transducers can also be used for monitoring the process. When the cavity of the tool is filled with the resin, the diaphragm of the pressure transducer deflects. This strain-gage, which is attached to the diaphragm of the pressure sensor, causes a change of electrical resistance, which is proportional to the pressure [117]. The pressure sensors are helpful for measuring the cavity pressure, which mostly deviates from the pressure set at the machine. Thus, they are also very valuable to monitor and control the cavity pressure. Those mentioned methods, however, can only be useful in controlling the process conditions but not in monitoring the cure reaction of the resin.

Ultrasonic monitoring is one of the common technique both for monitoring resin cure and the flow front of the resin. Piezoelectric elements generate an acoustic wave, which propagates through the material with a specific velocity. When any irregularities or boundaries exist on the way, some of the signals are reflected and some travel through to the second sensor, which collects the signal. Thus, ultrasonic measurement usually requires two sensors; one to generate the acoustic pulse, the other to collect the signals, which should be mounted on opposite side of the tool [119]. There is also a direct reflection method which requires only one sensor for transmitting and collecting the signal; however, some disturbing echoes can be recorded in this case which can cause improper measurement [110]. The transmitted and reflected waves are collected by so-called ultrasonic transducers. The ultrasonic sound speed is calculated based on the distance and the time information. When the resin arrives to the sensor, it leads to a variation in the velocity and the attenuation of the sound wave [117]. Two types of information can be derived from the ultrasonic measurements: sound velocity and attenuation. The correlation of the gathered information from ultrasonic monitoring to the progress of the cure reaction of the EMC are studied by numerous authors [110], [111], [119]. The change in the sound velocity is associated with the change in the viscosity and the cure state. When the viscosity of the material decreases, the acoustic wave velocity decreases as well. With the propagation of the cure reaction, larger molecular structure is formed irreversibly, the degree of cure increases, thereby decreases the diffusivity. Due to the reduced diffusivity, the configurational motion of the molecules increases, which raises the acoustic wave velocity [120], [121]. Rath et al. investigated different types of molding compounds and the impacts of various parameters such as fiber filler volume of molding compounds, moisture content, storage duration and amount of hardener on the sound velocity with ultrasonic cure monitoring [121]. It was stated that each material has a specific sound velocity like fingerprint depending on their chemical composition and reactivity. To understand the impact of storage duration on the epoxy resins, the epoxy molding compounds were stored for 3 hours and 24 hours at 90 °C to generate thermal degradation in the properties and measured with the ultrasonic cure monitoring in compression molding. The results showed that the sound velocity and the minimum of sound velocity increased for the stored materials in comparison to the fresh materials. This indicates that the resin and hardener already started curing under thermal load during storage time, which leaded to an increase in storage modulus, and thus on the sound velocity of the material. The values at the end of reaction also indicated that the samples had a certain amount of cross-linking during the storage time. In addition, the samples were stored in a humidity cabinet to observe the impact of humidity on the sound velocity of the material. An increased amount of water in epoxy resins caused a remarkable decrease on the minimum sound velocity. It was emphasized that absorbed water molecules in the resin do not disappear, stay entrapped and lead to a micro-porous structure in the material, which causes crack or moisture induced mechanical damage. This can be observed with the ultrasonic monitoring, where the absorbed water acts as plasticizer and decreases the elastic moduli, and thus decreases the sound velocity [121].

Another suitable method for in-situ cure monitoring is DEA. With DEA, the capacitance of the media between the plates and conductance in accordance to temperature, time and frequency are measured [122], [123]. DEA delivers information such as degree of cure, change in ion viscosity in real-time during the process. DEA is a suitable method to characterize the polymeric materials to obtain information about the thermal, rheological and dielectric information for a wide range of materials. In

addition, it correlates well with the chemo-rheological properties of the resin during polymerization [122], [124], [125].
DEA is usually compared with the ultrasonic methods in terms of sensitivity of monitoring the cure reaction of the resins. The advantages and disadvantages of these two methods are frequently discussed [126], [127]. The advantages of the ultrasonic cure monitoring are stated as that the sensors can be implemented in the tool without having any contact with the material, and hence the sensors leave no marks on the molded parts. On the other hand, special attention needs to be given during mold tool construction to achieve a good contact between the piezoelectric element of the ultrasonic sensor and the tool. Furthermore, in ultrasonic measurement, perpendicularity of the sensor to the sample geometry is very determining since to have a correct signal, the wave should meet perpendicularly with the surface boundary, otherwise it will change the direction. Thus, the tool must be precisely machined to achieve this necessary perpendicularity for the measurement technique [119], [120]. In addition, for the ultrasonic measurement, the part must have a significant thickness (at least 2 mm), and it should be of homogeneous material [126]. Non-homogeneous parts can cause spurious reflection, which can prevent successful measurements. This feature can make it difficult to use the ultrasonic method for electronic packages as they involve many different components inside. Moreover, for an accurate measurement the part thickness needs to be measured. If the part thickness changes during processing, it may also prevent an accurate measurement [126].
Compared to the ultrasonic technique, DEA is a highly sensitive method detecting the small variations in the material characteristics, especially at molecular level [128]. Moreover, DEA is the most sensitive method of measuring especially the local motions of the polar molecule chains due to the fact that polar molecules are strongly influenced by the electrical stimulation [129]. Furthermore, DEA is also found to be extremely sensitive to the end of the cure reaction [130], [131], [132]. Another advantage of the DEA is that the cure state can be measured simultaneously with multiple sensors and at various positions on the sample [133].
DEA sensors are available in many different forms i.e. implantable or one-way disposable sensors which can be embedded into the measured material. Thus, the ability to use DEA method in many different applications makes it a suitable method in diverse online monitoring applications [126]. In addition, DEA results show good correlation with other analytical methods such as DSC, Raman spectroscopy and rheology [103], [134], [135]. Large amount of information about the rheological state of the epoxy-based polymers during polymerization can be derived from DEA. Accordingly, among other online monitoring methods, DEA is named the most promising method to monitor the cure state of thermosetting materials [103], [136].
Therefore, based on the given overview, as the most promising online monitoring method, DEA can be a suitable selection for in-situ cure monitoring of EMC in transfer molding process. Thus, the measurement principle of DEA method will be highlighted in more detail in following section.

Dielectric Analysis

DEA can be used for process control, where cure reaction of the polymers is measured in-situ continuously in process. In a DEA measurement, the ion viscosity of the material is measured, which originates from ions and the dipoles movements, which exist as impurities like charged ions such as sodium and chloride ions [137], [138]. A DEA sensor measures the alteration in the ionic mobility of the samples in correlation to the curing time. According to Senturia and Sheppard [139], during the polymer manufacturing dielectric response is a function of the ionic conductivity, which is caused by the impurities and the components. Although the concentration of ions in the EMC is in ppm range, it has been shown that even an amount below 1 ppm is sufficient to cause a significant change in the ionic conductivity [139]–[142].
In DEA measurements, the EMC sample is in direct contact with the sensor. A thermosetting resin which is a dielectric material forms a capacitor when placed between the electrodes [136]. Ions and dipoles have a random orientation prior to application of an electrical field [138]. A sinusoidal voltage (AC

signal of frequency) is applied on one electrode and the resulting current is received by the second electrode along with the phase shift between the voltage and current [143]. When the sinusoidal voltage is applied, the electrical field is created in the sample. The sample becomes electrically polarized, the dipoles orient with the electrical field and the charge carriers in polymers such as ions, electrons, charged atoms or charged molecules and impurities are forced to move in the direction of the electrode with opposite charge [139], [143]. This results in a phase shift in the response between the voltage and current which is a function of ion and dipole mobility [130], [137]. Figure 2.8 depicts an excitation and a response between two electrodes and the behavior of dipoles and ions between two electrodes. Dielectric measurement can be performed in a large range of frequencies from 1 mHz to 100 kHz [144].

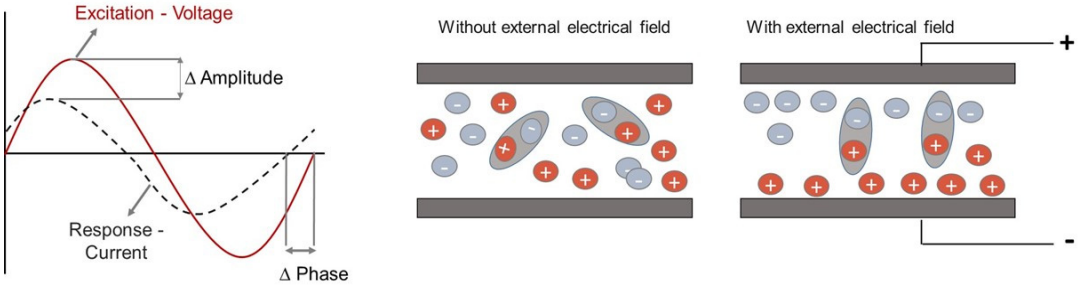

Figure 2.8: Excitation and response of the polymeric material between two electrodes (left), orientation of dipoles and charged ions in a polymer due to an external electrical field (right) [130], [143]

When the exact distance between the electrodes, frequency of the excitation, and the exact area of the electrodes are known, the change in the phase shift and the amplitude can be converted into two fundamental dielectric properties: dielectric permittivity έ and dielectric loss factor ε" [143]. The phase shift can be correlated with the dielectric loss factor ε", whereas the change in amplitude can be correlated with dielectric permittivity έ [143]. Dielectric permittivity indicates the number of dipolar groups in the resin and is a measure of the polarization of the medium per applied electric field [141]. Dielectric loss factor is associated with the conductive nature of a material and is a measure of the total energy lost due to the work done while aligning dipoles and moving ions in a material [128], [141]. Predominantly, permittivity changes due to the dipole motion during a typical polymerization. The dielectric loss factor is affected by both dipole motion and ionic conductivity. During polymerization, the contribution of the dipole motion on the loss factor is relatively small, thus the loss factor is mainly dominated by the ionic conductivity [126]. As the ionic conductivity indicates the ion mobility in the samples, it is inversely proportional to the viscosity before gelation and the rigidity after gelation [126]. Dielectric loss factor ε" is defined as shown in Equation (1) where R_p is equivalent AC parallel resistance, d is the distance between the electrodes, A is the electrode plate area, f is the measurement frequency and ε_0 is the permittivity of vacuum (8.854 pF/m) or also named as dielectric constant [144].

$$\varepsilon'' = \frac{d}{R_p\, \varepsilon_0 2\pi f\, A} \tag{1}$$

The relative permittivity can be calculated as following (Equation 2) where C_p is the parallel capacitance, C_{sub} is the substrate capacitance.

$$\acute{\varepsilon} = \frac{\left(C_p - C_{sub}\right) d}{\varepsilon_0\, A} \tag{2}$$

Ionic conductivity, σ is proportional to the dielectric loss factor, ε" and is a reciprocal value of the ion viscosity $\boldsymbol{\rho}$. Equation (3) represents the calculation of the ion viscosity, $\boldsymbol{\rho}$. Ion viscosity is the most relevant parameter in terms of the cure reaction of the EMC.

$$\rho = \frac{1}{\sigma} = \frac{1}{\varepsilon'' \, \varepsilon_0 \, 2\,\pi\, f} = \frac{R_p A}{d} \tag{3}$$

The dissipation factor, or loss tangent of a medium, tan (δ) is defined as the ratio of the dielectric loss factor ε" to the dielectric permittivity έ (Equation 4).

$$\tan(\delta) = \frac{\varepsilon''}{\acute{\varepsilon}} \tag{4}$$

The changes in the dielectric properties of the resin can be correlated with the variations of chemical and rheological behavior of the epoxy resin during polymerization process [104], [145]. During polymerization of the thermoset resin in the transfer molding process, the resin undergoes different transitions. At the beginning of the process, when the epoxy resin pellets come into contact with the hot wall of the mold tool, the resin starts melting and liquidizes. In DEA measurements, the ionic conductivity indicates the ease of the movements of the ionic impurities in resin, thus directly correlated with the viscosity [126], [137]. For epoxy resins, chloride and sodium ions are considered to dominate the ionic conductivity since their concentration remains constant during the polymerization reaction [122], [146], [147]. Figure 2.9 shows the DEA curve during the polymerization reaction of EMC in transfer molding process. As seen in Figure 2.9, the moment, where the conductivity reaches its maximum matches with the moment where the viscosity has the lowest point [118], [148], [149].

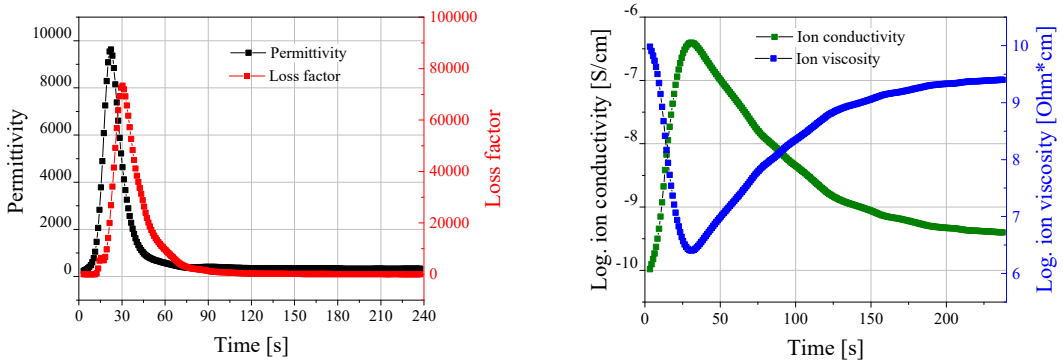

Figure 2.9: Permittivity and loss factor with respect to time (left), and logarithmic ion conductivity as well as logarithmic ion viscosity with respect to time (right)

Following the minimum viscosity, the resin polymerization continues, larger molecules are formed and another important stage, where significant transformations in the physical properties of the thermosetting polymer occur, is achieved, namely gelation. In gelation, the system changes its state and resin transforms from a liquid into a covalently cross-linked gel [150]. Gel point indicates the point that all monomers are attached to the network by at least one chemical bond, and three dimensional network is formed [96], [151]. Gel point is a critical point in polymer processing, since after epoxy resin reaches this point, the flowability of the resin is reduced dramatically. Large efforts have been done to define the gelation point by using the DEA method [122], [148], [152]–[155]. Maistros et al. defined the point for initiation of the gelation as the inflection point in the drop of the logarithmic ion conductivity [149]. Inflection point is defined as the time, where the cure reaction begins to slow down [156]. The gelation point in the DEA curve is described as a point of inflection which is $d^2(LIC)/dt^2=0$ where LIC is the logarithm of the ionic conductivity. Mcllhagger et al. correlated this defined onset of gelation point for composite materials from DEA measurements with gel point obtained from the dynamic mechanical analysis (DMA) measurements [122]. They have found that the gel point obtained in DEA with a point

of inflection is very close to the gel point determined with the DMA measurements, where the *tan (δ)* is equal to 1 is taken as the gel point. Slight variations between gel points obtained from two measurements were observed, which is attributed to the small variations in the temperature-time profile between the measurements. However, it should be pointed out that the definition of the gel point with the DEA is difficult to generalize for all chemical systems, since the experiments were based on specific epoxy systems, where the ionic conductivity was dominated by the species of that certain system. Thus, to meet a universal conclusion for identification of the complex phenomenon of gelation with DEA, more research is required [131], [150].

With the propagation of the curing reaction, 3D network of the polymer forms, cross linking degree increases, thus causing an increase in T_g [157]. T_g indicates the temperature required to change the molecules from glassy to rubbery state. The logarithmic ion viscosity curve is also found in a good correlation with the rate of change in T_g and DEA is taken as sensitive method to detect the changes in T_g [132], [138]. Another important point in polymerization reaction is vitrification. Vitrification is defined as the point where the polymer chains get closely packed, the network becomes tighter due to the cross-linking and there is no sufficient volume for the ionic motions in the structure [130], [158]. During vitrification, the system transforms from a gel into a glass, and vitrification ends when the T_g of the material reaches the isothermal cure temperature [122], [150].

According to the information given above, some crucial information about the polymerization reaction of the resin can be obtained in-situ from the DEA such as reaction onset, processing time of the resin, minimum ion viscosity, time at minimum ion viscosity, maximum ion viscosity, and the reaction rate. During the curing process, the ion viscosity of the polymers can increase in a range of several decades, thus data for ion viscosity is represented usually in a logarithmic scale [159]. The slope of the logarithmic ion viscosity versus time curve correlates with the reaction rate of curing. Higher temperature leads to a higher reaction rate, hence faster curing [152]. Moreover, the differences between the maximum and minimum viscosity can deliver information about the degree of cure of the thermoset material [160]. A typical DEA curve, which is taken in-situ during polymerization of the EMC during the transfer molding process, and the characteristic information, which can be derived from the DEA signal, are depicted in Figure 2.10.

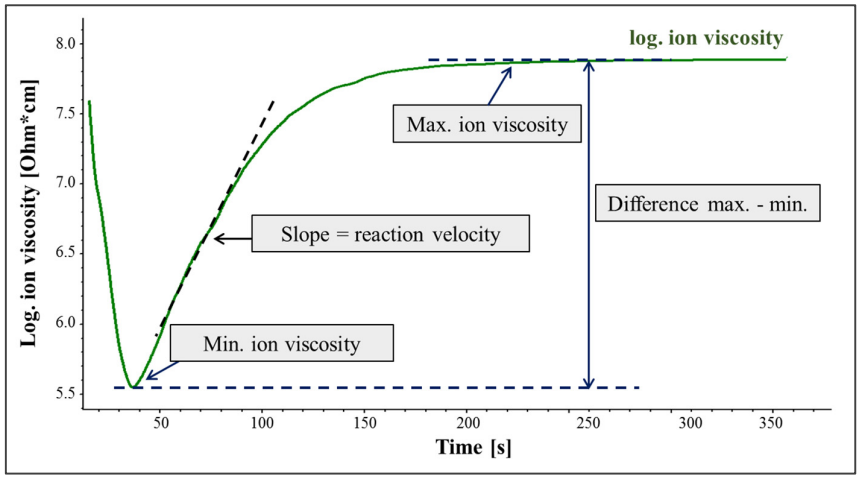

Figure 2.10: Ion viscosity with respect to curing time in transfer molding process and the important characteristic information derived from the DEA signal

There are different types of DEA sensors available in various configurations, which make them suitable for different applications such as monitoring the curing reaction for dental filling, composite materials for aircraft or military applications [122], [161], [162]. Some of the DEA sensor types are parallel-plate sensors, disposable one way sensors or implantable sensors. Disposable one way sensors and implantable sensors require one single surface with comb structures or interdigitated electrodes, whereas

the parallel-plate sensors must be implemented on both side of the tool. Disposable sensors have a comb electrode structure and they measure the penetration depth of the alternating electric field of the sensor which is the distance between the electrodes [130], [162]. Parallel plate sensors allow the measurement through bulk material, however, the dimensional change of the resin matrix during polymerization, which is typical for most of the resins, can cause some difficulties to keep the spacing between the electrodes. Thus, it can be difficult to maintain the calibration of the parallel-plates and this can lead to artifacts during measurement [139]. One of the key advantages of the comb electrodes over the parallel-plate configuration is that the calibration of the interdigitated electrodes is independent of the temperature and other changes, which leads to more reproducible measurements [139], [163]. Modern dielectric measurement setups, namely monotrode sensors, employ two interdigitated electrodes, which enable one sided measurement without employing two sensors [141]. With the monotrode sensor, it is possible to measure the dielectric constant of samples even for those which have a thickness of a few millimeters [159], [164], [165].

Therefore, with the help of the DEA sensors, detailed information about the molding compounds can be determined during the polymerization regarding any possible change in the rheological state of the EMC. Moreover, the actual cure state of the polymers during processing, the optimum molding cycle time for the required curing of the polymers can be detected online which can help to increase the productivity and molded part quality [86].

Due to such advantages, as already mentioned, DEA finds application in various processes such as dental application, composites manufacturing for aircraft industry or wind energy applications. Surprisingly, in spite of its numerous advantages in terms of process monitoring, there is only little work done on using the DEA for transfer molding process characterization in the field of electronic packages. One of the rare reports is provided by Chen et al. where DEA was used as an in-situ monitoring method to observe the cure state of the plastic encapsulated EMC in transfer molding process [166]. They implemented at six locations the reusable, monotrode DEA sensors with a diameter of 6 mm. The measurements were performed in a conventional single pot mold transfer molding process. Influence of the process parameters such as mold temperature, transfer pressure, preheat time on the ion viscosity of EMC were investigated with DEA. They conducted statistical analysis and selected full factorial analysis with three parameter sets in three different levels. The results showed that the minimum ion viscosity was strongly influenced especially by the mold temperature. With increasing mold temperature from 155 °C to 195 °C, the minimum ion viscosity decreased. On the other hand, transfer pressure and preheat time demonstrated very little effect on the minimum ion viscosity.

All in all, although not many work on the topic of implementing the DEA for transfer molding process analysis is published, it is possible to conclude that by given advantages DEA can be a suitable online monitoring method for in-situ cure monitoring of EMC in transfer molding process for encapsulation of electronic packages.

2.6 Statistical Analysis

In this section, methods of statistical analysis, also known as Design of Experiments (DoE), are introduced. In many technical areas, experiments are performed to examine the characteristics of process, and to improve and optimize the operations. DoE is a method to plan experiments and to analyze the results systematically [167]. The aim of a DoE is to obtain knowledge from experimental investigations and determine the correlations between input and output parameters with least possible effort, time and costs. Thus, for this work statistical analysis is applied to design experiments and to evaluate the results systematically as well as to describe the relationship between process parameters, material characteristics and package quality in a model. Hence, detailed description of the statistical analysis methods is given in this section. The major aspects on designing the experiments are highlighted. The essential steps to achieve a process model with the help of the statistical analysis are explained in detail.

Definition of Models in Statistical Analysis

The goal of statistical analysis is to establish models, which deliver the relationship between the input parameters and the output parameters. In Figure 2.11 a schematic description of a system for a process is represented with influencing quantities, target quantities and errors.

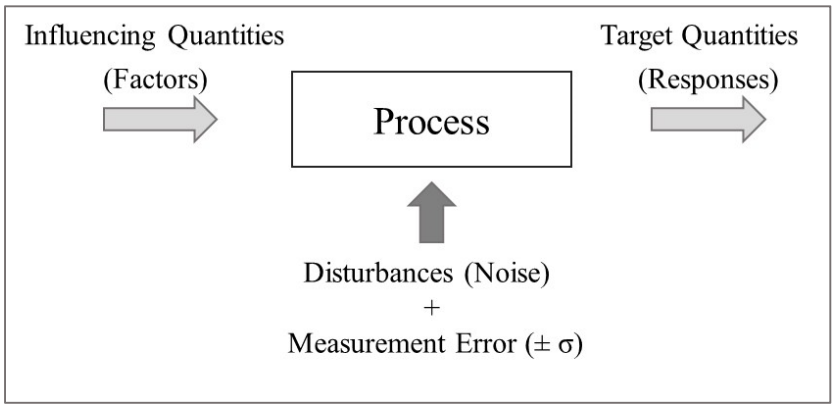

Figure 2.11: A schematic description of a system, adopted from [168]

As shown in Figure 2.11, the system involves the input parameters, which are the influencing quantities (factors), and the output parameters, which are the target quantities (responses). As an input in the system, the factors are chosen in which their variation affects the responses, hence they help to improve the performance of a process [167]. In almost all operations, there are known and unknown disturbance factors or noises, which influence the process [168], [169]. The disturbance factors cannot be easily controlled, thus they must be kept as constant as possible [170]. Therein, the aim is to determine the relationship between the input parameters and the target quantities, which can be quantified despite of disturbances in the system [168]. To determine the correlations between the influencing factors and target quantities and to describe the relationship mathematically in a model, regression analysis is used in statistical analysis. When the responses or the target quantities are denominated as y, the influencing factors are chosen as $x_1, x_2 \ldots x_p$ and the measurement error as well as the noises are considered together as errors, e, the relationship in a system between the influencing quantities and target quantities can be described in a model with a regression function as $y = f(x_1, x_2, \ldots x_p) + e$.

One of the most important steps to achieve a good model for this system is to list the influencing factors and the target quantities [170]. Definition of the system is very crucial in terms of obtaining a good correlation between the influencing factors and target quantities. The selection of the influencing and target quantities determines the success of the experiments, and thus the quality of the generated models. If many parameters are included into the system, the influences of the input parameters on the target quantities cannot be determined easily due to the participation of too many factors, which may prevent a clear correlation. On the other hand, if the system is kept too small and less factors are selected, some important factors may be neglected, thus the generated model cannot describe the correlations adequately due to the lack of important factors.

Selection of Target Quantities (Responses) and Influencing Quantities (Factors)

In many systems, the target quantities are the quality characteristics and the purpose is to improve them by adjusting the influencing input parameters and eventually to find an optimum for the system. However, to improve the target quantities, it is important that the target quantities are quantitatively measurable and in best case they are known to be influenced by the selected input parameters. Moreover, selection of too many target quantities or quality characteristics makes it difficult to define an optimum for a system.

By the selection of the influencing quantities, i.e. the factors in a DoE, it is important to ensure the reproducibility of the factors in the course of an experimental plan [169]. In an experimental analysis,

factors are varied in different levels to test their effects. Levels are the set or defined values for each factor [167], [169]. In an experimental plan, each factor should be varied at least in two levels to determine their respective influence on the responses [169]. When the factors are varied in two levels, the correlations can be described with a linear model. For some system, when quadratic influences and the interactions between the parameters are not significant, the linear model can describe the relationship between the influencing quantities and the target quantities adequately. However, when complex correlations between the parameters exist, such as the parameters have interactions with each other, the correlations between factors and responses cannot be described with a linear model thoroughly. At this point, quadratic models should be selected, which involve the interactions between the parameters and the quadratic influences of the parameters. To achieve quadratic models, the factors should be varied at least in three levels.

In addition to the number of levels, the distance between the set levels is also very crucial. The distance between the levels can strongly influence their impact on the responses (target quantities). When the distance between the levels for a factor is selected too small, only small influences of the corresponding factor can be observed on the target quantity. Hence, a higher number of experiments is required to examine some distinguished effects on the responses. Moreover, in a small distance between the set levels, influences of the factors on the responses are considered as chance due to some possible overlapping effects between the factors, so the clear effects cannot be detected [171]. On the contrary, the distance between the levels should not be selected too large either. If the distance between the levels is too large, some side effects can appear between the levels, which prevent determining the clear effects on the responses and decrease the model precision [171]. The large distance between the levels is recommended usually at the very early phase of the experiments, when the impacts of the factors on the responses are not known in order to get to know the system and to induce greater effects on the responses. However, it is also important to limit the levels in the realistic parameter range in order to assure the operability of a system. For this reason, it is recommended to prove with the help of the preliminary experiments, if the process operates with the planned parameter range [169].

Selection of Experimental Plan

In DoE, various experimental designs exist to set up an experimental plan, which can be selected depending on the system and the purpose. Based on the selected design, generally the correlations can be expressed either with a linear model or a quadratic model. With some experimental designs, only the main effects of factors can be investigated on the responses, whereas some other designs can deliver the impacts of the interactions between the factors on the responses as well. Interactions between two factors means that the effect of one factor depends on the set value of another factor [171]. In addition, there are some designs, where quadratic influences can be investigated as well. Table 2.1 summarizes some of the main experimental designs in DoE and the corresponding effects, which can be investigated with the respective design.

Table 2.1: Selection of the experimental design

Experimental design	**Investigated Effects**	**Mathematical Model**
Full factorial	Main effects, Interactions	Linear
Fractional Factorial	Main effects	Linear
Placket-Burman	Main effects	Linear
D-optimal	Main effects, Interactions, Quadratic	Non-linear
Central composite	Main effects, Interactions, Quadratic	Non-linear
3^K	Main effects, Interactions, Quadratic	Non-linear

With the full factorial design, the main effects and influence of the interactions between the parameters can be studied. To generate the experimental design, the factors are varied in two levels and the design includes all possible combinations between the factors. With K factors, 2^K single experiments are

required for this design. The drawback of the full factorial design is that if the investigated number of factors is high, the number of experiments can raise dramatically. The schematic representation of the experimental designs is shown in Figure 2.12, where the experimental design is depicted in a building block. The building block represents the experiment zone (room) for three factors, where each factor is represented through one dimension and corners show the factor combinations. As shown in Figure 2.12, in full factorial design all the corner points are covered. If necessary, some center-point experiments can be also supplemented to the full factorial design.

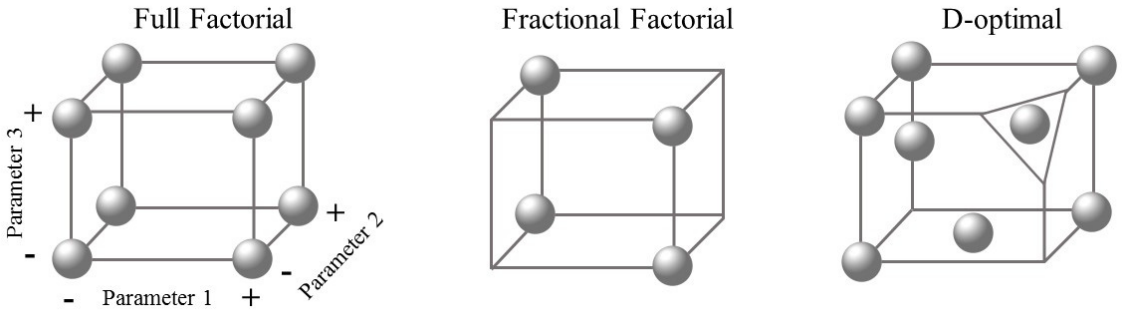

Figure 2.12: Experimental design illustrated schematically for three factors, full factorial design (left), fractional factorial (middle), and the D-optimal design (right)

Statistical experimental designs are orthogonal and balanced. In this sense, orthogonal means that the columns in the experimental matrix in the design are independent and balanced means that all factors are tested with the same repetitions in the design [170].

When a new problem occurs in the process and an expanded process knowledge does not exist to solve the problem, usually many factors are studied to understand the main influencing factors on the target quantities. In that point, it is mainly important to know which factors are the major influencing factors, and how those factors are affecting the target quantities [171]. In such cases, screening experiments can be used. Screening experiments are usually recommended when eight or even more factors are examined in order to reduce the number of experiments. For the screenings experiments Plackett-Burman or fractional factorial designs can be used to obtain required information with a least possible number of experiments. With those designs, only the main factors are determined and interaction between the factors is not considered [168]. The correlations between the factors and the responses can be described only with a linear model. As depicted in Figure 2.12, fractional design does not consider all corner points. The design selects only a fraction of full factorial design, thus reducing the number of experimental runs.

One of the most straightforward methods to evaluate the effect of each factor on the responses is to use one factor at a time (OFAT) design [171]. In OFAT design, only one factor is varied while the other factors are kept constant. Thus, the impact of each factor can be easily detected on the responses [171]. However, one of the disadvantages of the design is that the number of required experiments can increase rapidly with increasing factors [171]. In addition, with this plan the interactions between the parameter cannot be identified and the optimum for a process can be found only by chance [172].

For non-linear dependency of the target quantities, the factors should be varied at least in three levels. As shown in Table 2.1, DoE offers some experimental designs, which help to achieve quadratic models with reduced number of experiments. 3^K, central composite design or D-optimal design are some of the known experimental designs to generate quadratic models.

In 3^K experimental design all corner points of the building block, edges and side middle points as well as the middle points of the building blocks are covered. The drawback of the 3^K design is with increasing number of factors, the number of experiments in the experimental design can increase enormously. For instance, for four factors 3^4 equally 81 experimental points are required for this design.

Another experimental design for quadratic models is the central composite design. This design is constructed in three parts, from a complete factorial plan (corners in building block, the corner points of a star and one central point). The design is usually used if the number of the required experiments does not increase with increasing factors [169].
An alternative experimental design for the quadratic model is the D-optimal design. The "D" is the designation for determinant. Determinant includes the total amount of information for the design matrix, which is formed from all factors and the factor levels [173]. D-optimal design is computer aided design, and it delivers the best parameter set considering all possible combinations to cover the experimental room with less possible number of experiments [174]. The experimental design of D-optimal method is depicted schematically in Figure 2.12. The advantage of the D-optimal plan is that the experimental plan can be adapted depending on the focus of the system. This means that in a conventional experimental design, all the factors should vary in the same level whereas in D-optimal design the levels for factors can be selected freely. For D-optimal design, an algorithm method is used, the desired combinations of the factors are designed in the experimental plan selectively and unnecessary combinations are taken out from the experimental plan so that the required number of experiments can be reduced. The selected experimental points in the design are distributed into the experiment zone in such a way that is adequate to generate a quadratic model. To illustrate the remarkable difference between the conventional full factorial design and D-optimal design, the necessary number of experimental points for both designs are shown in Figure 2.13 with the same number of factors, namely with two factors X and Y and the target quantity Z.

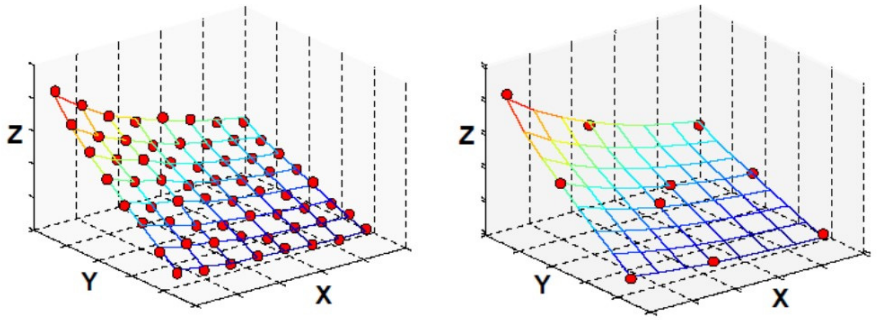

Figure 2.13: Comparison between full factorial design (left), and D-optimal design (right) with two factors X, Y and a target quantity Z [175]

As seen apparently from Figure 2.13, D-optimal model-based design can cover the investigated room for the experimental plan with a reduced number of experiments compared to the conventional approach of full factorial plan. Another advantage of the D-optimal experimental design is that it is possible to consider the experimental results, which already exist for a given system. The results from previous experiments can be included into the model and be evaluated together. Moreover, after all necessary experiments are included in the design, and the experimental plan can be broadened by supplementing new single experimental points or by supplementing new factors into the design [171]. On the other hand, a drawback of the D-optimal design is that due to its complex algorithms, D-optimal designs can only be designed with a suitable software.
After obtaining the experimental results with a selected design, the regression models can be generated and the fitting quality of the regression models can be evaluated. Fitting quality determines how good the model fits to real data. One of the most important terms to describe the model quality is the "R^2", which is the coefficient of determination. This term indicates the determination quality of the model. In other words, this quantity describes the proportion of the variability in the responses. R^2 varies between 0 and 1 and higher values of R^2 indicate that the model follows the responses very closely. One important aspect regarding R^2 is, that when extra terms are added to the model, R^2 always increases, although the supplemented terms do not necessarily improve the model quality. Thus, the increase in the R^2 does not

inevitably mean the improvement in the model quality. For this reason, it is more consistent to use the modified version of the R^2 namely, R^2_{adj}, for an estimation of the model quality. R^2_{adj} is an adjusted version of R^2 in regard of the terms, which means that R^2_{adj} does not increase by an addition of the new terms into the model, unless the added terms improve the model quality. In other words, R^2_{adj} increases only if the new added term improves the model more than it would be expected by chance. Therefore, R^2_{adj} delivers more steady results in terms of estimating the model quality. As a matter of fact, there are also the errors in the model. The errors in other words the residuals in the regression function give an estimation of the standard deviation in a model due to the measurement error or disturbances in the process, which are also illustrated in Figure 2.11. As addressed earlier, regression analysis is applied to generate a mathematical model based on the selected design, which estimates the relationship between the factors and the responses. It is important to emphasize that the models can only express the correlations in the defined process window (experiment zone) and the extrapolation outside of the process window is risky since the system behavior can change outside of the system borders drastically [169], [171].

After generation of the regression models, optimization for the target quantities can be done. In the optimization step target quantity or the quality characteristics can be minimized, maximized, or a target value can be defined [167], [176]. The target quantity gets an optimum value at the end of the optimization process. For statistical reasons, usually the average value is considered for an optimum value of the target quantities [171]. In most of the systems, there is more than one target quantity, which should be optimized at the same time. Moreover, the parameter adjustment, which is the optimum for one target quantity, is not always an optimum for the other quantity. Based on the quantitative knowledge of the dependency of all target quantities on the factor and with the help of the generated mathematical model, a compromise can be found, which delivers optimum values for more than one target quantity at the same time [171].

Consequently, by considering the aforementioned designs, if the objective is to generate a quadratic model, which defines the correlation between the input parameters and the target quantities mathematically and optimize the system, one can follow three steps to achieve this goal: screening, modeling and optimization [177]. The number of steps can be decreased depending on the knowledge on the system and if enough knowledge on the system is available, one can reduce the number of the steps.

2.7 Outline of the Dissertation

Based on the given overview in this chapter, it is shown that the quality of the molded packages heavily depends on the process parameters of transfer molding process, characteristics of EMC, package assembly inside and the design parameters. It is indicated that although transfer molding is a common process for producing electronic packages, parameter settings of a transfer molding process are mostly done in a trial and error manner and defining the optimum process parameters is laborious. Many works are represented in this section, which were done to optimize the process parameters of transfer molding process, however, no systematic approach has been established so far to obtain optimum process parameters and to establish a process model, which describes the correlation between the process parameters and the quality of the package. Additionally, it is shown that the material characteristics have a drastic influence on the quality of the molded packages. The viscosity and cure behavior of EMC are of prime importance for understanding the influence of the material on the package quality. The reactive nature of the epoxy resins can be influenced by prolonged storage duration, moisture content and the possible variations from batch to batch. Such impacts may cause alterations in the characteristics of the EMC such as moldability and change in the flow behavior of the material in the cavity. However, no systematic investigations are conducted to understand the influence of the variations in the cure behavior of the EMC prior to molding process on the quality characteristics. Additionally, the material investigations are performed usually in laboratory conditions with conventional methods, but it is shown that online monitoring methods in the transfer molding process are necessary to gather some

consequential information about the cure behavior of the EMC directly from the cavity to diminish the defects. In literature there are not sufficient studies available on the investigation of the mentioned variations in the cure behavior of EMC directly in transfer molding process to date. Due to this limited knowledge of the process and the impact of EMC characteristics on the package quality, several defects may occur in the package during the encapsulation of the semiconductor devices such as voids, wire sweep and delamination, which may cause total package failure at the end. Therein, understanding the influence of the material characteristics of the EMC and the process parameters on the package quality is essential. In this context, an online monitoring technique can deliver consequential information about the cure reaction behavior of the EMC to yield a stable package quality in transfer molding process.

Considering the aforementioned aspects, an established correlation between process parameters, material characteristics and the package quality can improve process understanding and diminish the failure mechanisms in the molded package, thus reducing the failure costs. Therefore, this work aims to give a conceptual understanding on the influence of the process parameters and the impact of material characteristics of EMC on the package quality in transfer molding process in order to reduce the failure costs in the molded packages. In addition, in this work an approach is evaluated to establish models, which deliver the correlation between the process parameters, material characteristics and the package quality. With established process models, the optimum process parameters of the transfer molding process can be defined. Three quality characteristics are investigated in this work, namely void formation, warpage and wire sweep in the molded packages. According to quality criteria given in Section 2.2, the target of this work is to reduce the wire sweep below 4 % in the molded package, which is the half of the distance between the wire bonds attached on the layout (More information about the wire bonds on the layout will be given in Chapter 4). As void formation is one of the major concerns in terms of the reliability aspect, the aim of this work is to obtain void-free packages. However, it is important to mention that the smallest detectable void diameter is 100 µm with a corresponding area of approximately 0.009 mm^2 for the selected package geometry with an applied transducer for the SAM analysis, thus the voids with a diameter smaller than 100 µm cannot be detected (Details on the SAM analysis will be given in Section 3.4). In addition, to provide good thermal interconnection between the power module and the heat sink, as a warpage quality criterion for the used package, warpage bigger than 100 µm is considered critical in terms of an effective thermal management. Most important, for all quality features studied in this work the major condition for the quality features is that the selected quality characteristics, namely void formation, wire sweep and warpage should be influenced by the variations in the process parameters. As this work aims to generate the models, which can be used to estimate the quality characteristic as a function of the process parameters, the selected quality characteristics should be influenced by the variation in the process parameters. Thus, to analyze the influences of the process parameters on the quality features, extensive process analysis is carried out in this work. DoE methods are used to design and evaluate the experiments and in addition to the OFAT design, due to the aforementioned advantages (Section 2.6), D-optimal design is selected to establish the process model and regression analysis is performed. In addition to the process model, the material model is also generated, which delivers the correlation between the variations in the material characteristics of EMC in terms of storage duration, humidity and batch to batch variations and the package quality. Due to the given advantages, DEA method is selected as an online monitoring of the material characteristic in the transfer molding process to investigate the variations in the properties of the EMC. Additionally, temperature and pressure sensors are implemented in transfer molding process to control the process. As indicated earlier in Section 2.1, manufacturing of electronic packages requires different assembly processes. However, it is important to emphasize that this work concentrates on the transfer molding process itself and the variations which are originated by the transfer molding process. The influences of other assembly processes on the package quality are not the scope of this work. Figure 2.14 displays the schematic representation of sequence of the assembly processes employed in this work with a focus on the transfer molding process.

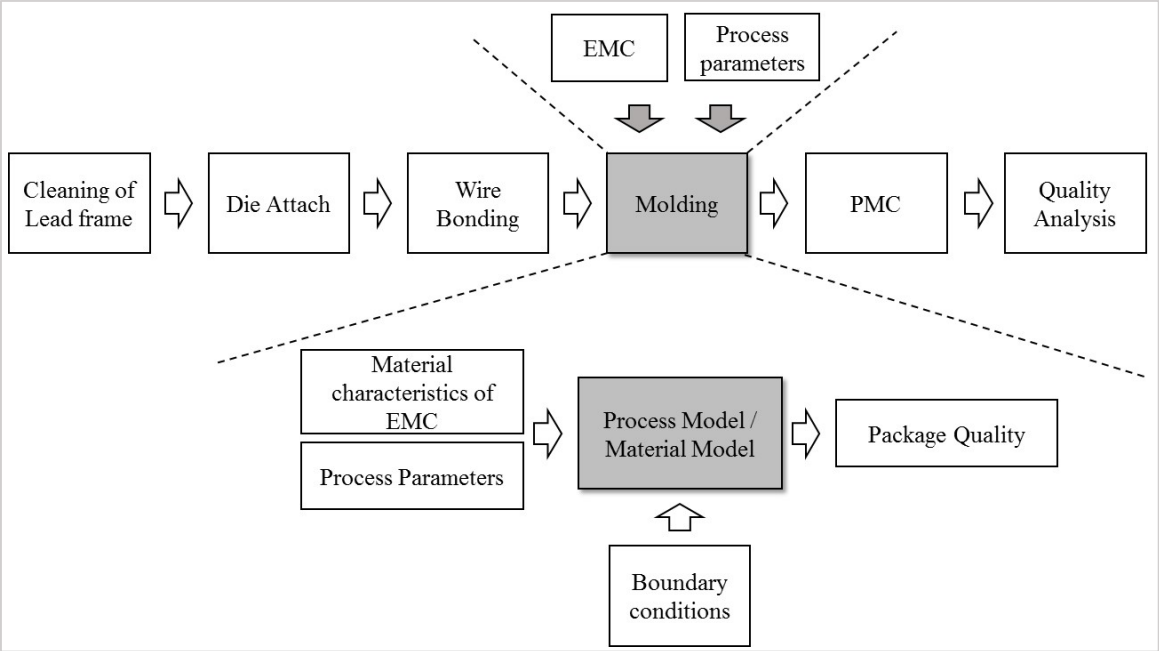

Figure 2.14: Schematic illustration of the processes employed in this work, and the transfer molding process as a focus of this work

As shown in Figure 2.14, to construct and evaluate the demonstrator in this work, many different assembly processes are employed. However, the focus of this work is on the transfer molding process and parameters for the rest of the assembly processes are kept constant after obtaining a suitable parameter set for a qualified assembly. As illustrated also in Figure 2.14, the aim of this work is to describe the relationship between the process parameters, material characteristics and the package quality with the help of the process and material models. The objective of the process model is to describe the relationship between the process parameters and the package quality. With the help of this model, it should be also possible to predict the quality characteristics. Additionally, the model represents a systematic approach to identify the process parameters which enable optimal package quality. The goal of the material model is to describe the relationship between the material characteristics and the package. With the help of the model, it is possible to describe the impact of preconditioned EMCs on package quality. Additionally, the model represents a systematic approach to estimate the processing limitations of EMCs which are subjected to the different preconditioning (storage duration and humidity) in order to achieve a predefined package quality. Moreover, the validation of both models is performed to determine the possibility and the limitations of the models with other EMC. Therefore, these systematic approaches described above which are used to generate these models can also be applied for other molded packages and for different EMCs to describe the relationships between the input and output parameters and to generate different models for such systems. Accordingly, in the following an outline of this thesis is briefly explained.

Chapter 3 provides a brief overview on the materials and instrumentation used in this work. The selection of the sensors for process control and the positions of the DEA sensors in the cavity of the tool for in-situ cure monitoring in transfer molding process are introduced.

Chapter 4 presents the assembly steps, which are used to prepare the demonstrator in order to study the package quality. The important features of the preparation steps from cleaning the lead frame until wire bonding process are explained.

Chapter 5 is dedicated to the preliminary experiments and their results, where the basis characterization of the process and material are performed. Preliminary experiments are conducted to determine the dominant process parameters, which have an impact on the quality characteristics and to examine the package qualities, which are strongly influenced by the process parameters. In addition, the main

characterization of the EMC and the impact of storage duration, humidity and the batch variations on the cure behavior of the EMC are examined with thermal and mechanical analysis methods. Furthermore, the suitability of the DEA method for online monitoring in transfer molding process is assessed in terms of observing possible variations in the cure behavior of EMC due to prolonged storage duration, humidity and batch variations.

Main experiments of this work and their results are shown in Chapter 6. The influence of the process parameters in D-optimal design on the package quality are discussed. The sensor signals and the process stability are evaluated. Furthermore, the influence of the variations in the EMC characteristics originating from prolonged storage duration, humidity and batch variations on the package quality are analyzed.

Chapter 7 involves the evaluation of the results of main experiments with the statistical analysis. Regression analysis is applied to evaluate the results and the important results of regression analysis are introduced. Moreover, a mathematical process model is established which expresses the correlation between the process parameters and the package quality and estimates the quality characteristics of the package. Optimum process parameters of the transfer molding process are determined. Furthermore, the estimation quality of the process model is assessed. In addition to the process model, a material model is established, which expresses the influence of the variations of the material characteristics on the quality characteristics.

The established process model and the material model are verified with validations experiments. The applied experimental design and the results of validation experiments are given in Chapter 8. Based on the comparison between the predicted quality characteristics given by the process model and the results of validation experiments, the prediction quality of the process model is assessed. Additionally, to determine boundary conditions of the established models, further experiments with another molding compound, which has substantially different material properties, are conducted. The limitations and the possibilities of the process and the material models are discussed.

Chapter 9 summarizes the main findings from the conducted research work. Conclusions are drawn and recommendations for further work are proposed.

3 Materials and Instrumentation

In this chapter an overview of the materials and the instrumentation employed in this work is given. The first part of the chapter focuses on the properties of the EMC and transfer molding processes which are used to produce the specimens of EMC. The properties of the selected EMCs as well as the lead frame are given in Section 3.1. Online monitoring of the transfer molding process is one of the important aspects investigated in this work. To accomplish this aspect, several temperature and pressure sensors are implemented into the transfer molding tools to gain more information about the process parameters in the cavity and filling behavior of the EMC. The selected sensor types for this purpose are described in detail in Section 3.2. The properties of EMC have significant impact on the quality of the molded packages. Hence, monitoring the polymerization reaction of EMC during molding process can deliver crucial information, which can be correlated with the final package quality. In this manner, DEA is chosen as an online monitoring method to observe the curing reaction of EMC in molding process. The characteristic information about the cure reaction of the EMC, which can be determined in-situ with DEA is described extensively in Section 3.2.3. To characterize the EMC, and to correlate the information about the cure reaction of EMC obtained from DEA, several characterization tools such as rotational rheometer, DSC, squeeze flow rheometer and DMA are employed in this work. Information about the corresponding testing equipment is provided in Section 3.3. Due to the ineligible process conditions and poor material characteristics several defects such as void formation, wire sweep and warpage can occur in the molded packages. The methods, which are employed to analyze the defects in the molded packages, are introduced in Section 3.4. The important features on the analysis of void formation, warpage and wire sweep are discussed.

3.1 Materials

In this section the properties of the two selected EMCs and the lead frame are given in Section 3.1.1 and in Section 3.1.2 respectively.

3.1.1 Epoxy Molding Compounds

As an encapsulation material, highly filled EMC is used. An ash test is applied according to the ISO 3451-1 to determine the filler content in the EMC in which the filler content is calculated by decomposing the EMC in the furnace at 600 °C under air and subsequently by weighing the remaining material, which are the silica filler particles. The filler content of EMC is found to be approx. 83 % by weight of molding compound, where the filler particle has around 75 µm cut off size as a datasheet value. Formulations of the EMC are mostly considered as a black box, since the supplier keeps the information about the chemical composition of the EMC strictly confidential. Nevertheless, some information can be derived from the material datasheet about the EMC. EMC used in this work is specified as phenol novolac type epoxy resin, which is produced by polyaddition reaction as typical for the cure reaction of the epoxy resins. Based on the information and the chemical substances given in material datasheet, it is assumed that the structure of resin system of the EMC is formulated by composing different types of epoxies such as multiaromatic and multifunctional epoxy resins. As a hardener phenol novolac resin is used for the curing reaction. Schematic of chemical structures of multiaromatic, multifunctional epoxy resins and phenol novolac are illustrated in Figure 3.1.

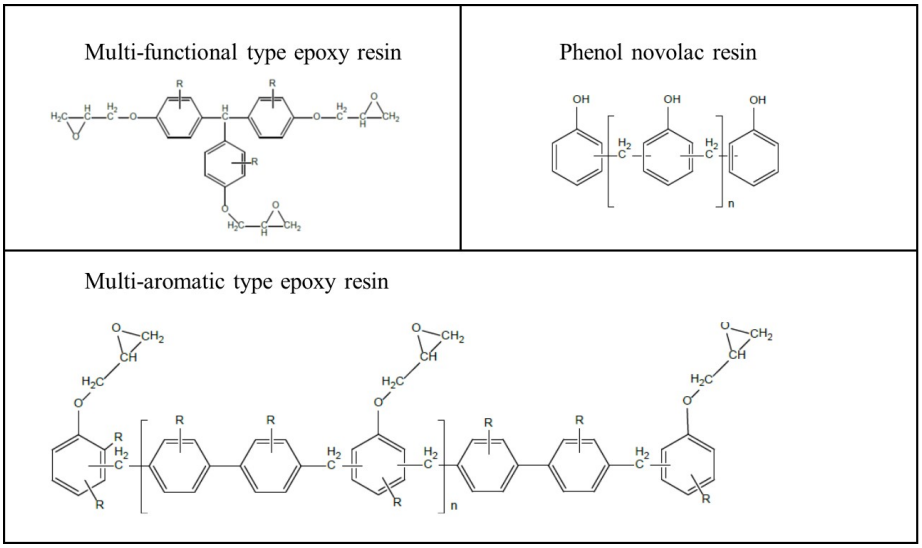

Figure 3.1: Schematic of chemical structures of multi-functional, multi-aromatic epoxy resins, and phenol novolac as a hardener for the curing reaction of EMC

For the validation of process and material models, a second EMC is selected, which is purchased from a different supplier. To prevent any confusion in nomenclature between selected EMCs, main EMC used in this work is designated simply as EMC 1 and the second EMC, which is only used for the validation experiments (Chapter 8) is marked as EMC 2. Although both EMCs are employed for encapsulation purposes, which requires generally having similar properties in terms of moldability, the chemical formulations of different suppliers are usually different. The resin structure of EMC 2 contains only multifunctional resin system and phenol resins. The material properties of EMC 1 and EMC 2 are summarized in Table 3.1.

Table 3.1: Material Properties of EMC 1 and EMC 2 (According to material datasheets)

Properties	**EMC 1**	**EMC 2**
Filler type	Silica spherical	Silica spherical
Filler cutoff size (µm)	75	75
Max. filler content (%)	82.9	83.5
Spiral flow (cm)	104	73
Gelation time (s)	40	46
Melt viscosity (Pas.)	16	16.3
Hot hardness (Shore D)	81	85
Specific gravity / Density (g/cm^3)	1.93	1.88
Flexural strength (MPa) at RT	95	136
Flexural modulus (GPa)	17	16
Glass transition temp (°C)	185	192
CTE α1 (ppm/C)	12	11
CTE α2 (ppm/C)	44	44
Post mold cure condition	180 °C x 4 h	180 °C x 4 h

Due to its different chemical formulation, EMC 2 shows also different flow behavior. Differences in the viscosity behaviors between EMC 1 and EMC 2 are evaluated with DEA at 175 °C and are shown in Figure 3.2.

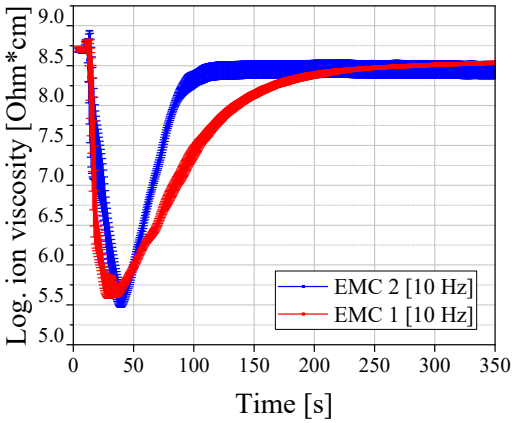

Figure 3.2: Logarithmic ion viscosities of EMC 1 and EMC 2 measured with DEA at 175 °C

The detailed description of the interpretation of the DEA signal will be given in Section 3.2.3, nonetheless some elementary points in terms of comparison of viscosity behaviors of two EMCs can be discussed here. As seen from Figure 3.2, which illustrates the viscosity behavior of EMCs versus time, the cure reaction behavior of the two EMCs is quite different. The propagation of the cure reaction of EMC 2 is faster compared to EMC 1, which can be identified from the slope of the curves. The minimum ion viscosities of the mold compounds are also differentiating. At the end of 350 s, both molding compounds arrive the same maximum level of ion viscosity. However, EMC 2 achieves this level much faster in comparison to EMC 1. Due to such significant differences in the flow behavior, EMC 2 is seen as a suitable material for the validation of process and material models.

As already explained in Section 2.4, EMCs are usually delivered in pellet form, which contains resin and hardener together. To prevent any undesired chemical reaction between the resin and hardener prior to the molding process, the pellets are usually stored at -20 °C in refrigerator. Before each measurement, the pellets are firstly thawed at ambient temperature for 1 hour in a desiccator so the temperature of EMC pellets reaches room temperature. According to the requirements of the transfer molding machines, pellets with a diameter of 14 mm with a weight of 6.5 g are used in this work. Standard deviation of the pellet weight is calculated by measuring 100 pellets and is ± 0.04 g.

3.1.2 Lead Frame

A copper based alloy lead frame with a thickness of 1 mm is used as a substrate to provide mechanical support to the components and the wire bonds. The chemical composition of lead frame is shown in Table 3.2.

Table 3.2: Chemical composition of copper based lead frame (According to the material datasheet)

Composition of lead frame	%
Cu	≥ 99.95 %
P	≈ 0.003 %

The dimensions of the lead frame and the tolerances of corresponding dimensions which are averaged out of 50 lead frames are illustrated in Figure 3.3.

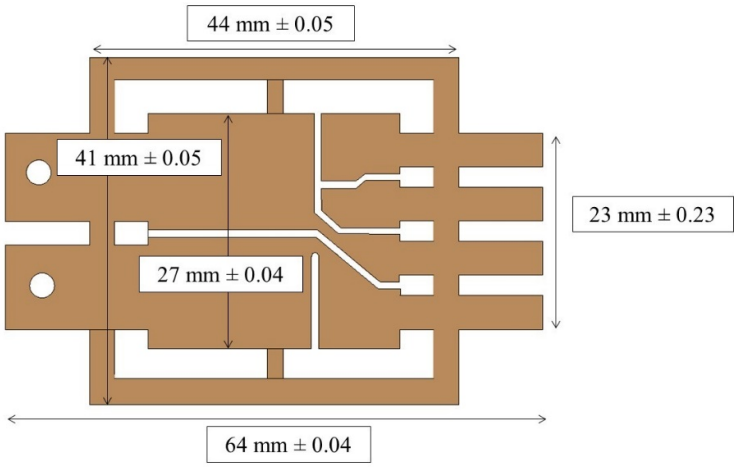

Figure 3.3: Design and dimensions of lead frame with corresponding tolerances

3.2 Transfer Molding Process and Online Monitoring Methods

The main process, namely transfer molding is performed by using two different molding machines and tools to produce different types of specimens in this work: One is to produce sample bars for the thermal and mechanical measurements and the other is to encapsulate the demonstrator to evaluate the quality characteristics such as wire sweep and voiding. In each molding machine, additional sensors are mounted into the tool to monitor the process parameters and to ensure the process stability. The dimensions and type of sensors selected for this purpose are introduced in Section 3.2.1 and 3.2.2. In addition, to observe the material characteristics of EMC in the cavity during the molding process, DEA is employed. For this reason, DEA sensors, more precisely monotrode sensors, are integrated in both molding tools in the two different machines. The DEA sensors and typical signals obtained from DEA sensors with its main characteristics are explained in more detailed in Section 3.2.3.

3.2.1 Molding Machine for Encapsulation of Demonstrator with Integrated Sensors

Lauffer transfer molding machine LHMS 28 with a clamping force of max. 28 kN is used to encapsulate the demonstrator. Transfer molding machine with lower and upper halves of the tool are depicted in Figure 3.4. The layout of the demonstrator will be described in detail in Section 4.1.

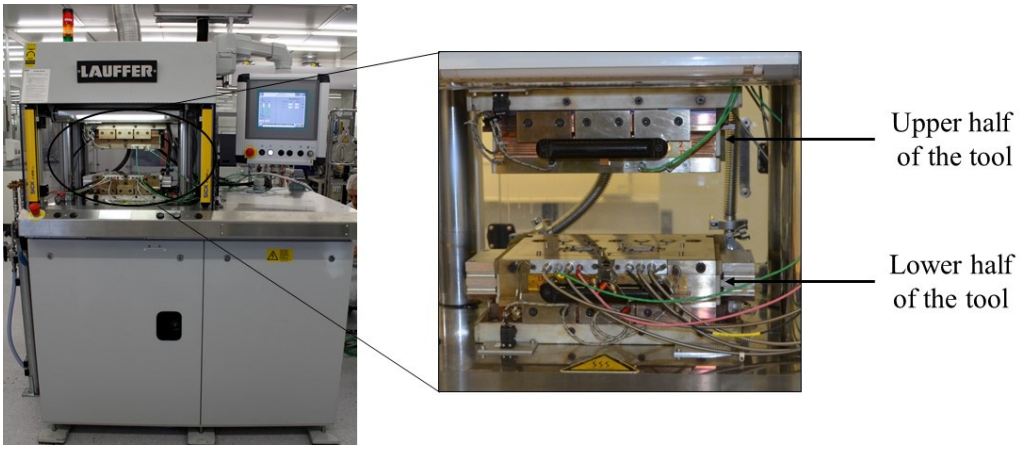

Figure 3.4: Transfer molding press LHMS 28 (left), upper and lower half of the tool (right)

The tool has two cavities and four plungers. Each cavity volume can be filled with two EMC pellets. A vacuum system is integrated into the tool to prevent the air entrapments in the package and to obtain homogeneously filled mold packages. The schematic of the mold form used in this transfer molding press is demonstrated in Figure 3.5.

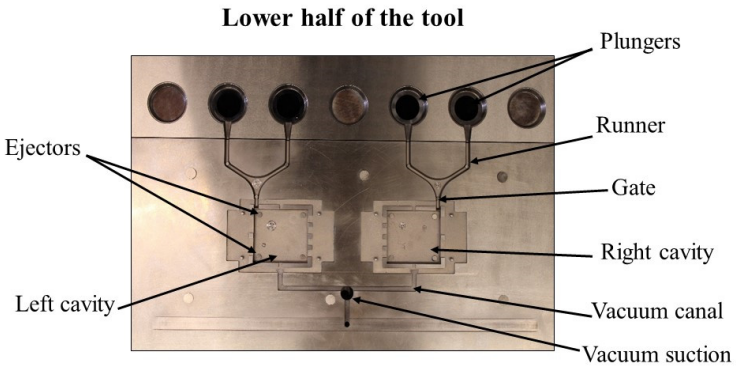

Figure 3.5: Mold tool used to encapsulate the demonstrator in transfer molding machine

The molding process includes several steps, which are demonstrated sequentially in Figure 3.6. The step 1 illustrates the pots and cavities at starting position of the molding. As a beginning of the mold process, first the lead frame based demonstrator, which contains the assembled dummy chips and wire bonds, is placed in the mold tool and preheated for 45 s before the cycle time starts in order to enhance the adhesion between the EMC and the lead frame as depicted in step 2. As a next step, the EMC pellets are brought into the pots (step 3) with a special carrier for better handling, which assists to put the EMC pellets at the same time into the pots to avoid any unequal preheating time in pots. Subsequently, the tool is closed and the clamp pressure is applied to provide a tight contact between two halves of the tool (step 4). After the closing of the tool, the desired preheat time of EMC follows. When the set preheat time is over, the plungers move forward, and with the help of the applied transfer pressure the now liquid EMC is injected into the cavities. After the in-mold cure cycle is finished, the molded packages are ejected as shown in step 5 with the help of the ejectors. Finally, the packages are fully encapsulated as illustrated in step 6. As it can be understood from the aforementioned steps, some process parameters such as preheat time, transfer speed of the plungers, clamping pressure, molding temperature, holding pressure and time are major relevant process parameters of transfer molding process for a successful encapsulation of the packages.

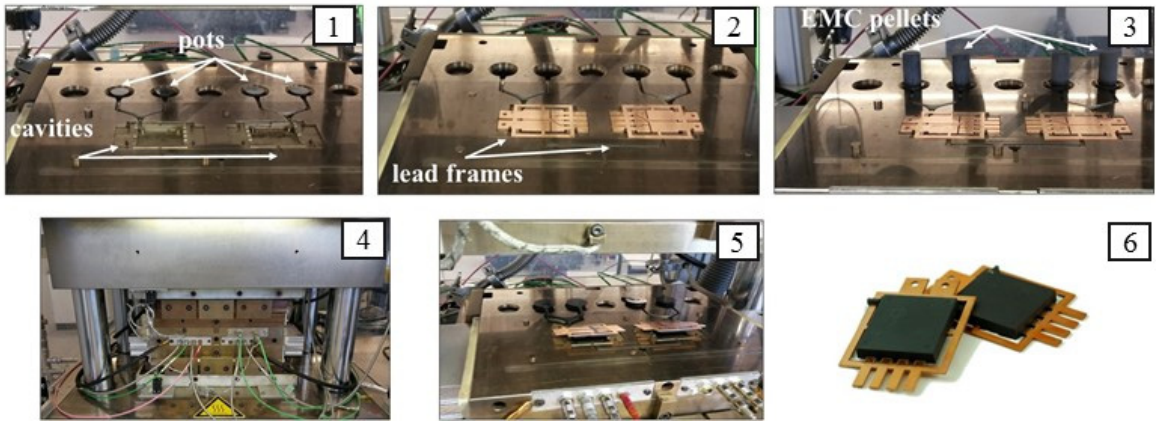

Figure 3.6: Process steps of the transfer molding for encapsulation of the semiconductor packages, mold tool with cavities and pots (1), lead frames are placed in the cavities of heated mold (2), EMC pellets are brought to the pots (3), tool is closed for injection of EMC and in-mold cure (4), ejection of the encapsulated lead frames after cycle time is over (5), encapsulated electronic packages after the molding process (6)

The filling behavior of the EMC during the molding process can be observed with short-shots in which the cycle time is interrupted and the final position of the plunger is set in different values prior to complete filling. In this way, the flow front of the EMC can be observed in different filling positions in the cavity. Figure 3.7 shows the short-shot images, which demonstrate the filling behavior of the EMC into the cavity from the beginning of the filling until the complete filling of the cavity.

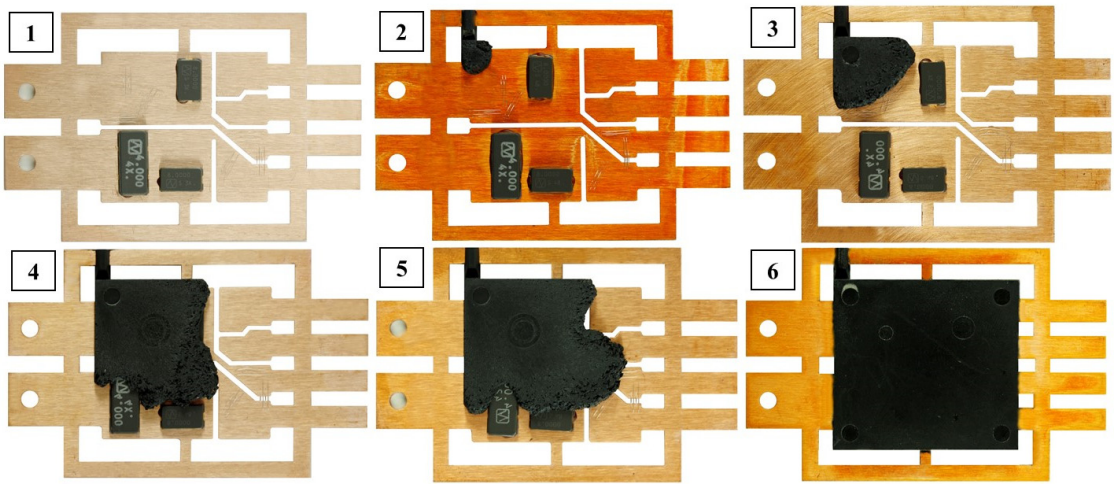

Figure 3.7: Short-shot images demonstrate flow front of the EMC during the cavity filling

To monitor the process parameters and to ensure stable temperature and pressure profile in the tool cavities throughout the process, in total eight temperature and pressure sensors are implemented into the cavities. Except one temperature sensor from Priamus System Technologies AG, all temperature and pressure sensors are purchased from Kistler Instrumente GmbH. The sensors are mounted at different positions in the cavities. In addition, two DEA Sensors are implemented in runner areas of two cavities. The positions of the sensors are shown in Figure 3.8. The types of the sensors implemented into the tool with corresponding diameters and the positions are illustrated in Table 3.3.

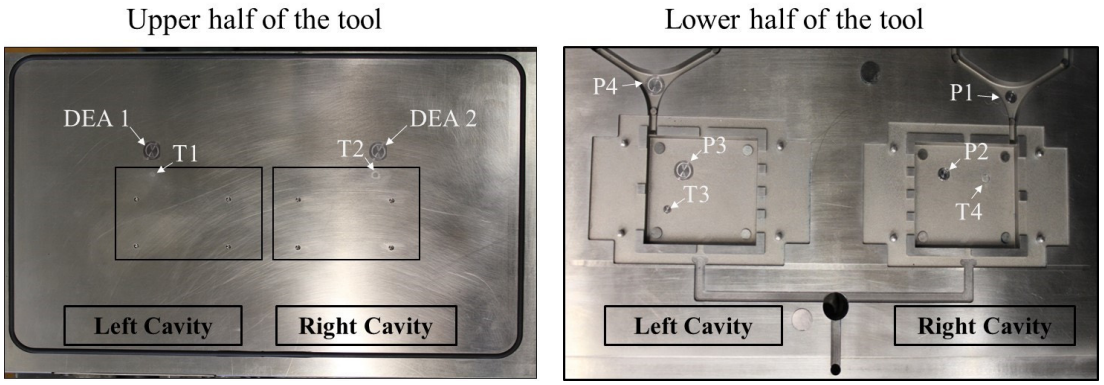

Figure 3.8: Mounted sensors to the upper half of the tool (left) and to lower half of the tool (right)

Table 3.3: Types, diameters and positions of the sensors implemented in the tool cavities in transfer molding machine

Description	Sensor	Type	Diameter	Position
T1	Temperature	Kistler 6195B	2.5 mm	Upper half of the tool – left cavity
T2	Temperature	Kistler 6195B	2.5 mm	Upper half of the tool – right cavity
DEA 1	Dielectric	Netzsch Monotrode 4/3RC	6 mm	Upper half of the tool – left cavity
DEA 2	Dielectric	Netzsch Monotrode 4/3RC	6 mm	Upper half of the tool – right cavity
P1	Pressure (diaphragm sensor)	Kistler M5 SKB	4 mm	Lower half of the tool – right cavity
P2	Pressure (diaphragm sensor)	Kistler M5 SKB	4 mm	Lower half of the tool – right cavity
P3	Pressure (diaphragm sensor)	Kistler 6163AA	6 mm	Lower half of the tool – left cavity
P4	Pressure (diaphragm sensor)	Kistler 6162AA	6 mm	Lower half of the tool – left cavity
T3	Temperature	Kistler 6195B	2.5 mm	Lower half of the tool – left cavity
T4	Temperature	Priamus 4014A0.2-101	2.5 mm	Lower half of the tool – left cavity (Implemented under the cavity surface)

On the lower half of the tool, three temperature sensors and four pressure sensors are mounted in cavities as well as at the gates. As seen in Table 3.3, different types of pressure sensors are chosen, which also have different measurement sensitivities, so that the suitable sensors can be tested and identified providing the largest amount of information with accuracy about the cavity filling behavior of the EMC. Two pressure sensors are located at the same positions in the left and in the right cavity on the lower half of the tool, opposite to the temperature sensors to ascertain possible pressure differences. As temperature sensors, mostly Type K thermocouples are used in this work apart from one Type N temperature sensor. On the upper half of the tool, two temperature sensors are implemented, where one temperature sensor is located in the left cavity and another temperature sensor is located in the right cavity. Two temperature sensors are mounted at the same position in two cavities to detect the temperature difference between the cavities. Typical signals obtained from different temperature and pressure sensors during the mold filling process are shown in Figure 3.9.

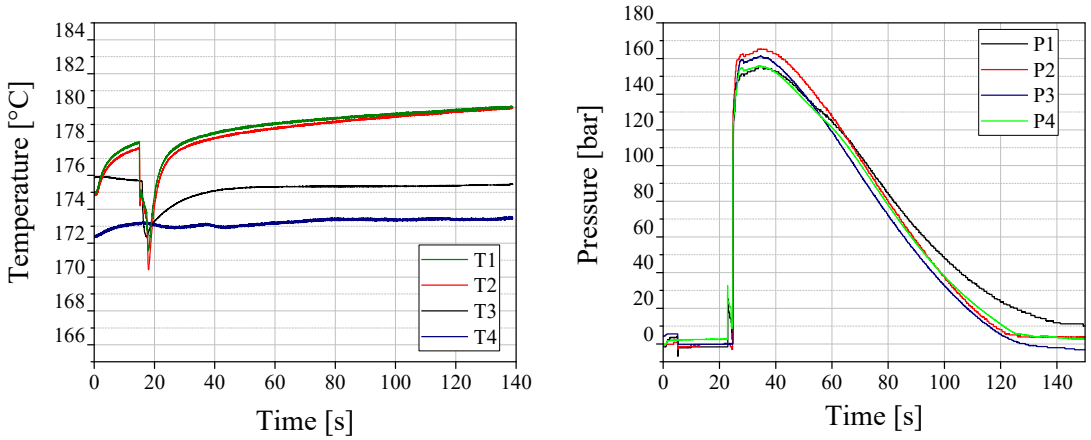

Figure 3.9: Signals obtained from various temperature (left) and pressure (right) sensors during the mold filling in transfer molding process

As seen in Figure 3.9 on the left hand side, T1 and T2 sensors show a sharp temperature decrease after around 16 s. This indicates the arrival of the EMC at the temperature sensor, which causes a temperature drop since EMC has a lower temperature compared to the tool surface at the beginning. Similar behavior is also observed at T3 sensor with slight difference due to the fact that T3 resides on the lower half of the tool in the cavity. In contrary to other temperature sensors, T4 does not show such drop in temperature since the sensor is implemented under the tool surface and has no contact with the molding compound. As seen on the right hand side of Figure 3.9, all pressure sensors show dramatic increase in the pressure profile exactly at the same time around 24 s. This sharp increase of pressure signal indicates the complete filling of the cavity. The slight differences observed in the pressure signals can be due to different positioning of pressure sensors namely in the cavities, gate area as well as in upper and lower half of the tool. The signals obtained from temperature and pressure sensors are used to inspect the process stability and also to compare the process parameters measured in the cavities with the set machine parameters. As T1 and T2 are mounted at similar positions in both cavities, for practical reasons only T1 and T2 sensor signals will be shown in the results, in order to compare the temperature profiles between two cavities. Due to similar reasons, the pressure sensors, P1 and P2 which are implemented in two cavities at the similar positions will be used to compare the filling behavior of the molding in the cavities.

In addition to temperature and pressure sensors, to measure the material characteristics of EMC in the molding process, two reusable monotrode sensors are implemented in the upper half of the tool, where one is in the left cavity at gate, and the other one is at the same position in the right cavity. The monotrode sensors are explicitly located at the gate area, because this position can deliver all steps of the curing behavior of the EMC from being liquid state during injection phase while flowing into the cavity until the gelation of epoxy resin. Moreover, since the viscosity of EMC is strongly influenced by the temperature, it is important to measure the temperature profile near the monotrode sensors. Thus, for more precise measurements and better interpretation of the results, monotrode sensors are mounted closely to temperature sensors of T1 and T2 (see Figure 3.8).

3.2.2 Molding Machine for Producing the Sample Bars

Lauffer transfer molding machine VSKO 25 with a max 25 kN clamping force is used to produce the sample bars to characterize the EMC with various analytical tools. With the molding press, it is possible to produce the sample bar geometry of 80 x 10 mm^2 with thickness variations of 1, 2 or 4 mm.

A reusable monotrode sensor with overall 6 mm diameter is implemented into the cavity of the transfer molding press to analyze characteristics of EMC with DEA during molding process. Additionally, to monitor the process and to ensure the process stability during molding process, temperature (Kistler Instrumente GmbH, Type K, 2.5 mm) and pressure (Kistler Instrumente GmbH, diaphragm sensor,

6 mm) sensors are mounted in the cavity. As in the other molding machine (see Section 3.2.1), in this molding machine the temperature sensor is also implemented very close to the DEA sensor in the tool. As temperature has a significant influence on the viscosity behavior of the molding compound, implementing a temperature sensor closer to the DEA sensor allows to correlate the viscosity behavior directly with temperature. All sensors are mounted on the upper half of the molding tool. Considering that the sensors can leave marks on the sample bars, the sensors are implemented on two ends of the cavity and as far as possible from the middle of the cavity to prevent any marks in center of the specimen bar which can influence the results of mechanical analysis such as DMA. The cavity of the molding tool and the positions of the integrated sensors are shown in Figure 3.10.

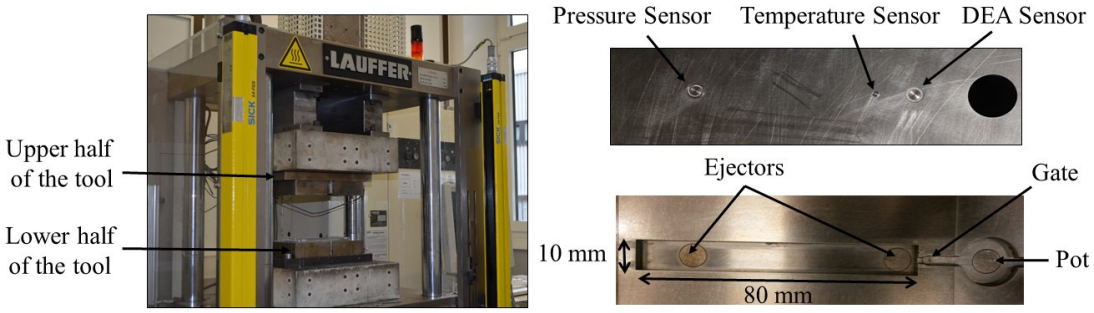

Figure 3.10: Transfer molding press to produce the sample bars (left), mold tool geometry for production of the sample bars (right)

3.2.3 Dielectric Analysis (DEA)

DEA is employed as monitoring technique to observe the variations in the material characteristics in transfer molding process. For this reason, reusable sensors are implemented in the tool cavities of both transfer molding presses, which are already explained in detailed in Section 3.2.1 and 3.2.2. The same type of monotrode sensors are mounted in cavities of both transfer molding presses in order to compare the results. The monotrode sensor 4/3RC is selected, which has overall 6 mm diameter. The sensing surface of the monotrode sensor 4/3RC is only 4 mm and the rest of 2 mm is the isolation layer as it can be seen from Figure 3.11. The isolation layer is necessary according to measurement principle in order to separate the sensing surface of the sensor from the tool surface to create an electrical field between the tool and the sensor. With the help of the generated electrical field the mobility of the ions can be measured. DEA measurements are carried out with dielectric cure analyzer, DEA 288 Epsilon, Netzsch-Gerätebau GmbH, Selb. The DEA 288 offers two dielectric channels, which allow to conduct two simultaneous measurements at the same time. Thus, two channels are used at the same time during the measurements in the transfer molding press with two cavities having two monotrode sensors (Section 3.2.1). The monotrode sensor and dielectric analyzer used in this work are shown in Figure 3.11.

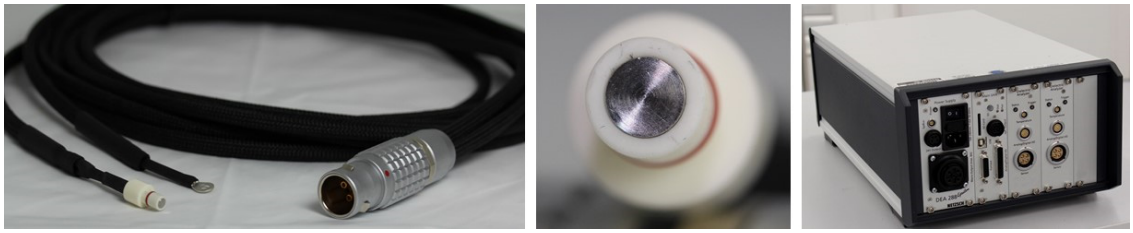

Figure 3.11: Monotrode sensor with its plug to connect to the analyzer (left), the surface structure of the monotrode sensor (middle) and the dielectric analyzer with two measurement channels (right)

In a DEA curve the logarithmic ion viscosity is plotted over curing time of the EMC in the transfer molding process. The implemented DEA setup allows also to monitor the temperature and the pressure

sensors together with the DEA signal during the molding process. A typical DEA signal obtained from DEA analyzer and corresponding temperature and pressure signals from the molding cycle are shown in Figure 3.12. The cycle time in transfer molding is typically in the order of 2 minutes. For the DEA measurements, however, the cycle time is prolonged to 4-6 minutes to record the curing behavior of the EMC until the end stages. All DEA measurements in both transfer molding presses are started with trigger signal beginning with a plunger movement conveyed from the machines to DEA analyzer to avoid any manual triggering, which can cause an undesired time shift at the beginning of measurements.

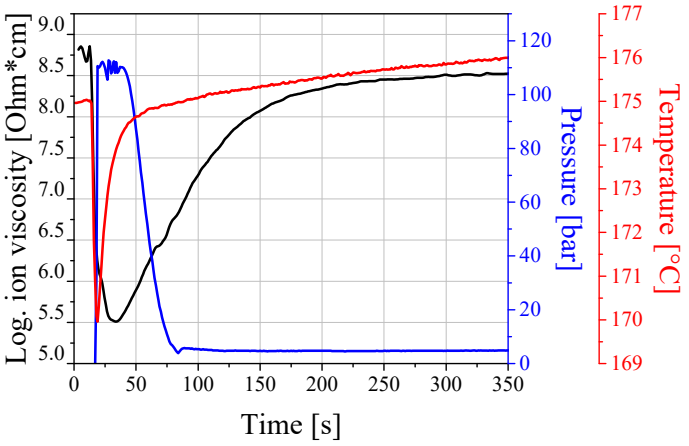

Figure 3.12: DEA signal of EMC 1 in-situ monitored with DEA Analyzer and corresponding temperature and pressure signals from the molding cycle

As seen in Figure 3.12, temperature drops sharply at the beginning of a cycle indicating that the material arrives at the sensor. At the same time, ion viscosity starts dropping also revealing the material arrival at the DEA sensor. The following continuous drop on the ion viscosity until around 30 s is due to the melting of EMC, which is heated through the hot molding tool and causing the decrement in the ionic viscosity. Subsequently, the EMC reaches the minimum ion viscosity at around 35 s. After this point, the reaction propagates quickly and the slope of reaction increases. As the time goes by, the slope of the viscosity curve decreases by indicating that the reaction rate slows down. After around 250 s, ion viscosity achieves its maximum indicating that the cure reaction is terminated.

DEA is a temperature and frequency dependent method. Thus, before conducting any measurement with DEA, it is important to evaluate the temperature influence on ion viscosity as well as the ion viscosity curve with different frequencies for the selected material. The selection of the right measurement frequency is very crucial to pursue the ion viscosity signal throughout the curing time in all phases of the molding compound continuously without any noises and interruptions. To determine the measurement frequency for EMC 1, ion viscosities are examined with five different frequencies; 1 Hz, 10 Hz, 100 Hz, 1 kHz and 10 kHz at a constant molding temperature of 175 °C as depicted in Figure 3.13. As a criterion for the selection of suitable frequencies, frequencies which deliver the lowest minimum ion viscosity combined with maximum ion viscosity level in a smooth curve is applied. In other words, the frequencies, which can demonstrate the highest delta (Δ) between the minimum ion viscosity and maximum ion viscosity, are selected as the suitable frequencies. Among measured frequencies from 1 Hz to 10 kHz, the frequencies 1 Hz, 10 Hz, and 100 Hz are selected as suitable frequencies for the DEA measurements of EMC 1 (see Figure 3.13). Nevertheless, as the choice of 10 Hz delivers the smoothest signal with largest delta between the minimum ion viscosity and the maximum ion viscosity, the ion viscosity curves at 10 Hz will be used as representation in the results.

As mentioned, the second important aspect when interpreting the DEA results is the temperature. Temperature has a direct impact on capacitance, on the energy of the system, yet on the mobility of the ions. In Figure 3.13 DEA measurements are illustrated which are conducted with EMC 1 with different molding temperatures from 155 °C to 185 °C at 10 Hz. Higher temperatures show faster cure reaction

by owning higher slope and achieving the corresponding maximum ion viscosities faster. On the other hand, as it can be seen in Figure 3.13, at the very beginning of reaction, the starting level of the logarithmic ion viscosities varies depending on the molding temperature. Additionally, maximum ion viscosities achieved at the end of measurement are also varied remarkably depending on the molding temperatures. Therefore, it is important to keep in mind that, when comparing the results of DEA with each other, the similar temperatures and frequencies should be selected for the correct interpretation of the results.

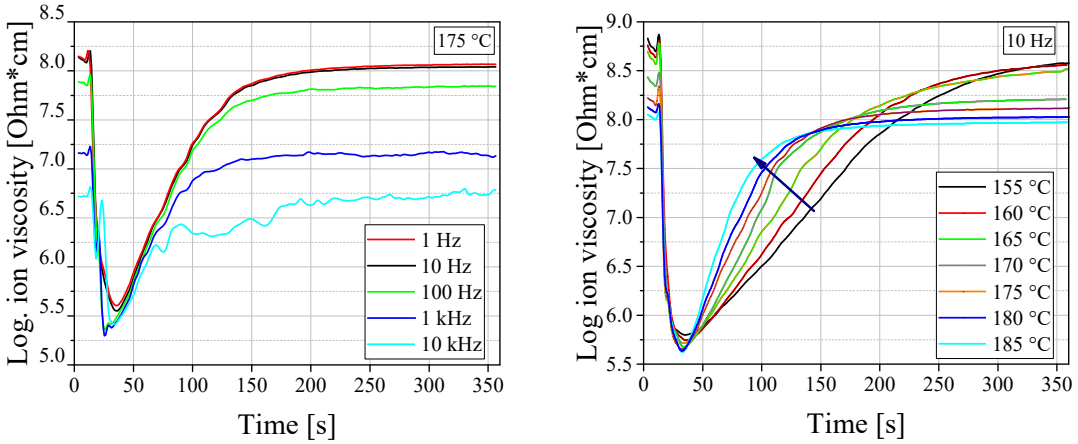

Figure 3.13: DEA signals measured with different frequencies; 1 Hz, 10 Hz, 100 Hz, 1 kHz and 10 kHz at constant molding temperature of 175 °C (left), influence of molding temperature on the ion viscosity curves; temperature is varied from 155 °C to 185 °C at constant frequency of 10 Hz (right)

3.3 Material Characterization Methods

In this section, thermal and mechanical measurements are explained, which are performed to characterize the properties of EMC. DMA method is used to measure glass transition temperature (T_g) of the EMC. The applied measurement mode of the DMA and more information about the parameters are given in Section 3.3.1. DSC measurement is conducted to determine the degree of cure of the EMC. Detailed information about the selected parameters for the DSC as well as the calculation of the degree of the cure of EMC are introduced in Section 3.3.2. As highlighted in Section 2.3, the viscosity behavior of the EMC plays an important role on the quality of the molded package. Therefore, to understand and simulate the viscosity behavior of EMCs under different conditions, rheological measurements with different analysis equipment are performed. As a standard method, rotational rheometer measurements are performed to examine the shear viscosity of EMC. The selected parameters for the rotational rheometer measurements are explained in Section 3.3.3. As an alternative viscosity measurement, a squeeze flow rheometer is used. A squeeze flow rheometer allows to examine the viscosity behavior of EMCs at higher temperatures in comparison to the rotational rheometer. Moreover, as the tool setup of the squeeze flow rheometer is constructed in a similar way as the molding process, it allows to simulate the cure reaction of EMCs as in the transfer molding process. Detailed information about the tool setup and the measurement principle of the squeeze flow rheometer are introduced in Section 3.3.4. Since the DEA is used as an online monitoring technique in this work, for better understanding of the ion viscosity curves in terms of the progress of the cure reaction, it is important to compare the ion viscosity with the shear viscosity. Thus, simultaneous DEA-Rotational Rheology method is conducted, which is shown in Section 3.3.5. Last but not least, as the influence of the humidity of the EMC on the quality features are the focus of this work, for a precise measurement, Karl-Fischer titration method is used to measure the moisture content in the pellets. The detailed information about the Karl-Fischer method is given in Section 3.3.6.

3.3.1 Dynamic Mechanical Analysis (DMA)

Dynamic mechanical analysis (DMA) yields information about the viscoelastic behavior of the thermoset materials. T_g and the modulus of elasticity of the material can be determined with DMA. DMA measurements are carried out in a Bose ElectroForce 320 under a harmonic load application. Maximum force used in this instrument can be selected from 100 N to 450 N in a temperature range of -50 °C to 260 °C. Three-point bending mode is applied on the specimen with a sinusoidal deformation of 0.03 mm. DMA delivers also information about the frequency dependency of properties of molding compound when measured at different frequencies. However, this aspect of investigation is not a focus of this work. DMA is employed in this study to correlate the T_g of the material with curing degree of the EMC, thus only one frequency is used to determine the T_g of the material and to compare the results of different preconditioned EMC with each other. For this reason, the typical frequency of 1 Hz is selected in DMA measurement. The specimens are heated from ambient temperature to the 250 °C with a heating rate of 10 K/min. The molding compound specimens have the dimensions of 10 mm length x 8 mm width x 4 mm thickness. Typically, loss modulus (*E´´*), storage modulus (*E´*) and tangent delta (*tan δ*) can be measured with DMA. Usually, the loss modulus is correlated with viscous part of the material, storage modulus is with the elasticity of the compound, and tangent delta delivers the ratio of loss modulus to storage modulus [178]. A typical DMA curve obtained for EMC 1 is shown in Figure 3.14.

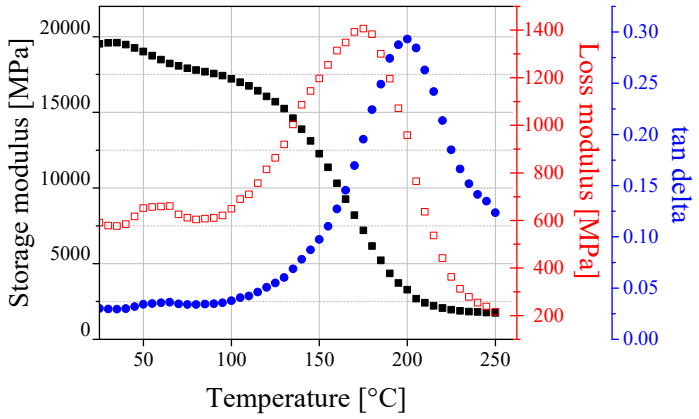

Figure 3.14: Storage modulus, loss modulus and tangent delta obtained from DMA measurement for EMC 1 at 1 Hz

The continuous decrease in the storage modulus and the peak observed in loss modulus in Figure 3.14 are due to the T_g of the EMC in which the sample becomes rubbery above this temperature. T_g can be measured in different positions of the curves; by the *E´* onset point, by the peak of *E´´* or the peak of *tan δ* [179]. However, the position of the peak of *tan δ* is usually used to determine the T_g of polymeric materials [32], [157], [180]. Thus, *tan δ* will be used to define the T_g of EMC 1 in this work.

3.3.2 Dynamic Scanning Calorimetry (DSC)

Differential scanning calorimetry (DSC) is frequently used to study the cure kinetics of epoxy based materials. According to ASTM standard E473, in DSC measurement the heat flow rate difference into the specimen and an inert reference sample is measured as a function of temperature under a controlled temperature program [181]. Two kinds of DSC measurements can be performed, namely isothermal and non-isothermal. In an isothermal DSC, the sample is heated up rapidly to a defined temperature and the temperature is held constant until no change in enthalpy is detected. Isothermal DSC can have some drawbacks due to the fact that during heating up the sample to a certain temperature, the sample can already start curing, and for a fast curing sample the reaction can be over before the desired temperature is reached. In non-isothermal or dynamic DSC, the sample is heated up with a constant heating rate to the desired temperature and the change in enthalpy is recorded [182]. Several crucial information can

be derived about the curing reactions from DSC curves. The starting temperature of the reaction, T_g, reaction enthalpy generated by curing are some of the important information [183]. Additionally, the degree of cure can be calculated from the DSC curves, which is also the main purpose of employing the DSC in this work. The degree of cure, α , can be determined by calculating the enthalpy at time t, $\Delta H(t)$ and dividing by the reaction enthalpy of a fully cured sample ΔH_{total} [47], [184], [185].

$$\alpha = \frac{1}{H_{tot}} \int_0^t \left(\frac{dH(t)}{dt}\right) dt \tag{5}$$

DSC measurements are performed with TA Instruments Q2000 having a measurement accuracy around 0.2 µW and a temperature accuracy around ± 0.1 °C in a temperature range of -180 °C to 725 °C [186]. For the measurements, the pellets are smashed into granular form and put in the aluminum pans in the DSC. DSC measurements are performed with a heating rate of 10 K/min over a range of -30 °C to 260 °C under nitrogen purge. Figure 3.15 shows a representative DSC curve of EMC 1 under non-isothermal condition.

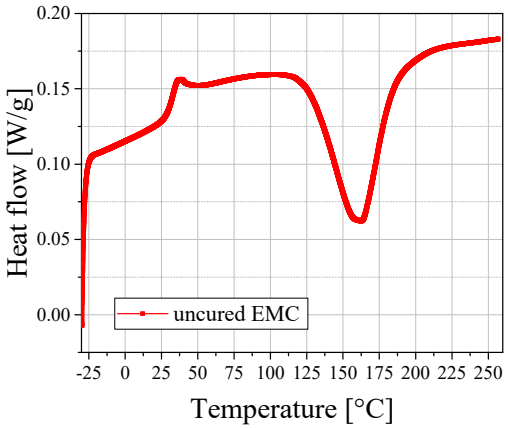

Figure 3.15: DSC curve of EMC 1 under non-isothermal condition from -30 °C to 260 °C with a heating rate of 10 K/min

The curing reaction of EMC is mostly exothermic, which can be identified from the positive value of the heat flow and the peak of the reaction pointing downwards [187]. Moreover, the area under the peak delivers the enthalpy of reaction. The first peak seen around 40 °C is due to the melting of some additives in EMC 1.

3.3.3 Rotational Rheometer

Rheology measurements are performed using a parallel-plate rotational viscometer. A rotational viscometer AR G2 from TA Instruments with a plate diameter of 6 mm and a gap height of 1.5 mm is employed. The measurements are carried out under isothermal condition at 100 °C and under non-isothermal condition with a heating rate of 2 K/min starting at 70 °C until the end of measurement range. The viscosity is measured in oscillation mode with a frequency of 1 rad/s and 2 kPa oscillation stress. For the measurements, the pellets are smashed into the granulate form, then pressed together as a tablet having 12 mm diameter and a thickness of 1.5 mm. The rheology measurements are repeated three times.

3.3.4 Squeeze Flow Rheometer

The molding temperature for the EMC is usually at 175 °C. To understand the viscosity behavior of the EMC during the molding process, determining the viscosity behavior at elevated temperatures is important. Unfortunately, the measurement of the viscosity behavior of EMC 1 at 175 °C with a rotational rheometer is mostly challenging and the viscosity behavior of the EMC can be measured only

up to a temperature around 140 °C. The reason for that is that the reactive EMC can start curing very fast at elevated temperature before the measurement even starts and the information about the initial phase of viscosity behavior cannot be recorded with a rotational rheometer. Only possibility to yield rheological data at process temperature is an extrapolation of measurements taken at lower temperatures. Alternatively, another method can be applied to measure the viscosity behavior of the EMC at 175 °C, a squeeze flow rheometer. Squeeze flow rheometry is designed as an annular gap rheometer, to simulate the viscosity behavior of the EMC in the molding machine. The construction of the tool is shown in Figure 3.16. During the measurement, the plunger moves downwards with a constant displacement and presses on the EMC pellet. The EMC, which melts at elevated temperature, flows through the both open side of the plunger in the capillary. The force required to move the plunger is recorded during measurements and is used to calculate the viscosity of the EMC.

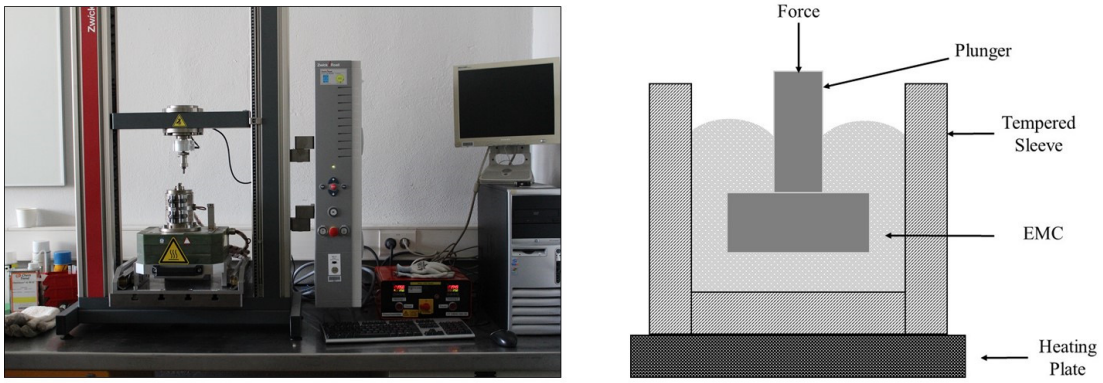

Figure 3.16: Squeeze flow rheometer setup (left), assembly of the squeeze flow rheometry (right) [188]

3.3.5 Simultaneous DEA-Rheology Measurements

The simultaneous DEA-Rheology measurements are conducted at Fraunhofer IZM with an impedance spectroscopy system Alpha AN from Novocontrol Technologies and with a AR G2 rheometer from TA Instruments. A rheometer with plate-plate geometry is used with a gap height of 1 mm in oscillation mode with a frequency of 1 rad/s. The impedance of EMC 1 is measured and then converted to the ion viscosity of EMC 1. Simultaneous rheology and impedance spectroscopy with an integrated interdigital capacitor is performed under isothermal condition at 100 °C and under non-isothermal condition from 70 °C at a constant heating rate of 2 K/min until the gelation. The frequencies of 10 Hz, 100 Hz and 1 kHz are selected. The measurements are repeated two times.

3.3.6 Karl-Fischer Titration

To measure the amount of water in the pellets, the gravimetric determination of the water content in the pellets before and after preconditioning in humid atmosphere is done. The weight difference of the pellets before and after preconditioning are compared. In addition to gravimetric determination, for a more accurate determination of the amount of water in the pellets the calorimetric Karl-Fischer titration is used according to DIN EN ISO 15512 [189]. Calorimetric Karl-Fischer titration is a method for precise measurements of especially the low level of humidity in the sample [82]. To determine the amount of water, the water in the sample is evaporated by heat and transferred into the titration cell. Then, the Karl-Fischer titration starts, which is based on the reduction of the iodine by sulfur dioxide in the presence of water to form sulfurtrioxide and hydroiodine acid [189]. Titration is performed until the water is consumed. After the endpoint is reached, the amount of water in the sample is recorded.
Karl-Fischer-Titrator AQUA 40.00 from Jena Analytic is used to measure the water uptake in EMC pellets. The measurement parameters for the titration are set to 200 °C oven temperature, 20 min measurement time and 8.0 µg/min drift. The measurements are repeated three times for an accurate determination of the amount of water in the EMC pellets and the average values are shown in the results.

Moreover, the samples for the measurement are taken from the same outer layer of the pellets to prevent any deviation in the water content due to the position of the samples in the pellets.

3.4 Quality Analysis Methods

In this section, quality analysis methods are introduced which are applied to examine the quality characteristics of the package after the molding process. First, the void formation in the molded packages is analyzed with scanning acoustic microscopy (SAM) after the molding process. The detailed information about the setup and the measurement is given in Section 3.4.1. Subsequently, the warpage analysis is conducted with the molded packages, which is shown in Section 3.4.2. As a last step, the molded packages are sent to laser opening, to remove the EMC and to relieve the wire bonds in order to analyze the wire sweep in the packages. After package opening, the wire bonds are inspected with optical microscopy and initial and final position of the wire bonds are compared. More information about the wire sweep analysis is given in Section 3.4.3. The methods to analyze the void formation and warpage are non-destructive, whereas the laser opening process, which is used to examine the wire sweep of aluminum wire bonds, is a destructive method. Thus, the order of the analysis steps is important to complete all quality characteristics examinations. Figure 3.17 shows the sequence of the analysis steps after the molding process. The quality analysis methods are given in this section in a respective order as shown in Figure 3.17.

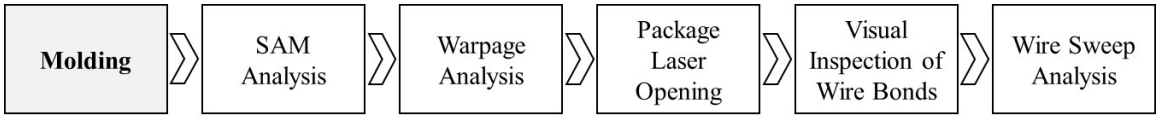

Figure 3.17: Sequence of quality analysis examinations after the molding process

3.4.1 Scanning Acoustic Microscopy (SAM)

For the analysis of voids in the molded packages, scanning acoustic microscope (SAM) is used. The analysis is carried out in SAM Winsam Vario III with a transducer of 15 MHz frequency. SAM is a non-destructive method, which can detect inhomogeneities and discontinuities in the specimens. Ultrasound can be spread through gases, liquids as well as solids. Typical frequency range used for the ultrasonic measurement is in the range of 5 MHz to 500 MHz. In SAM there are two different types of measurement methods, namely through-transmission method and pulse echo method. In through transmission method, two components are required, where the transmitter sends the signal, and the receiver records it. The other method is the pulse-echo method, where only one component, a transducer is used, which transmits and receives the signal. In this work, pulse-echo method is used. The pulse with a high frequency is generated by pulse generator and directed to the sample through the acoustic lens. After transmitting the signal to the specimen, a pause follows and the transmitter switches to the receiver mode. Transducer transmits the signal to the specimen and also receives the signal, which is reflected from the specimen. Reflections occur due to the surfaces of the specimens as well as the presence of the discontinuities. Between the transducer and the specimen, a medium is required in order to transmit and receive the signal. To prevent any undesired inhomogeneities between the transducer and the specimen, distilled water is used as a medium in an ultrasonic bath. The setup of the SAM and an exemplary signal detected during the measurement are illustrated in Figure 3.18.

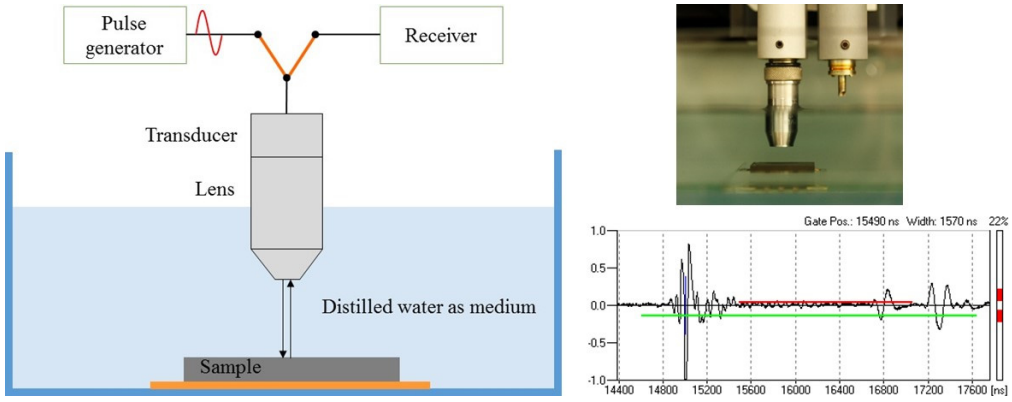

Figure 3.18: Scanning acoustic microscope, schematic of the test setup (left), the transducer on top of the sample measured (right above), and the amplitude signals during the measurement which are reflected from the surface and from the inhomogeneities (right below)

For the pulse-echo acoustic microscopy, there are different scan modes, which allow to obtain all required information and details regarding to specimen. The scan modes of A, X, B and C are applied in this work. X-scan delivers information in different horizontal levels, A-scan allows to identify only one point in a vertical line, B-scan can be applied to obtain a picture on a cross-section, and C-scan gives a picture on horizontal level with a defined thickness. The principle of A, B and C scan modes in SAM can be seen in Figure 3.19. Although frequently C-scan is used in this work as a scan mode, other scan modes are also applied to acquire necessary information. The thickness range of the C-scan level is adjusted to the thickness of the molded packages to deliver all the information through the package within one picture.

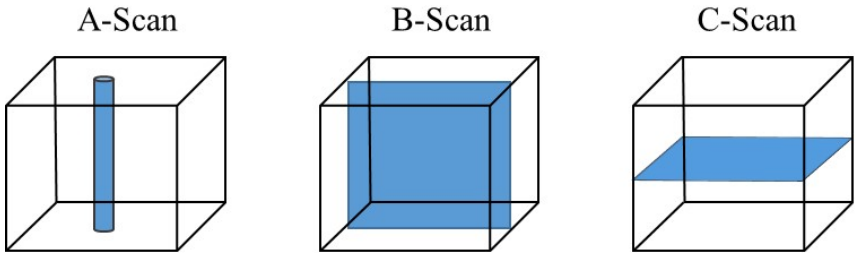

Figure 3.19: Principle of A, B and C Scan modes in SAM which are employed in this work for the measurement of the void formation in the molded packages

After measuring the samples with SAM, the pictures are evaluated to obtain the number of voids, the size of the voids as well as the location of the voids on the layout. For a precise evaluation, a software is used. The open source image processing program ImageJ is used, which includes the analysis modules such as plugins, which are developed for the void analysis purpose of the selected demonstrator for this work. The software detects the voids by setting the threshold in terms of the resolution. Threshold for the resolution is set in such a way that software selects the dark points (potentially voids) on the SAM image which can also be discretely identified by a visual observation. Nonetheless, the software has difficulty to differentiate the voids, in other words the darker points on the SAM image, which are close to contours, edges or the borders of the layout, which are also seen as black areas on the SAM image. Therein, for an accurate void analysis, the images, which are examined with the software, are examined subsequently by an additional visual inspection. Additionally, as a transducer frequency of 15 MHz is selected in SAM analysis, which allows through-thickness measurement for this demonstrator geometry, the minimum detectable void size is determined as 100 µm.

3.4.2 Warpage Analysis

The warpage analysis is measured with the help of digital image correlation. The investigations are carried out with the DANTEC Analysis Q400. For the preparation of the samples, the surfaces of the molded packages are marked with a white spray to distinguish the small impurities on the surface. For each sample, the images are recorded from different angles of the cameras and the obtained images are analyzed with the program Istra4D. First step in the evaluation of the images is to define the examination area on the sample. For this reason, a mask is placed on the surface and the area within this mask is analyzed with the software. The software measures the surface contour of the packages within the defined mask and create a false-color image (Figure 3.20 left). After obtaining the false-color images, a circle is placed in the middle of image and four lines are set within the circle (Figure 3.20 right). The purpose of the circle is to ensure that all four lines have the same length within the circle and the position of the lines are the same for each sample. The four line contours on the false-color image deliver the information about deviation in z-direction on the surface. The values obtained from the software about the z-direction for each line are analyzed. The type of warpage is identified between concave or convex. All the warpage analysis for the molded packages are performed after PMC.

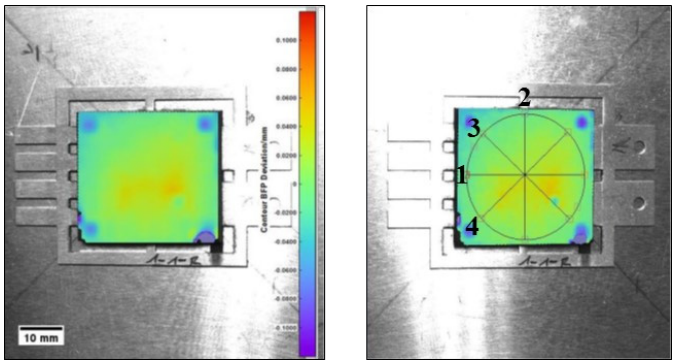

Figure 3.20: Image correlation, the variation is shown with the colored scale (left), the four lines placed within the circle on the false-color image to evaluate the deviation in z-direction (right)

For the warpage, firstly the maximum value on the line in z direction is calculated and selected as the maximum warpage. However, some surface defects on the molded package can cause one single maximum point although the other measured values on the lines lie significantly under this value, yet this may result in false interpretation of the results. Therefore, in addition to maximum points of warpage, the area under the curve of the lines are also evaluated.

3.4.3 Wire Sweep Analysis

Wire sweep is evaluated by visual inspection. Each wire bond is examined before and after the molding process with an optical microscope. To analyze wire sweep after the molding process, the package is opened up with laser ablation technique at two locations of the specimen to expose the aluminum wire bonds (Figure 3.21). For the laser ablation process, Laser VMC1 from Trumpf GmbH + Co KG is used.

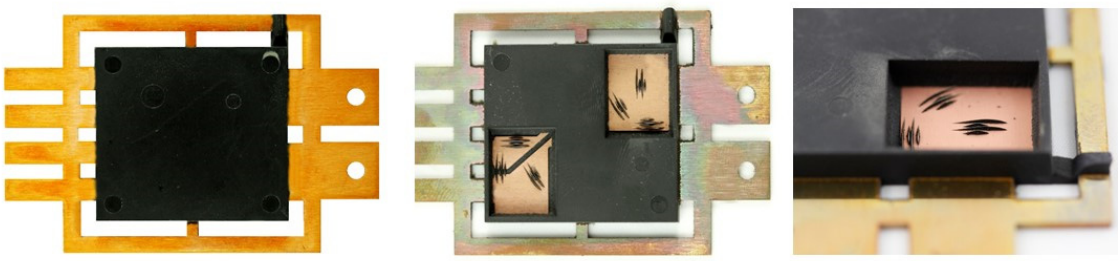

Figure 3.21: Molded package after the molding process (left), opened molded package to expose the wire bonds which are bonded on two locations on the lead frame (middle), wire bond groups close to the gate (right)

Wire sweep evaluation is done with an image editing software ImageJ. To ensure reproducible wire sweep measurement, on each wire bond 10 points are replaced on an outer vertical line of the wire bond as it is shown in Figure 3.22. The coordinates of these 10 points for each wire bond are measured and recorded before and after the molding process. To compare the points before and after the molding process, the coordinates are calibrated and the vertical displacement is measured. The maximum displacement between initial position and the position after the molding process is measured and defined as a wire sweep. Wire bonds images before and after the molding process as well as the definition of wire sweep are shown in Figure 3.23.

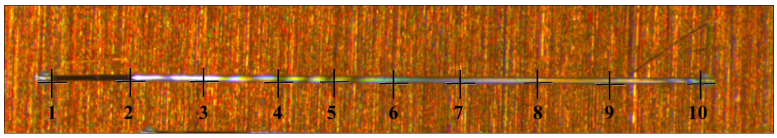

Figure 3.22: Wire sweep analysis with 10 points placed on the outer line of a wire bond

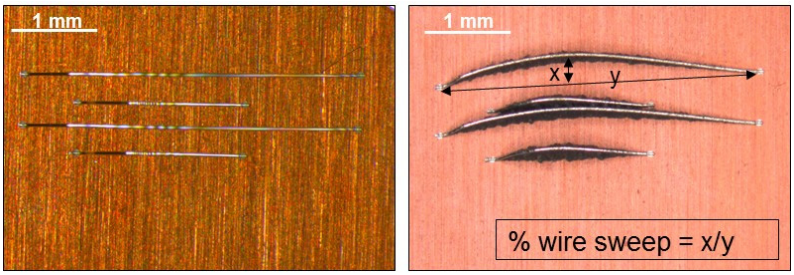

Figure 3.23: Wire bonds before the molding process (left), after the molding and laser ablation process, definition of wire sweep (right)

As explained previously, wire sweep is accomplished by manual evaluation of the obtained images by locating 10 points on the outer vertical layer of one wire bond (Figure 3.22). This is done for each wire bond before and after the molding process. To find out the deviation caused by the manual wire sweep evaluation, each 24 wire bonds on the test vehicle are measured 10 times before and after the molding process. The wire sweeps of the wire bonds are examined and the standard deviation between the measured wire sweep values are calculated. The maximum standard deviation observed in wire sweep for the same wire bond is found as ±10 µm.
In addition, during the visual inspection of the wire bonds before and after the molding process, the wire bonds cannot be positioned exactly at the exact area on the image. In order to identify, whether this positioning of the wire bond on the image causes any significant deviation in wire sweep examination, four images are taken with optical microscope, where the same wire bond group is positioned purposely in different areas on the images and possibly far from the middle area of the image. The images are shown in Figure 3.24.

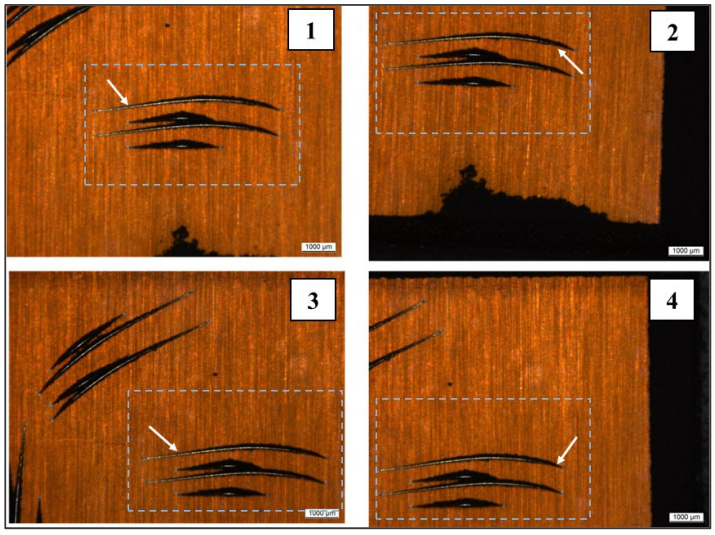

Figure 3.24: Same wire bond group is inspected by locating the wire bonds in different area of the image and the standard deviation of the positioning of the wire bonds on the image is calculated.

Wire sweep for the same wire bond such as the first long wire bond from above which is marked with white arrow in Figure 3.24 is measured in four images and the standard deviation of the wire sweep values are calculated. The standard deviation is found as 9 µm. As explained above, 10 µm standard deviation in wire sweep originated due to the manual evaluation of the wire sweep, which implies that this 9 µm standard deviation measured in the same wire bond located at different positions on the four images (Figure 3.24) is to a large extent due to the manual evaluation, and not due to the positions of the wire bonds on the image.

4 Experimental Preparation

To study the quality characteristics in the molded packages, firstly it is necessary to define a suitable layout. In this chapter, the layout of the test vehicle including respective wire bonds and components as well as the steps necessary to prepare this layout for the test vehicle are introduced. The overview of the quality analysis after the molding process is already schematically described is Section 3.4. In this chapter, the steps which take place before the molding process in order to prepare the test vehicle, in other words the demonstrator, are introduced. Figure 4.1 depicts the steps, which are essential to apply in order to prepare the test vehicle before the molding process. The sequence of the steps is adopted to the respective layout of the demonstrator used in this work.

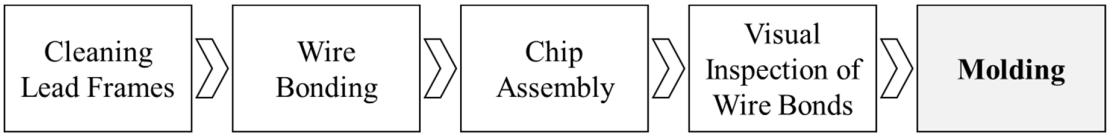

Figure 4.1: Overview of the steps required to prepare the demonstrator before the molding process

In Section 4.1, the defined layout for the demonstrator for instance the positions, the lengths and the types of the selected wire bonds is introduced. Subsequently, the steps, which are necessary to produce the test vehicle with a defined layout are given in Section 4.2. The cleaning process of the lead frames, bonding process and chip assembly are given in detail in a respective order as shown in Figure 4.1.

4.1 Layout Definition

In this work, as a test vehicle similar geometrical dimensions as a power module package is chosen. The demonstrator package is a test vehicle and not a functional power module, thus to realize the components volume in the package dummy components are used and thin aluminum wire bonds are bonded directly on a lead frame. The layout of the demonstrator is designed in a way enabling to study different wire bond characteristics on the wire sweep. 50 µm aluminum wire bonds (Al + 1 % Si) from Heraeus are used and all wire bonds are bonded directly on the copper lead frame. The influence of various wire bond properties on wire sweep is examined in this work. To analyze the influence of the wire bond length on the wire sweep, two different lengths of wire bonds, namely 2.75 mm and 5.5 mm with an identical loop height of 0.5 mm are chosen. Long wire bonds and high loop heights are preferred so that the wire sweep is sufficiently large to be measured accurately and to identify the corresponding effects of investigated parameters. In addition, the influence of the wire bond location with respect to the gate on the lead frame are investigated. To accomplish this, wire bonds are placed in two locations on the lead frame at near to the gate and far from the gate areas. Furthermore, in order to study the impact of angle of the wire bonds to the gate, the wire bonds are bonded at three different angles to the gate; 180°, 90° and 45°. In total, each test vehicle consists of 24 wire bonds, in which 12 wire bonds are attached close to the gate and 12 wire bonds are bonded far from the gate. The 12 wire bonds of each group are divided into three subgroups and each subgroup is attached in three different angles to the gate. Each subgroup contains 4 wire bonds, 2 short and 2 long wire bonds with an identical loop height. Bond to bond distance is kept identical for all wire bonds on the layout and is approximately 450 µm. The schematic description of layout of the test vehicle is shown in Figure 4.2. The amplified images of the wire bond groups, which are bonded close to the gate and far from the gate with corresponding subgroups are depicted in Figure 4.3. To sum up, following three effects of wire bond properties are studied with this layout with regard to wire sweep:

- Influence of wire bond length: 2.75 mm and 5.5 mm with an identical loop height of 0.5 mm

- Influence of position of the wire bonds on test vehicle: wire bonds attached in near gate and far from the gate areas
- Influence of angle of wire bonds to the gate: wire bonds attached at 180°, 90° and 45° to the gate in near gate and far from the gate areas

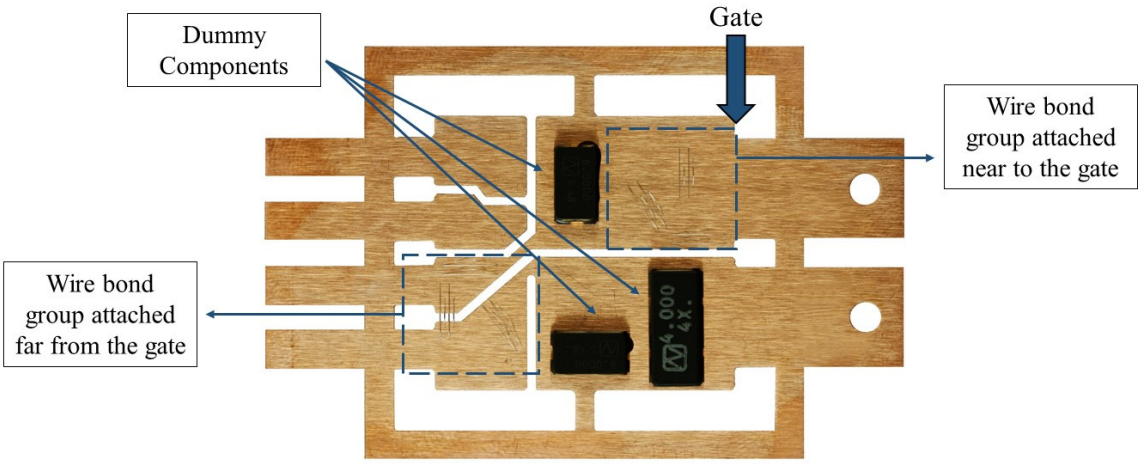

Figure 4.2: Test vehicle with three dummy components and two groups of wire bonds with respect to gate position, wire bonds attached at three different bond angles at 180°, 90° and 45° relative to gate position

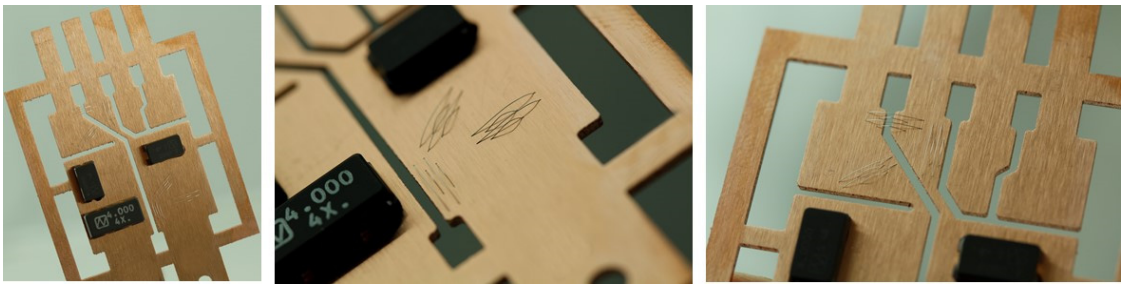

Figure 4.3: General overview of the layout of the demonstrator with all wire bonds (left), amplified image of the wire bonds attached at three directions to the gate 180°, 90° and 45° in near gate area (middle), and amplified image of the wire bonds attached in far from the gate area at three directions to the gate 180°, 90° and 45° (right)

As already mentioned, the wire bonds are directly bonded on the lead frame surfaces. This is also the reason of the modified assembly sequence shown in Figure 4.1. Nevertheless, to realize the volume of the electronic components in the package, passive units like resistors and condensers are assembled on the lead frame substrate [190]. Since an electrical functionality of the package is out of the scope of this work, passive dummy components without an electrical function are selected for the layout of the demonstrator. Two different sizes of the dummy components, which have the identical volume, as active components are chosen (Quartz NX8045GB 8,000MHz and NX1255 GB 4,000MHz FRG Frischer Electronic GmbH). Overall three dummy components are implemented onto the substrate, where two of them have a package size of 8 mm x 4.5 mm x 1.8 mm and one bigger component has a package size of 1 x 5.5 mm x 2.5 mm (Figure 4.3).

4.2 Sample Preparation

Test vehicles are prepared in three steps. Firstly, the lead frames are cleaned to remove any surface contamination in order to prepare the surface for the bonding process. The detailed information about steps of the cleaning process is introduced in Section 4.2.1. As the wire bonds are bonded directly on the copper lead frame and not on a chip for this defined layout of the demonstrator, the bonding process is done subsequent to the cleaning process. More information about the bonding process is given in

Section 4.2.2. As a last step, the dummy components are assembled onto the lead frame substrate. The selected adhesive and the setup for a chip assembly is explained in Section 4.2.3.

4.2.1 Cleaning

Lead frames are cleaned to remove the contamination from the surface and to provide a good surface cleanliness for the subsequent bonding process. To achieve the highest cleanliness on the surface without any impurities or flux residues, water-based cleaning medium, namely Vigon A200 (Zestron, Dr. O.K. Wack Chemie GmbH) is used as a cleaning agent. In addition, to prevent any possible oxidation or corrosion on the lead frame, corrosion inhibiter Vigon plus Cl 20 (Zestron, Dr. O.K. Wack Chemie GmbH), which is an aqueous mix of corrosion preventing additives, is supplemented into the solution. The preparation of the cleaning solution is completed by adding up deionized water. The mixing ratios for the ingredients in the cleaning solution are shown in Table 4.1.

Table 4.1: Mixing ratios of ingredients for the cleaning solution

Medium	Concentration
Vigon A200	30 vol. %
Vigon Cl20	2 vol. %
Deionized water	68 vol. %

Lead frames are first placed into a carrier and dipped into the beaker glass, which contains the cleaning solution. Then, the beaker glass is transferred into the ultrasonic bath, which has a temperature of 45 °C. Lead frames are cleaned for 5 min at 45 °C in the ultrasonic bath. Subsequently, lead frames are rinsed into the next beaker, which is filled with deionized water, and cleaned for 5 min at 45 °C further in ultrasonic bath to remove the rest of cleaning solution. After the cleaning of the lead frames in distilled water is completed, the cleaning step in the cascade rinsing follows. The cleaning of the lead frame in the cascade rinsing helps to remove the possible rest of cleaning solution or impurities and to achieve highest possible surface cleanliness on the lead frames. For this purpose, the lead frames are rinsed into three separate beakers filled with deionized water. The cleaning process in the ultrasonic bath and the cascade cleaning are shown in Figure 4.4.

Figure 4.4: Cleaning process of the lead frames, first placing of lead frames into the carrier (left), cleaning in the ultrasonic bath in cleaning solution and in distilled water (middle), cleaning solution, which changes the color from transparent to violet after the cleaning (right)

When the cleaning process is finished, each lead frame is dried by blowing nitrogen gas onto the lead frame surface to remove the remaining humidity. Finally, the lead frames are transferred into the storage cabinet under nitrogen atmosphere before the lead frames are conveyed to the bonding process.

4.2.2 Bonding

To attach the Al wires to the lead frame an ultrasonic wedge wedge bonding process is employed, which is typically applied to bond aluminum wires and does not require higher temperature [39], [191], [192]. The required ultrasonic energy is produced by the vibration of the bonding tool typically in a frequency range of 20-300 Hz [191]. For bonding the aluminum wire bond onto the lead frame, wire wedge bonder

Model 3700 from Kulicke & Soffa Industries is used, which has a capability to be utilized in a fully automatic production line, and the bonding process is conducted at room temperature in this work. The bonding process should be performed directly after cleaning process to have the highest cleanliness of surface for a good quality of bonding. The wire bond quality is crucial to ensure that no lift-off occurs due to the poor bonding quality, and that the wire bonds can withstand the high transfer speed during the molding process.
The precision of the positioning of the wire bonds with the bonding machine is evaluated by measuring the position of different wire bonds on the lead frames 50 times and the standard deviations are calculated. The standard deviation obtained from the measurements is found to be approximately 12 µm.

4.2.3 Chip-Assembly

In the last step of the sample preparation, the dummy chips are assembled on the surface of the lead frame with Infotech IP 520 from Infotech AG. PD 955 SMT thermosetting polymer adhesive is used in order to fix the dummy components on the lead frame. Firstly, the adhesive is dispensed by the machine on a defined target position and the dummy components are picked and placed on top of adhesive depots automatically. After placing all the components on the lead frame, the adhesive is cured at 125 °C in an oven for 10 minutes.

4.3 Statistical Process Analysis

Statistical evaluation software, Cornerstone, is used in this work to generate the experimental plan and to analyze the results obtained from the measurements. The correlation between the input parameters such as process parameters and material characteristics and output parameters such as wire sweep, voiding and warpage are done by using regression analysis. The process and material models, which will be presented in Chapter 7 are also generated with the help of regression analysis.

5 Preliminary Experiments and Results

In this chapter preliminary experiments are introduced, which are performed to gain more understanding on the influence of the process parameters on quality characteristics such as void formation, wire sweep and warpage. In addition, the variations in the material characteristics of EMC 1 due to the preconditioning in prolonged storage duration in dry and humid environment are analyzed. The information acquired in this chapter in terms of material characteristics and the influence of process parameters on the quality features are essential to constrain the main experiments in Chapter 6. In this chapter focus is on two main matters. The first matter is to determine dominant process parameters of transfer molding process on void formation, wire sweep and warpage and to analyze the quality characteristics, which are strongly influenced by the process parameters. The second matter is to evaluate the suitability of the DEA in terms of observing the possible variations in the material characteristics of EMC due to prolonged storage duration, humidity and batch variations. Moreover, the basic characterization of the preconditioned EMC 1 is carried out with rheology methods to gain more understanding in the cure reaction of EMC 1 and to comprehend the variations in the material characteristics of EMC 1.

The planned experiments to study the impact of individual process parameters on the package quality are introduced in Section 5.1. In this study, four main process parameters are examined, which are molding temperature, transfer speed, preheat time of the pellets and holding pressure. To study the significance of process parameters on the package quality, a DoE is designed. The results of the DoE, and the dominant process parameters on the void formation, wire sweep and warpage are discussed in Section 5.2. Based on the acquired results, the quality features, which are strongly influenced by the variation in the process parameters, are determined.

In Section 5.3 the investigations to assess the suitability of the DEA as an in-situ cure monitoring for the transfer molding process are shown. At first, for a better understanding of the DEA as an online monitoring method, DEA results are correlated with standard laboratory techniques of DSC and rotational viscometer. The applied approaches for correlation of the methods are introduced in Section 5.3.1. Subsequently, the impact of the prolonged storage duration, humidity and the batch variations on the cure behavior of EMC 1 is studied with DEA in-situ in transfer molding process. The obtained DEA results are correlated with the rheology results. The results of the correlation of the DEA with DSC and rotational rheometer as well as the feasibility of the DEA as an in-situ cure monitoring in transfer molding process are given in Section 5.4.

5.1 Preliminary Experiments of Process Parameters

Preliminary experiments of process parameters are performed to investigate three aspects. The first aspect is to examine the dominant process parameters on void formation, wire sweep and warpage. For this reason, molding temperature, holding pressure, preheat time and transfer speed are selected as molding parameters. In order to define a suitable process window, which does not lead to any incomplete filling of the package for the selected molding parameters, three steps are applied for process analysis.

In the first step, an experimental setup with 13 experimental points is conducted to test the limitations of the process and to decide for a suitable range of the process window which allows a complete filling of the package. The molding parameters are varied as following: temperature between 155 °C – 185 °C, preheat time between 0 s – 20 s, transfer speed between 0.5 mm/s – 6.5 mm/s and holding pressure between 80 bar – 180 bar. The demonstrators are molded with critical parameter combinations such as fast transfer speed with a low temperature and no preheat time to analyze whether the cavity is filled completely or whether the selected process parameter combinations cause incomplete filling of the demonstrator or strong sticking of the molding material at the cull area, which requires long cleaning time of the cavity after the cycle is over. The selected process parameter combinations for this experiment and the results in terms of incomplete filing of the demonstrator are given in Appendix A1.

Based on the results from the first step of process analysis, the process window is selected, which assures the complete filling of the demonstrator. The selected process window of the molding parameters and the levels are shown in Table 5.1.

Table 5.1: Process parameters and levels used in the DoE for preliminary experiments

Factors	**Level**		
	-1	***0***	***+1***
Molding temperature [°C]	165	175	185
Holding pressure [bar]	80	110	140
Preheat time [s]	0	8	16
Transfer speed [mm/s]	1.5	4	6.5

In the second step of the process analysis, an additional set of experiments is conducted with the defined range of the process window as shown in Table 5.1 to determine whether package quality can be improved and void free packages can be obtained within this selected process window. Since the selected process window will be used also for the main experiments, which includes an optimization step, it is important to verify that the voids can be diminished within the selected process parameters. Otherwise, a real optimum process parameter combination for void free packages lies outside of the selected process window and cannot be achieved with the defined process window. Voids are one of the easily investigated quality features in comparison to warpage and wire sweep, thus for this feasibility analysis of the process window only the void formation is evaluated. In addition, the impact of vacuum is also investigated to decide whether the vacuum has significant impact on void formation and should be used during the experiments throughout this work. Therefore, an additional set of 9 experimental runs is performed. The selected process parameter combinations and the results of void formation analysis are given in Appendix A2. Based on the obtained results, it is observed that the selected process range of the process parameters yields void free packages and the vacuum should be used during the rest of the experiments in this study since it shows a positive impact on reduction of the voids in the package. These two steps of process analysis do not involve a detailed investigation of the quality characteristics and are done only to define the processing conditions and limitations of the transfer molding process to prepare a suitable process window for the third step, which is the main focus of this chapter.

In the third and main step of the process analysis, a detailed analysis of the influence of process parameters on void formation, wire sweep and warpage is done. In previous steps of the process analysis, since the goal is only to determine the complete filling and the void free packages, only the lead frames without any wire bonds and dummy components are used. In this step of the process analysis, the demonstrator with a given layout as shown in Figure 4.2 is utilized. As all the named quality features are analyzed in detail with the defined layout, the results of this step of the process analysis are elementary for definition of the experiment matrix and the quality features which will be then analyzed in the main experiments. Thus, the results of this main process analysis are the focus of the preliminary experiments and they will be given in detail. To identify the dominant process parameters, DoE is generated and designed in a way that only one process parameter is varied in each parameter set. As previously explained in Chapter 2, such kind of experimental design is called one-factor-at-a-time (OFAT) where a direct impact of individual process parameters on the quality characteristics can be identified. On the other hand, the interactions between the process parameters and the quadratic influences of the process parameters on the package quality cannot be studied with this design. Only a linear correlation between the input parameter such as varied process parameters and output parameters such as quality characteristics is possible.

In OFAT design four process parameters; molding temperature (T), transfer speed (v), preheat time (t) and holding pressure (P) are set in three levels, which gives altogether nine parameter combinations. In addition, one central point, that is the middle of three levels for each process parameter, and three additional extreme case combinations are supplemented in the DoE such as parameter set no. 2, no. 3 and no. 12. Extreme case combinations are the parameter sets which affect the material viscosity at most such as low temperatures, short preheat time and very fast transfer speed. Experiment no. 5 is the central point, where all the process parameters are in their middle level. In total 13 different combinations are studied and each parameter set is run 5 times to maintain repeatable results. Considering that the mold tool has two cavities, overall ten samples are investigated for each parameter set. The experimental design for the preliminary experiments is illustrated in Table 5.2. In all experimental designs studied throughout this work, the parameter set no. is arranged based on the ease of varying the process parameter. Considering the fact that varying the temperature between the parameter set numbers requires the longest time until to reach the set temperature, the experimental plan is sequenced from lower temperature to higher temperature.

Table 5.2: Experimental design for the preliminary experiments

Parameter set no.	**T [°C]**	**v [mm/s]**	**t [s]**	**P [bar]**
1	165	4	8	110
2	165	1.5	0	80
3	165	6.5	0	140
4	175	1.5	8	110
5	175	4	8	110
6	175	4	0	110
7	175	4	8	80
8	175	6.5	8	110
9	175	4	16	110
10	175	4	8	140
11	185	4	8	110
12	185	6.5	16	140
13	185	1.5	16	140

The second aspect studied in preliminary experiments is the identification of the quality characteristics, which are strongly influenced by the process parameters. Accordingly, among void formation, wire sweep and warpage, the quality characteristics, which are significantly influenced by the change in the process parameters are determined. This is an important aspect since this work aims to improve the package quality with the variations of the process parameters, thus only the quality features which are greatly affected by the variations in the process parameters are relevant for this work.
Third aspect of the preliminary experiments is to analyze the suitability of the layout of demonstrator. This work considers the wire bonds on the layout as mechanical structures in which their deformations due to the selected process parameters are the focus. Hence, it is important that the selected layout for

the test vehicle is qualified to study the influence of process parameters on wire sweep. To evaluate that, the layout of the test vehicle is tested with preliminary experiments in order to determine whether the wire bonds withstand the extreme process parameter combinations such as high transfer speed, short preheat time and low molding temperature so that no wire bond lift-off occurs due to selected process parameters.

5.2 Results of Preliminary Process Experiments

In this section the results of preliminary experiments are given where the influence of the individual process parameters on the void formation, wire sweep and warpage are illustrated respectively. The quality characteristics, which are strongly influenced by the process parameters are determined.

5.2.1. Identification of Significant Process Parameters

Before the results of the quality characteristics are shown in this section, it is important to emphasize that all the examinations on the quality characteristics are performed after the PMC process. First, the demonstrators are molded with transfer molding process and subsequently transferred to an oven for PMC process. PMC is done at 180 °C for 4 h to achieve complete polymerization of the EMC. The results of the investigations on the influence of the process parameters on the void formation, warpage and wire sweep are given in following.

Void Formation

In Figure 5.1 the results of the void formation with respect to 13 experimental runs (Table 5.1) are shown. In this work not only the number of voids is measured, but also the area of the voids is evaluated. The reason for that is, that a package may contain large number of voids but the voids can have very small areas. On the contrary, a package may have a low number of voids, however, those voids can have very large areas, which may be critical for package quality. Hence, analysis of the number of voids as well as the area of voids can give an idea about the proportion of the number to the corresponding area of the voids in the package. The number of voids and the area of voids with respect to parameter set no. can be seen in Figure 5.1.

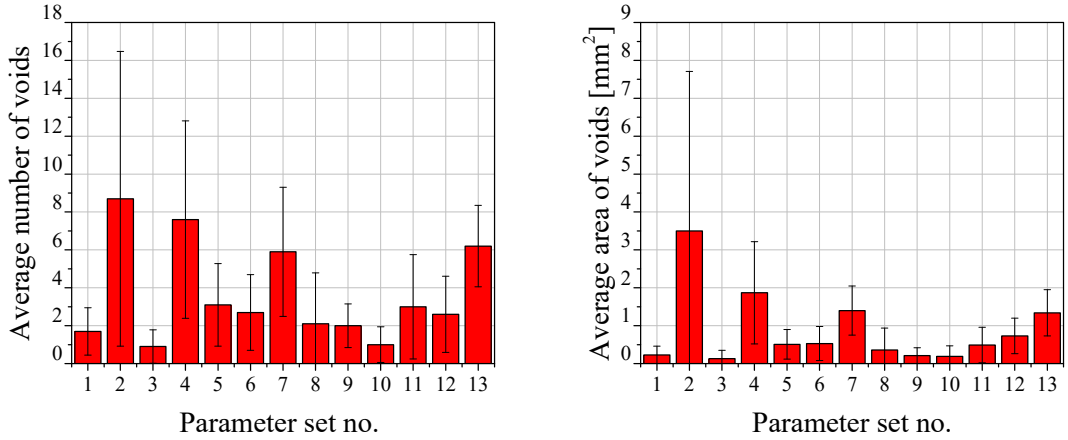

Figure 5.1: Effect of processing parameters on void formation, average number of voids with respect to 13 experimental runs (left), and corresponding average area of voids with respect to 13 experimental run (right)

It is obvious, that the number of voids formed in the molded package is influenced by different parameter settings. Some parameter combinations cause large void formation, whereas some process parameter combinations lead to less void formation in the packages. For instance, the packages, which are molded with parameter set no. 3, show a low number of voids in combination with very small areas. On the other hand, one of the extreme process parameter such as parameter set no. 2 causes large void formation in the package. Figure 5.2 displays the example of such packages with large void formation as well as the molding package with very little void formation to visualize the effect of processing parameters on

the void formation in the package. The package on the left hand side in Figure 5.2 is molded with an experiment run no. 10, from which very low void formation is observed in the packages. As a matter of fact, in some of the packages, which are molded with experiment run no. 10 no void formation in the package is observed. In Figure 5.2 (left), one of such molded packages is presented. In addition, in Figure 5.2 (middle), another package is depicted, which is molded with the experimental run no. 2, and has many large voids having different sizes in the package.

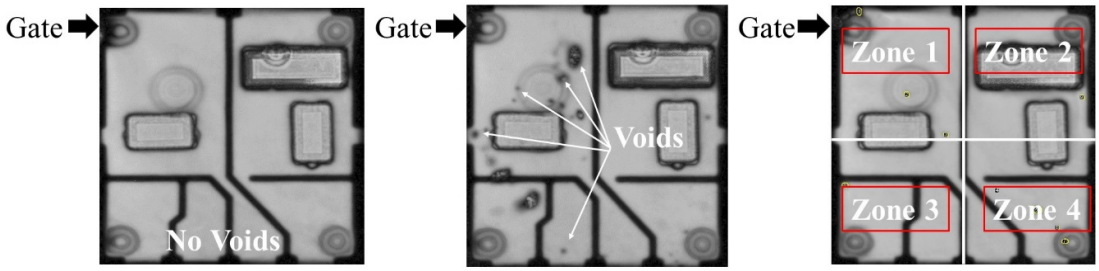

Figure 5.2: SAM images of the molding packages which show the influence of the processing condition on the void formation in the molded packages. The package which is molded with experimental run no. 10 shows no voids (left), the package which is molded with experimental run no. 2 shows many voids (middle). To analyze the positions of the voids on the layout, the layout of the demonstrator is divided into four zones and the voids detected by the software are indicated with yellow circles on the image exemplarily (right)

As seen in packages depicted in Figure 5.2, voids are formed in different positions in the package. Identification of the positions of the voids in the package is important to determine the zones, where the voids are formed at most and to define the critical areas on the layout. For this reason, the voids are divided into four different zones as illustrated in Figure 5.2 (right), where the zone 1 is the area close to the gate and the zone 4 is the area which is far from the gate. Figure 5.3 depicts the average number of voids, and the corresponding area of voids which are observed in different zones on the layout of the molded package.

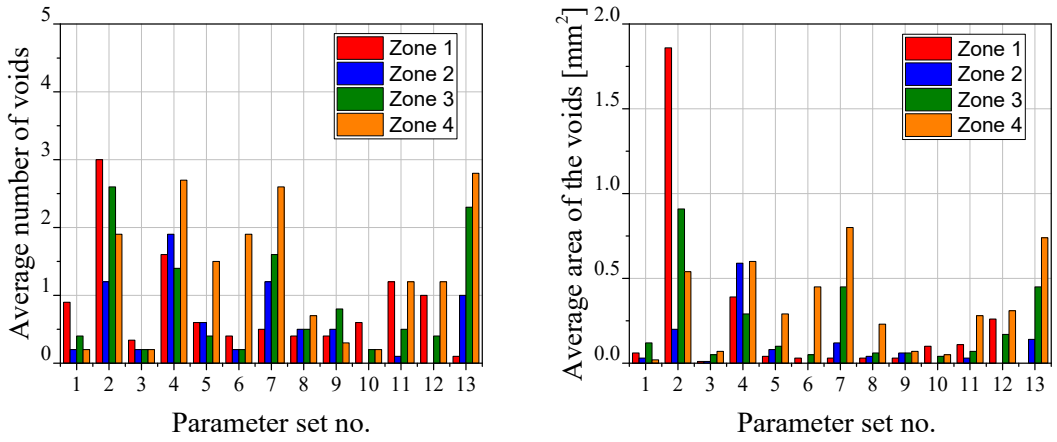

Figure 5.3: Void formation in different zones on the layout of the package with respect to different process parameters, the number of voids formed in four different zones (left), the corresponding area of the voids in four different zones (right)

Apart from the extreme process parameter combinations, such as parameter set no. 2, in which very large voids are formed (see Figure 5.2 middle), the voids are formed usually in zone 4, which is far away from the gate. On the other hand, reduced void formation is observed near the gate area.
According to the DoE plan given in Table 5.2, when the void formation in the parameter set no. 6, 5 and 9 are compared with each other, the influence of preheat time on the void formation can be analyzed. Similarly, when the void formation in the parameter set no. 1, 5 and 11 are compared, the impact of the

mold temperature on the void formation can be analyzed. The influence of holding pressure on the void formation can be observed by comparing the results of the parameter set no. 7, 5 and 10. Moreover, the effect of transfer speed can be determined by comparing the results of parameter set no. 4, 5 and 8. The influence of the individual process parameters on the void formation by comparing the aforementioned parameter set numbers are depicted in Figure 5.4 and Figure 5.5.

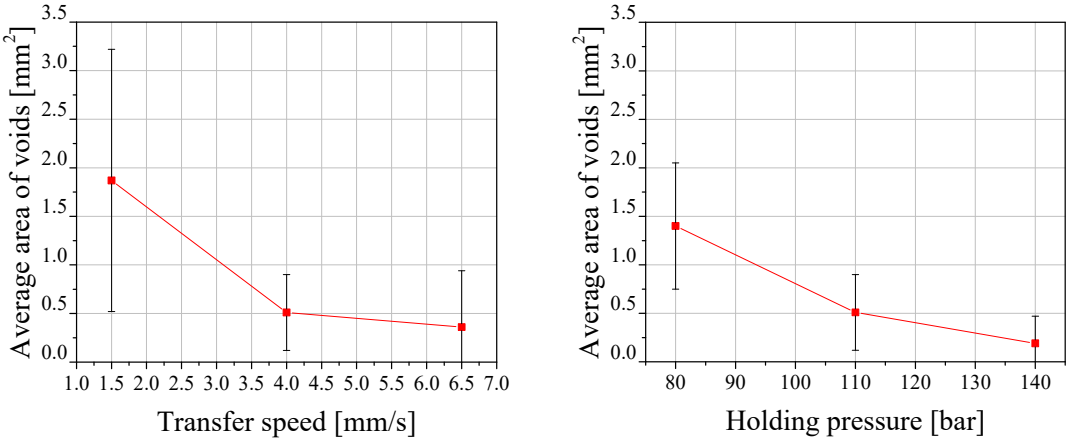

Figure 5.4: Influence of transfer speed of plunger (left) and holding pressure (right) on the average area of voids

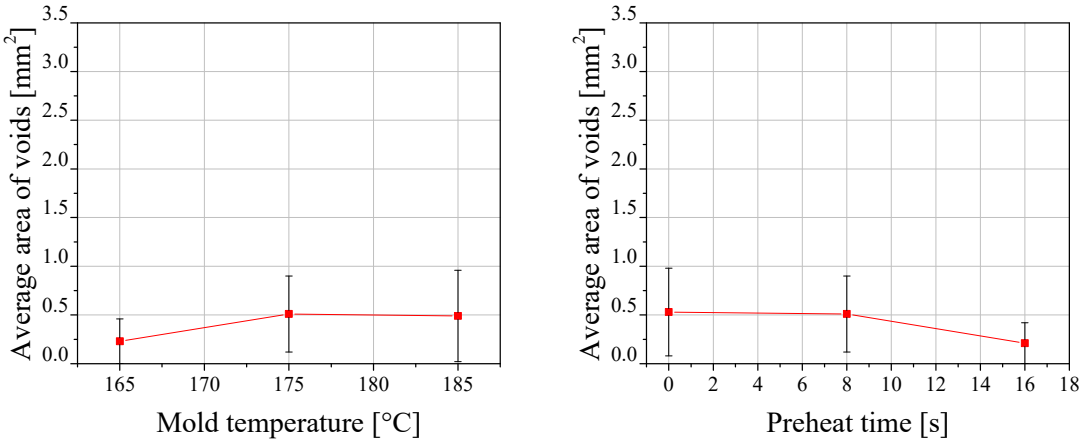

Figure 5.5: Influence of mold temperature (left) and preheat time (right) on the average area of voids

Among four varied process parameters, transfer speed and holding pressure show the major impact on the void formation. By increasing transfer speed, less voids are formed in the package (Figure 5.4 left). The largest influence is observed in holding pressure. The voids are formed at low holding pressure and with increasing the holding pressure, the void formation is reduced (Figure 5.4 right). According to Figure 5.3, when the void formation in parameter set no. 7, 5 and 10 are compared which delivers the influence of holding pressure, it can be seen that the number of voids as well as the corresponding area of the voids, especially which are formed in the zone 4, are decreased by increasing the holding pressure. On the other hand, as seen in Figure 5.5, molding temperature and preheat time show only slight impact on the void formation. Thus, void formation is not strongly affected by the change in mold temperature or preheat time.

Wire Sweep

In Figure 5.6, the effects of processing conditions on the wire sweep of the long wire bonds attached in near gate and far from gate area as well as short wire bond attached in near gate and far from gate area are presented.

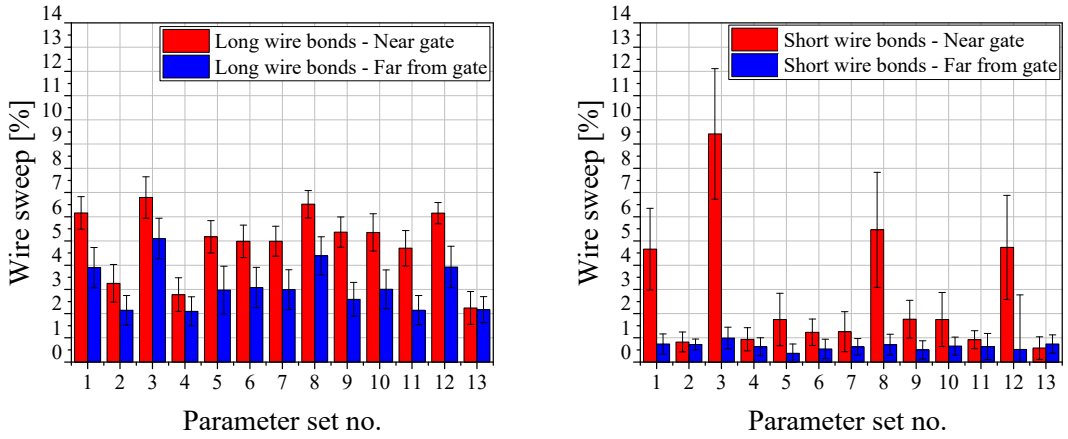

Figure 5.6: Effect of processing conditions on long wire bonds located in near gate and far from the gate (left), and on short wire bonds located in near gate and far from the gate (right). For the represented comparison of the positions and the lengths, wire bonds with a direction of 45° to the gate are chosen.

According to Figure 5.6, the long wire bonds attached in both positions on the test vehicle, namely near gate and far from the gate area are strongly influenced by the process parameters. Long wire bonds attached close to the gate area show more wire sweep compared to the long wire bonds attached far from the gate. Similarly, the short wire bonds attached close to the gate area show more wire sweep compared to the short wire bonds located far from the gate area. Moreover, long wire bonds exhibit larger wire sweep in comparison to the short wire bonds. Nevertheless, in certain parameter combinations, short wires attached at the close to the gate area also exhibit large wire sweep. Short wire bonds represent especially large wire sweep in parameter set no. 1, 3, 8 and 12. According to Table 5.2, those are the processing conditions, which are characterized by an increased transfer speed. In particular, in parameter set no. 3, where the extreme process parameter combination is selected, the short wire bonds represent excessive wire sweep.

Figure 5.7 depicts the influence of the processing conditions on the long wire bonds which are attached at different angles to the gate, namely at 90°, 180° and 45° in near gate and far from the gate area on the test vehicle (see Figure 4.2 for the layout).

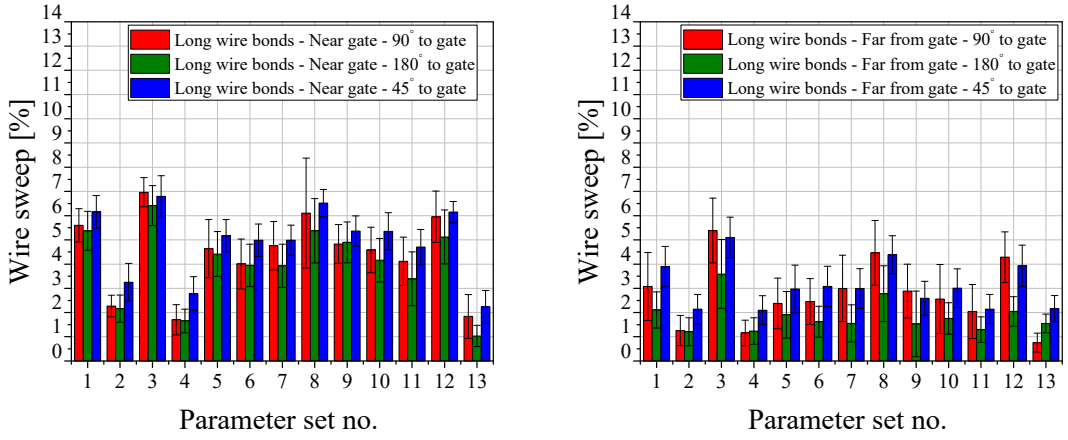

Figure 5.7: Effects of the processing conditions on the different direction of the long wire bonds which are attached at 90°, 180°, and 45° to gate in near gate (left), and far from the gate area (right)

Different processing parameters show the similar impact on the wire bonds which are attached at different angles to the gate. The tendency of the wire sweep with respect to the different process parameters is very similar in all angles of the wire bonds. Nonetheless, slight variations in the wire

sweep are observed within different angles of the wire bonds to the gate. Among different wire bond angles to gate, the mean values of the wire sweep for the long wire bonds which are attached in near gate area with 180° to the gate is slightly lower compared to the mean values of the wire sweep for the wires bonded at 90° and 45° to the gate. Similar results are also observed for the long wire bonds attached far from the gate (Figure 5.7 right).

Figure 5.8 illustrates the influence of the process parameters on the short wire bonds attached at 90°, 180° and 45° angle to the gate which are bonded in near gate (Figure 5.8 left) and far from the gate area (Figure 5.8 right).

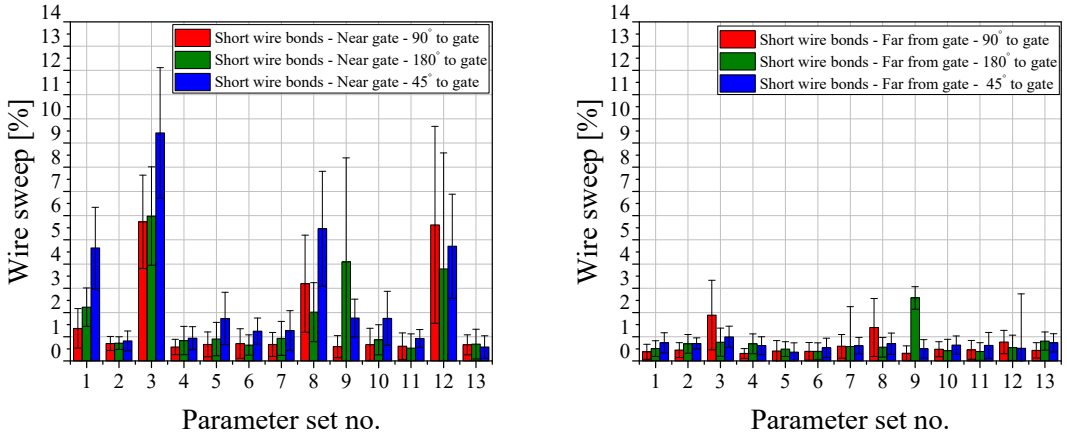

Figure 5.8: Effects of the processing conditions on the different direction of the short wire bonds which are attached at 90°, 180°, and 45° to gate in near gate (left), and far from the gate area (right)

For the short wire bonds, especially for the ones which are bonded far from the gate area, it is difficult to identify any difference in wire sweep for different angles of the wire bond due to minimal wire sweep observed in all wire bond directions (Figure 5.8 right). For the short wires attached in near gate area, especially for the parameter set no. 1, 3, and 8, where large wire sweep occurs, the difference in the wire sweep between the different angles of the wire bonds can be recognized easily. In these parameter sets, the mean values of the wire sweep for the wire bonds attached at 45° to the gate is slightly higher in comparison to the mean values of the wire sweep for the wire bonds attached at 180° and 90° to the gate. Figure 5.9 and Figure 5.10 show the influence of transfer speed, mold temperature, preheat time as well as holding pressure on the wire sweep of short wire bonds and long wire bonds attached in near gate and far from the gate area.

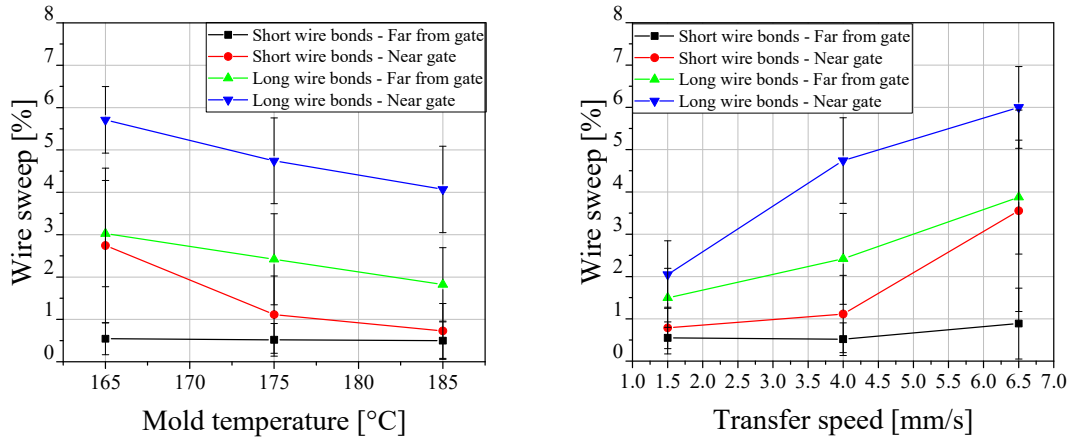

Figure 5.9: Influence of mold temperature on wire sweep (left), influence of transfer speed on wire sweep (right) for short and long wire bonds attached in near and far from the gate area

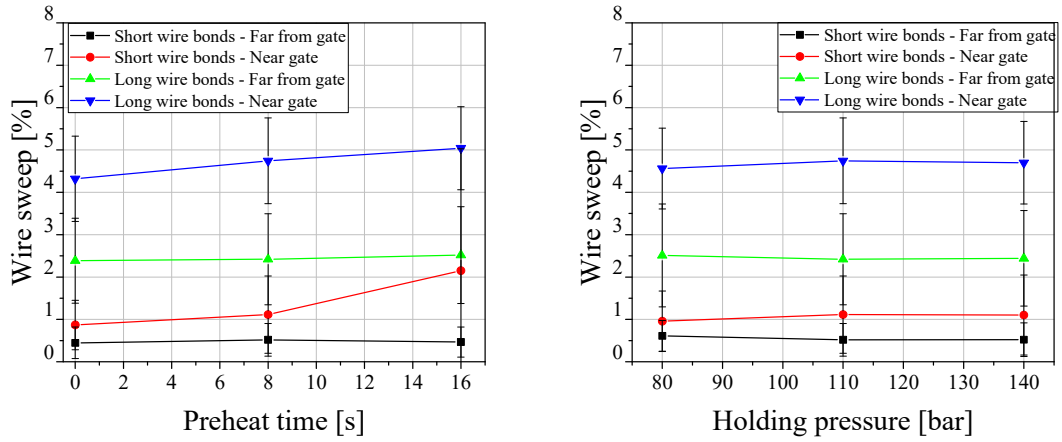

Figure 5.10: Influence of preheat time on wire sweep (left), influence of holding pressure on (right) for short and long wire bonds attached in near and far from the gate area

Among four process parameters, transfer speed and mold temperature are found as the most significant process parameters on the wire sweep. As seen in Figure 5.9, raising the mold temperature leads to less wire sweep for short wire bonds and long wire bonds attached in near gate and far from the gate area. Increasing transfer speed, however, causes more wire sweep on short and long wire bonds. As previously shown in Figure 5.4, increasing transfer speed causes less void formation in the package which is the opposite effect of transfer speed observed on wire sweep. Therefore, to achieve better package quality, which involves improving both quality features, a compromise should be done when defining optimum process parameters. On the other hand, as seen in Figure 5.10, the variations in holding pressure and preheat time do not demonstrate any significant changes in the wire sweep for short and long wire bonds both in near gate and far from the gate area. Only for the short wire bonds attached near to gate, increasing preheat time causes slightly more wire sweep. On the other hand, the impact of the different process parameters on the short wire bonds at the far from the gate area cannot be determined clearly as the short wire bonds at far from the gate area illustrate minimized wire sweep almost in all parameter combinations (see Figure 5.8 right).

Warpage

For the warpage analysis four line contours, namely line 1, line 2, line 3 and line 4 are set on the molded package, which are already depicted in Figure 3.20 and the deviations in the z-direction are measured along these lines. The maximum values obtained in z-direction on the surface of the package deliver the maximum warpage, which is presented in Figure 5.11. In addition to the maximum warpage value measured for each of those lines, the average warpage is also calculated, which represents the mean value of all four lines (Figure 5.11 right).

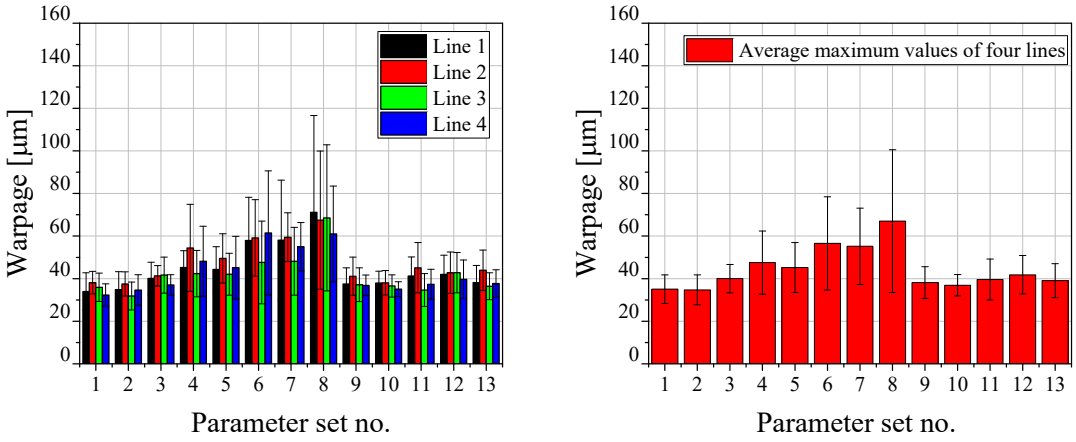

Figure 5.11: Maximum warpage value for each measured line on the molded packages with respect to 13 process parameter no. (left), average value obtained considering all four lines together with respect to parameter set no. (right)

Based on the results obtained from the warpage measurements, it is observed that the surface of the molded packages bends upwards in all packages and the data of the warpage has a positive value. This indicates that the type of the warpage in the package is convex. Nevertheless, based on the results of all 13 process parameter set numbers, which are illustrated in Figure 5.11, the average of the maximum warpage value lies under 100 µm. However, as it can be seen from the plotted curves, there are also large standard deviations within a single process parameter set, such as parameter set no. 8. Moreover, the standard deviation in such parameter sets, e.g. parameter set no. 8 show a large scatter that it covers all the range of variations in warpage values within the 13 parameter set numbers. Thus, to analyze the differences in the warpage values more precisely, the measured warpage for each molded part for all parameter set numbers is plotted in Figure 5.12. Considering left and right cavity as well as the five repetitions of each parameter set, ten parts are analyzed for every single parameter set, which are represented between the black vertical lines in Figure 5.12. The warpage of overall 130 parts are illustrated in the diagram.

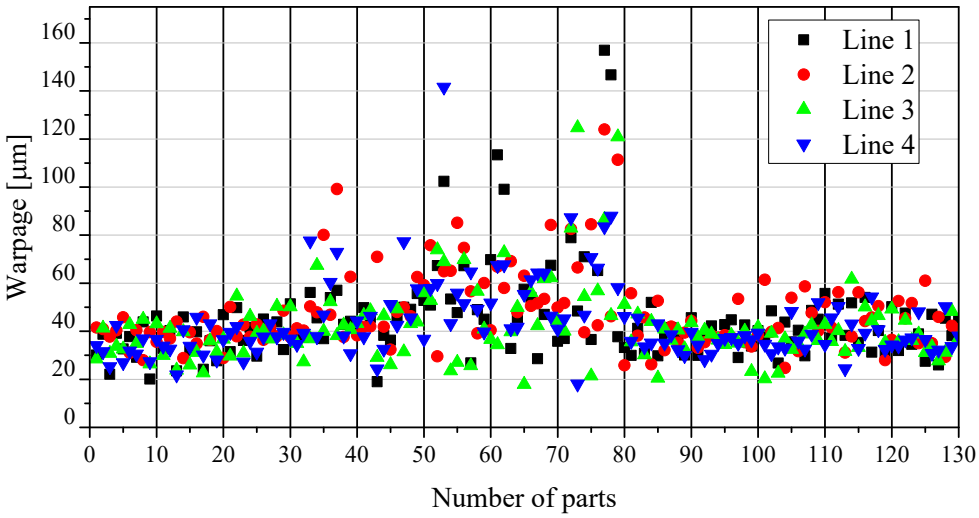

Figure 5.12: Maximum warpage values in four line contours for all measured parts. The points between the black lines belong to one parameter set beginning from the parameter set no. 1 until parameter set no. 13. For instance, the number of parts between 70 and 80 belongs to the parameter set no. 8.

The results show that in some parameter sets, such as parameter set no. 6, 7 and 8, there are large deviations between the measured maximum warpage values within one single process parameter set. For instance, for parameter set no. 8 the warpage values vary from 20 µm to 160 µm. On the contrary, although there is 20 °C difference in temperature between the number of parts until 30, and the number of parts after 80, no big variation is observed in maximum warpage. Therefore, based on the warpage values shown in Figure 5.12 it is evident that, the deviation of the warpage values within one single parameter set is much larger in comparison to the deviation in the warpage values between 13 different parameter sets.

It is important to mention that, during the measurements, it is recognized that across the measured lines, in some cases there may be one or two points having very high values in the z direction possibly due to some surface artifacts on the surface of the molded package. Only considering the distinct maximum value as a warpage, which may be caused possibly due to some surface artifacts can lead to false interpretations. Thus, to assure the results, in addition to the maximum point observed along the lines which are illustrated in Figure 5.12, the area under the four lines, namely line 1, line 2, line 3 and line 4 (see Figure 3.20) are also calculated to build an overall image in terms of the package surface. The results of the area under the curve of the lines are compared with the results of the maximum point observed on the lines. However, the warpage values obtained by calculating area under the lines also show similar results as the maximum warpage value shown in Figure 5.12. No significant difference in the warpage values obtained from the area under the curves are observed between the different process parameters and still a large scatter exists within a single parameter set. Thus, hereby the results are approved with an additional consideration. Therefore, considering the obtained results, it can be stated that, although the process parameters are significantly varied such as 20 °C difference in the mold temperature between the process parameter sets, which may indeed influence the package warpage, no significant variations in the warpage are observed between the different process parameters. Additionally, the deviation of the warpage values observed within one parameter set is found much larger in comparison to the deviation of the warpage values between different process parameter sets.

5.3 Preliminary Investigations of Material Characteristics

In this section the preliminary experiments are introduced, which are conducted to assess the suitability of the DEA method to observe the possible variations in the material characteristics of EMC 1 in-situ in the transfer molding process. However, before explaining the DEA results, it is crucial to understand and interpret the DEA results correctly. Thus, the obtained DEA signals are correlated and compared with rotational rheometer and DSC measurements. The approaches used for the correlation of the DEA with DSC and rotational rheometer are introduced in Section 5.3.1.

Furthermore, the influence of prolonged storage duration, humidity and batch variations on the material characteristics of EMC 1 are studied. Rotational rheometer and squeeze flow rheometer are used to analyze the variations in the viscosity of EMC 1. The preconditioned materials are also measured with DEA in-situ in transfer molding process to evaluate any possible changes in ion viscosities of the material. All measurements performed with DEA in the transfer molding process in this section are conducted with central process parameters at a temperature of 175 °C, transfer speed of 4 mm/s, preheat time of 8 s and a holding pressure of 110 bar. The experimental approach performed to investigate the influence of storage duration, humidity and batch variations on EMC 1 characteristics are introduced in Section 5.3.2, 5.3.3 and 5.3.4 respectively. To assure whether humidity and temperature stay constant during humid and dry storage in the chambers and also to control the measurements, a data logger Multimetrix DL 53 is used. Humidity and temperature are recorded with data logger during the whole storage duration time in the chambers for each measurement in this work. To produce the sample bars for the analysis with thermal and mechanical methods, the transfer molding press Lauffer VSKO 25 is used. More information about the mold tool and the cavity geometry can be found in Section 3.2.2. The results of the measurements described in this section are given in Section 5.4.

5.3.1 Correlation of DEA with Rotational Rheometer and DSC

DEA is chosen in this work as an online monitoring method in transfer molding process in order to observe small variations in the characteristics of the EMC. To interpret the information delivered from the DEA correctly, it is essential to understand the course of ion viscosity curve and the important characteristics of the ion viscosity curves. Therefore, the DEA is compared and correlated with the rotational rheometer and DSC measurements. The specific details about the DEA-Rotational Rheometer and DEA-DSC correlation are explained in this section respectively.

DEA-Rotational Rheometer Correlation

DEA is a monitoring technique where the mobility of ions in a sample is measured during the polymerization of EMC and indicated as ion viscosity as explained previously in Chapter 2. Since the rotational rheometer measurement is a standard conventional laboratory method to measure the shear viscosity of the material and to analyze the rheological behavior of the EMC, dynamic viscosity in other words, shear viscosity is more straightforward in understanding compared to the ion viscosity. Thus, the correlation of the ion viscosity to shear viscosity can help to comprehend the course of ion viscosity curve. Simultaneous rotational rheometer-DEA measurement is performed to determine the correlation between ion viscosity and the dynamic viscosity. The progress of curing reaction, which is observed simultaneously with DEA and rotational rheometer are correlated.

Correlation of Degree of Cure Obtained from DEA with DSC

The DEA signal represents the curing reaction of the EMC from the beginning of the uncured stage of epoxy resin until the end of cure. An ion viscosity curve shows the progress of reaction step by step during polymerization of EMC, however, the degree of cure at different stages of the reaction cannot be directly measured with DEA. DEA can only deliver the ratio of the crosslinking degree at a corresponding time, by taking the maximum ion viscosity as 100 % and minimum ion viscosity as 0 % crosslinking degree. However, that does not exactly reflect the real situation of crosslinking degree in the EMC because neither the crosslinking degree reaches 100 % at maximum ion viscosity nor the polymer has 0 % crosslinking degree at the minimum ion viscosity. EMC already starts curing at early stages of the reaction even before reaching the minimum ion viscosity. For this reason, to determine the actual cross linking degree of EMC, DSC measurements are performed and the reaction enthalpy of EMC 1 is measured and correlated with the ion viscosity curve obtained from DEA. To examine the degree of curing in EMC 1 at different stages of cure reaction, the molding process is stopped after the defined cycle times such as 30 s, 60 s, 90 s, 120 s, 180 s, and 240 s, then the sample bars are successfully removed from the molding machine. To suspend the cure reaction after the termination of the molding process, the sample bars are cooled down in a liquid nitrogen chamber and immediately submitted to DSC to measure the residual heat of reaction of the samples corresponding to the portion that is not polymerized during molding. In addition to EMC 1 pellets, which are molded at various lengths of cycle times in the molding machine, 0 h EMC 1 pellets in other words fresh EMC 1 pellets, which are only thawed in room temperature for 1 hour are also measured with DSC to determine the initial status of EMC 1. The experimental approach applied is shown schematically in Figure 5.13.

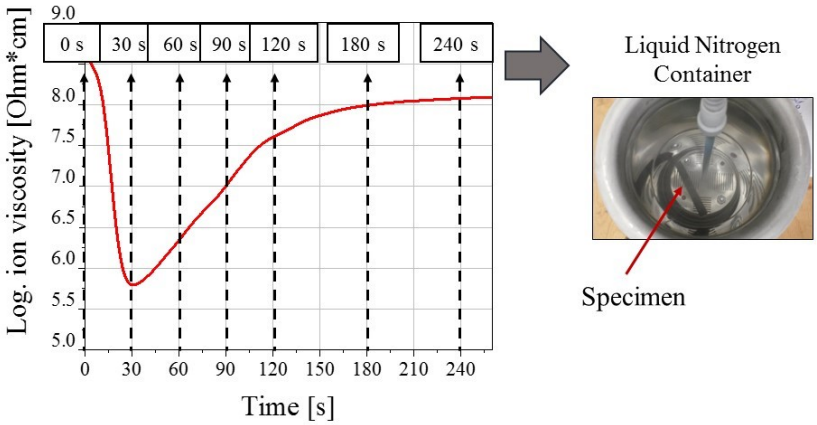

Figure 5.13: Experimental approach to correlate the ion viscosity curve with reaction enthalpy obtained from DSC measurements, the molding cycles are terminated after certain times i.e. 0 s, 30 s, 60 s, 90 s, 120 s, 180 s , 240 s and the specimens are cooled down in a liquid nitrogen container to terminate the reaction and conveyed immediately to DSC measurement

After the measurement with DSC, the residual heat of reaction of the samples is measured and the degree of crosslinking of the samples at corresponding molding cycle time is calculated as described in Section 3.3.2.

5.3.2 Storage Duration

The impact of the prolonged storage duration on the characteristics of EMC 1 is investigated by preconditioning the samples for 0 h, 8 h, 16 h and 24 h in a vacuum oven at 0 % RH and 30 °C. Before preconditioning EMC 1 pellets, all pellets are thawed at room temperature in a desiccator for 1 hour. The preconditioned EMC 1 pellets are then measured with a rotational rheometer to examine the influence of the storage duration on the viscosity behavior of EMC 1. Furthermore, additional pellets which are preconditioned with similar approach are molded in transfer molding process and measured with DEA simultaneously. Each DEA measurement for the preconditioned samples is repeated at least 8 times and the average value of the measurements is calculated. The rheology behavior of the preconditioned EMC 1 pellets obtained from the rotational rheometer measurements and the DEA measurements are compared with each other.

In order to clarify whether a period of storage time longer than 24 h has an influence on EMC 1 curing characteristics, the storage duration is extended until 72 h. The pellets are preconditioned additionally for 48 h and 72 h at 30 °C and 0 % RH. The preconditioned pellets are measured with rotational rheometer to determine the influence of the extended storage duration of 48 h and 72 h on the viscosity behavior of the EMC. Moreover, the preconditioned pellets are molded in transfer molding process by monitoring with DEA. The results of DEA are compared with the results obtained from rotational rheometer.

5.3.3 Humidity

The impact of the moisture on the EMC characteristics is analyzed by preconditioning EMC 1 pellets in a climate chamber with 90 % RH, at 30 °C. First, all samples are thawed in a desiccator for 1 hour and subsequently preconditioned for 0 h, 8 h, 16 h and 24 h in humid environment. The pellets with different preconditioning durations in humid environments are analyzed with rotational rheometer under isothermal and non-isothermal conditions to understand the effect of humidity on dynamic viscosity of EMC 1. Moreover, additional pellets, which are preconditioned in the same way, are molded in transfer molding process and measured with DEA simultaneously. The effects of the humidity on the ion viscosity behavior and the dynamic viscosity behavior of EMC 1 are discussed.

The similar approach as in the storage duration is also used here in terms of prolonging the storage duration of EMC 1 pellets in a humid environment. EMC 1 pellets are further stored in a climate oven

at 90 % RH and 30 °C for 48 h and 72 h to observe whether the pellets reach any saturation point in terms of water uptake and whether the ion viscosity is influenced by the extended preconditioning in humid environment. The preconditioned pellets are molded and measured with DEA to identify any possible effects of humidity of EMC 1 on the ion viscosity. To determine the moisture uptake during the humidity storage time in EMC 1 until 72 h, preconditioned pellets are analyzed with Karl-Fischer Titration. To identify the water uptake trend in EMC 1 pellets until 8 h storage duration, additional 2h and 4 h storages are performed and the moisture content of the pellets is measured with Karl-Fischer Titration as well.

To understand the humidity influence on curing behavior of EMC in detail, it is important to differentiate, whether the effect originates from the extended storage duration itself only by preconditioning in dry environment, or whether the effect results due to humidity storage. Thus, the results obtained from Section 5.3.2 are compared with the results obtained from Section 5.3.3. Table 5.3 summarizes the investigations performed in terms of preconditioning the pellets in dry and humid environments.

Table 5.3: Preconditioning of the samples in dry and humid environment

Fresh samples	Preconditioning at 30 °C / 0 % RH	Preconditioning at 30 °C / 90 % RH
0 h	-	-
-	8 h	8 h
-	16 h	16 h
-	24 h	24 h
-	48 h	48 h
-	72 h	72 h

5.3.4 Batch Variations

Possible alterations between different batches are examined by selecting three batches marked as batch 1, batch 2 and batch 3. Among all batches, batch 3 is the one characterized by a minimum storage duration, whereas batch 1 is characterized by a longest storage duration. The rheological behavior of three batches is analyzed with rotational rheometer to identify any variations in properties. In addition, DEA measurements are performed to detect possible alterations in the properties of EMC 1 batches in the transfer molding process.

5.4 Results of Preliminary Investigations of Material Characteristics

In this section, the results of the characterization of EMC 1 are introduced, which are described in Section 5.3. The results obtained from the simultaneous DEA-Rotational Rheometer measurement and DEA-DSC correlation are represented in Section 5.4.1. The obtained correlation should help to gain more understanding on the cure reaction of EMC 1 and the progress of ion viscosity curve observed with DEA. The results of the impact of the prolonged storage duration, humidity and batch variations on the curing characteristics of EMC 1 are given in Section 5.4.2. The preconditioned EMC 1 pellets are characterized with rheological methods as well as with DEA and the results obtained from the methods are compared. The suitability of the DEA to detect the possible variations in the material characteristics of EMC 1 due to storage duration, humidity and batch variations is discussed.

5.4.1 Results of Correlation of DEA with Rotational Rheometer and DSC

In this section, the results of the correlation of DEA with rotational rheometer as well as with DSC method are given respectively. The important features of the obtained correlations are discussed.

Correlation of DEA with Rotational Rheometer Measurement

Figure 5.14 depicts the results of the simultaneous DEA-Rotational Rheometer measurement, where the ion viscosity measured with impedance spectroscopy at 10 Hz and the shear viscosity is measured with a rotational rheometer.

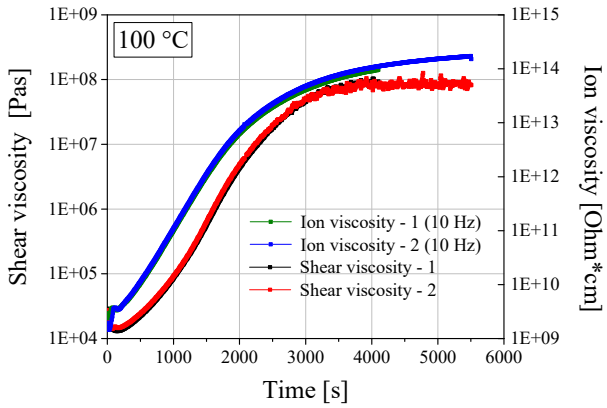

Figure 5.14: Simultaneous DEA-rotational rheometer measurement conducted at isothermally at 100 °C measuring the ion viscosity with an interdigital capacitor at 10 Hz and the shear viscosity with rotational rheometer

The results of the simultaneous DEA-rotational rheology measurement show that the cure reaction behavior of EMC 1 represents the similar behavior at the same time scale in both methods. At the time around 300 s, where the molding compound has its minimum viscosity, the ion viscosity measured with DEA shows also its minimum value. When the cure reaction starts accelerating, the shear viscosity of material raises quickly, correspondingly the ion viscosity of EMC 1 is raising as well. The slopes of the curves, which represent the reaction speed of EMC 1, match very well with each other in both methods. After around 2000 s the slope of the dynamic viscosity curve starts decreasing which indicates that the reaction comes slowly to the end. At the same time, the slope of the ion viscosity curve decreases as well. When the dynamic viscosity reaches its maximum value after around 4000 s and no significant changes in the viscosity occurs anymore, the ion viscosity also reaches its maximum value. Therefore, the simultaneous DEA-rotational rheology measurement shows that the ion viscosity of EMC 1 observed with DEA shows very good correlation to the shear viscosity measured with the rotational rheometer.

Correlation of DEA with DSC measurement

A typical DEA curve measured with EMC 1 is shown in Figure 5.15 (right). The indicated points on the diagram of the DEA curve are the samples, which are molded for 30 s, 60 s, 90 s, 120 s, 180 s and 240 s in transfer molding and subsequently measured with DSC to determine the residual heat of reaction. Figure 5.15 (left) illustrates the results of measured residual heat of reaction of the samples which are molded in corresponding cycle times. Moreover, in Figure 5.15 (right) the degree of cure calculated based on the DSC results according to the selected points are also implemented in the DEA curve to illustrate the correlation of the progress of the ion viscosity with the degree of cure schematically. Additional information derived from the DSC measurements such as heat of reaction and T_g for different cycle times are listed in Table 5.4.

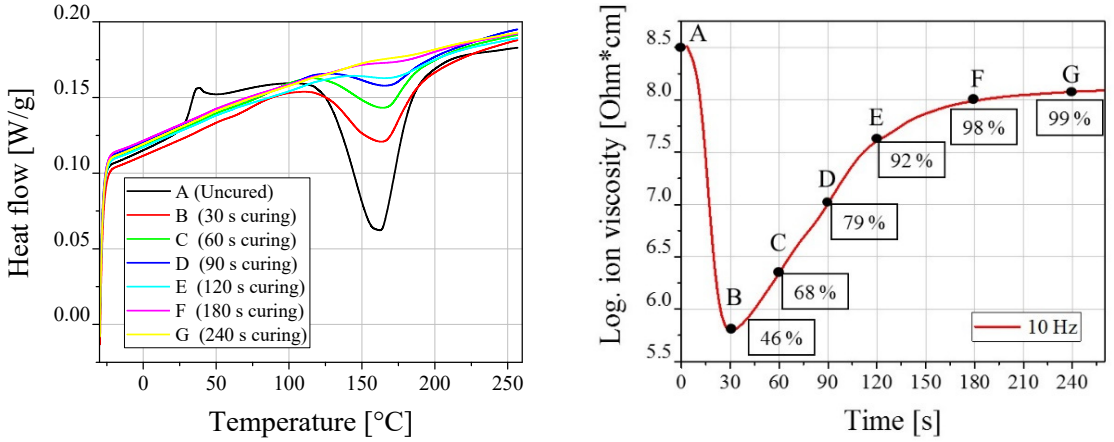

Figure 5.15: Results of the non-isothermal DSC curves for the samples, which are molded for different molding cycle times of 30 s, 60 s, 90 s, 120 s, 180 s and 240 s in transfer molding (left), DEA curve with a calculated degree of cure from DSC results for the corresponding cycle times (right)

Table 5.4: Results of non-isothermal DSC measurements with different molding cycle times

Represented points	**Cycle time [s]**	**Reaction onset [°C]**	**Reaction yield [J/g]**	**T_g 1st Run [°C]**	**T_g 2nd Run [°C]**	**Degree of cure [%]**
A	0	97	25.1	31	177	-
B	30	94	13.5	78	167	46
C	60	109	8.1	91	163	68
D	90	118	5.2	105	162	79
E	120	133	2.0	111	162	92
F	180	152	0.6	135	162	98
G	240	162	0.2	140	161	99

Based on the DSC results (Figure 5.15), it is apparent that the residual heat of reaction of the samples decreases with increasing cycle time indicating the progress of curing. At 30 s molding time, the ion viscosity of EMC 1 first reaches its minimum value, where the material has the lowest network density (Figure 5.15 (right), point B) and large heat of reaction (Table 5.4). As the cure reaction propagates, the ion viscosity escalates indicating the increase in the network density. By the time at around 240 s, ion viscosity reaches the plateau revealing that the cure reaction is almost completed. This correlates very well with the DSC results, as the remaining heat of reaction at point G with 240 s cycle time is very low, which signifies that the cure reaction is almost finished. Based on the measured residual heat of reaction, the degree of cure with respect to selected points is calculated (Table 5.4), which is also illustrated in Figure 5.15 (right). The results apparently show that the progress in the ion viscosity observed with DEA correlates very well with the degree of cure results, where with increasing in ion viscosity, the degree of cure of EMC 1 increases. When the cure reaction is almost over at 240 s, the material reaches its maximum network density. In fact, T_g of the samples also increases with increasing network density. Highest T_g in the first run can be observed with 240 s molding. Therefore, considering the results observed from the DSC, it is evident that the results of the DEA show good correlation with the results of the DSC. The ion viscosity expresses the progress of the cure reaction and the network density of EMC 1 excellently.

5.4.2 Results of Investigations of Material Characteristics

In this section, the results of the investigation in regard of the influence of the prolonged storage duration, humidity and the batch variations on the cure reaction of EMC 1 are presented. The variations in the viscosity of EMC 1 are characterized with a rotational rheometer as well as with a squeeze flow rheometer. The obtained results from the rheology methods are compared and correlated with the results obtained from the DEA. The suitability of DEA to determine possible variations in the EMC characteristics in-situ during transfer molding process is discussed. All DEA results, which are shown in this section, are performed with 10 Hz and the average values of the ion viscosities out of 8 measurements are represented in the diagrams.

Investigation of the Influence of Storage Duration on EMC Characteristics

Figure 5.16 illustrates the average logarithmic ion viscosity for the samples preconditioned for a time interval of 0 h, 8 h, 16 h and 24 h in vacuum oven with 0 % RH at 30 °C.

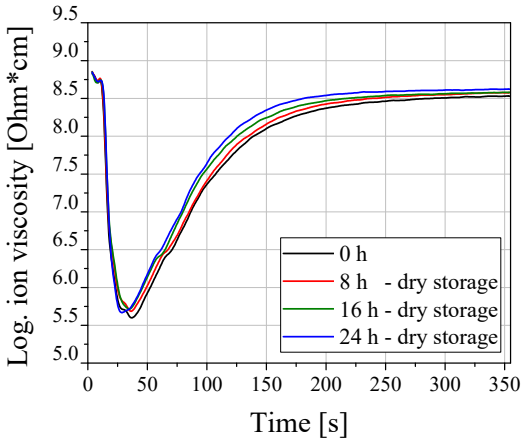

Figure 5.16: DEA curves for preconditioned EMC 1 pellets for storage time of 8 h, 16 h and 24 h in dry environment at 30 °C / 0 % RH as well as fresh pellets (0 h)

Only slight differences in the cure reaction of EMC 1 are observed with different storage durations. The minimum ion viscosities slightly increase with prolonging the storage duration. Correspondingly, the maximum ion viscosities at the end of the curing time also illustrate slight variations, which may however deliver the similar delta (Δ), which is the difference between the maximum and minimum ion viscosities. As mentioned previously, the delta can deliver information about the degree of cure of the molding compound [160]. The slopes of the reactions for different storage durations are found to be almost identical. In order to ascertain whether the storage duration has an impact on the dynamic viscosity behavior of EMC 1, rheological measurements are performed. Figure 5.17 depicts the isothermal and non-isothermal rotational rheometer results, where the viscosity behavior of the preconditioned pellets with respect to time and temperature are plotted respectively.

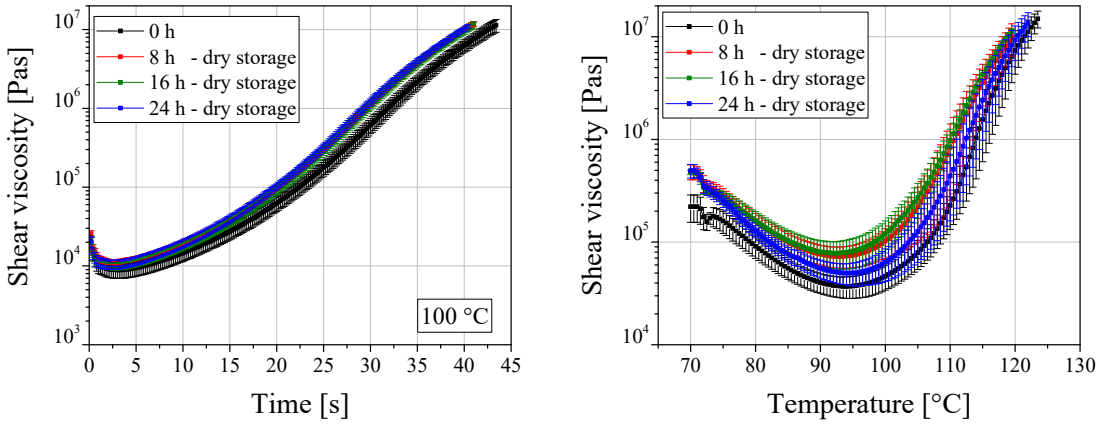

Figure 5.17: Isothermal rotational rheometer measurement at 100 °C (left) and non-isothermal rotational rheometer measurement with 2 K/min (right) for EMC 1 pellets preconditioned for 8 h, 16 h and 24 h in dry environment as well as fresh pellets (0 h)

The storage duration until 24 h does not affect the dynamic viscosity of EMC 1 remarkably. Only a slight difference on the dynamic viscosity between the fresh samples (0 h) and the samples preconditioned for an extended period of time can be observed. The gel time diminishes moderately with extended storage duration, which can be identified by the shift of the curve to the left on time scale. Similarly, no distinguishable trend for the dynamic viscosity of EMC 1 can be noticed with increasing storage time under temperature ramp in Figure 5.17 (right). Only a slight increase in the minimum viscosity of the pellets can be seen in the viscosity curves, which also confirms the results of the ion viscosities obtained from the DEA.

The storage duration is extended until 72 h to assure whether the material characteristics of EMC 1 stay further constant or any changes happen in the ion viscosity with the storage time exceeding 24 h. The pellets, which are preconditioned for 48 h and 72 h, are measured with DEA and the ion viscosity curves are analyzed. Figure 5.18 shows ion viscosities of the pellets as well as characteristic information derived from these ion viscosity curves such as minimum ion viscosity and the delta, which is the difference between the maximum and minimum ion viscosity.

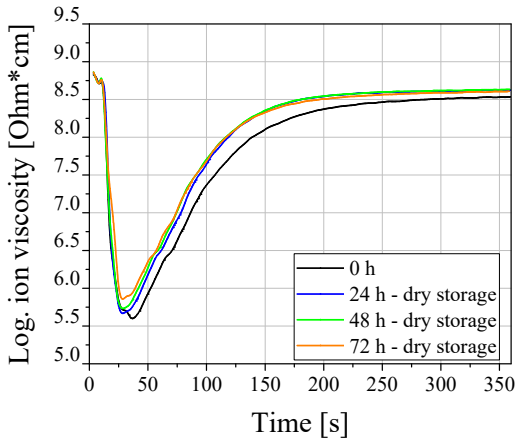

Storage duration	Minimum ion viscosity [Ohm*cm]	Δ (Difference max-min ion viscosity) at 350 s [Ohm*cm]
0 h	5.60	2.93
24 h	5.67	2.93
48 h	5.71	2.89
72 h	5.88	2.74

Figure 5.18: Logarithmic ion viscosity (left) and the characteristic information derived from the DEA curves such as minimum ion viscosity and the delta (right) for EMC 1 pellets, which are preconditioned for a storage time of 24 h, 48 h, 72 h at 30 °C / 0 % RH as well as fresh pellets (0 h)

No significant differences can be seen in the slope of the curves between the 24 h storage and 72 h storage, the speed of the reaction are almost found to be identical for all ion viscosity curves. Except the

ion viscosity curve for fresh samples (0 h), all curves arrive at the same maximum ion viscosities at the end of the reaction at around 350 s. However, the minimum ion viscosity slightly increases with prolonging storage duration which causes a difference in the delta. The delta between the maximum ion viscosity at 350 s and the minimum ion viscosity are calculated from the curves for each storage duration and depicted in Figure 5.18 (right). As it can be seen from the calculated values, the delta decreases with increasing the storage duration. However, to determine whether the difference in measured deltas are significant, the process stability analysis is done for the transfer molding machine with DEA measurements. The process stability analysis is conducted in a Lauffer VSKO 25 transfer molding press by performing 25 molding cycles with the same process parameter to observe the maximum deviations in the characteristics features of the DEA curves at 10 Hz such as maximum standard deviation observed in minimum ion viscosity, maximum ion viscosity, and the delta between the maximum and minimum ion viscosity. In this way, it can be possible to determine whether the difference between the measured deltas are significant. The maximum standard deviation measured in the delta out of 25 molding cycles is found as 0.08 Ohm*cm. Similarly, the standard deviation for the minimum ion viscosity are found as 0.08 Ohm*cm whereas the standard deviation for the maximum ion viscosity is found fairly lower and as 0.02 Ohm*cm. Thus, any difference bigger than these deviations can be considered as significant. Yet, based on the difference in the minimum viscosities and the differences in the delta given in Figure 5.18, it is evident that there is slight difference in characteristics of EMC 1 with prolonging storage duration. To approve the results obtained from the DEA and to determine whether the dynamic viscosities of EMC 1 also affected by the prolonged storage duration, rotational rheometer measurement are conducted. In Figure 5.19, the dynamic viscosities obtained from the rotational rheometer measurement are shown.

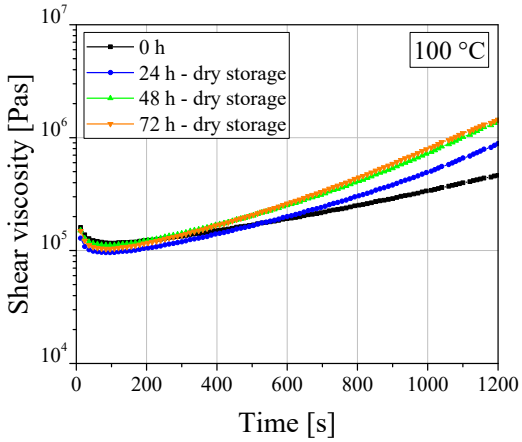

Figure 5.19: Dynamic viscosity of the preconditioned EMC 1 pellets for 24 h, 48 h, 72 h at 30 °C / 0 % RH as well as 0 h samples with respect to time measured with rotational rheometer at 100 °C

As seen in Figure 5.19, the dynamic viscosity or also-called shear viscosity shows similar results as in the ion viscosity where the viscosity of EMC 1 is influenced by extended storage duration. The viscosities of the pellets, which are preconditioned for 48 h and 72 h are found to be higher at the same time scale such as at around 1000 s in comparison to the pellets preconditioned for 24 h as well as fresh samples. This may indicate pre-crosslinking of the material during storage duration. The material may start already cross-linking at room temperature which may cause a raise in the viscosity.
In addition to the rotational rheometer, squeeze flow rheometer measurements are also conducted. In Figure 5.20, the measurements are illustrated, which are performed with the preconditioned pellets for storage durations of 0 h, 8 h, 16 h, 24 h, 48 h and 72 h in squeeze flow rheometer at 175 °C. Additional 4 h storage duration is also implemented in the diagram.

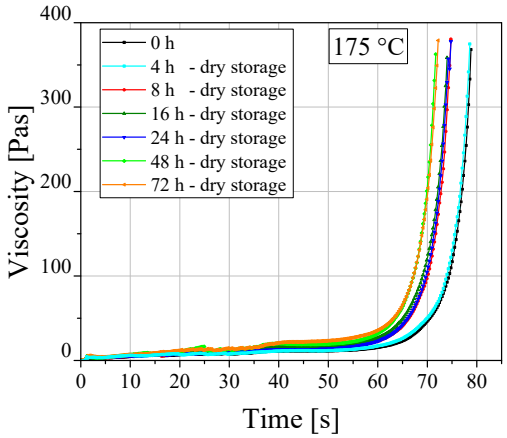

Figure 5.20: Viscosity measurement with squeeze flow rheometer at 175 °C for preconditioned EMC 1 pellets with storage durations of 0 h, 4 h, 8 h, 16 h, 24 h, 48 h, 72 h in dry environment at 30 °C / 0 % RH

The results of the squeeze flow rheometer also approve the results obtained from the rotational rheometer, where with extended storage duration, the viscosity behavior of EMC 1 changes. The squeeze flow rheometer results, which are obtained at 175 °C, illustrate that with increasing storage duration the gel time of the pellets decreases in which the viscosity curves shifted to left in the time scale. The first most significant change in the viscosity happens between the fresh pellets and the pellets preconditioned for 8 h. Subsequently, no remarkable changes happen in the viscosities of EMC 1 between the storage duration of 8 h and 24 h. These results also confirm the results obtained from the rotational rheometer shown in Figure 5.17, where no large deviation happen in the dynamic viscosity curves of the pellets between the storage duration of 8 h to 24 h. The next variation in the curves is seen, when the storage duration is extended to 48 h, where the viscosity curves shift further to the left and indicate a decrease in the gel time. Following, no significant changes happen in the viscosities between the pellets stored for 48 h and 72 h. Therefore, by considering the results obtained from the rheology measurements, it is possible to say that the extended storage duration in dry environment shows some influence on the cure reaction of EMC 1. Additionally, the rheology measurements obtained from the rotational rheometer as well as squeeze flow rheometer represent good correlation to the results obtained from the DEA. Hence, the variations in the cure reaction and the viscosity of EMC 1 due to the prolonged storage duration can be also observed from the DEA curves in-situ during transfer molding process.

Investigation of the Influence of Humidity on EMC Characteristics

In Figure 5.21, average logarithmic ion viscosity curves for the preconditioned pellets in humid environment at 30 °C and 90 % RH for 8 h, 16 h, 24 h as well as fresh samples (0 h) and the characteristic information about the cure reaction of EMC 1 derived from the ion viscosity curves are shown.

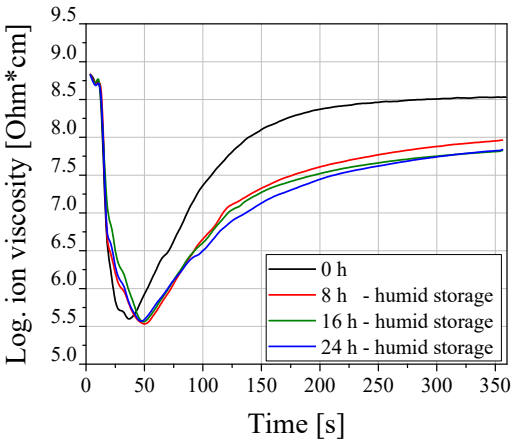

Storage duration	Minimum ion viscosity [Ohm*cm]	Δ (Difference max-min ion viscosity) at 350 s [Ohm*cm]
0 h	5.60	2.93
8 h	5.53	2.42
16 h	5.59	2.23
24 h	5.59	2.23

Figure 5.21: Logarithmic ion viscosity with respect to time (left) and characteristic information (right) of preconditioned EMC 1 pellets for 8 h, 16 h and 24 h at 30 °C and 90 % RH as well as fresh samples (0 h)

The progress of the cure reaction changes remarkably when the pellets are exposed to humid environment. The slope of the reactions for the preconditioned pellets differentiate to a great extent from the fresh samples (0 h). The time required to reach the maximum ion viscosity is longer when the pellets are preconditioned. The ion viscosity curves are different for humid samples in comparison to the dry samples. The delta between the maximum and minimum ion viscosity is significantly larger for the fresh samples in comparison to the preconditioned samples, which can be also seen from the values given in Figure 5.21 (right). To determine whether the dynamic viscosities of EMC 1 pellets are also influenced by the storage duration in humid environment, the rotational rheometer measurements are performed for preconditioned pellets. Figure 5.22 depicts the results of the rheology measurements which are conducted under isothermal and non-isothermal conditions for pellets preconditioned in humid environments in climate oven at 30 °C and 90 % RH.

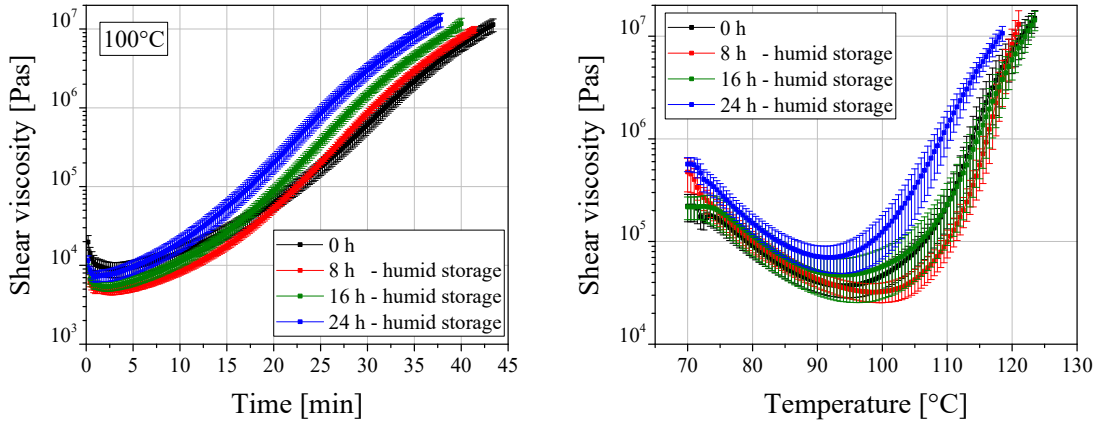

Figure 5.22: Isothermal at 100 °C (left) and non-isothermal with 2 K/min (right) viscosity plot for EMC 1 pellets preconditioned in humid environment for 8h, 16 h and 24 h at 30 °C / 90 % RH and for fresh pellets

Both rheological measurements with isothermal and temperature ramp of EMC 1 with different storage durations in a climate chamber show differences in viscosities with extended storage duration in humid environment. The gel time decreases gradually by increasing the preconditioning duration of EMC 1 in

humid environment. As a matter of fact, the alteration in the viscosity becomes more pronounced with 24 h humid storage. As seen in Figure 5.22 (right), the minimum viscosity of EMC 1 raises when the pellets are preconditioned for 24 h in humid environment.
As explained in the previous section, there is a slight change in the viscosity of EMC 1 with prolonged storage duration in dry environment. Hence, to determine solely the effect of humidity on the cure reaction of EMC 1 and to eliminate the effect of dry storage duration, the viscosity curves for the pellets, which are preconditioned for 24 h in dry environment and for 24 h in humid environment, are represented together in Figure 5.23. In addition, the viscosity curve for the 0 h samples are supplemented into the diagrams to consider the viscosity of EMC 1 at initial state.

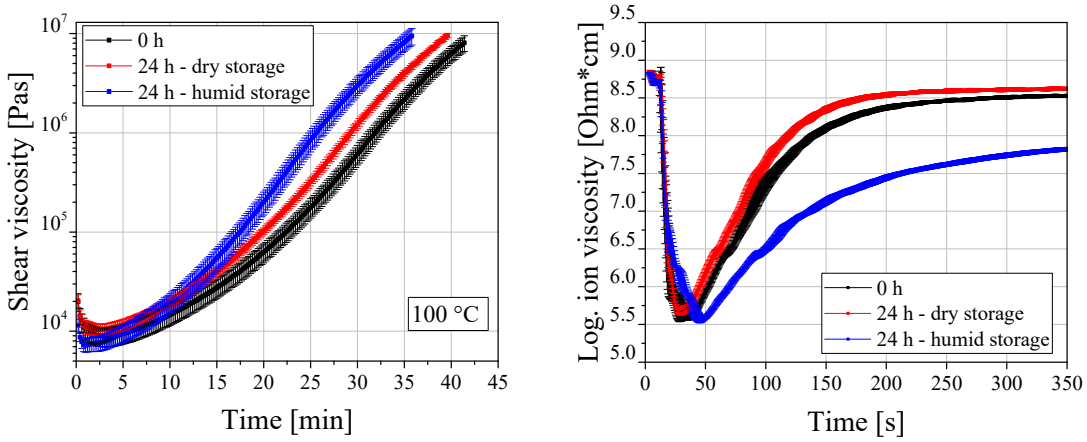

Figure 5.23: Dynamic viscosity curve (left) and the ionic viscosity curve (right) with respect to time for EMC 1pellets which are preconditioned for 24 h at 30 °C / 0 % RH and for 24 h at 30 °C / 90 % RH as well as fresh samples

The excessive impact of the humidity on the dynamic viscosity of EMC 1 as well as on the ion viscosity of EMC 1 can be seen in Figure 5.23. As the difference between the ion viscosity curves under humidity are significantly larger and easily identifiable, the standard deviation of the curves is also implemented in the ion viscosity diagram in Figure 5.23 (right) to visualize the deviation in the ion viscosities. The ion viscosity of the samples preconditioned for 24 h in humid storage differs remarkably from 0 h and 24 h dry samples. The minimum ion viscosity for 24 h humid samples is found lower in comparison to the fresh samples as well as 24 h stored dry samples. In addition, the ion viscosity curve for 24 h humid samples propagates much slower than the ion viscosity curve for dry samples and fresh samples. Similarly, the difference between maximum and minimum ion viscosity is larger for fresh samples and for 24 h stored dry samples in comparison to the 24 h stored humid samples. To analyze whether the differences in maximum and minimum ion viscosity, namely delta observed in DEA are caused by the variations in the degree of the cure of the preconditioned EMC, T_g‘s of EMC 1 are measured with DMA. Figure 5.24 depicts the results of the DMA measurement of molded samples made from fresh pellets and from pellets stored in humid and dry environment. It is important to note that as the purpose to perform the DMA measurement is to find correlation between the T_g and the delta observed in DEA, DMA measurements of the samples are carried out directly after the molding process and without conducting PMC to prevent any PMC effect in between.

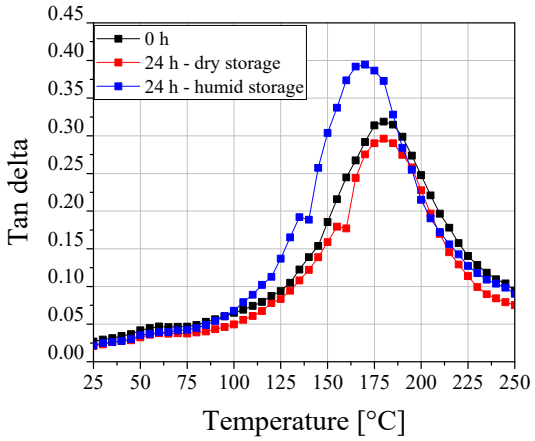

Figure 5.24: DMA measurements of the EMC 1 pellets preconditioned for 24 h in humid and dry environment as well as fresh samples (0h)

As previously explained in Section 3.3.1, the peak point observed at the curve of *tan delta* versus temperature is defined as T_g of the material in DMA measurement. According to the DMA results, the T_g for 0 h fresh samples and for the 24 h dry samples are found very similar which is around 180 °C. On the other hand, the T_g of 24 h humid samples shifts to the left to a value of 170 °C and decreases. Yet, 10 °C difference is observed in the T_g of EMC 1 between the humid and dry samples of 24 h of storage. This implies that the difference observed in the delta in the ion viscosity curve reflects the change in the T_g of the molding compound. Thus, a good correlation is found between DEA and DMA measurement where the variation in the delta in the ion viscosity curve correlates well with the variation in the T_g of the molding compound.

As a next step, the pellets are further preconditioned for 48 h and 72 h to determine the limit of the humidity influence whether the humidity has further impact on the viscosity behavior or whether the pellets achieve saturation point. Figure 5.25 depicts the ion viscosity curve as well as the characteristic information derived from the ion viscosity curves for 0 h, 24 h, 48 h as well as 72 h of storage duration in humid environment.

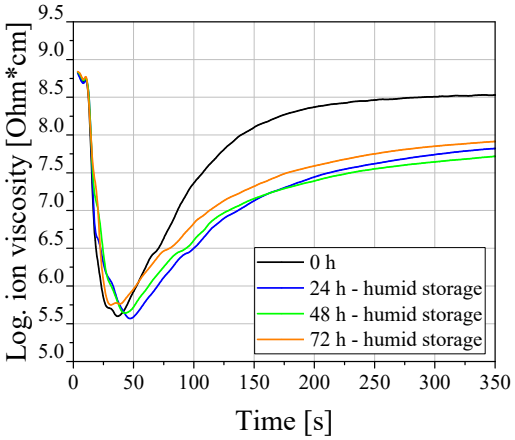

Storage duration	Minimum ion viscosity [Ohm*cm]	Δ (Difference max-min ion viscosity) at 350 s [Ohm*cm]
0 h	5.60	2.93
24 h	5.59	2.23
48 h	5.67	2.04
72 h	5.66	2.04

Figure 5.25: Average logarithmic ion viscosity with respect to time for EMC 1 pellets preconditioned for 24 h, 48 h and 72 h in humid environment at 30 °C / 90 % RH as well as fresh samples (0 h) (left), the minimum ion viscosities and the difference in delta measured with prolonged storage duration at humid environment (right)

With extended storage of the molding compound, the cure reaction of EMC 1 is further influenced. The minimum viscosity of the samples increases and the time of minimum viscosity shifts slightly to earlier time with further storage of 48 h and 72 h in humid environment. The variation in the minimum ion

viscosity and the delta between the maximum and minimum ion viscosity (Figure 5.25 right) shows that the largest change in delta happens between the fresh samples and 24 h humid samples. Afterwards, the delta varies slightly between the 24 h humid samples and the 72 h humid samples.
DMA measurements are carried out also for the samples and T_g of the samples which are preconditioned for 24 h, 48 h as well as 72 h are measured. Figure 5.26 illustrates the results of the DMA measurements of the preconditioned samples as well as fresh samples.

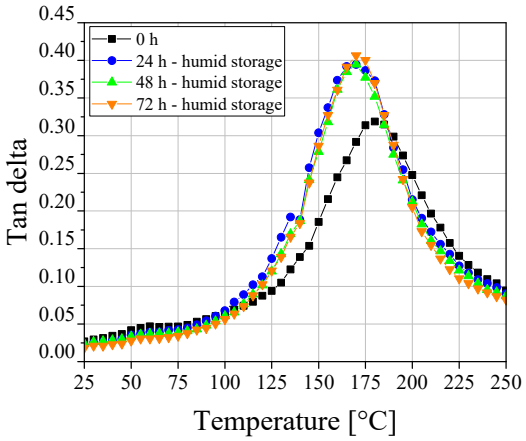

Figure 5.26: DMA measurements of EMC 1 pellets preconditioned for 24 h, 48 and 72 h at 30 °C and 90 % RH as well as fresh samples (0h)

The preconditioned samples for 24 h, 48 h as well as 72 h have almost identical T_g, which is around 170 °C. The unconditioned samples, in other words fresh samples (0 h) have the T_g around 180 °C. This implies that the most significant variation in T_g happen between the fresh samples and 24 h humid samples. No remarkable changes happen in T_g with further extension of longer than 24 h in humid environment. This also verifies the results of delta obtained from the DEA, where the large variation in the delta happens between the fresh samples and 24 h humid samples. After analyzing the mechanical properties of the preconditioned samples with the DMA measurements, rotational rheometer measurements are conducted to observe whether the viscosity of the EMC 1 varies with extended storage duration of the pellets in humid environment. Figure 5.27 depicts the shear viscosities of the preconditioned samples for 24 h, 48 h, 72 h as well as 0 h fresh samples.

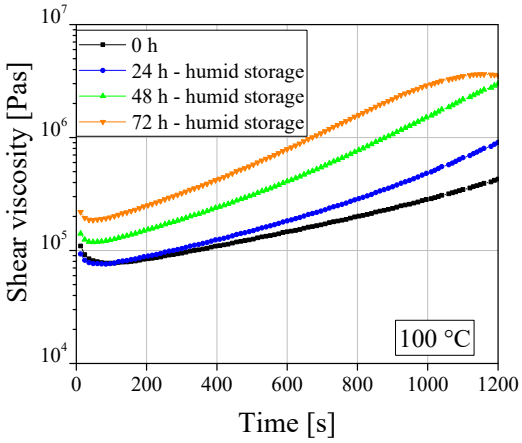

Figure 5.27: Isothermal rheology measurement at 100 °C for preconditioned EMC 1 pellets for a storage time of 0 h, 24 h, 48 h as well as 72 h at humid environment at 30 °C / 90 % RH

The extended storage duration has an influence on the shear viscosity of the analyzed pellets. The viscosity increases with further preconditioning of the pellets for 48 h and 72 h in humid environment.

As seen in Figure 5.27 after 1000 s a minimal decrease in the viscosity curve of 72 h humid samples can be observed. The reason for that although the measurements are repeated three times, each time 72 h preconditioned humid EMC 1 samples lose their contact to the measurement tool most probably due to the significant alterations in the material characteristics, which does not allow a good adhesion to tool surface. Additional rheology measurements are carried out with the squeeze flow rheometer to observe the viscosity behavior at molding temperature. Figure 5.28 illustrates the results of the squeeze flow rheometer for all preconditioning durations in humid environment, namely for 4 h, 8 h, 16 h, 24 h, 48 h, 72 h as well as fresh samples.

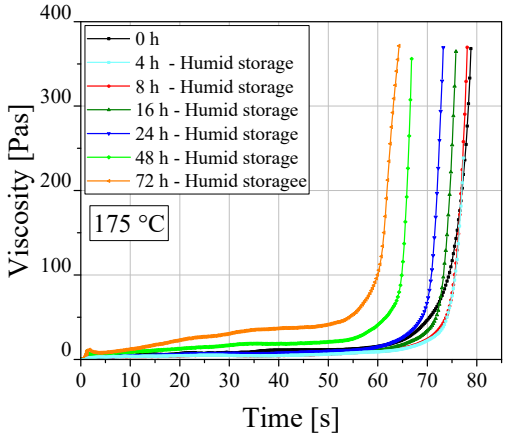

Figure 5.28: Viscosity measured with squeeze flow rheometer at 175 °C of preconditioned EMC 1 pellets for 4 h, 8 h, 16 h, 24, 48 h, 72 h as well as fresh samples

The variations in the viscosities of all analyzed pellets, which are preconditioned until 72 h as well as fresh samples, can be observed in Figure 5.28. With extended storage duration, the sharp increase of the viscosity curves shifts to the earlier time intervals, indicating a decrement in gel time. Pronounced differences in the viscosities are observed with further preconditioning of the pellets from 24 h to 72 h which correlate well with the results obtained from rotational rheometer. Thus, the results of the rheology measurement show that cure reaction of EMC 1 is remarkably influenced by extended storage duration in humid environment.

To determine the moisture content of the pellets with prolonging storage duration in humid environment, Karl-Fischer titration is applied. Figure 5.29 illustrates the moisture content in the pellets stored until 72 h in humid environment as well as the moisture content of the pellets, which are stored in dry environment for comparison. To observe the trend of the ion viscosity curves for all storage durations in humid environment by taking into account the moisture content in the pellets, ion viscosity curves are illustrated together in Figure 5.29 (right). As the moisture content of the preconditioned pellets for 4 h is measured, DEA measurement for 4 h humid storage duration is also conducted additionally to compare the variation in the ion viscosity by considering the raise in the moisture content of the pellets.

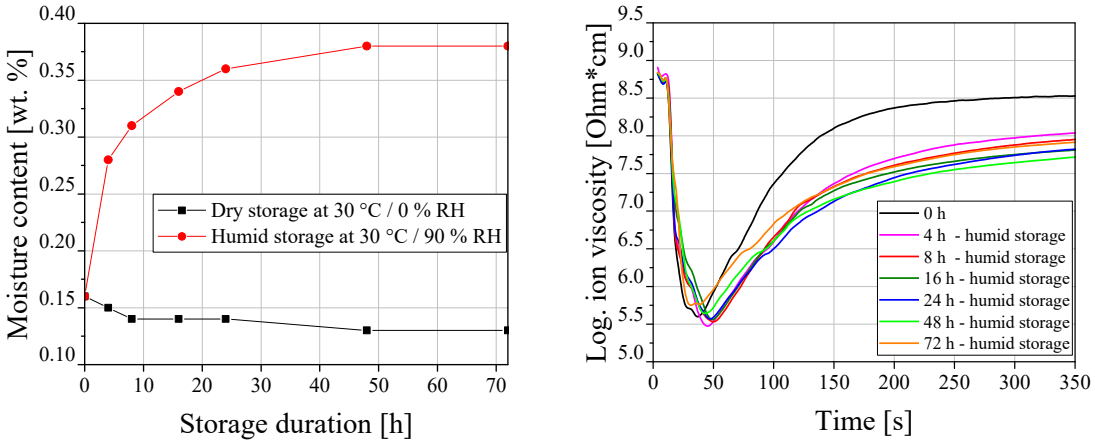

Figure 5.29: Moisture content in EMC 1 pellets preconditioned in dry and humid environment (left), ion viscosity curves for EMC 1 pellets preconditioned for 4 h, 8 h, 16 h, 24 h, 48 h, 72 h as well as fresh samples (0 h) (right)

Karl-Fischer titration results show that the moisture content of the pellets preconditioned in dry environment at 30 °C and 0 % RH stays constant during 72 h storage duration. Around after 24 h dry storage, the moisture content in the pellets decreases slightly most probably due to drying of the moisture initially present in the pellets. On the other hand, the moisture content of the preconditioned pellets in humid environment raises with prolonging storage duration at 30 °C and 90 % RH. Approximately around 48 h, pellets arrive saturation point and the moisture content does not change significantly after 48 h humid storage and stays almost constant until 72 h of storage. The influence of the moisture content on the ion viscosity curves can be observed for all storage durations in Figure 5.29 (right). The humidity plays a major role on the ion viscosity of the pellets especially until 24 h of storage. Ion viscosity curves for the pellets, which are stored until 24 h, show similar cure reaction. However, after 48 h of humid storage, the minimum ion viscosity changes its behavior and the ion viscosity curve shifts to earlier time scale as seen in Figure 5.29 (right). When taking into account the results observed from the rheology measurements for the preconditioned samples in dry environment, where the viscosity of EMC 1 is influenced by the prolonged dry storage duration, it is apparent that there are some overlapping effects on the viscosity of EMC 1 seen in Figure 5.29 (right). The variation in the ion viscosities after 48 h and until 72 h observed in Figure 5.29 (right) is most probably a combination of the impact of absorbed humidity in the pellets and also starting cross-linking reaction due to the prolonged storage duration.

Investigation of Influence of Batch Variations of EMC with DEA

Figure 5.30 demonstrates the dynamic viscosity of three batches of EMC 1 namely batch 1, batch 2 and batch 3 with respect to time and temperature.

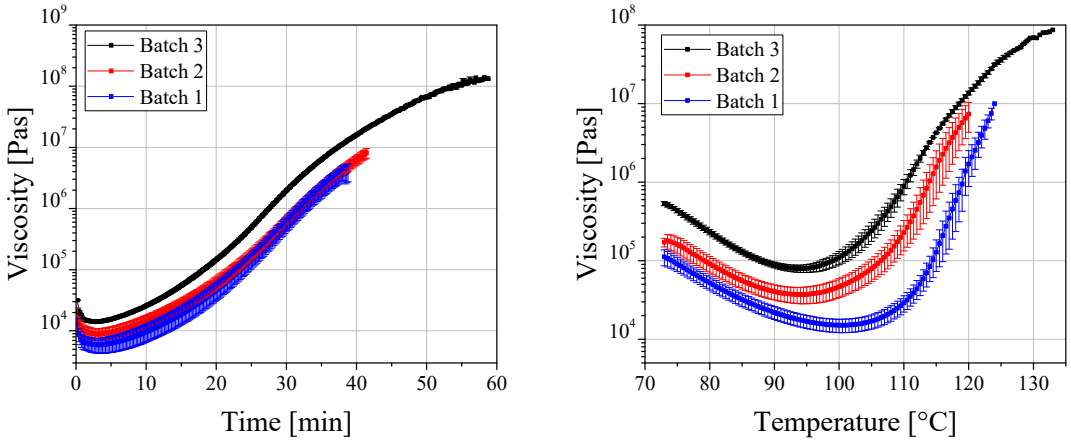

Figure 5.30: Isothermal rheology measurement (left), non-isothermal viscosity curves (right) of batch 1, batch 2 and batch 3 of EMC 1

Three batches of EMC 1 show different viscosity behavior under non-isothermal condition. The minimum viscosities of three batches at the same temperature differentiate from each other. On the other hand, under isothermal condition, batch 1 and batch 2 show almost identical viscosity behavior, whereas viscosity of batch 3 differs notably regarding dynamic viscosity behavior as well as reaction time. To determine whether similar differences can be also observed from the ion viscosity curve of the three batches of EMC 1, DEA measurements are performed. Figure 5.31 presents the ion viscosities of three batches of EMC 1.

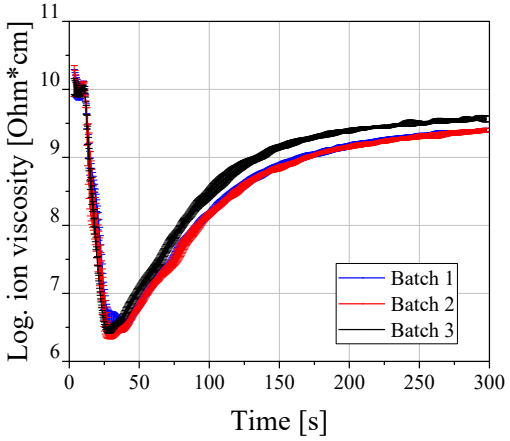

Figure 5.31: Ion viscosities for batch 1, batch 2 and batch 3 of EMC 1

The ion viscosity curves for batch 1 and batch 2 are almost identical and no significant differences are noticeable in the cure reaction curves e.g. regarding the slope of the curve. Batch 3, however, shows a slightly different reaction path. The slope of the reaction is rather larger, thus cure reaction for batch 3 is faster and the maximum ion viscosity is reached in a shorter time in comparison to batch 1 and batch 2. This result correlates well with the rheology results obtained under isothermal condition, which shows that the dynamic viscosity curves for batch 1 and batch 2 behave almost identical and dynamic viscosity of batch 3 differs from batch 1 and batch 2.

5.5 Summary

The results of the preliminary process experiments show that the void formation in the molded packages is strongly influenced by the process parameters. Some process parameter combinations cause reduced void formation in the molded packages, whereas some process parameters such as parameter set no. 2, one of the extreme process parameter combinations, causes large void formation in the package. It is assumed that the reason for this large void formation in the package is the high viscosity during the molding stage, caused by low molding temperature, low preheat time, as well as low holding pressure applied in parameter set no. 2. In addition to that, it is observed that the voids are formed as a tendency in the zone 4 area which is far from the gate. This tendency of the void formation to form in the zone 4 can be attributed to the fact that the flow behavior of the mold compound where the flow front collapses at the very end of the layout in zone 4 and forms some voids especially in this area. However, the detailed analysis in regard of the origin of the void formation in the molded packages is not the scope of this thesis. Thus, to comprehend and to analyze the actual origin of the voids in the molded package in detail, additional work should be done. Furthermore, among the investigated process parameters, transfer speed and holding pressure are found to be dominant process parameters on the void formation, whereas the preheat time and the temperature does not show pronounced impact on the void formation.

Moreover, wire sweep in the package is also strongly influenced by the process parameters. In contrary to the results seen in the void formation, parameter set no. 2 causes reduced wire sweep, whereas parameter set no. 3 leads to large wire sweep in the package. The reason for the large wire sweep in parameter set no. 3 can be possibly attributed to the fact that the parameter set no. 3, which has high transfer speed combined with the least preheat time and low mold temperature, can cause high viscosity of EMC. This high viscosity of the EMC can cause large viscous drag forces on the wire bonds, which then leads to such large wire sweep even on the short wire bonds. In general, the long wire bonds show more wire sweep in comparison to the short wire bonds. The wire bonds attached in far from the gate area show less wire sweep compared to the wire bonds attached in near gate area. For the wire bonds attached at different angles to the gate, the wire bonds attached at 180° to the gate show slightly smaller wire sweep in near gate and far from the gate area. Among the selected process parameters, the temperature and the transfer speed are found to be the dominant process parameters on the wire sweep. The impact of the temperature on the wire sweep can be directly correlated with the viscosity of the molding compound, where the higher temperatures lead to a reduction in the viscosity of the molding compound, thus less force is applied on the wire bonds.

Furthermore, the warpage measurement results show that the warpage of the selected package is not influenced by the variations in the process parameters and the deviation in the warpage in one parameter set is much larger in comparison to the variations in the warpage within 13 parameter sets. In addition, the maximum average warpage value observed in all 13 process parameters is under 100 µm, which is considered as non-critical regarding the defined quality criterion for this test vehicle (see Section 2.7). The reason for the small variations in the warpage observed in this test vehicle can be due to the stable thickness of the lead frame which is around 1 mm and the small surface area of the test vehicle.

Therefore, by considering all quality characteristics investigated in this chapter, it is possible to say that the wire sweep and the void formation of the molded packages are strongly influenced by the variations in the process parameters. Thus, it is possible to improve these quality features of the molded packages by the variations in the process parameters. On the other hand, the warpage for the investigated test vehicle is not affected remarkably by the change in the process parameters due to the selected substrate dimensions. Hence, as the target of the work is to find an optimum set of process parameters of the transfer molding process which deliver the best package quality, warpage will not be investigated further as a quality characteristic in the main experiments.

In the second part of this chapter, it is observed that the prolonged storage duration has an influence on the cure reaction of EMC 1. With extended storage duration, the degree of cure increases, which implies that cross-linking reaction starts already during storage in vacuum oven and EMC 1 achieves certain

cross-linking degree before the pellets are molded. In addition, the storage duration in humid environment shows a more pronounced influence on the cure reaction of EMC 1. The ion viscosity signal is strongly influenced when EMC 1 pellets are subjected to humid environment. Good correlation between the delta in the ion viscosity and T_g from the DMA is found, which implies that the ion viscosity delivers also consequential information about the variation in the T_g of the material. Moreover, the rotational rheometer results show that a variation in the curing reaction between different batches exist, and this difference can be observed also with DEA measurement in-situ in transfer molding process. Additionally, the results obtained from the DEA match very well with the results obtained from the rotational rheometer, DSC and squeeze flow rheometer. The feasibility analysis of the DEA demonstrates that DEA delivers valuable information about the cure reaction of the EMC and is found suitable as an in-situ monitoring technique in transfer molding process to observe the variations in the EMC characteristics due to batch variation, and prolonged storage duration in dry and humid environment.

6 Main Experiments and Results

After gaining a comprehensive understanding with the preliminary experiments in terms of significant process parameters and the impact of the variations in the material characteristics on the cure behavior of EMC 1, the main experiments are conducted. The main experiments are performed to define a process model and a material model which delivers the correlation between the process parameters, material characteristics and the package quality. Hence, in this chapter, the selected experimental designs and applied approaches are shown, which are employed to generate models, and the results of the main experiments are discussed. Since different experimental plans are conducted for the generation of process and the material models, the main experiments consist of two parts. The first part is dedicated to the main experiments for process analysis, which are conducted to establish a process model. The selected experimental design to generate a process model, which expresses the relationship between the process parameters and the quality characteristics parameters is introduced in Section 6.1. The quality analysis of the conducted experimental design is given in Section 6.2. The important findings about quality analysis of void formation and wire sweep and relevant aspects, which are necessary to consider in generation of the process model, are discussed. Before the results of the quality analysis are introduced, the process is examined in order to determine the possible variations in temperature and pressure. Thus, the pressure and temperature sensors are analyzed and important features on the observed signals are assessed. Moreover, process stability analysis is conducted to determine the maximum deviations in the temperature and the pressure sensors in the process as well as in void formation and wire sweep.

In the second part of the main experiments, an applied experimental approach to generate a material model, which delivers the impact of the variations in the material characteristics on the quality features is given. In the preliminary experiments, the influence of the variations in the material characteristics on the cure behavior of EMC 1 are discussed. In the main experiments, however, the impact of the variations in the material characteristics of EMC 1 directly on the wire sweep and void formation in the molded packages are examined. The experimental approach, which is carried out to assess the influence of the variations in the material characteristics due to the storage duration, the batch variations and the humidity on the quality characteristics is illustrated in Section 6.3. The results of the experimental analysis are discussed in Section 6.4. In Section 6.5 the summary of the important findings about the main experiments is given.

6.1 Main Experiments for Process Analysis

The objective of the main experiments in this work is to establish a correlation between the process parameters and the quality characteristics in order to estimate the quality characteristics beforehand as well as to define optimum process parameters, which delivers the best package quality. In that manner, it is crucial that the selected quality characteristics are influenced by the process parameters. For this reason, as already mentioned warpage by being a quality characteristic, which is not influenced by the variations in the process parameters for this package geometry, will not be further investigated in the main experiments.

For the main experiments D-optimal design is selected. The reason for the selection of the D-optimal design is that with D-optimal design, the interactions between the process parameters and the impact of quadratic influences of parameters on the void formation and the wire sweep can be studied. Thus, a quadratic model can be established based on the results of the experimental plan which is constructed according to D-optimal design. Four process parameters, which are molding temperature, holding pressure, preheat time and transfer speed, are investigated within the selected process window which is already shown in Table 5.1. The process parameters are set in 3 levels. For four factors, which are set in 3 levels, the minimum number of the required parameter set in D-optimal design is 15. As explained in Chapter 2, in D-optimal design, the parameter combinations which are chosen based on the algorithm,

are distributed within a given matrix or in other words within a process window, and some of the corner points in the matrix may not be occupied. In order to cover the investigated process window thoroughly to obtain better interpolation with the established model, five additional parameter combinations are supplemented into the experimental design. In total 20 different parameter combinations are studied. The experimental plan executed to generate a process model is shown in Table 6.1.

Table 6.1: D-optimal experimental plan in main experiments with four process parameters set in 3 levels to generate a process model

Parameter set no.	T [°C]	v [mm/s]	t [s]	P [bar]
1	165	6.5	0	80
2	165	6.5	16	140
3	165	1.5	0	80
4	165	1.5	16	80
5	165	1.5	0	140
6	165	4	8	110
7	175	6.5	0	110
8	175	4	0	80
9	175	6.5	8	80
10	175	1.5	16	110
11	175	1.5	0	140
12	175	4	8	110
13	185	1.5	16	80
14	185	1.5	16	140
15	185	6.5	16	80
16	185	1.5	0	140
17	185	6.5	0	140
18	185	6.5	0	80
19	185	4	16	140
20	185	4	0	110

Each parameter set is repeated five times to evaluate the reproducibility of the results. Considering the left and right cavity together, the void formation and the wire sweep of overall ten samples are analyzed for each parameter set.

6.2 Results of Main Experiments for Process Analysis

To gain more insight into cavities of the molding process, pressure and temperature signals and their important characteristics are discussed in Section 6.2.1. Furthermore, to examine the deviations in the temperature and the pressure of the transfer molding process during molding, a process stability analysis is performed. The process stability analysis is carried out by conducting 25 molding cycles at the same process parameter set to observe the deviations in the pressure and the temperature as well as in the quality characteristics, namely void formation and wire sweep in the package. Results of the process stability analysis are given in Section 6.2.2. Moreover, the influence of the process parameter combination sets depicted in Table 6.1 on the void formation and the wire sweep are investigated. The main aspects of the experiments on the void formation and the wire sweep are introduced in Section 6.2.3 in the quality analysis part.

6.2.1 Machine and Sensor Signal Analysis

As already illustrated in Chapter 3, the transfer molding process is monitored with temperature and pressure sensors during molding in this work. Monitoring the molding process is crucial to assure the process stability and to disclose any possible variations from cycle to cycle. Moreover, the machine settings are usually not reflecting the real situation in the cavity. There are certain deviations between the set parameters in the machine and the real conditions measured in the cavity. Thus, it is important to measure the temperature and the pressure directly in the cavity to control the process.
In addition to the difference between the set machine parameter and the cavity conditions, there may be also deviations between the left and the right cavities. To highlight the situations in the left and the right cavities, some of the sensor signals from the cavities are analyzed. Considering the nine temperature and pressure signals implemented in the cavities of the molding tool (see Chapter 3 for exact position of the sensors), only representative examples of the signals from the selected sensors are shown in this section. Figure 6.1 illustrates the temperature signals measured in the left cavity and in the right cavity for three parameter set no. 1, 7 and 18 where the tool temperature is varied as 165 ˚C, 175 ˚C and 185 ˚C respectively.

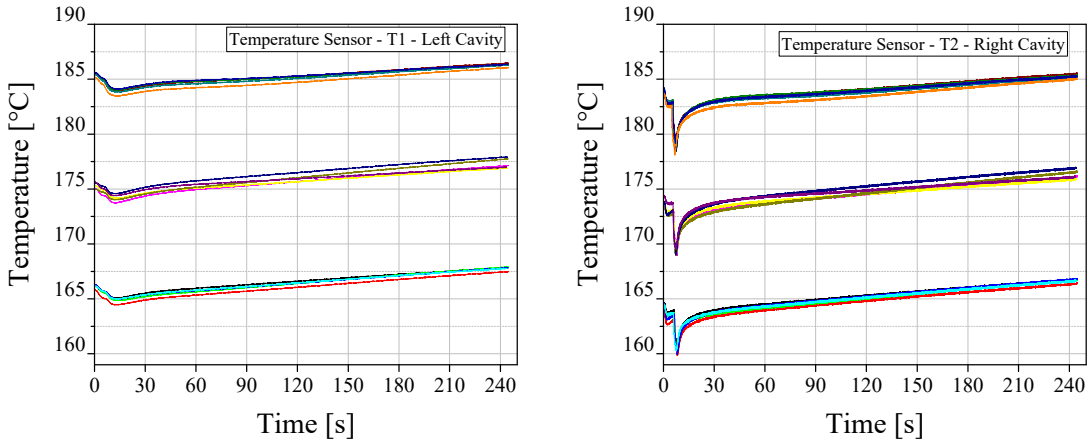

Figure 6.1: Temperature signals obtained from temperature sensor T1 in left cavity (left), and from temperature sensor T2 in right cavity (right). As an illustration of signals parameter set no. 1, 7, 18 are selected.

According to Figure 6.1, the temperature for five cycles within each parameter set number stays constant. The representative parameter set no. 1, 7 and 18 are selected purposely, since all those parameter sets have the same preheat time (0 s) and transfer speed (6.5 mm/s) but have different molding temperatures. The set transfer speed and preheat time are decisive for the peak in which the temperature goes down. Exactly at this point, which is circa after 12 seconds for the parameter set with 6.5 mm/s transfer speed and 0 s preheat time, the molding compound reaches at temperature sensor and causes this peak in downwards due to its colder temperature in comparison to the tool temperature. The similar peak can be also observed on the temperature sensor in the right cavity only with a small difference that in the right cavity the measured temperature has a sharper peak. The reason for that is there is a minimal position difference (~ 2 mm) between the T1 in the left cavity and T2 in the right cavity and due to the irregular cross section of the gate area, slightly more material flows through T2 sensors, which causes larger down peak. However, for the comparison of the temperature between the sensors in left and the right cavity, it is more representative to inspect the start temperature at time 0 s. As seen in signals from T1 in the left cavity, for the set temperatures of 165 °C, 175 °C and 185 °C, the left cavity has a slightly higher temperature whereas in the right cavity the temperature lies slightly below the set temperature. The difference between the temperatures in the left and the right cavity is between 1 °C – 2 °C. This variation is also confirmed with the other temperature sensors in the cavities namely T3 and T4 implemented on the lower half of the tool as well as with an additional examination by a temperature

measuring device which is also performed regularly during the experiments to control the cavity temperatures. This variation in the temperatures between two cavities can be attributed to construction of the tool especially the position of the heat strip. Nevertheless, for temperature stability in the process, the most important condition is that the offset of the machine temperature setting to the measured molding temperature in the tool stays constant independent from the set molding temperature. This can be assured by the temperature signals shown in Figure 6.1, where the molding temperatures measured in temperature sensors at time 0 s have always the same offset to the set temperature in the machine in the left as well as in the right cavity. Figure 6.2 depicts the pressure signals obtained from the pressure sensors from the left and right cavities.

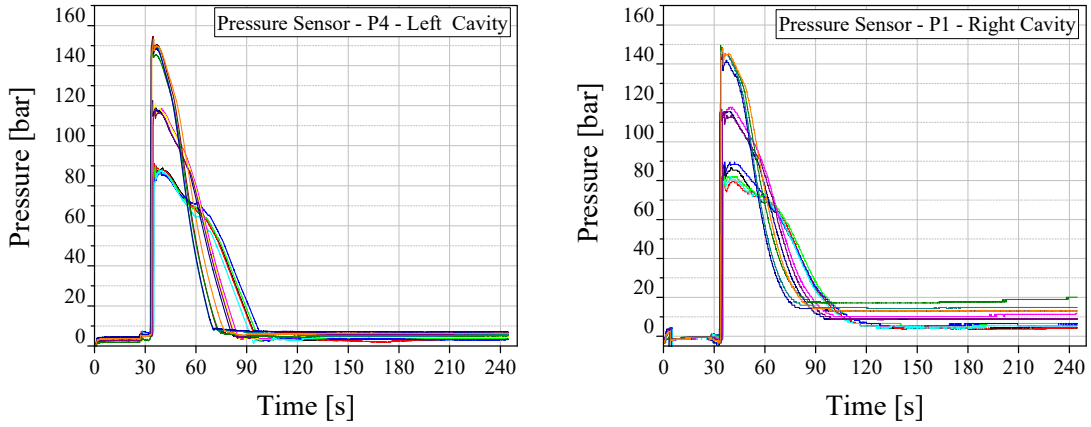

Figure 6.2: Pressure signals obtained from pressure sensor P4 in left cavity (left), and from pressure sensor P1 in right cavity (right). As an illustration of signals parameter set no. 4, 10 and 14 are selected.

For the pressure signals, the parameter set no. 4, 10 and 14 are selected since those parameters have the same preheat time (16 s) and transfer speed (1.5 mm/s) but have different holding pressures, which are varied as 80 bar, 110 bar and 140 bar. The set preheat time and transfer speed determine the time in which the pressure goes up dramatically. This point indicates the complete filling of the cavity, which is around 34 seconds for the selected transfer speed and preheat time. Considering the fact that the preheat time is 16 s and pressure goes up in 34 s, the cavity is filled in 18 s with the lowest transfer speed of 1.5 mm/s. Moreover, the width of the pressure signals is varied when changing the set value from 80 bar to 140 bar. The reason for that is not only the pressure variation itself but also the differences in the tool temperatures, where the parameter set no. 14 has the highest holding pressure (140 bar) and highest tool temperature (185 °C) in the experimental plan. In contrary, the parameter set no. 4 has the lowest holding pressure (80 bar) as well as the lowest temperature (165 °C). This combination of the high temperature and high pressure can promote the curing reaction of the molding compound and the curing reaction can be completed faster. When the molding compound is cured, it loses slowly its contact with the tool surface and automatically with the pressure sensor, yet causes a drop in the pressure signal. Thus, with the help of the sensor signals some substantial information can be gathered about the characteristics and the curing behavior of the molding compound directly from the cavity. Furthermore, as seen from the diagrams in Figure 6.2, the measured pressure in the pressure sensors is around 5 bar higher than the set pressure. As implied previously, there are certain deviations between the set temperature, pressure values in the machine and the measured temperature and pressure in the cavity. However, the difference of 5 bar can be seen in almost all process parameter combinations as well as in left and the right cavities and no fluctuations in the difference value is observed, yet the obtained results are reproducible. The pressure sensors in left and the right cavities show similar signals and both sensor types deliver essential information about the dynamic phase of pressure signals, which correlate with the curing behavior of the EMC in the cavity.

Apart from the pressure and temperature signals, another important characteristic in the process is the vacuum. The vacuum has especially influence on the void formation, thus it is important to assure that it stays constant throughout the experimental plan. Figure 6.3 illustrates the vacuum signals for 20 parameter sets for all 100 cycles in the main experiments.

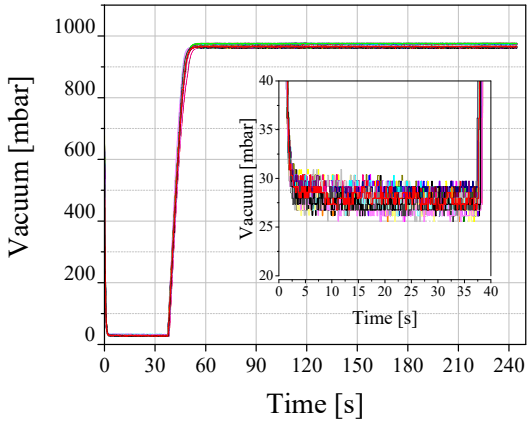

Figure 6.3: Vacuum signal with respect to molding cycle time for 100 cycles

The vacuum from the cavities is sucked during 40 seconds. The 40 seconds of vacuum is essential to cover the filling phase of the molding compound in the cavity, where the material is in liquid form to remove any possible air or gas. The minimum vacuum around 28 bar can be achieved with this tool construction. As seen from Figure 6.3, the vacuum stays perfectly stable during 100 cycles of the main experiments.

6.2.2 Analysis of Process Stability

In this previous section, the temperature and the pressure signals from different process parameter sets are introduced to compare different parameter settings and to explain the important characteristics of the pressure and temperature signals with respect to the curing behavior of the molding compounds. After acquiring some fundamental information from the temperature and pressure signals about the cavity of the mold tool, in this section, the process stability is investigated. Process stability analysis is essential in terms of determining the maximum deviations in the pressure and temperature sensors as well as in the void formation and the wire sweep. In this context, the process stability analysis is conducted with EMC 1 by performing 25 molding cycles with only one process parameter combination to observe the maximum deviation in the temperature and pressure sensors as well as DEA sensors in the cavities more precisely. Furthermore, void formation and wire sweep in the molded packages are also measured to determine the maximum variations in the defects under the same parameter condition. This investigation is especially important to differentiate after which range the variations in the wire sweep or in the void formation become significant. Thus, the results of this process stability analysis are also determining in the material investigation analysis in terms of the evaluation of the alteration in the material characteristics on the wire sweep and void formation. In that manner, the central process parameter combination, which is the process parameter set no. 12 with 175 °C molding temperature, 4 mm/s transfer speed, 8 s preheat time and 110 bar holding pressure, is selected for process stability analysis. Figure 6.4 and Figure 6.5 illustrate the temperature and pressure signals for 25 cycles and the deviations inspected in the signals.

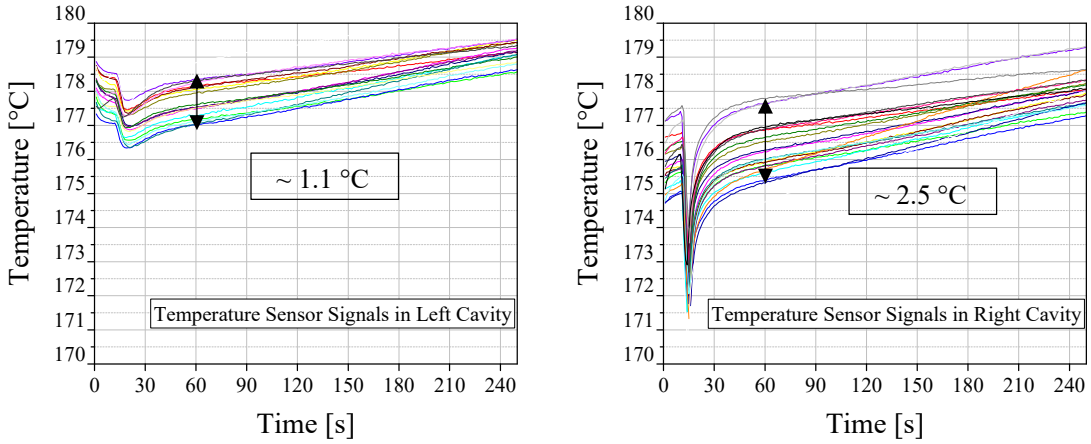

Figure 6.4: Temperature sensor signals in left cavity (left) and right cavity (right)

The temperature measured in the left cavity shows circa 1.1 °C deviation within the 25 molding cycles. The measured temperature in the right cavity, however, depicts larger deviation in comparison to the left cavity, and the maximum deviation observed is around 2.5 °C. With the represented temperature signals between the left and the right cavities, it is apparent that the temperature measured between the left and right cavities show deviations. The left cavity has a slightly higher temperature at around 2 °C in comparison to the right cavity. Figure 6.5 illustrates the pressure signals of P3 and P2 sensors from the left and the right cavities.

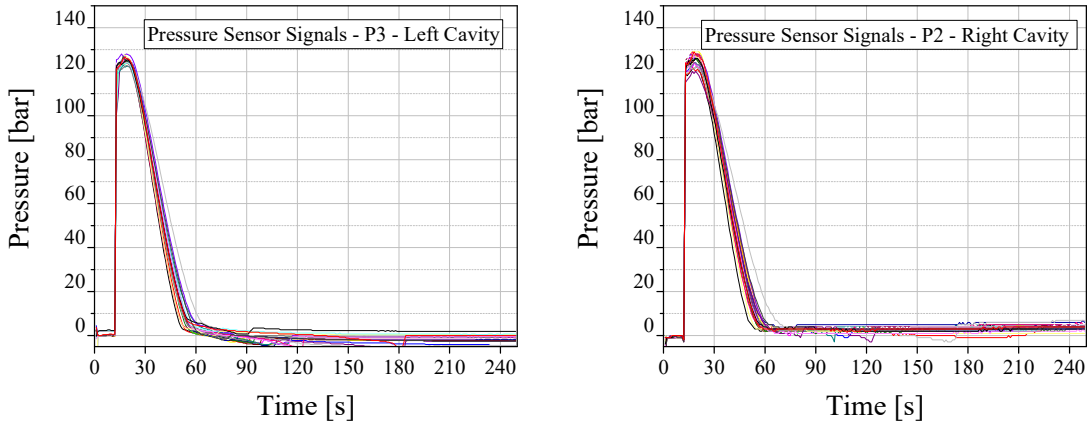

Figure 6.5: Pressure sensor signals in left cavity (left) and in right cavity (right)

Pressure sensor, P3, which is implemented in the left cavity, shows very reproducible results. The deviation observed in the pressure signals is less than 4 bar within 25 molding cycles. Pressure sensor P2 also shows maintainable results with a slightly higher deviation at around 9 bar in 25 molding cycles. Nonetheless, it is evident that the pressures measured in both cavities are stable and reproducible. In addition to the temperature and pressure sensors, the deviations in the DEA sensors are also measured. Figure 6.6 depicts the DEA signals for 25 molding cycles from the left and the right cavities.

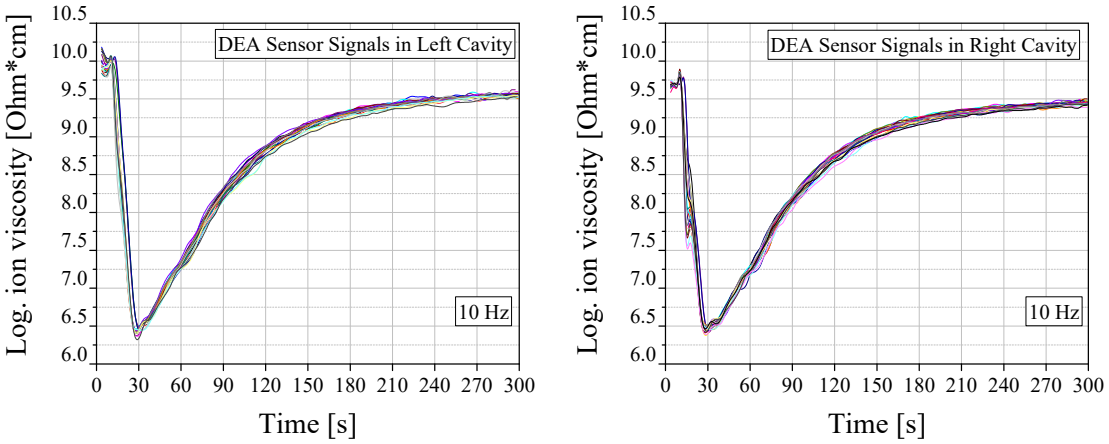

Figure 6.6: DEA sensor signals obtained from the sensors in left cavity (left) and in right cavity (right)

The starting logarithmic ion viscosity in the left cavity at the beginning (between 0 s and 7 s before the material reaches to the sensor) is slightly higher in comparison to the logarithmic ion viscosity obtained from the right cavity. This difference in the beginning phase of the ion viscosity can be attributed to the temperature difference between the left and the right cavity, where the left cavity has a slightly higher temperature, thus it causes higher ion viscosity at the beginning. However, apart from this difference the logarithmic ion viscosities observed in the left and the right cavities are very similar. It is evident that the logarithmic ion viscosity shows reproducible results and minimum deviations. The determination of the maximum standard deviation of the logarithmic ion viscosities are substantial for this work, since DEA is selected as a monitoring method to examine the slight variations in the material characteristics of the EMC. In this context, the maximum standard deviation observed in the DEA signal is found around 0.095 Ohm*cm for the left cavity and 0.10 Ohm*cm for the right cavity. This means, any deviations which are bigger than this measured standard deviations should be contemplated and considered as significant variation in the ion viscosity.

In addition to the sensor signals, the void formation and the wire sweep of the 25 molded packages are compared. To examine any possible deviations between the cavities, the left and right cavities are considered separately and the deviations in the wire sweep and the void formation for each cavity are listed individually. Table 6.2 represents the standard deviations measured for void formation, namely number of voids and the area of voids, as well as each wire bond on the layout of the demonstrator.

Table 6.2: Standard deviations of void formation and wire sweep for each wire bond on layout of demonstrator

Position and angle of the wire bonds to the gate		Quality Characteristics	Left Cavity	Right Cavity
		Number of voids	0.4 ± 0.9	0.3 ± 0.7
		Area of voids [mm^2]	0.1 ± 0.3	0.1 ± 0.2
Near gate	90° to gate	Short wire bond 1 (s1) - wire sweep [%]	0.8 ± 0.4	1.7 ± 0.9
		Short wire bond 2 (s2) - wire sweep [%]	0.5 ± 0.5	0.7 ± 0.5
		Long wire bond 1 (l1) - wire sweep [%]	4.3 ± 0.6	5.5 ± 0.6
		Long wire bond 2 (l2) - wire sweep [%]	6.0 ± 1.1	7.1 ± 0.8
	180° to gate	Short wire bond 1 (s1) - wire sweep [%]	2.3 ± 1.2	1.1 ± 1.3
		Short wire bond 2 (s2) - wire sweep [%]	1.6 ± 0.9	1.0 ± 1.0
		Long wire bond 1 (l1) - wire sweep [%]	5.7 ± 0.6	5.1 ± 0.6
		Long wire bond 2 (l2) - wire sweep [%]	6.6 ± 0.6	5.8 ± 0.5
	45° to gate	Short wire bond 1 (s1) - wire sweep [%]	3.4 ± 1.7	1.5 ± 0.6
		Short wire bond 2 (s2) - wire sweep [%]	2.8 ± 1.4	1.9 ± 0.8
		Long wire bond 1 (l1) - wire sweep [%]	6.1 ± 0.8	5.6 ± 0.5
		Long wire bond 2 (l2) - wire sweep [%]	6.8 ± 0.7	6.5 ± 0.5
Far from gate	90° to gate	Short wire bond 1 (s1) - wire sweep [%]	0.7 ± 0.4	0.4 ± 0.3
		Short wire bond 2 (s2) - wire sweep [%]	0.4 ± 0.3	0.3 ± 0.3
		Long wire bond 1 (l1) - wire sweep [%]	2.9 ± 0.7	2.3 ± 0.5
		Long wire bond 2 (l2) - wire sweep [%]	4.3 ± 0.8	3.3 ± 0.5
	180° to gate	Short wire bond 1 (s1) - wire sweep [%]	0.7 ± 0.3	0.4 ± 0.3
		Short wire bond 2 (s2) - wire sweep [%]	0.6 ± 0.4	0.3 ± 0.3
		Long wire bond 1 (l1) - wire sweep [%]	2.0 ± 0.5	2.0 ± 0.5
		Long wire bond 2 (l2) - wire sweep [%]	2.8 ± 1.0	2.7 ± 0.7
	45° to gate	Short wire bond 1 (s1) - wire sweep [%]	0.7 ± 0.4	0.6 ± 0.4
		Short wire bond 2 (s2) - wire sweep [%]	0.6 ± 0.4	0.5 ± 0.4
		Long wire bond 1 (l1) - wire sweep [%]	3.7 ± 0.7	3.1 ± 0.6
		Long wire bond 2 (l2) - wire sweep [%]	5.5 ± 0.8	5.3 ± 0.9

With the help of the mean values and the standard deviations stated in Table 6.2, it is possible to determine whether the measured difference in the wire sweep such as due to process parameters or variation in the material characteristics lies within the standard deviation or whether the observed difference in the wire sweep should be treated as significant variation. Apart from the determination of the standard deviation of each wire bond, Table 6.2 allows the comparison of wire sweep of every single wire bond with each other under central process parameter conditions. The standard deviation represented in this table is especially important when investigating the influence of the material characteristics, since the small variations in the material characteristics can lead also to small differences in the wire sweep and void formation. Thus, in order to determine whether the observed differences in the quality characteristics are significant, it is essential to determine the maximum standard deviation of each wire bond as well as the area and the number of voids.

6.2.3 Quality Analysis

In this section, the results of the quality analysis in terms of void formation and wire sweep are discussed respectively. The important aspects, which are necessary to consider for an establishment of the process model, are pointed out.

Void Formation

Figure 6.7 illustrates the average number of the voids and the corresponding area of voids from left and the right cavities together with respect to 20 different process parameters combinations.

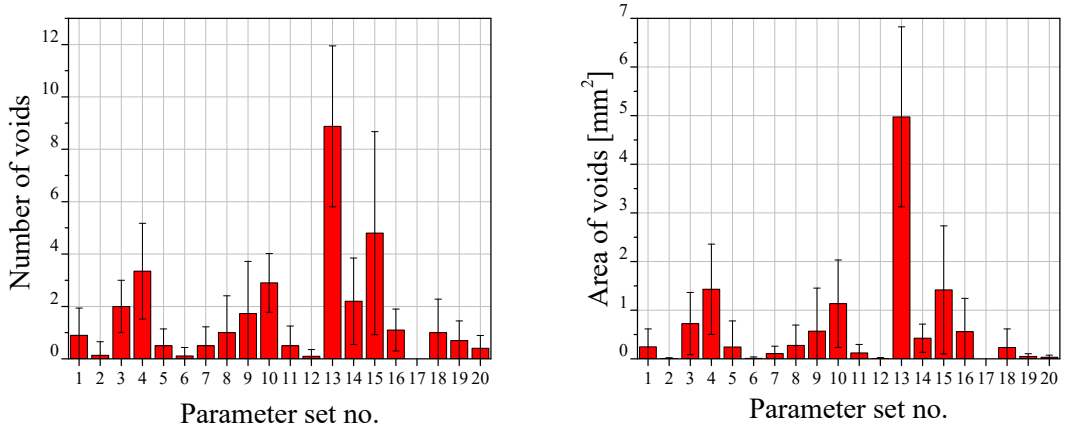

Figure 6.7: Average number of voids (left) and average corresponding area of voids (right) averaged from left and right cavity with respect to 20 different process parameter set

The number of voids and the corresponding area of the voids are varied remarkably with respect to different process parameters. Some process parameter combinations such as parameter set no. 13 and 15 cause large void formation in the package. On the other hand, in some parameter combinations such as parameter set no. 2, 6, 12 and 17 almost no voids are observed in the package. Figure 6.8 displays the number of voids and the corresponding area of the voids formed in different zones with respect to the gate on the layout which are averaged from the left and the right cavities together.

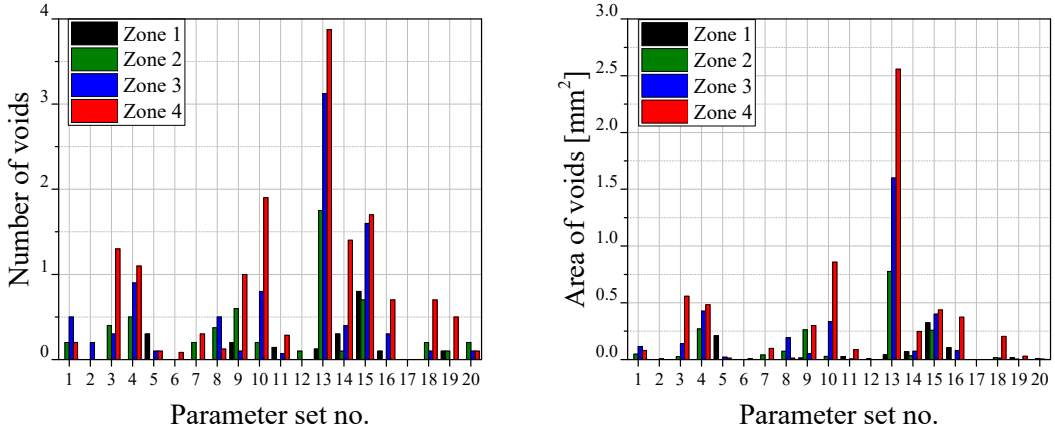

Figure 6.8: Number of voids (left) and corresponding area of voids (right) averaged from left and right cavity, located in four different zones on layout of the package with respect to 20 different process parameter set

Similar to the results obtained in the preliminary experiments, the voids are formed mostly in the zone 4 for almost all process parameter set numbers. In contrary, the reduced void formation is observed in close to the gate area, namely in zone 1.

As mentioned in Chapter 3, for an accurate void analysis, the images, which are examined with the software tool ImageJ, are checked subsequently by an additional visual inspection. In order to assure that the selected dark points on the SAM images, which are considered as voids, are real existing voids in the molded packages and not any kind of inhomogeneity on the surface of the mold package, the intersections of the mold packages are taken. Yet, two demonstrators are selected, which include many voids inside the package according to the SAM images. Demonstrator 1 includes voids, which are selected by the software and demonstrator 2 includes voids, which are added in the additional visual observation due to the fact that voids reside very close to the layout contours and are not recognized by the software (see Section 3.4.1 for more detail). For the demonstrator 1, one zone is selected, where three voids reside in almost at the same y - coordinate and very close to each other. This allows to investigate three points with one cross sectional cut. The area of the voids and the line for the cross section is indicated in Figure 6.9 (left). In demonstrator 2, three small voids residing very close to the border of the layout, which are slightly difficult to recognize on the SAM image, are selected to assure the results (Figure 6.9 right).

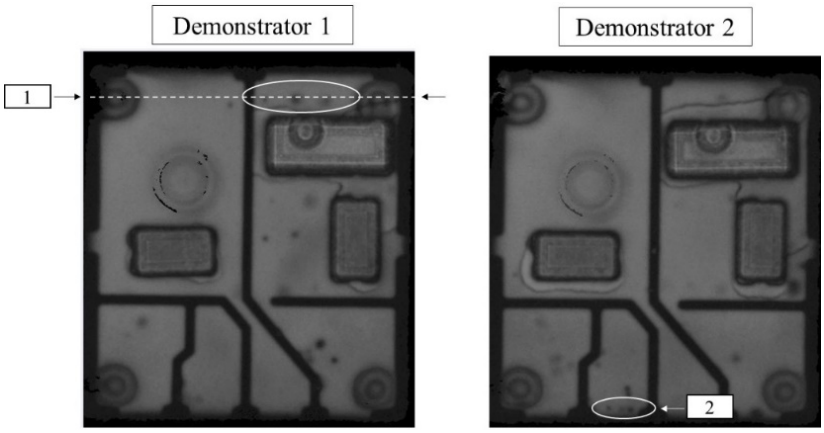

Figure 6.9: Intersections of selected voids for the demonstrator and corresponding SAM Images

Figure 6.10 displays the lateral view of the demonstrator 1. It is important to emphasize that in Figure 6.9 the images of the demonstrator are the top view taken by a transducer in ultrasonic bath, whereas in Figure 6.10 the lateral views of the demonstrator are shown. In lateral view, the position of the voids such as the deepness of the voids in the package between the surface of the mold package and the lead frame can be determined.

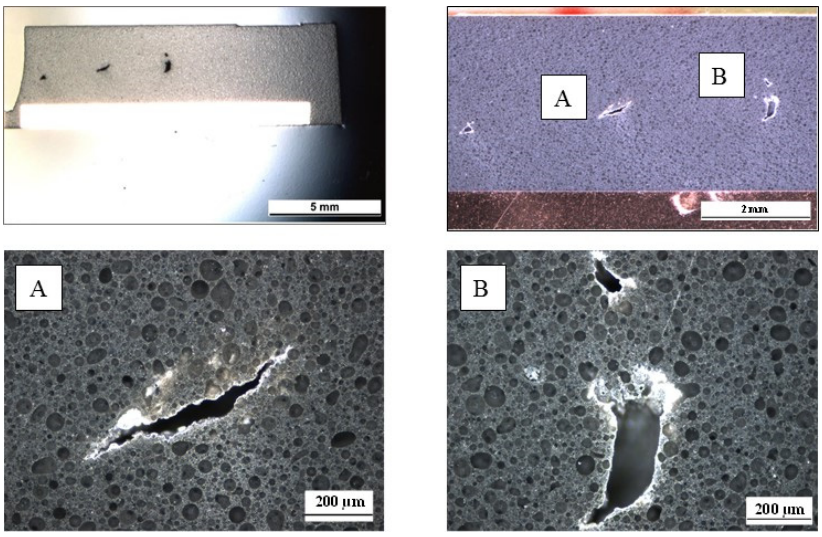

Figure 6.10: Intersection of the demonstrator 1

The images shown in Figure 6.10 confirm that three dark points on the SAM image, which are considered as voids, exist in the molded package and are not any kind of surface artifacts. The shape and the size of the points differentiate from each other. The points, which look like round structures from top view, have in fact irregular shape when they are examined from the lateral section. Point A has more like an elongated structure whereas point B illustrates a more rounded structure. Figure 6.11 depicts the lateral view of the demonstrator 2 for the voids in the zone 2.

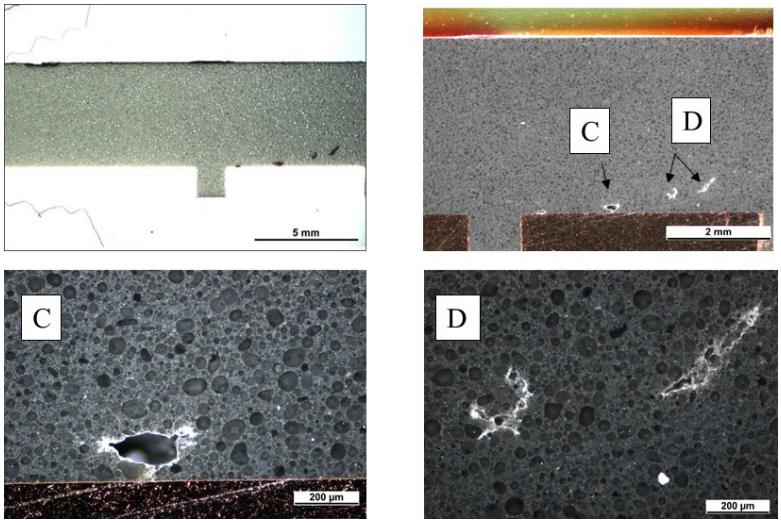

Figure 6.11: Intersection of the demonstrator 2

The lateral views for the demonstrator 2 also prove that all three dark points, which are visible on the SAM images, exist in the mold package. Point C has more round structure in comparison to the point D. Therefore, as observed with both demonstrators, the results prove that the points considered as voids, which are detected by the software and by the visual observation fully exist in molded packages and are not any kind of surface artifacts.

Another important aspect in the void formation is that the standard deviations in the number of voids or the corresponding area of the voids, which are seen in Figure 6.7, are quite large for almost all process parameter set numbers. It is realized that there is a certain deviation in the void formations of the molded packages between the left cavity and the right cavity. Figure 6.12 illustrates the difference in the number of voids and the corresponding area of voids observed in the packages from the left cavity and the right cavity.

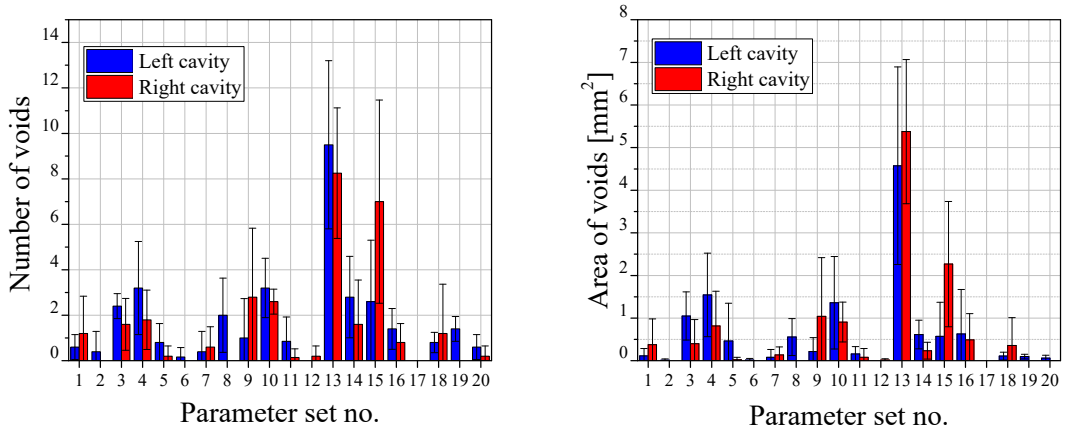

Figure 6.12: Comparison of number of voids (left) and area of voids (right) between left and right cavity with respect to 20 different process parameter set

As seen in Figure 6.12, in most of the process parameter sets, the mean values of the number of voids and the area of the voids in the left and the right cavities show differences. The void formation in the molded packages of the left cavity is slightly higher in comparison to void formation of the molded packages from the right cavity. These differences observed in the void formation can be originated due to the temperature differences between the left and the right cavities, which are demonstrated in Section 6.2.2. The approximately 2 °C of temperature difference between the left and the right cavities can lead to such deviations in the number of voids and the corresponding area of voids between the cavities. Apart from the differences observed in void formation between the left and right cavities, large standard deviation in number of voids and in area of voids can be seen in Figure 6.12 within each cavity. This variation of void formation within each cavity can be originated from the fluctuations of the temperature and the pressure from cycle to cycle, which are also mentioned in Section 6.2.2.

Wire Sweep

Figure 6.13 represents the wire sweep with respect to 20 different process parameters set for long and short wire bonds in both positions on the layout, namely in near gate and in far from the gate areas for left and right cavities together.

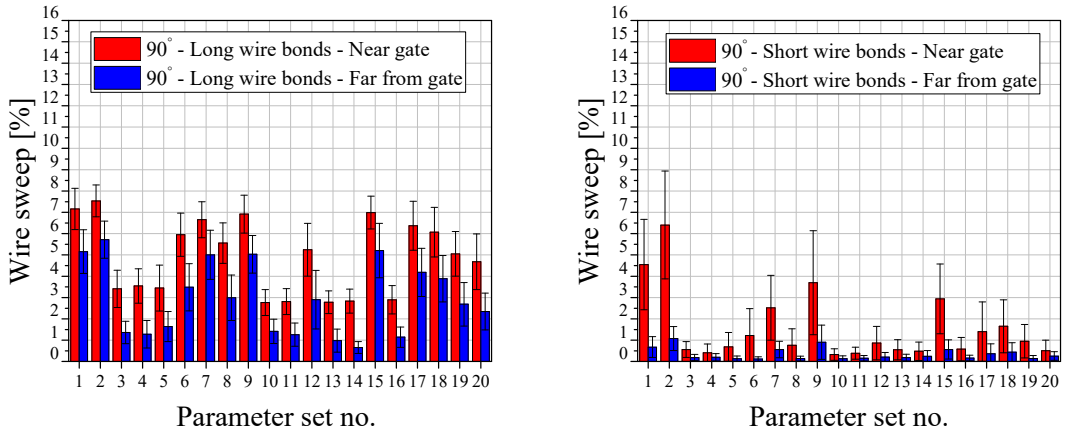

Figure 6.13: Wire sweep with respect to 20 process parameter set for long wire bonds attached at 90° (left) and for short wire bonds attached at 90° (right) to gate in near gate and far from the gate area, averaged from left and right cavity

According to Figure 6.13, the wire sweep for long wire bonds in both positions on the layout are influenced by the variations in the process parameters. The long wire bonds near gate show more wire sweep compared to the long wire bond in far from gate area, which confirms the results obtained in preliminary experiments. The short wire bonds in near gate area are also influenced by the different process parameters, whereas the short wire bonds far from gate show in general very reduced wire sweep. For the short wire bonds, especially in some process parameter combinations such as parameter set no. 1, 2, 7, 9 and 15 large wire sweeps are observed. Those are the parameter combinations having the highest transfer speed of 6.5 mm/s in the experimental plan shown in Table 6.1. The least wire sweep for long wire bonds and short wire bonds in all positions on the layout is observed for the parameter set no. 13 and 14. Figure 6.14 displays the influence of the process parameters on wire sweep of the long and short wire bonds, which are attached at different angles to the gate in near gate area.

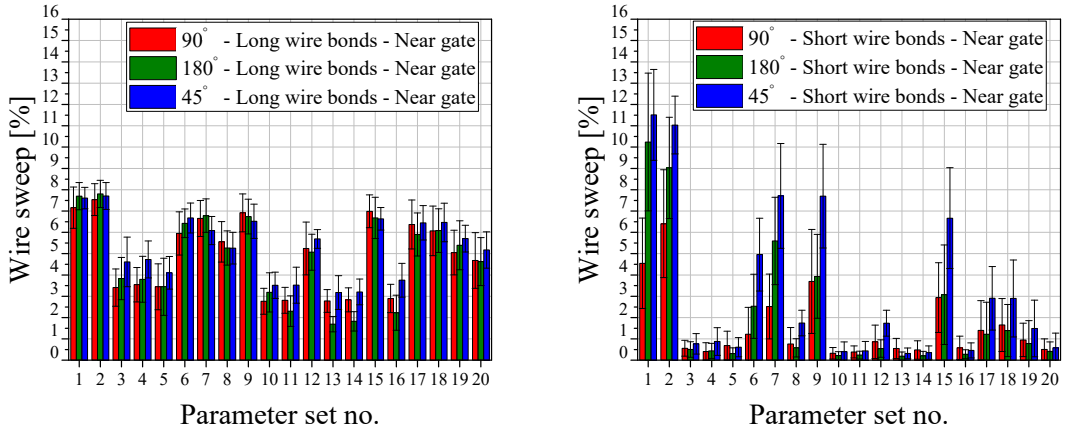

Figure 6.14: Wire sweep of long wire bonds (left) and short wire bonds (right) attached at different angles i.e. 90°, 45° and 180° in near gate area with respect to 20 different process parameter set, averaged from left and right cavity

Different wire bond angles with respect to the gate show similar wire sweep almost in all process parameter set numbers. The mean values of the wire sweep for the long wire bonds attached at 45° to the gate is slightly higher in comparison to the mean values of the wire sweep for the wire bonds attached at 90° and 180° to the gate, which confirms the results obtained in the preliminary experiments. In addition, for the short wire bonds the wire sweeps show differences depending on the angle of the wire bonds to the gate. Especially for some parameter set numbers such as no. 1, the short wire bonds have an excessive wire sweep and large deviations between different angles of the wire bonds to the gate. The wire sweep is varied remarkably in different angles of the short wire bonds especially for the parameter set numbers 1, 2, 7, 9 and 15, where the transfer speed is high. Despite the fact that the short wire bonds usually show less wire sweep in comparison to the long wire bonds, when the transfer speed is high, the short wire bonds in particular in the near gate area show large wire sweep as well. In fact, wire sweep observed in the short wire bonds is in the same micrometer range as wire sweep observed in the long wire bonds. However, since wire sweep is illustrated in percent, where the measured wire sweep is divided to the length of the corresponding wire bond, the short wire bonds represent in percentage also larger wire sweep.

Furthermore, according to Figure 6.14, when the short wire bonds show large wire sweep such as in the parameter set no 1, 2 and 9, the wire bonds with an angle of 45° illustrate the largest wire sweep in mean value compared to other groups, which confirms the results observed in preliminary experiments. It is important to mention that the abbreviated directions of 90°, 45° and 180° are only the directions to the gate, and not the directions to the flow front. The flow front becomes irregular especially when the molding compound passes the dummy components. Yet, especially for the wire bonds which are far from the gate it is difficult to determine the exact angles of the wire bonds to the flow front. Thus, to meet an abbreviation which is valid for all the wire bond groups on the layout, namely in far from gate and near gate area, wire bonds are marked in regard of their direction to the gate.

As seen in Figure 6.13 and Figure 6.14, the standard deviation in wire sweep is quite high. The reason for that is the wire sweep represented in those diagrams are the average values of the two wire bonds, which have the same lengths and which are in the same group in terms of the direction of the wire bonds to the gate. For instance, wire sweeps are averaged for long wire bond (l1) and long wire bond (l2) which are bonded at direction of 45° to the gate in the near gate area. Detailed schematic illustration of the wire bonds with corresponding abbreviations of each single wire bond is given in Figure 6.15.

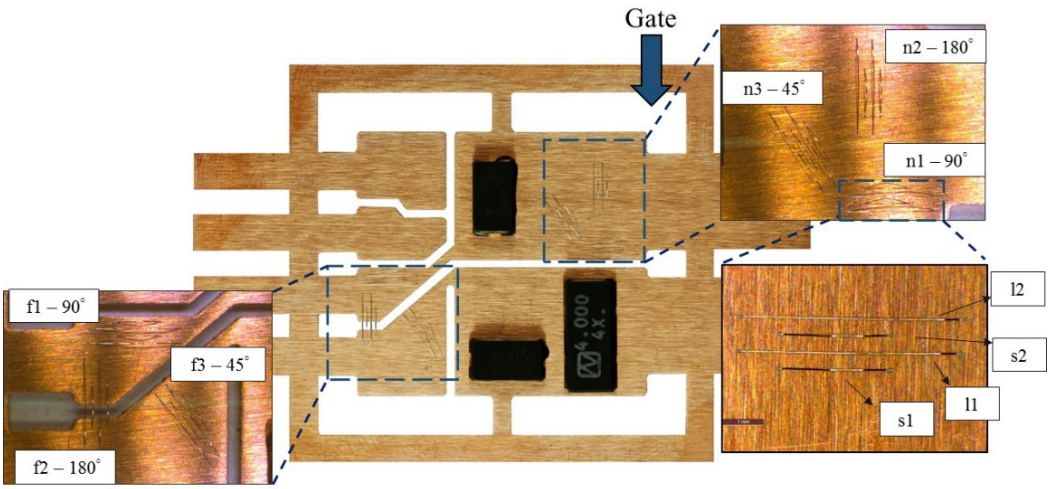

Figure 6.15: Detailed schematic representation of wire bonds on layout with corresponding positions and abbreviations. “n” is an abbreviation for wire bonds bonded in near gate area whereas “f” states for far from gate. “s1” and “l1” are abbreviations for short wire bond 1 and long wire bond 1 respectively. Numbering of wire bonds of 1 to 2 starts always from the first wire bond, which is closest to gate, such as s1, is closer to gate compared to s2. 45°, 90° and 180° represent the groups of wire bonds depending on their angles to gate.

It is recognized that both wire bonds with the same lengths in the same group such as 45° to gate do not necessarily show the similar wire sweep. Figure 6.16 illustrates the wire sweep measured for long wire bond 1 and for long wire bond 2 as well as the wire sweep observed in left and right cavity for long wire 2.

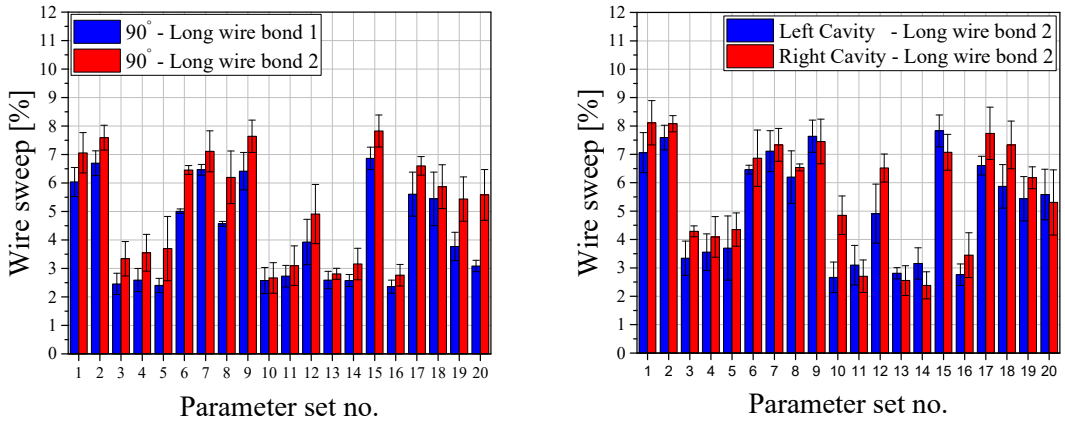

Figure 6.16: Difference in measured wire sweep between long wire bond 1 and long wire bond 2 for group of 90° to gate (left), and difference between wire sweep for long wire bond 2 at 90° to gate measured in left and right cavity (right) with respect to 20 different process parameter sets

As illustrated in Figure 6.16, the long wire bond 2 shows more wire sweep compared to the long wire bond 1. In addition to that, certain deviation in the wire sweep values for the molded package between the left and the right cavities are observed. As previously mentioned, it is inspected that the temperature measured in the left cavity is slightly higher than the temperature measured in the right cavity circa around 2 °C. According to the results given in preliminary experiments, temperature is found as one of the most significant process parameters for the wire sweep. Thus, the wire sweep value obtained in the molded packages from left and right cavities can remarkably differentiate from each other due to the temperature difference. To assure whether the wire sweeps measured in left and the right cavities are significantly different from each other, t-test is conducted. The results of the t-test show that there is significant difference in the wire sweep values between the left and right cavities ($p<0.05$, null

hypothesis is rejected) when comparing the same wire bond at the same position in two cavities. Therein, for the precision of the process model each wire bond as well as the right cavity and the left cavity will be considered separately when establishing the process model.

6.3 Analysis of Influence of Material Characteristics on Package Quality

After the preliminary experiments are performed which involve the basis characterization of EMC 1 in terms of understanding the impacts of batch differences, humidity and storage durations with DEA and rheological methods, as a next step the main experiments are carried out. The goal of the main experiments is to understand the influence of batch differences, storage duration and humidity of EMC 1 on the quality of the molded package such as on void formation and wire sweep. For this reason, the experiments are conducted in molding machine LHMS 28 to mold the test vehicle with the wire bonds and dummy components. The tool geometry with an implemented temperature, pressure and DEA sensors are shown in detail in Section 3.2.1. The influence of batch variation, storage duration and humidity of EMC 1 on void formation and wire sweep are analyzed. Based on the experiments conducted in this section, a material model is generated, which expresses the correlations between the variations in the EMC 1 properties and void formation as well as wire sweep in the molded packages. The performed measurements to examine the influence of storage duration, humidity and batch variations on the voids and wire sweep are introduced in Section 6.3.1, 6.3.2 and 6.3.3 respectively. The results of the experiments are given in Section 6.4. Since in this section the impacts of the variations in the material characteristics on selected quality characteristics are the focus, the process parameters are kept constant. All experiments are carried out with a central process parameter set, namely 175 °C molding temperature, 4 mm/s transfer speed, 8 s preheat time and 110 bar holding pressure.

6.3.1 Storage Duration

Investigation of the impacts of storage duration of EMC 1 on the wire sweep and void formation is conducted as the same way described in Section 5.3.2 but only with a different specimen geometry, namely with a demonstrator which consists the wire bonds and the dummy components. Initially, the pellets of EMC 1 are thawed for 1 hour in desiccator, then preconditioned for 0 h, 8 h, 16 h, 24 h, 48 h and 72 h in a vacuum oven at 0 % RH and 30 °C. Similar to the preliminary experiments, the data logger Multimetrix DL 5 is used during preconditioning in vacuum oven to assure that the temperature and the humidity stay constant. The demonstrators are then molded in transfer molding machine with the preconditioned pellets. The viscosity behavior of the preconditioned pellets during molding are recorded with DEA simultaneously. After the molding process, the molded demonstrators are conveyed to an oven for PMC at 180 °C and for 4 h. The void formation in the package due to the prolonged storage duration is examined. Subsequently, the specimens are sent to the laser ablation process to open the package in order to analyze the wire sweep.

6.3.2 Humidity

To understand the effect of humidity of EMC 1 on quality characteristics in the molded package, EMC 1 pellets are preconditioned for 0 h, 8 h, 16 h, 24 h, 48 h and 72 h in a climate oven at 90 % RH and 30 °C. The humidity and the temperature are recorded during preconditioning with the data logger Multimetrix DL 5 to control the stability of the humidity and the temperature in climate oven. The water uptake of EMC 1 pellets is then measured with Karl-Fischer titration directly after the preconditioning. Additionally, the remaining parts of the preconditioned pellets in the cull area after the molding process are also measured with Karl-Fischer titration to determine the variations in water content before and after the molding process. The demonstrators are molded with preconditioned pellets in transfer molding process and the viscosity behavior of EMC 1 are recorded with DEA during molding process. Subsequently, PMC process is applied for the molded demonstrators. After PMC process, the voids in the package are analyzed with SAM. After completing the SAM analysis, the molded packages are sent

to the laser etching process and wire sweep is measured after the package opening. The influence of the humid storage of EMC 1 on the void formation and wire sweep in the package are investigated.

6.3.3 Batch Variations

Influence of the batch variations on the quality characteristics is investigated with three batches, which are already described in Section 5.3.4. The demonstrators are molded with three different batches namely with batch 1, batch 2 and batch 3 and the DEA signals are recorded. Among three batches, batch 3 is characterized by a minimum storage time, whereas batch 1 has the longest storage duration. Following the PMC process, SAM analysis is carried out to examine the void formation. The molded packages are sent to laser opening to analyze the wire sweep. After the laser opening process, the influence of the batch variations on the void formation and wire sweep are determined.

6.4 Results of Influence of Material Characteristics on Package Quality

The results of the influence of material variations due to storage duration, humidity and batch variations of EMC 1 on void formation and wire sweep are presented in this section. It is important to emphasize that as indicated previously, all measurements for the analysis of void formation and wire sweep are performed after the PMC process. Additionally, standard deviations, which are calculated in the process stability analysis out of 25 repetitions (see Table 6.2), are used in this section as an additional approval to determine whether the variations in the wire sweep are significant.

6.4.1 Influence of Batch Variations on Package Quality

Figure 6.17 illustrates the impact of the batch variations on the number of voids and area of voids.

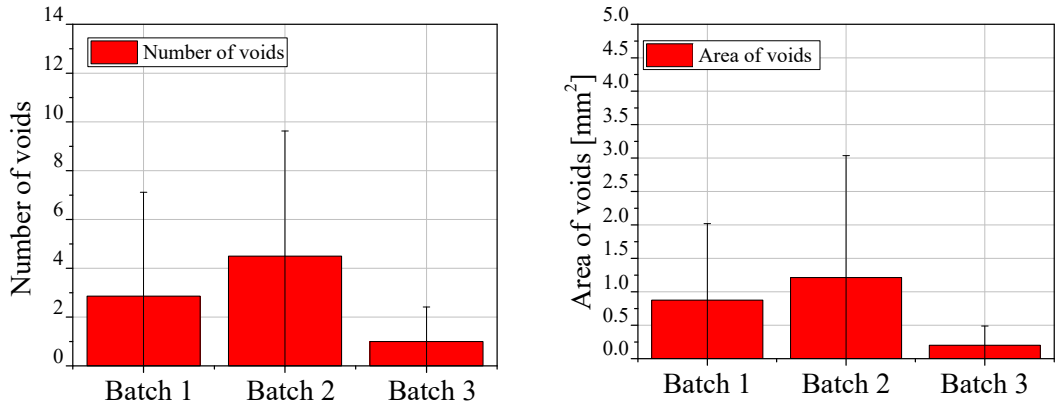

Figure 6.17: Number of voids (left), corresponding area of voids (right) measured in packages molded with three different batches of EMC 1 i.e. batch 1, batch 2 and batch 3

As seen in Figure 6.17, the number of voids and the corresponding area of voids for three batches show slight variations. Batch 3, which has the shortest storage time, illustrates slightly less void formation in comparison to batch 1 and batch 2.

Figure 6.18 demonstrates the wire sweep for short wire bonds bonded in two locations on the layout with respect to different batches. It is important to emphasize that due to the mentioned variations between the wire sweep of the similar wire bonds in Section 6.2.3, wire sweep of long wire bond 1 and long wire bond 2 attached at 90° to the gate will not be averaged in this section. The wire sweep of each wire bond will be treated individually and shown correspondingly in the diagrams. Short wire bond 2 and long wire bond 2 are selected generally in Section 6.4 for the comparison purpose of the wire sweep.

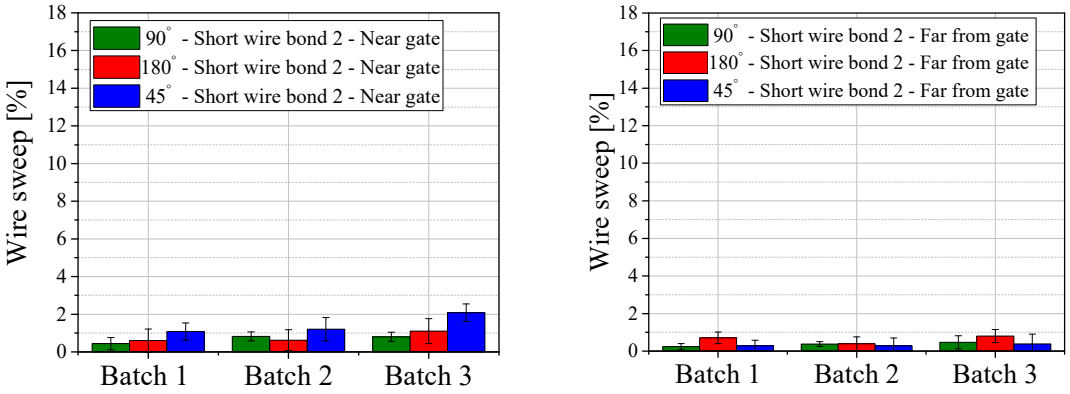

Figure 6.18: Comparison of wire sweep in the packages molded with batch 1, batch 2 and batch 3 for short wire bond 2 attached at 90°, 180° and 45° to the gate in near gate (left) and far from gate area (right)

As seen in Figure 6.18, short wire bonds in any directions to the gate do not show any significant variations with respect to different batches neither in near gate area nor in far from the gate area. The short wire bond 2 attached at 45° to the gate in the near gate area shows slightly larger wire sweep in comparison to the other directions. It is important to note that, the scale in Figure 6.18 is kept purposely the same as in Figure 6.19 to compare the results. Figure 6.19 depicts the wire sweep for long wire bond 2 in near gate and far from the gate area attached at different directions to the gate. In addition to the standard deviation measured out of the five samples in the diagrams, to determine whether the variations are significant, the standard deviations calculated from the process stability analysis out of 25 repetitions (see Table 6.2) are also implemented as horizontal dashed lines in the diagrams. The horizontal dashed lines assist to evaluate whether the observed variations between wire sweep for different batches lie within the standard deviations measured in process stability analysis. The dashed lines shown in the diagrams represent standard deviation in wire sweep of one certain wire bond, and for clear representation standard deviation of only one wire bond is shown in the diagrams. Either long wire bond 2 or short wire bond 2 attached at 90° angle in near gate or far from the gate area is selected for this purpose. Thus, the vertical dashed lines can only be used to evaluate the variation of one specific wire bond. For example, the dashed lines in Figure 6.19 refer the standard deviation observed out of 25 repetitions for long wire bond 2 attached at 90° angle to the gate in near gate (Figure 6.19 left) and far from the gate area (Figure 6.19 right), which refer to the variations within green columns.

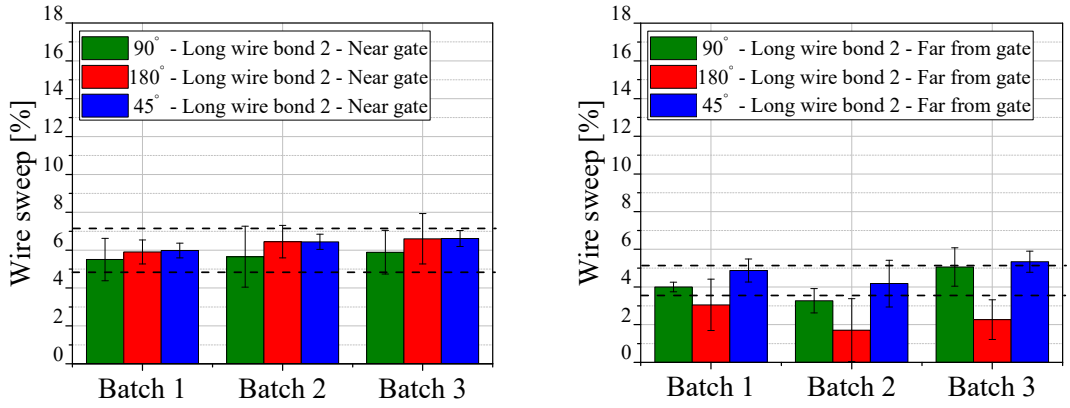

Figure 6.19: Comparison of wire sweep in packages molded with batch 1, batch 2 and batch 3 for long wire bond 2 attached at 90°, 180° and 45° to the gate in near gate (left) and far from gate area (right)

Wire sweep of long wire bonds attached at 90°, 180° and 45° to the gate in near gate area does not show pronounced variation with respect to different batches. As represented with additional dashed lines in Figure 6.19, the variation in wire sweep for long wire bond 2 attached at 90° angle to gate lie within the standard deviation observed in process stability analysis. On the other hand, for long wire bonds far from the gate area, wire bonds which are attached at different directions to the gate show different wire sweep. The long wire bond attached at 90° to the gate in far from the gate area displays larger wire sweep for batch 3 in comparison to batch 1 and batch 2. However, considering the standard deviation from the process stability analysis for long wire bond 2 attached at 90° to the gate shown with dashed lines in Figure 6.19, the variation is within the standard deviations. Although the mean value of wire sweep for long wire bond 2 attached at 90° to the gate molded with batch 2 lies slightly below, no significant variations can be observed in wire sweep between different batches.

6.4.2 Influence of Storage Duration on Package Quality

Figure 6.20 displays the results of void formation in the molded packages with respect to prolonged storage duration in dry environment in vacuum oven at 30 °C and 0 % RH. The illustrated results are the average values of the 15 molded packages.

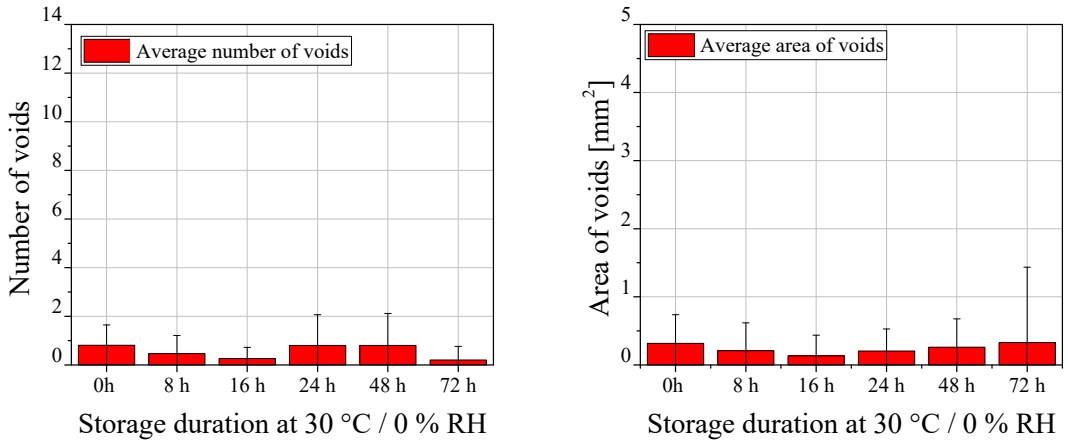

Figure 6.20: Average number of voids (left) and area of voids (right) with extended storage duration of 8 h, 16 h, 24 h, 48 h, 72 h at 30 °C / 0 % RH as well as 0 h fresh samples

Increasing storage duration at dry environment at 30 °C and 0 % RH does not demonstrate any impact on void formation in the package. The void formation which is observed at 0 h in the molded packages, stays almost constant with prolonging the storage duration. Figure 6.21 represents the results of wire sweep with extended storage duration at dry environment. The dashed lines on the diagram again illustrate the standard deviation measured from the process stability analysis for long wire bond 2 attached at 90° to the gate for the fresh samples, namely for 0 h of storage.

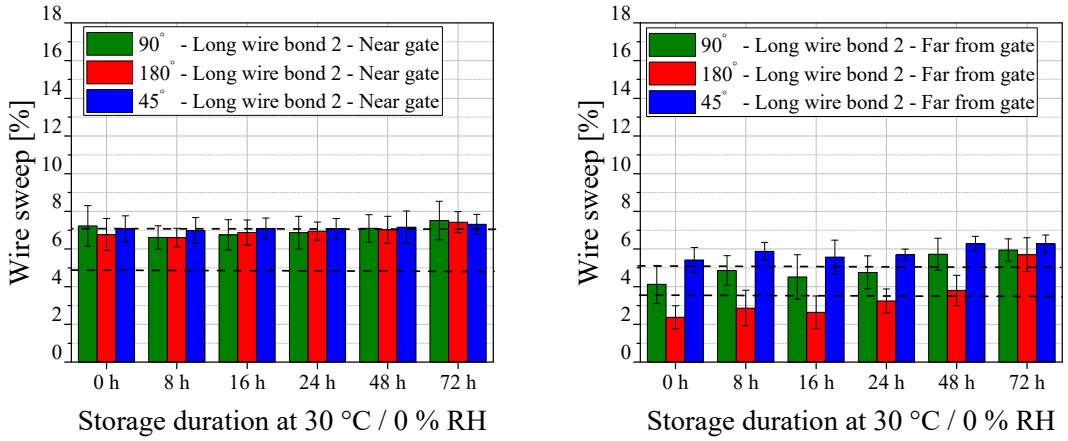

Figure 6.21: Influence of prolonged dry storage duration at 30 °C / 0 % RH on long wire bond 2 attached at 90°, 180° and 45° to the gate in near gate (left) and far from gate area (right)

No significant variations in wire sweep are observed with extended storage duration for long wire bonds attached at three different directions to gate in near gate area. Considering the standard deviation from the process stability analysis shown in Figure 6.21 with the dashed lines, only a slight increase is observed in the mean value of wire sweep for long wire bond 2 attached at 90° to the gate after 72 h of storage duration. On the other hand, for long wire bonds far from the gate, notable variations in wire sweep for different directions of the wire bonds are observed. In contrast to the long wire bond in near gate area, long wire bonds far from the gate show an increment in wire sweep with prolonged storage duration. Wire bonds attached at 180° to the gate illustrate the smallest wire sweep until 72 h of storage among other directions. After 72 h of storage, a sudden increase in the wire sweep of these wire bonds is observed. A slight increment in the wire sweep can also be seen in wire bond groups attached at 90° and 45° degrees to the gate. Based on the illustrated dashed lines, which represent the standard deviation for long wire bond 2 attached 90° to the gate, the variation in the wire sweep of these wire bonds becomes pronounced especially after 48 h of storage.

Figure 6.22 presents the wire sweep results for short wire bonds in near gate and far from the gate area. The dashed lines represent the standard deviation calculated from the process analysis for short wire bond 2 attached at 90° to the gate for fresh samples or in other words for 0 h samples.

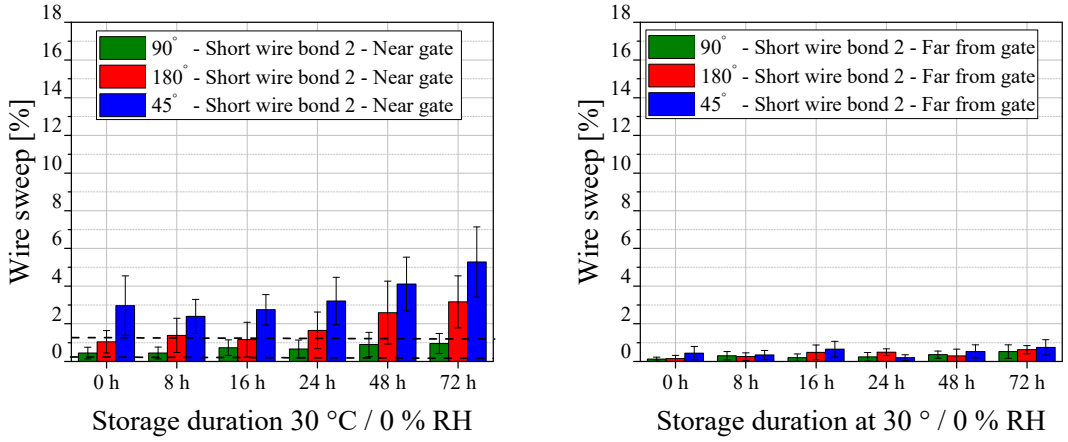

Figure 6.22: Influence of prolonged dry storage duration at 30 °C / 0 % RH on short wire bond 2 attached at 90°, 180° and 45° to the gate in near gate (left) and far from gate area (right)

The short wire bonds in near gate area are impacted by the prolonged storage duration. The wire sweep especially for the wire bonds attached with a direction of 45° and 180° to the gate illustrates large wire

sweep with extended storage duration. In Figure 6.22 only the standard deviation of wire sweep for a wire bond attached at 90° to the gate is implemented from the process stability analysis. Nevertheless, considering the standard deviations of wire sweep for the wire bonds attached at 45° and 180° to the gate given in Table 6.2, it is obvious that the variations in the wire sweep for those wire bonds lie outside of the standard deviations. Only the wire bond attached at 90° to the gate is not influenced considerably by the storage duration, where the variation in wire sweep stay within standard deviation. The short wire bonds in far from the gate area show minimal wire sweep and are not affected by the prolonged storage duration remarkably.

6.4.3 Influence of Humidity on Package Quality

Figure 6.23 illustrates the results of the void formation in the molded packages with respect to prolonged storage duration in humid environment in a climate chamber at 30 °C and 90 % RH. To comprehend the effect of humidity more clearly, the void formation with prolonged storage duration in dry environment is supplemented in the diagrams as well.

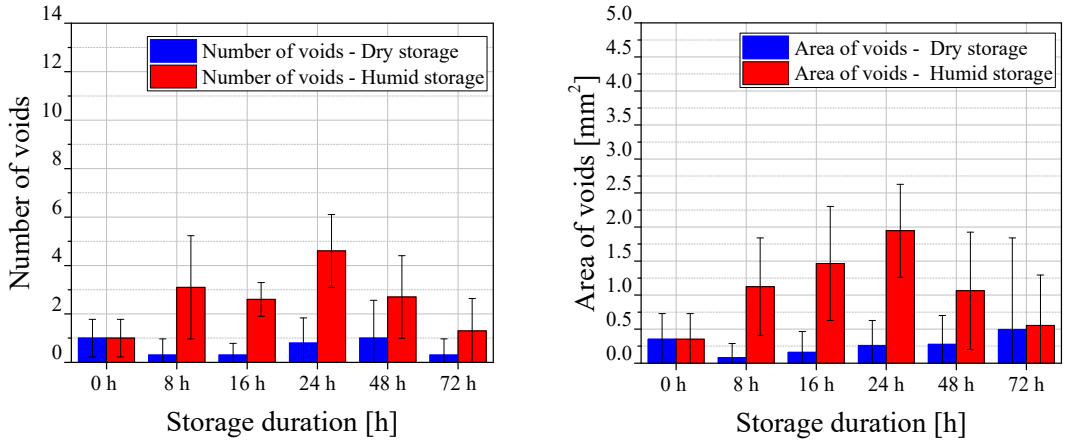

Figure 6.23: Number of voids (left) and corresponding area of voids (right) with prolonged storage duration of 8 h, 16 h, 24 h, 48 h, 72 h in humid and dry environment as well as fresh samples (0 h)

The number of voids and the area of voids are influenced by prolonged storage in humid environment and both increase with extended humid storage duration. The difference in the void formation between dry and humid storage duration can be recognized particularly with 16 h and 24 h of storage, where the void formation in the packages ascends notably due to an increase in the moisture content. The void formation seems to be reduced after 24 h of humid storage, however, the variation is within standard deviation of the number of voids and the area of voids. Figure 6.24 demonstrates the effect of humid storage duration on long wire bonds attached at 90°, 180°, 45° angle to the gate in near gate as well as in far from gate area. The dashed lines represent the standard deviation calculated from the process analysis for long wire bond 2 attached at 90° to the gate for 0 h samples.

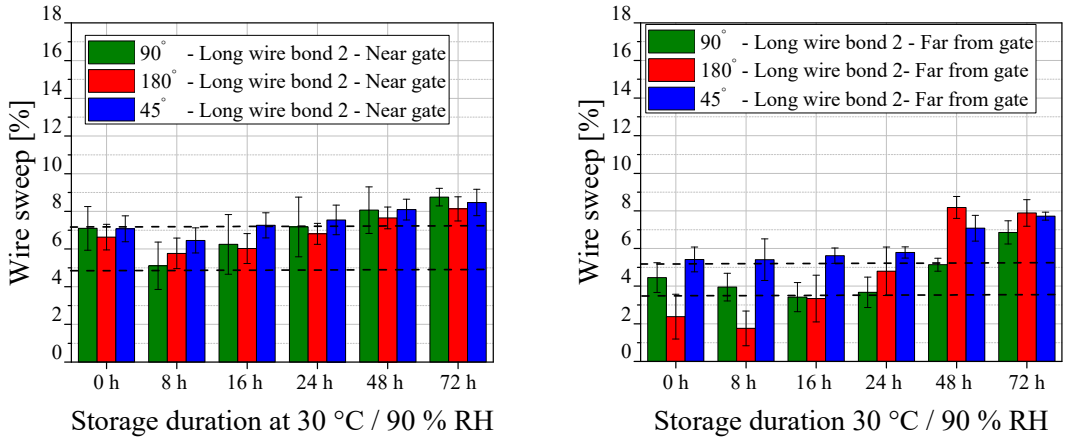

Figure 6.24: Influence of prolonged storage duration in humid environment at 30 °C / 90 % RH on wire sweep for long wire bond 2 attached at 90°, 180°, 45° to the gate in near gate (left) and far from the gate area (right)

The wire sweep of the long wire bonds is influenced by prolonged storage duration of EMC 1 in humid environment. It can be easily recognized from Figure 6.24 that all three different angles of the long wire bonds with respect to gate exhibit a raise in wire sweep with extended humid storage duration.
Apart from the individual standard deviations in Figure 6.24, considering the standard deviations shown as dashed lines from process stability analysis, the wire sweep of long wire bond 2 attached at 90° to gate becomes especially pronounced after 48 h of humid storage. Similarly, with prolonged storage duration in humid environment wire sweep for the wire bonds attached in other directions namely at 45° and 180° to the gate increases as well. On the other hand, long wire bonds in far from the gate show less wire sweep in comparison to the long wire bonds attached in near gate area (Figure 6.24 right). Similar to the wire sweep results obtained in the prolonged storage duration in dry environment, the wire sweep results vary between the wire bonds attached at 90°, 180°, 45° to the gate, when wire bonds are located in far from the gate area. Considering the standard deviations from process stability analysis, wire sweep raises significantly after 48 h humid storage for wire bonds attached at 90° to the gate. In addition, a pronounced increase in the wire sweep is distinguished after 48 h of storage also for wire bonds attached at 45° and 180° to the gate. Figure 6.25 depicts the impact of prolonged storage duration in humid environment on short wire bonds attached in near gate and far from the gate area attached at 90°, 180°, 45° to the gate.

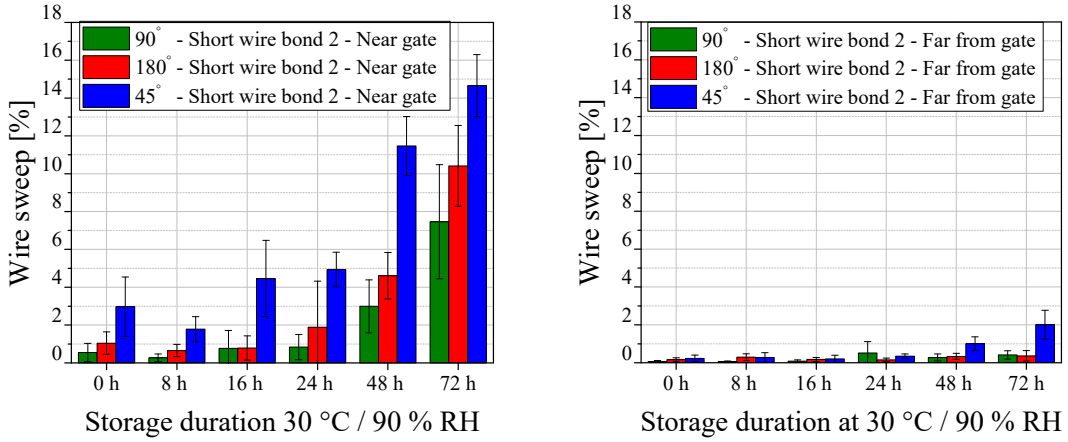

Figure 6.25: Influence of prolonged storage duration in humid environment at 30 °C / 90 % RH on wire sweep of short wire bond 2 attached at 90°, 180°, 45° to the gate in near gate (left) and far from the gate area (right)

The wire sweep for all wire bond groups attached at 90°, 45° and 180° to the gate in near gate area are remarkably impacted by the humidity storage of EMC 1. The wire sweep increases drastically with extended storage duration in humid environment. Excessive wire sweep for short wire bonds is observed for the wire bond attached at 45° to the gate when the humid storage duration exceeds 24 h. This remarkable increase in the wire sweep particularly for the wire bond attached at 45° to the gate can be also easily recognized from the optical microscope images, which are shown in Figure 6.26 for the packages molded with the pellets preconditioned for 48 h in humid environment.

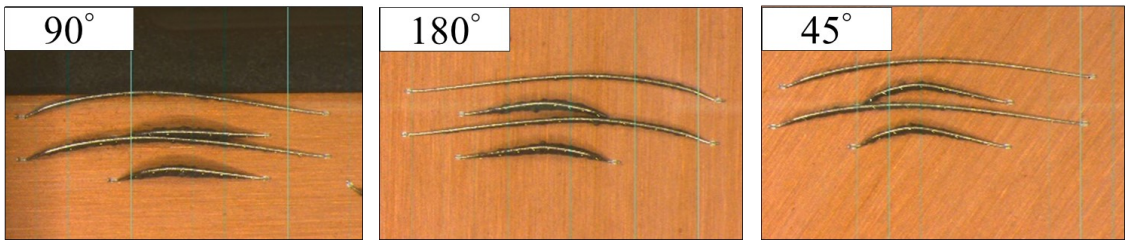

Figure 6.26: Optical microscope images of the wire bonds attached at 90° to gate (left), at 180° to gate (middle), at 45° to gate (right) in near gate area for the packages molded with pellets which are preconditioned for 48 h in humid environment at 30 °C and 90 % RH

Although the wire sweep of short wire bonds in near gate area are affected tremendously by the existence of the humidity in the pellets, the short wire bonds in far from the gate area demonstrate minimal wire sweep under humidity almost similar as in the dry preconditioning (Figure 6.25 right). Only a slight increase in the wire sweep is observed for the wire bonds attached at 45° to the gate after 72 h of storage in humid environment. This minimal wire sweep of short wire bonds in far from the gate area may be correlated with their corresponding positions on the layout. The humidity in the mold compound can be affected and possibly decreased by the mold temperature as the mold compound requires longer time to reach the wire bonds in far from the gate area. To investigate whether the absorbed water in the humid pellets is influenced by the mold conditions, the pellet remaining parts in the cull area after the molding process are collected and measured with Karl-Fischer titration. The moisture contents of the pellets which are preconditioned in humid environment before and after the molding process are compared in Figure 6.27.

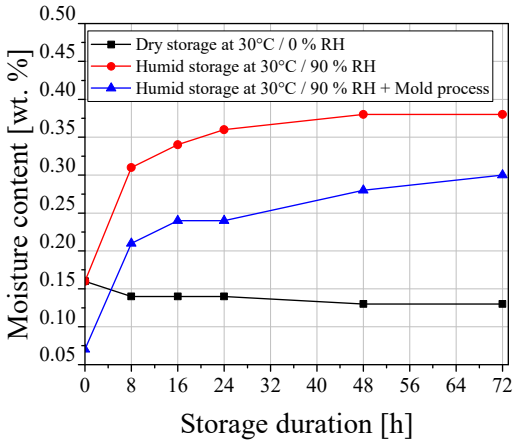

Figure 6.27: Moisture contents of the humid pellets preconditioned at 30 °C / 90 % RH before and after the mold process as well as dry pellets preconditioned at 30 °C / 0 % RH for a storage time of 0 h, 8 h, 16 h, 24 h, 48 h and 72 h

Karl-Fischer titration results illustrate that moisture content of the humid pellets after the mold process is below the moisture content level of the same humid pellets prior to molding in all storage durations. Although the water content of pellets does not reach the ultimate level of moisture content in dry storage,

the mold conditions contribute on reducing the existing water content in the pellets at around 0.10 %. Apart from the stable dimensions of short wire bonds, this may additionally contribute to the observed minimal wire sweep of the short wire bonds in far from the gate area under humidity, where the humidity impact is diminished to some extent and the short wire bonds are not affected from the humidity significantly.

This result leads to the next point of investigation to evaluate whether the absorbed humidity and its corresponding effects can be reduced at all. As discussed in Chapter 5, humid storage of pellets exhibits large influences on the dynamic viscosity behavior as well as on the ion viscosity of EMC 1. As seen in the results in Chapter 5, the delta, which is the difference between the maximum and the minimum ion viscosity observed in the ion viscosity curves for the humid samples are correlated very well with T_g of EMC 1. In order to understand the root cause of the variations in T_g in the existence of the humidity in EMC 1, further investigations are performed in this section together with the quality analysis. The variations observed in T_g of EMC 1, which are preconditioned in humid environment, can be supposedly originated on one side due to the change in the degree of the cure of EMC 1. T_g of the material usually is associated with the network density of the molding compound, where lower T_g implies lower network density or the degree of cure of molding compound [12]. On the other hand, the decrease in T_g can also be originated due to the plasticizer effect of the absorbed water molecules in the molding compound [67]. To highlight this topic and to determine whether the decrement in T_g of EMC 1 samples which are subjected to humid preconditioning is due to the reduced cross-linking degree of the humid EMC 1 samples, or due to the plasticizer effect of the water molecules in EMC 1, the preconditioned pellets, which are molded with transfer molding machine are further conveyed to PMC process. Applying the PMC process to the samples can help to understand whether the humidity effect in the samples is reversible and the water molecules can be removed from the preconditioned samples under higher temperatures. Figure 6.28 depicts T_g of the preconditioned samples for 24 h, 48 h, 72 h with and without PMC process. In addition, the sample bars, which are produced with fresh pellets (0 h), are also measured with DMA with and without PMC process to compare the results with the initial state of EMC 1.

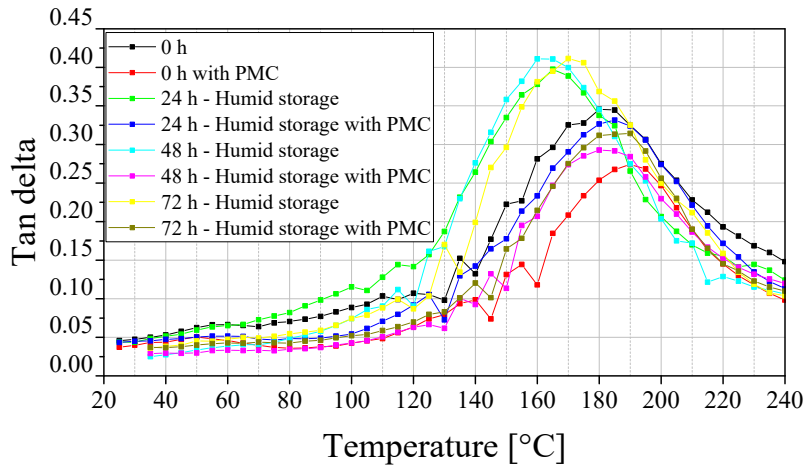

Figure 6.28: DMA measurements of EMC 1 sample bars with and without PMC process which are molded with the preconditioned pellets for 24 h, 48 h and 72 h at 30 °C and 90 % RH as well as fresh samples (0 h)

The influence of PMC process on T_g of EMC 1 can be seen in Figure 6.28. When comparing the initial state of EMC 1 (0 h), T_g of EMC 1 without PMC is found around 185 °C whereas with PMC T_g of EMC 1 rises to 190 °C. Thus, at initial state of EMC 1, when the pellets are not subjected to any preconditioning, the PMC process contributes in T_g of EMC 1 at around 5 °C. When EMC 1, however, is exposed to the humid storage, T_g of EMC 1 for 24 h and 48 h humid storage without PMC is found as 165 °C. T_g of EMC 1 for 72 h of storage without PMC is slightly higher with 170 °C. On the other hand, when sample bars, which are molded with preconditioned pellets for 24 h, 48 h as well as 72 h in

humid environment, are subjected to PMC process, T_g increases around 20 °C and arrives to 185 °C for all storage durations. Hence, T_g of all sample bars which are molded with preconditioned pellets reaches the same level of T_g of fresh samples when the PMC process is applied. This result may imply that the water molecules existing in EMC 1 pellets act as plasticizer in this case and the effect of humidity can be removed from the molding compound with an additional PMC process.

To confirm the results obtained from the DMA, and to observe whether the viscosity of the preconditioned pellets return to their original ion viscosity when the samples are dried, further investigations are performed with squeeze flow rheometer and DEA. The pellets are firstly preconditioned for 24 h at 30 °C and 90 % RH in climate oven, and subsequently dried in vacuum oven for 24 h at 30 °C and 0 % RH. The preconditioned pellets are then measured with DEA as well as with squeeze flow rheometer to determine the changes in the ion viscosity as well as the viscosity behavior of EMC 1. The results are depicted in Figure 6.29.

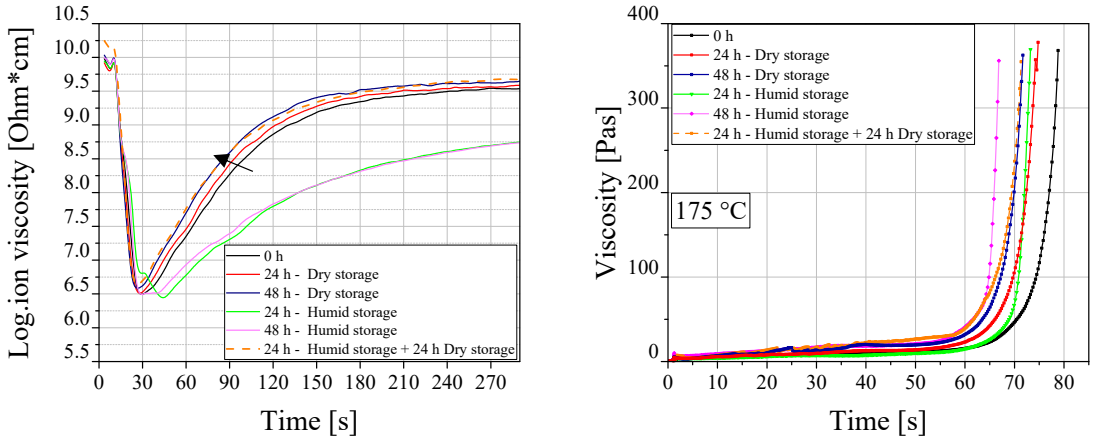

Figure 6.29: Ion viscosity curves (left) and viscosity curves from the squeeze flow rheometer (right) for the pellets preconditioned for 24 h, 48 h in dry and humid environment as well as the pellets preconditioned for 24 h in humid environment, and adjacent dried for 24 h at 30 °C and 0 % RH in vacuum oven

As the overall storage duration of the pellets, which are preconditioned for 24 h humid storage and adjacently dried for 24 h, which makes together 48 h, the ion viscosity curves of pellets that are preconditioned for 48 h in dry and humid environment are also supplemented in Figure 6.29. The ion viscosity curve for the pellets preconditioned for 24 h in humid storage and adjacent for 24 h in dry storage is depicted as dashed lines. As seen in Figure 6.29 (left), when the pellets are preconditioned for 24 h or 48 h in humid environment, the ion viscosity curves are completely different in comparison to the pellets preconditioned in dry environment. When the pellets are first exposed to 24 h humid storage and then dried for 24 h in vacuum oven, ion viscosity of the pellets changes drastically and becomes almost identical as ion viscosity signal for EMC 1 pellets which are preconditioned for 48 h in dry storage. This implies that, by 24 h of an extra drying of the pellets, which are already exposed to humid environment for 24 h, the humidity effect on the ion viscosity behavior can be reduced. The viscosity curves which are measured with squeeze flow rheometer also prove this result (Figure 6.29 right). Although the shear viscosity of EMC 1 is less sensitive to humidity in comparison to the ion viscosity curves, the viscosity of the preconditioned pellets, which are subjected to 24 h humid and adjacent 24 h dry storage, shows similar behavior and depicts almost identical viscosity behavior as the pellets, which are preconditioned for 48 h in dry environment in vacuum oven. Thus, the rheology measurements also confirm the results obtained from the DMA measurement and indicate that the humidity influence of the preconditioned pellets can be reversed. Nevertheless, one of the most crucial parts in terms of the humidity is to determine whether this situation has any impact on the quality features of the molded packages. Therefore, the packages are molded with pellets, which are preconditioned for 24 h in humid environment at 30 °C and 90 % RH and subsequently dried for 24 h in dry environment at 30 °C and 0 % RH, and void formation and wire sweep analysis are performed. Figure 6.30 represents the impact

of the humid and adjacent dried pellets for 24 h on void formation in the molded packages. For comparison of the results, the void formation in the packages molded with fresh EMC 1 as well as with preconditioned pellets for 24 h and 48 h in dry and humid environment are supplemented in Figure 6.30.

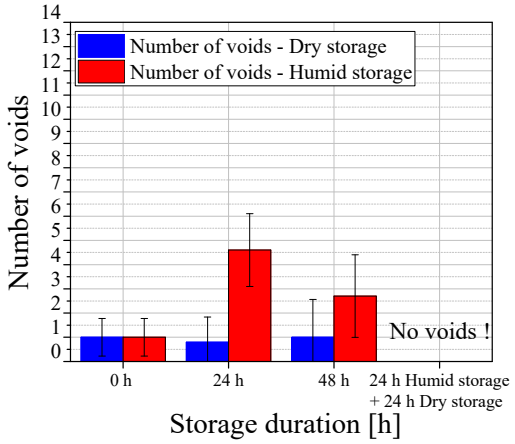

Figure 6.30: Influence of preconditioned pellets for 24 h in humid environment at 30 °C / 90 % RH and subsequently dried for 24 h in dry environment at 30 °C / 0 % RH on void formation in the molded packages

As seen in Figure 6.30, the packages, which are molded with the pellets preconditioned for 24 h in humid environment and subsequently dried for 24 h in dry environment, show no void formation. The drying process helps to remove the humidity effect and to obtain packages without any voids. To assure that the pellets achieve indeed the same humidity level as the initial situation (0 h), Karl-Fischer titration is performed. The moisture content in the pellets, which are preconditioned for 24 h at 30 °C and 90 % RH and subsequently dried for 24 h at 30 °C and 0 % RH, is measured. The moisture content in the pellets is found as 0.14 %. Considering the fact that 0 h fresh pellets have the moisture content of 0.16 %, this result implies that the existing humidity can be completely removed from the pellets. After drying process, the moisture content in the pellets returns back to the similar level as in the fresh pellets (0 h) but more correctly to an exact moisture content of the pellets stored for 24 h in dry storage (0.14 %).
In addition to the void formation, wire sweep analysis is also executed with the preconditioned pellets for 24 h in humid environment and subsequently dried for 24 h in vacuum oven. Figure 6.31 depicts the results of long wire bond 2 attached at 90° to the gate in near gate area as well as the short wire bond 2 attached at 45° to the gate, which shows the largest wire sweep among the short wire bonds in near gate area.

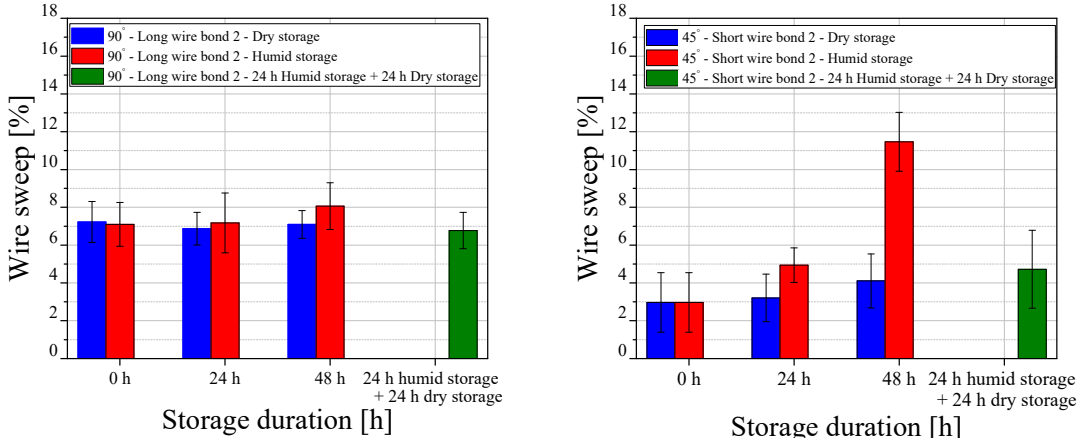

Figure 6.31: Wire sweep for long wire bond 2 attached at 90° to the gate in near gate area (left) and for short wire bond 2 attached at 45° to the gate in near gate area (right) from the package molded with the pellets preconditioned for 0 h, 24 h, 48 h in dry and humid environment as well as 24 h in humid environment at 30 °C / 90 % RH and subsequently dried for 24 h in dry environment at 30 °C / 0 % RH

When the package is molded with the pellets, which are preconditioned for 24 h in humid environment, and subsequently dried for 24 h in vacuum oven, the wire sweep for the long wire bond 2 has the same wire sweep level as for the packages molded with the pellets preconditioned for 48 h or similarly 24 h in dry storage. The largest effect of drying the pellets can be observed more clearly in the short wire bond 2 attached at 45° to the gate (Figure 6.31 right). As previously explained, the humidity shows remarkable influence on the wire sweep of the short wire bonds in near gate area. Particularly the short wire bonds attached at 45° to gate illustrate excessive wire sweep when the package is molded with the humid pellets. Nevertheless, as seen in Figure 6.31 on the right hand side, when the pellets are dried and the humidity is removed from the pellets, reduced wire sweep is observed in the molded packages. By drying the pellets in vacuum oven at 30 °C in 0 % RH for 24 h, humidity effect on the wire sweep is diminished, and the mold package shows similar wire sweep level as the packages molded with the pellets preconditioned for 48 h in dry environment. This result can be explained by the viscosity behavior. As the wire sweep is strongly influenced by the viscosity of the molding compound, when the viscosity of the molding compound returns back to the initial situation after drying step (see Figure 6.29), the effect on the wire sweep is also eliminated.

6.5 Summary

The detailed analysis of the pressure and temperature sensors shows that the sensors deliver consequential information about the flow and cure behavior of the molding compound. Moreover, the process stability is assured considering the sensor signals obtained from pressure and temperature sensors. However, some deviations between left and right cavity are observed.

The results of the main experiments for the process analysis show that most of the voids evaluated in 20 process parameter combinations are formed in zone 4. This confirms the assumption made in preliminary experiments that the voids are formed as a tendency in the area far from the gate very likely due to the flow front end. Since zone 4 is diagonally the farthest area on the layout, the molding compound reaches this area at latest after flowing the longest way in the cavity. Along this way, the viscosity of the molding compound increases. Moreover, as observed in the short-shots images, the flow front of the molding compound has bubble-like structures (see Figure 3.7). When the molding compound reaches at the end of the cavity, flow front collapses here and it causes void formation predominantly in this area. Therefore, when the holding pressure is increased, this may especially compress the voids formed in this area and cause reduction in the void formation. In opposition to this situation, least void formation is observed in the close to the gate area such as zone 1 most probably due to the fast propagation of the flow front.

Furthermore, the void formation and wire sweep results show that there are differences between the results observed in the left and right cavity. For the wire sweep evaluation, it is determined that the wire sweep values vary for the wire bonds which are attached in the same area and which have the same length. Thus, each wire bond will be evaluated separately to meet more precise estimation on the wire sweep with the process model.

As a second part of the main experiments, material investigations are conducted and the results show that batch variation has only slight impact on void formation and wire sweep. Storage duration does not show major impact on void formation, however, wire sweep for the short wire bonds and long wire bonds are influenced by prolonged storage duration. The storage duration influences especially the wire sweep for long wire bond 2 attached at 180° to the gate in far from the gate area. The reason for the observed raise in wire sweep for the wire bonds in far from gate area can be explained with an increase of the viscosity of material with extended storage duration. As previously shown in the preliminary experiments, the viscosity of EMC 1 raises with prolonging storage duration in dry environment. The difference in the viscosity may especially be critical for the wire bonds far from the gate area, in which the flow front of the material arrives at latest. When the material reaches to the wire bonds at far from the gate area, material may access the wire bonds with higher viscosity and exert more force on wire bonds. On the other hand, the short wire bonds far from the gate show almost negligible wire sweep and

are not influenced by the prolonged storage duration. This can be attributed most probably to the stable dimensions of the short wire bonds, which offer less contact area for the viscous melt.
The largest impacts on the void formation and wire sweep are observed when the pellets are exposed to humidity. The void formation increases with prolonged storage duration of the pellets in humid environment especially until 24 h storage. Based on the Karl-Fischer titration results, it is evident that the largest water absorption happens until 24 h of humid storage. The wire sweep for the long wire bonds as well as for the short wire bonds increase with extended humid storage duration. It is observed that the minimal wire sweep examined in the short wire bonds in far from the gate area can be attributed also to the effect of the mold conditions on reducing the existing humidity in the pellets.
To comprehend the behavior of the water molecules in the pellets, further investigations are executed and the results show that the water molecules in the molding compound can be removed from the pellets with an extra drying step without causing any significant change in the material characteristics. The void formation as well as wire sweep are analyzed with pellets which are first stored in humid environment for 24 h at 30 °C and 90 % RH and subsequently dried for 24 h in vacuum oven at 30 °C and 0 % RH, and the results demonstrate that the pellets return to their initial moisture level after drying. Therefore, when the pellets are dried after exposure to humidity, the humidity influence on the material characteristics is removed, and the material behaves in a similar way as if it is preconditioned in dry environment for the corresponding storage time. Thus, it is important to consider that the humidity has a great impact on void formation and wire sweep, but when the existence of humidity in the pellets is known, it is also possible to remove the humidity from the pellets of the molding compound without causing any significant variation in the material characteristics.

7 Evaluation of Statistical Correlations and Model Definition

In this chapter, the process and material models are introduced. The process and material models are generated based on the results of the main experiments, which are given in Chapter 6. The generated models allow to describe the relationship between the process parameters, the material characteristics and the package quality. The general definition of the models is demonstrated schematically in Figure 7.1.

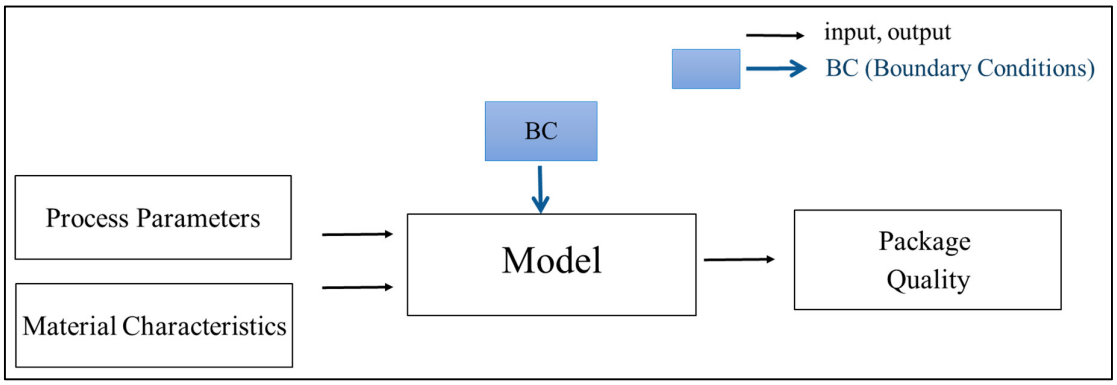

Figure 7.1: General definition of model

As seen in Figure 7.1, the process parameters and the material characteristics are the input of the model, whereas the package quality is the output of the model. The models provide understanding of the impact of the input parameters on the output parameters, and describe the relationship between the input and the output parameters mathematically.

In this work, regression analysis is used to generate the models. Thus, in this chapter, regression analysis based on the main experimental results is conducted. The approaches to establish the regression models are demonstrated. The process model and the material model are considered separately as two different aspects, and accordingly, the chapter is divided into two parts. In the first part of this chapter, in Section 7.1, the mathematical definition of the process model is demonstrated. An approach to generate a process model is evaluated. The generated process model is shown, which allows estimation of the wire sweep and the void formation in the package. The optimum process parameters of the transfer molding process to achieve the best package quality in terms of void formation and wire sweep are introduced.

In the second part of this chapter, in Section 7.2, regression analysis is conducted to generate the material model, which defines the relationship between the variations in the material characteristics and the void formation as well as the wire sweep. Regression analysis is performed based on the results of variations in the material characteristics, which are given in Chapter 6. The definition of the material model is illustrated, and important aspects, which are crucial concerning the material model, are discussed. Summary of the conducted approach as well as the established process and material models is given in Section 7.3.

7.1 Evaluation of Process Analysis and Process Model Definition

In this section, an approach to generate a mathematical regression model is given. The required steps to establish a process model are described in detail. First, a schematic description of the process model and the objective of the process model are introduced in Section 7.1.1. A systematic approach to establish a regression model is given and the required steps are described in detail in Section 7.1.2. Subsequently, regression analysis is performed to determine the interactions between the process parameters and to evaluate the significant terms that are necessary to consider in the process model. The results of

regression analysis are shown in Section 7.1.3. In addition, the generated process model with significant terms is demonstrated in Section 7.1.4. The generated process model allows to estimate the void formation as well as the wire sweep in the package, thus the prediction quality of the model is determined and shown in Section 7.1.5. Finally, based on the generated mathematical process model, the optimum process parameters which deliver the best package quality by considering the void formation and wire sweep are determined. The optimum process parameters of the transfer molding process are given in Section 7.1.6.

7.1.1 Objective of the Process Model

The process model describes a relationship between the process parameters and package quality. The generation of a process model has two objectives. The first objective is to predict the quality characteristics such as void formation and wire sweep in the molded package. The second objective is to determine the optimum process parameters of the transfer molding process, which delivers the best package quality in terms of void formation and wire sweep. Hence, a systematic approach is represented, which enables to establish a mathematical model based on regression analysis in order to predict the package quality and to identify the process parameters which enable optimum package quality. The schematic illustration of the process model is demonstrated in Figure 7.2.

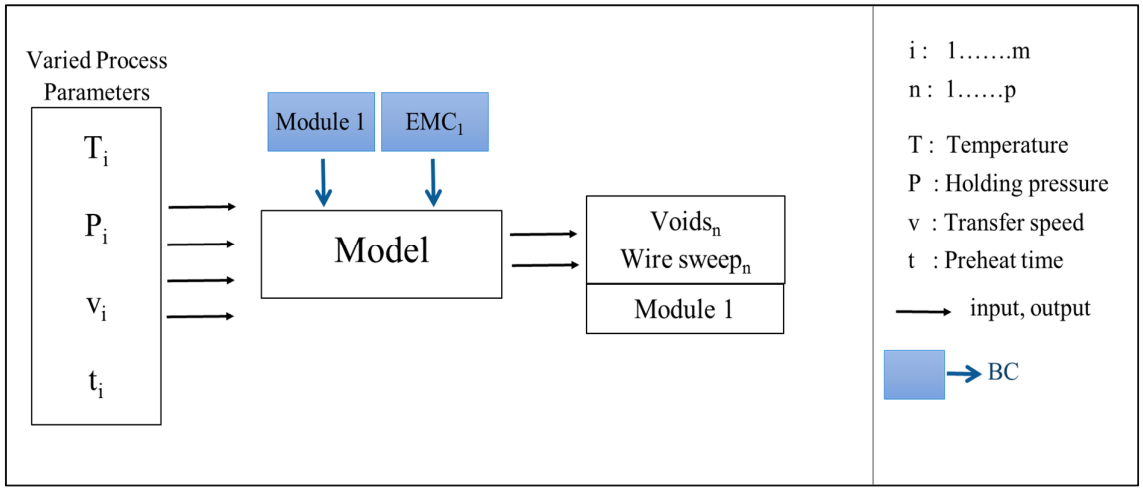

Figure 7.2: Schematic illustration of the process model

The model consists of four process parameters: temperature, holding pressure, preheat time and transfer speed and two quality characteristics of the package: void formation and wire sweep. The process model mathematically expresses the relationship between these input parameters, which are the varied process parameters and the output parameters, which are the quality features of the package, namely the void formation and the wire sweep. The process model, which expresses the correlations between the process parameters and the package quality, should on the one hand allow to predict the void formation and wire sweep, and on the other hand should determine the optimum process parameters. The shaded designated boxes in Figure 7.2 illustrate the boundary conditions of the model. As the main experiments are carried out with one certain module with a defined package geometry (see Chapter 4 for the package geometry) and with one molding compound with given material properties (see Chapter 3 for the EMC properties), module 1 and EMC 1 are the boundary conditions of this model.

7.1.2 Model Definition

To generate the process model, regression analysis is performed. With regression analysis, the significant process parameters and interactions between the parameters can be identified. The significant terms, which are determined with regression analysis, are then included into the model with corresponding coefficients depending on their significance level. Regression analysis is carried out with

a statistical software, namely with Cornerstone. A mathematical description of a regression model is illustrated in Equation 6.

$$\hat{y} = c_0 + \sum_{i=1}^{n} c_i\, x_i + \sum_{i=1}^{n} c_{ii}\, {x_i}^2 + \sum_{i=1}^{n-1} \sum_{j=i+1}^{n} c_{ij}\, x_i x_j + r \qquad (6)$$

In Equation 6, $\hat{y}$ is the target quantity such as area of voids or wire sweep; x_i and x_j are the factors that influence the target quantity such as process parameters; c_o, c_i ,$c_{ii,}$and c_{ij} are the coefficients; and r is designated for the residuals. Residuals are the difference between an actual response value and the value predicted by the fitted model.

There are several steps, which are necessary to follow in order to generate a regression model. The following steps shown in Figure 7.3 describe a path, which is essential to establish a regression model.

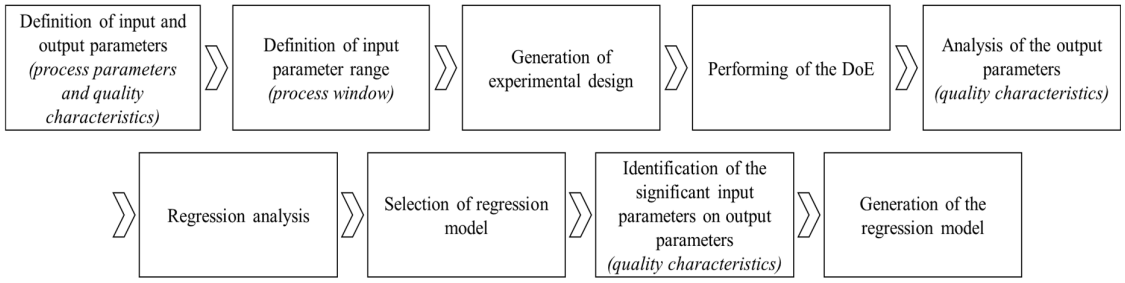

Figure 7.3: An approach to establish a regression model

According to Figure 7.3, at first the important input and output parameters are identified and a suitable process window is selected. Afterwards, an experimental plan is generated and a DoE is performed. After performing the DoE, the output parameters such as quality characteristics are analyzed. Until this step, the steps regarding the performing of the DoE and the analysis of the output parameters are already represented and discussed in Chapter 6. The reason for the selection of the D-optimal design for this work and important aspects in terms of definition of the process window are covered elaborately in previous chapters. After analyzing the output parameters (see Chapter 6), regression analysis is carried out. The detailed description of the steps beginning from regression analysis as shown in Figure 7.3 are highlighted in following sections of this chapter. In order to establish a process model, it is important to select a regression model. The regression model can be a linear or a quadratic model. As the process model for this work involves also the quadratic influences and the interactions between the parameters, a quadratic model is selected. As a next step, the input parameters with significant influence on the quality characteristics of void formation and wire sweep are analyzed. To do that, all process parameters and the quadratic terms and the interactions between the process parameters are analyzed with regression analysis in a so-called term significance table. In such a significance table, the terms important for the output parameters of void formation and wire sweep can be determined. For instance, in addition to the factors in other words process parameters (temperature, holding pressure, preheat time, transfer speed), the interactions between the process parameters and the quadratic influences of the input terms on the void formation and the wire sweep are analyzed in a significance table. The selected important terms are then included as factors in the regression model (Equation 6). Moreover, a coefficient table is generated, which delivers the coefficients of the terms depending on their influence on the target quantity. The significant terms with corresponding coefficients are then included into the regression model as shown in Equation 6. In the following section, regression analysis is conducted to determine the significant terms for the process model.

7.1.3 Evaluation of Process Parameter Correlations with Regression Analysis

Regression analysis is carried out based on the main experimental results given in Chapter 6. With regression analysis, the impact of the individual process parameters on quality features as well as the interaction between the process parameters are determined. The evaluation of the process parameters with regression analysis is crucial in terms of identifying the important terms which significantly influence the quality features.

At first, the impact of investigated process parameters (temperature, holding pressure, temperature and preheat time) on void formation and the wire sweep are analyzed with regression analysis. The impact of the individual process parameters on the area of voids and wire sweep is illustrated with the help of so-called "Adjusted Response Graphs" in Figure 7.4. Based on the results given in Chapter 6, it is indicated that each wire bond as well as the left and the right cavity should be considered separately in the process model to achieve an accurate model. Therefore, one certain wire bond is selected as a representation of regression analysis for the wire sweep in this chapter. The long wire bond 2 attached at a 90° angle to the gate in the near gate area in the left cavity is used as a representation in this chapter, but similar regression analysis is also carried out for all other wire bonds attached on the demonstrator.

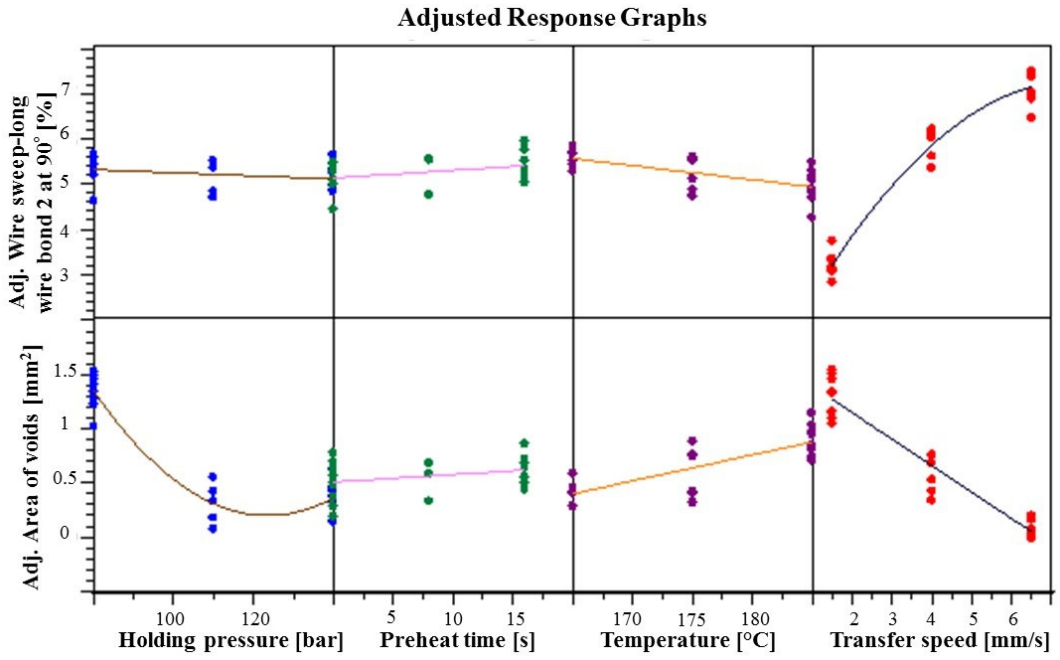

Figure 7.4: Influence of individual process parameters on the area of voids and the wire sweep of long wire bond 2 attached at a 90° angle to the gate

On the x-axis of Figure 7.4, four selected process parameters are shown, whereas on the y-axis, the adjusted values of the investigated quality characteristics, namely the area of voids and the long wire bond 2 attached in near gate at 90° angle to the gate are represented. Adjusted values are the values simplified from the impacts of other influencing factors, such that only the impact of a single process parameter on the void formation and wire sweep can be examined [168]. According to the top row of Figure 7.4, which is related to the wire sweep, holding pressure and the preheat time do not show pronounced impact on the wire sweep of the long wire bond 2. Temperature exhibits a slight influence on the wire sweep. On the other hand, the most remarkable impact is observed in transfer speed, and increasing the transfer speed causes a rise in the wire sweep. On the contrary, the area of voids is affected significantly by the holding pressure, and area of the voids in the package is reduced with increasing holding pressure. Temperature affects the void formation slightly, whereas the preheat time shows almost no influence on the void formation. Transfer speed demonstrates a pronounced effect on the area

of the voids in the package, and higher transfer speed leads to reduced void formation in the package. It is apparent from Figure 7.4 that transfer speed has major influence on both quality characteristics of void formation and wire sweep, but in opposite ways. As a next step in regression analysis, the interactions between the process parameters are examined. To determine whether two process parameters have an interaction and whether the interactions between the process parameters are important for the quadratic model, the interaction graph from regression analysis is investigated. Figure 7.5 illustrates the interaction graph for the area of voids.

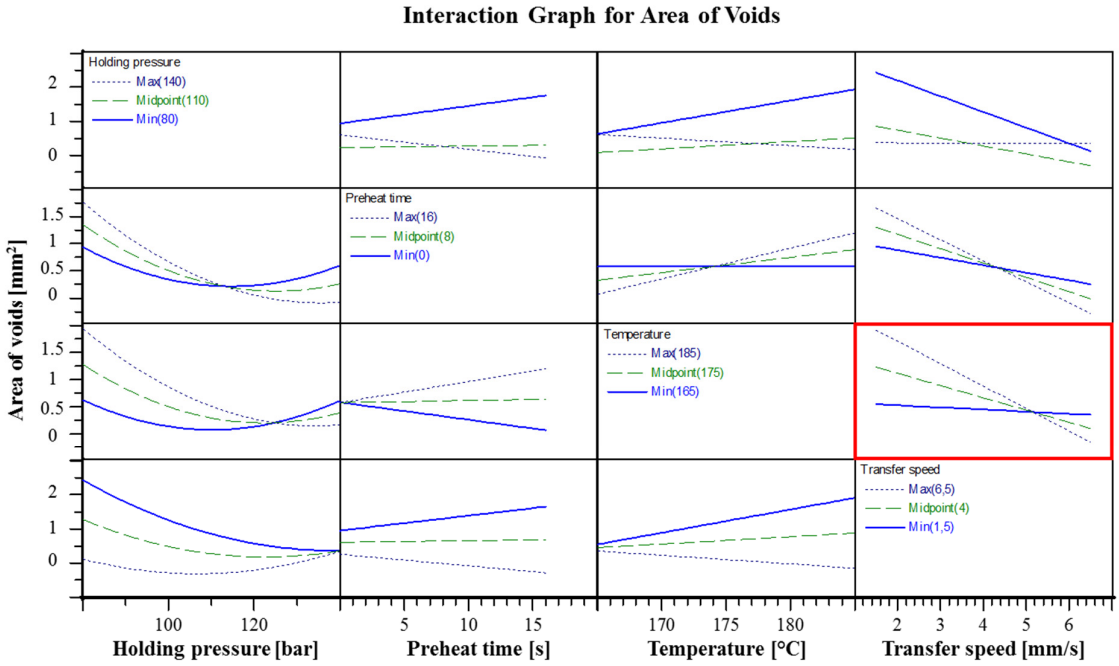

Figure 7.5: Representation of the interactions between the factors, namely the process parameters for the area of the voids

Any curves in this matrix shown in Figure 7.5, which cross or are not aligned parallel to each other, indicate a two-term interaction, which signals a considerable effect on the quality characteristic. Each graph in the matrix illustrates three curves since the process parameters are varied in three levels in D-optimal design. The curves with a dotted line display the maximum level of the corresponding process parameters, whereas the solid lines indicate the minimum level of the corresponding process parameters. In each of the graphs in the matrix, the response (area of the voids), which is shown on the y-axis, is depicted as a function of two predictors (two process parameters). For instance, the graph located in the fourth column at third row from above, which is indicated with a darker red outline in Figure 7.5, illustrates the interaction between the temperature and transfer speed. Transfer speed varies continuously as it is presented on the x-axis, whereas the temperature does not vary continuously and is fixed in three levels, which can be seen in the neighbor diagram with an indicated maximum, midpoint and minimum values. As the curves intersect, it implies that there is an interaction between these two process parameters. To achieve a minimum area of voids seen on y-axis, the line, which gives the minimum area of the voids, should be found. In this case, maximum temperature and the highest transfer speed deliver the minimal area of voids for this interaction. Similarly, different interactions can be determined further in Figure 7.5 that can also indicate the delivery of a reduced area of the voids in the package. Indeed, almost all the graphs shown in the matrix in Figure 7.5 are not aligned in parallel or have an intersection, which designates that there are high order interactions between the process parameters for the area of voids in the package. The interaction graphs between the process parameters for the wire sweep of the long wire bond 2 attached at 90° to the gate is depicted in Figure 7.6.

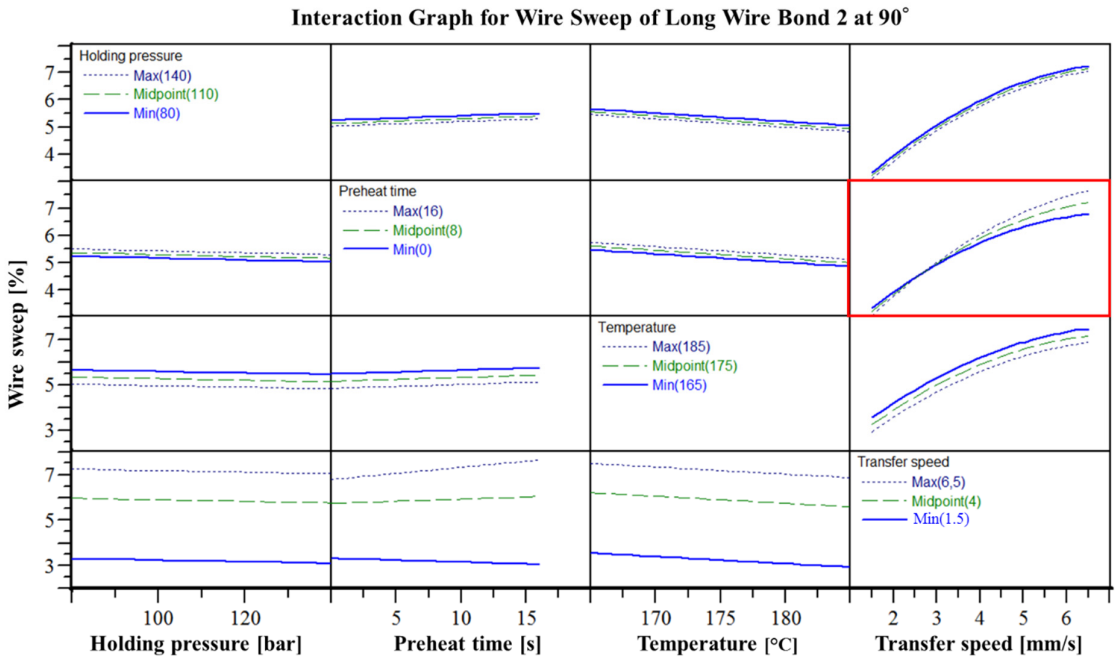

Figure 7.6: Representation of the interactions between the factors i.e. process parameters for wire sweep of long wire bond attached at 90° to the gate in near gate area

Most of the curves shown in Figure 7.6 are either aligned parallel to each other, or are identical and do not intersect nor cross each other. This implies that there are no significant interactions between the process parameters for the wire sweep. Only in some graphs slight interaction between the parameters can be observed. For instance, the graph, which is in the fourth column and second row and which is marked with a darker red outline, shows slight intersection for the parameters of transfer speed and preheat time, however, the interaction is still not as pronounced as in the void formation. Thus, in contrast to the high order of interactions between the process parameters observed in the void formation, for the wire sweep no significant interactions between the process parameters are determined.

After examining the dominant process parameters and the interactions between the process parameters, the relationship between the process parameters and the void formation and wire sweep can be presented graphically. The predicted response graph in regression analysis allows for determination of the variation in the quality characteristics as a function of the variation in the process parameters. Figure 7.7 depicts the predicted response graph in which the factors (process parameters) are shown on the x-axis and the target values in other words the quality features (void formation and wire sweep) are shown on the y-axis with the corresponding confidence interval for each quality characteristic. The diagrams in Figure 7.7 consist of three curves, one in the middle with two outer lines. The middle line is the estimated function and the outer lines define the confidence interval of the function. In this case, estimated values lie in this range with 95 % probability. The different widths of the confidence areas indicate that not all the areas are statistically distributed equally.

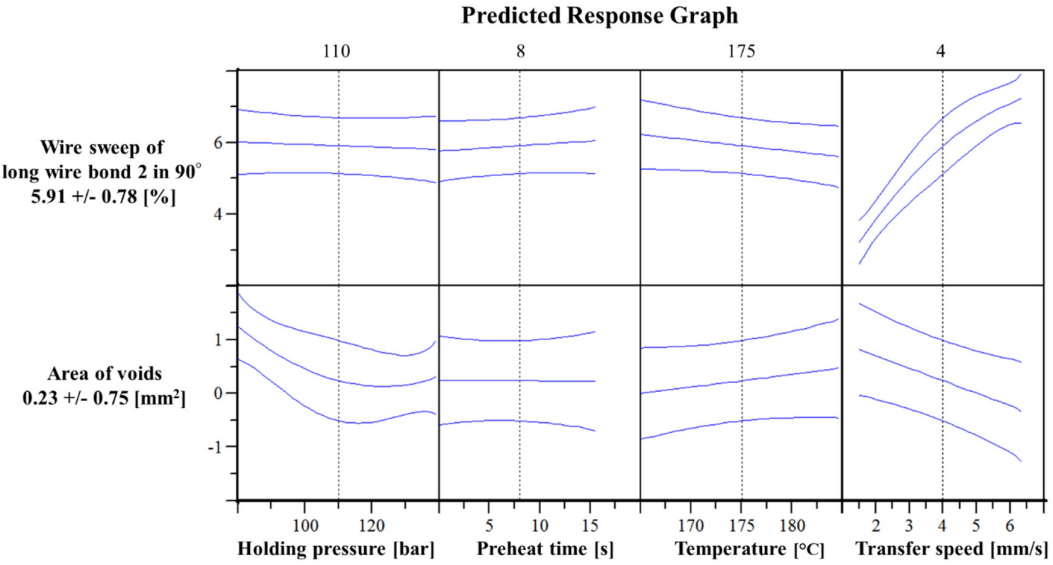

Figure 7.7: The overall model including the confidence intervals

The vertical dashed lines indicated in Figure 7.7 are the current points in the experimental room. In this case, the central process parameter combination (holding pressure 110 bar, preheat time 8 s, temperature 175 °C, transfer speed 4 mm/s) is shown, while a forecasted value of the respective target variable (quality characteristics) with a confidence interval is specified on the y-axis for this central point. At the upper end above these vertical lines, the set values of process parameters are displayed. The wire sweep and the area of voids with a confidence interval for the set values of process parameters, namely for the central point, can be seen on the y-axis. By moving the vertical lines, each point in the experimental room can be reached and the target value such as area of voids and the wire sweep can be read on the y-axis. The curves and confidence ranges can change by the respective shifting of the vertical lines. The reason for this change is the interactions between the various factors, which are also taken into account.

7.1.4 Generation of Process Model

As shown in Figure 7.3, after following the required steps, namely after conducting regression analysis, defining the important terms and selecting the regression model, the next step is the generation of the regression model for void formation and wire sweep. The corresponding coefficients for the significant terms, which are shown in Equation 6, are determined based on the significance level of the terms on the quality characteristics. As emphasized previously, due to the variations between the wire sweep of similar wire bonds as mentioned in Chapter 6, each wire bond is considered separately. Since each wire bond has a unique position on the layout, one process model is generated for each wire bond to be able to estimate the wire sweep more precisely. Since 24 wire bonds are attached on the layout, as a representation, the process model for one certain wire bond is shown in this section. As in previous chapters the results of the long wire bond 2 at 90° angle to the gate are mainly represented, the process model for this wire bond is given in this chapter. In addition, as previously mentioned, the left and the right cavity are considered separately due to temperature difference, thus a separate model of the quality characteristics is generated for each cavity. The process models shown in this chapter are generated based on the results obtained from the left cavity. However, similar approach can be used also for other wire bonds and right cavity as well. It is also important to emphasize that for the generation of the models, the average values of the five cycles from each cavity are used.

The generated process model for the area of voids and number of voids as well as the wire sweep for the long wire bond 2 attached at 90° to the gate in near gate area are shown in Equation 7, Equation 8 and Equation 9 respectively. In process model equations, as factors; T states for temperature, P is for holding pressure, t is for preheat time and v states for transfer speed. As target values y_1 is designated

for the number of voids, y_2 is for the area of voids, y_3 is for the wire sweep of long wire bond 2 attached at 90° to the gate in near gate area.

Process model for number of voids:

$$\begin{aligned} y_1 = -52.3759 &+ 0.43112\,\boldsymbol{T} + 3.50022\,\boldsymbol{v} + 0.15433\,\boldsymbol{P} - 1.16714\,\boldsymbol{t} \\ &- 0.03389\,\boldsymbol{T}\,\boldsymbol{v} - 0.00256\,\boldsymbol{P}\,\boldsymbol{T} + 0.00843\,\boldsymbol{t}\,\boldsymbol{T} \\ &+ 0.08974\,\boldsymbol{v^2} + 0.01339\,\boldsymbol{P}\,\boldsymbol{v} - 0.02093\,\boldsymbol{t}\,\boldsymbol{v} + 0.00099\,\boldsymbol{P^2} \\ &- 0.001767\,\boldsymbol{P}\,\boldsymbol{t} \end{aligned} \tag{7}$$

Process model for the area of voids [mm²]:

$$\begin{aligned} y_2 = -28.7629 &+ 0.23113\,\boldsymbol{T} + 2.31851\,\boldsymbol{v} + 0.09013\,\boldsymbol{P} - 0.38626\,\boldsymbol{t} \\ &- 0.01867\,\boldsymbol{T}\,\boldsymbol{v} - 0.00147\,\boldsymbol{P}\,\boldsymbol{T} + 0.00354\,\boldsymbol{t}\,\boldsymbol{T} \\ &+ 0.00764\,\boldsymbol{P}\,\boldsymbol{v} - 0.01554\,\boldsymbol{t}\,\boldsymbol{v} + 0.00060\,\boldsymbol{P^2} \\ &- 0.00156\,\boldsymbol{P}\,\boldsymbol{t} \end{aligned} \tag{8}$$

Process model for wire sweep of long wire bond 2 attached at 90° to the gate in near gate area [%]:

$$\begin{aligned} y_3 = 7.00802 &- 0.03340\,\boldsymbol{T} + 1.58942\,\boldsymbol{v} - 0.03142\,\boldsymbol{t} - 0.1097\,\boldsymbol{v^2} \\ &- 0.01259\,\boldsymbol{t}\,\boldsymbol{v} \end{aligned} \tag{9}$$

As seen from the equations above, the process models involve not only the single process parameters but also the interactions between the process parameters and the quadratic terms. It is apparent that the regression model for the wire sweep in Equation 9 includes less terms in comparison to the regression models for the area of voids and number of voids in Equation 7 and Equation 8. The reason for that is that as shown in Section 7.1.3 there are more significant interactions between the process parameters for void formation in comparison to the wire sweep. Thus, the process models for void formation consist of more terms in comparison to the process model for wire sweep. Furthermore, as seen in equations above, each term has a corresponding coefficient, which is determined depending on the significance of the term on the quality characteristics. Additionally, the illustrated models in Equation 7, Equation 8 and Equation 9 do not only show the correlations between the process parameters, the void formation and wire sweep, the models can also be used to estimate the number of voids and the wire sweep in the package. In that context, one of the most important aspects in regression model is the model fitting quality, which expresses how good the generated process model describes the correlation between the selected terms such as process parameters and the target quantities such as quality characteristics. The prediction quality of the generated models is given in detail in next section.

7.1.5 Model Prediction Quality

Table 7.1 represents the model quality of the Equation 7, Equation 8 and Equation 9 with R^2, R^2_{adj} and RMS Error, which states for the residuals.

Table 7.1: Fitting quality of the regression models

Quality characteristics	R^2	R^2_{adj}	RMS – Error
Number of voids	0.990	0.973	0.349
Area of voids	0.975	0.94	0.251 [mm²]
Wire sweep (90° - long wire bond 2)	0.968	0.956	0.384 [%]

According to the R^2_{adj} values depicted in Table 7.1, over 97 % of the number of voids can be explained with the help of the generated process model. The mean deviation, in other words the RMS error of the model is around 0.4 voids. In addition, over 94 % of the area of the voids can be explained with the generated process model with an RMS error of 0.251 mm^2. Based on the coefficient of determination, it is evident that good correlation is found between the process parameters and the void formation, and the generated mathematical model can express this correlation with a high fitting quality. Similarly, the R^2_{adj} value for the process model to estimate the wire sweep is found around 0.96, which indicates that over 96 % of wire sweep observed for the long wire bond 2 attached at 90° to the gate can be expressed with this model. The mean deviation is around 0.38 % wire sweep. The values of the process model for the wire sweep also imply that the wire sweep is correlated excellently with the process parameters and the generated mathematical model for the wire sweep can express this correlation with a high quality.
As mentioned in previous section, as a process model for the wire sweep, mathematical equation of only one wire bond is shown as representation in this chapter, however, for each wire bond in left and the right cavities, separate models are generated. The coefficient of determination, in other words the fitting of the process model for each wire bond is calculated. As left and right cavity are considered separately and each demonstrator has 24 wire bonds, overall the fitting quality of 48 wire bonds is determined. However, as a representation only the fitting qualities of the long wire bonds attached in near gate area in left cavity are given in detail in Table 7.2 to illustrate the deviation in the fitting qualities between different angles of the wire bonds.

Table 7.2: Fitting quality of the regression models for long wire bonds attached at 90°, 45°, 180° in near gate area on the layout of the demonstrator

Quality characteristics	R^2	R^2_{adj}	RMS - Error [%]
Long wire bond 1 at 90° to gate in near gate	0.948	0.934	0.44
Long wire bond 1 at 180° to gate in near gate	0.987	0.979	0.31
Long wire bond 1 at 45° to gate in near gate	0.957	0.942	0.40
Long wire bond 2 at 180° to gate in near gate	0.982	0.966	0.37
Long wire bond 2 at 45° to gate in near gate	0.879	0.848	0.49

The model qualities of the long wire bonds, which are bonded in near gate area at different direction to the gate vary between 0.85 – 0.98 (R^2_{adj}) for the left cavity as seen in Table 7.2. Apart from the given values in Table 7.2 similar fitting quality is also found for the wire bonds in the right cavity where the fitting quality lies between 0.96 – 0.98 (R^2_{adj}). Similarly, the R^2_{adj} of the process models for the short wire bonds in near gate area is found between 0.93 - 0.99 for the left cavity and between 0.77 – 0.98 for the right cavity. Although the short wire bonds far from the gate in general show minimal wire sweep, with the generated process model for the short wire bonds far from the gate also good correlation is found. R^2_{adj} for the short wire bonds in far from the gate area lies between 0.8 – 0.98 for the generated process models for wire sweep. This implies that over 80 % of the wire sweep shown in the short wire bonds in the far from the gate area can be explained with the process parameters. Only for the short wire bond attached in the far from the gate area attached at 180° to the gate, no good correlation is found in both cavities.
After determining the fitting quality of the generated models for the void formation and wire sweep, as an extra aspect, the model quality can be examined. As previously mentioned, residuals are the difference between the actual response value (quality characteristics) and the value predicted by the fitted model. To achieve a good model, the residuals should follow the normal probability distribution. In regression analysis with the help of the so-called “Residuals Probability Plot”, the distributions of the residuals in comparison to the values from a standard normal probability distribution as well as the outliers can be observed. The large deviations of the residuals from the normal distribution indicate the disagreements in the models. Furthermore, the unrecognized outliers can permanently distort the results

and thus reduce the model quality [168]. Figure 7.8 illustrates the distribution of the residuals for wire sweep of long wire bond 2 attached at 90° to the gate (left) and for area of the voids (right).

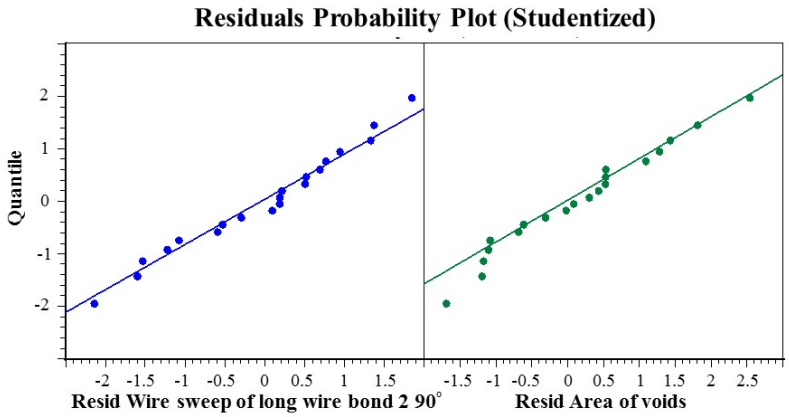

Figure 7.8: Normal distribution of the residuals

All points shown in Figure 7.8 in other words the residuals for wire sweep and the area of voids lie approximately along the straight line. Alignment of the residuals on the line indicates that the residuals for wire sweep and void formation follow the normal distribution. Another important point regarding Figure 7.8 is that the residuals do not show any discernible pattern and are distributed randomly along the line, which implies the good quality of the generated models. In addition to the normal distribution, to prove the model quality, it is also necessary to check, whether the residuals stay constant over the range of values of the target variable or whether they follow a trend such as they increase or decrease with increasing target size. Figure 7.9 depicts the residuals associated with the model, which are shown on x-axis and the fitted predicted response values, which are shown on y-axis.

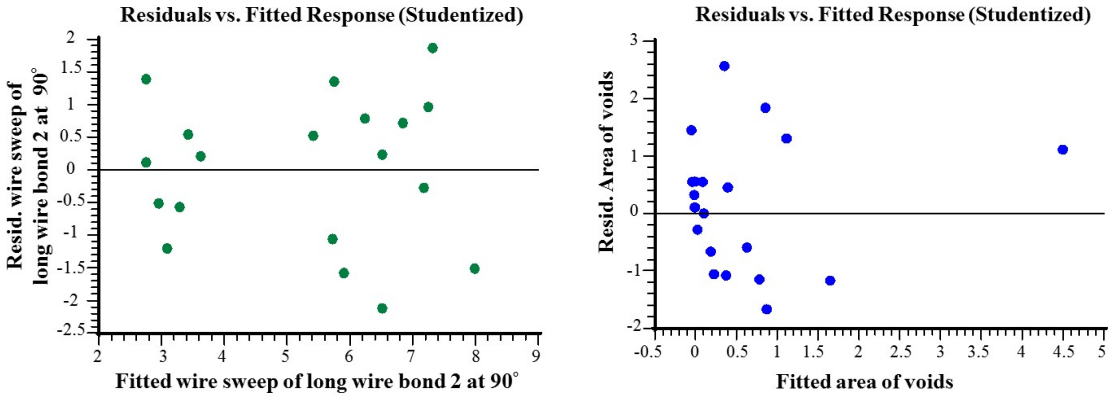

Figure 7.9: Examination of the constant residuals for the wire sweep of long wire bond 2 attached at 90° to gate (left) and for the area of voids (right)

In both diagrams in Figure 7.9, the residuals are at almost the same level, which can be seen on y-axis. The residuals do not increase or decrease with an increment of response value in any sort of way. The spread over the straight line is almost constant and no trend is recognized. Therefore, based on the residual analysis, it is evident that the residuals in generated models follow the normal distribution and no outliers or trend in the residuals can be observed, which prove the good quality of the generated models.

7.1.6 Optimum Process Parameters

As a next step, the optimum process settings can be determined by using the established regression models. Based on the results given in Chapter 6 and regression analysis shown in Figure 7.4, it is apparent that an increase in the holding pressure decreases the void formation in the package. The transfer speed, however, affects void formation and wire sweep in opposite directions. Increasing the transfer speed decreases the void formation, but raises the wire sweep in the package. Thus, to find optimum process parameter combinations, which delivers the best package quality for wire sweep and void formation at the same time, this aspect should be considered. To define the optimum process parameters in a best possible way, which deliver the best factor combination for both quality characteristics, an optimization tool of the software can be used. For the optimization, specification limits, target values and weightings must be entered for each quality feature. Depending on the objective of the optimization, two quality characteristics can be optimized either with the same weighing or more focus in weighing can be given to one quality characteristic. For instance, more weighing can be selected in optimization on wire sweep in order to decrease the wire sweep in a considerable degree and thereby allow slightly higher void formation in the package. However, the aim in the optimization of this work is to find the optimum parameter settings, which minimize the void formation and the wire sweep in the molded packages at the same time. Thus, the optimization is carried out with same weighing for area of voids and wire sweep, and the factor settings for the optimum are determined. As a representation, the wire sweep of the long wire bond 2 attached at 90° to the gate in near gate area is considered in optimization. The optimum process parameters, which minimize the wire sweep of the long wire bond 2 at 90° to the gate in near gate area and the area of voids in the molded package are found as:

- Temperature: 170 °C
- Transfer speed: 1.5 mm/s
- Holding pressure: 138 bar
- Preheat time: 16 seconds

The models estimate the area of voids and the wire sweep of long wire bond 2 attached at 90° to the gate in near gate area with the optimum process parameters as following:

- Area of voids: $3.88 \times 10^{-5} \pm 1.73$ mm^2
- Wire sweep: 3.13 ± 1.08 %

A similar approach can be applied also to determine the optimum parameters in terms of number of voids instead of the area of voids. The optimum parameters, which minimize the number of voids and the wire sweep of the long wire bond 2 attached at 90° to the gate in near gate area are determined as:

- Temperature: 168 °C
- Transfer speed: 1.5 mm/s
- Holding pressure: 129 bar
- Preheat time: 1.6 seconds

The optimum process parameters deliver the number of voids and the wire sweep for the long wire bond 2 attached at 90° to the gate in near gate area as:

- Number of voids: 0.6 ± 1.6
- Wire sweep: 3.53 ± 0.75 %

As seen from the optimum process parameters, to reduce the wire sweep in a considerable degree, the lowest transfer speed is selected in the optimization. On the other hand, to reduce the void formation also in considerable amount high holding pressure is selected in optimization so that the wire sweep and void formation can be reduced at the same time in molded package. As the preheat time does not show a significant impact on the wire sweep or the void formation, significant difference in preheat time for the optimization of the area of voids and the number of voids can be seen above. The reason for that is that as the preheat time is not one of the dominant process parameter which does not need to be minimized or maximized for the best package quality, the confidence interval is taken into account in

optimization. For all process parameters, the confidence intervals, which give the less uncertainty in prediction of the quality features are chosen during optimization.
Therefore, considering the optimum process parameters for the void formation and the wire sweep, it can be seen that the void formation is reduced to almost 0 in the package and the wire sweep for the long wire bonds decreases to circa 3.5 %. Both quality criteria, namely void formation and wire sweep are reduced in considerable amount with the optimum process parameters which are achieved with the given approach.
As the mathematical models are established for the estimation of the void formation and the wire sweep, the mathematical models can be implemented also in other tools for geometrical visualization of the multi-objective optimization. For this reason, Pareto front diagrams are used to visualize the variations in the void formation and the wire sweep at the same time by changing the process parameters. To constitute the Pareto front diagrams, all possible combinations between the process parameters within the selected process window are generated and the number of voids and the wire sweep are calculated according to the process models. Such kind of diagrams are especially advantageous for multi-objective optimization. Figure 7.10 and Figure 7.11 depict the Pareto front diagrams, where the variation in the wire sweep and the void formation are shown with respect to the variation in the process parameters.

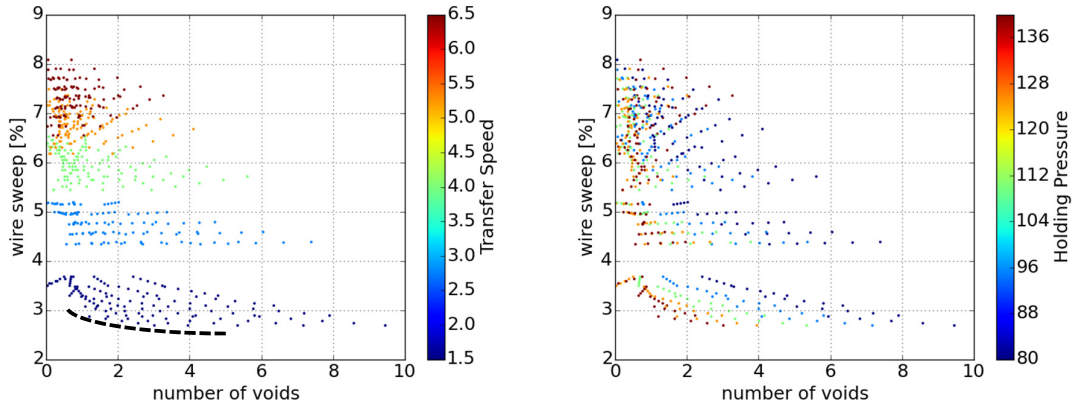

Figure 7.10: Pareto front for transfer speed (left) and holding pressure (right)

Figure 7.10 represents the wire sweep on y-axis and the number of voids on x-axis and the variations of these two quality features as a function of transfer speed (left) or holding pressure (right). The variation in the corresponding process parameter is shown on the color scale from blue to red on the right hand side of each diagram. Figure 7.10 (left) represents the variations in the wire sweep and voids with respect to the variations in the transfer speed. The dots on the diagram correspond to the color on the transfer speed scale, which is shown on the right hand side of the diagram. Transfer speed is varied at five different levels between 1.5 mm/s and 6.5 mm/s, which can be also identified from the five different colors of the dots on the diagram. As seen in Figure 7.10 (left), the dots follow a certain pattern of color on the diagram and the color of the dots changes regularly by moving in the y direction. As a matter of fact, this implies that the quality characteristic presented on the y-axis is strongly influenced by the selected process parameter. The red dots on the diagram imply that selection of the high transfer speed causes larger wire sweep. Thus, to reduce the wire sweep, the dark blue dots should be selected, which requires reducing the transfer speed. It is important to emphasize that every single dot shown in diagrams represents the responses of the factor combinations, not the response of the variation of only one process parameter. However, with the help of such representation, the influence of one single parameter on both quality characteristics can be visualized distinctly. For instance, to achieve less void formation and less wire sweep, so-called front should be selected, which is marked as black hemicycle in Figure 7.10 (left). To decrease the wire sweep as well as the void formation in the package at the same time, the low transfer speed should be selected. This also explains the reason regarding the selection of low transfer

speed in optimization of both quality features given previously. In Figure 7.10 (right), influence of the holding pressure on quality characteristics is shown. This time the color pattern changes in the x-axis direction. This indicates that the quality characteristics represented on the x-axis is influenced by that process parameter. Thus, the number of voids, which is presented on x-axis, is strongly affected by the holding pressure. The Pareto front here shows that to reduce the number of voids in the package, higher holding pressure should be selected. The wire sweep, however, is not influenced by the holding pressure significantly. Figure 7.11 illustrates the influence of preheat time and temperature on the voids and wire sweep.

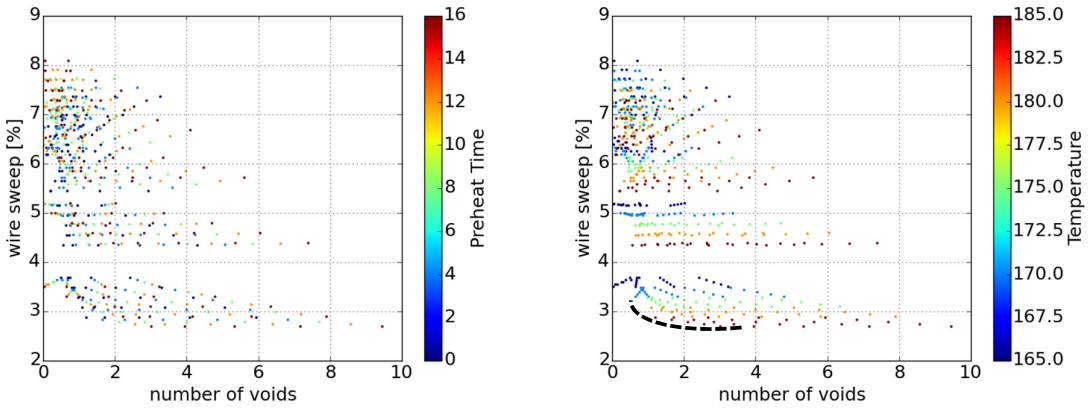

Figure 7.11: Pareto front for preheat time (left) and temperature (right)

On contrary to the results seen in Figure 7.10, no discernible pattern in the color of the dots can be observed in preheat time in Figure 7.11 (left). This indicates that the preheat time does not show a pronounced influence on the wire sweep and void formation. On the other hand, in Figure 7.11 (right) there are some patterns in the dots of the colors, but the color of the dots is mixed in each level of the temperature. However, the impact of the temperature still cannot be distinguished easily. Nevertheless, the front as shown in Figure 7.11 (right) should be followed to decide for the temperature, which reduces both defects at the same time. Depending on the weighing of the optimization one can decide between the two ends of the black hemicycle, either having less wire sweep but slightly higher void formation, or vice versa. Therefore, the Pareto front diagram not only helps to visualize and understand the reason for selection of the optimum process parameters but also to define the optimum process parameters by following the fronts in the diagrams.

7.2 Evaluation of Material Analysis and Material Model Definition

In this section, regression analysis for the material investigations is performed, which are based on the results given in Chapter 6. Similar approach as in the process model is followed for the generation of the material models, which is shown in Figure 7.3. At first, the objective of the material model and the boundary conditions of the model are shown in Section 7.2.1. Afterwards, regression analysis is conducted to determine the influence of the variations in the material characteristics on the void formation and the wire sweep and the results are given in Section 7.2.2. Based on regression analysis, the regression models are generated, which define the relationship between the variations in the material characteristics and void formation as well as wire sweep, and are introduced in Section 7.2.3. The model prediction quality and the important aspects, which are necessary to consider in material models are discussed in Section 7.2.3.

7.2.1 Objective of the Material Model

The aim of the material model is to describe a relationship between the variations in the material characteristics due to humidity and storage duration and package quality such as void formation and wire sweep. Additionally, the model represents a systematic approach to estimate the processing

limitations of EMCs, which are subjected to different preconditioning (storage duration and humidity) in order to achieve a predefined package quality. Figure 7.12 depicts the schematic illustration of the material model.

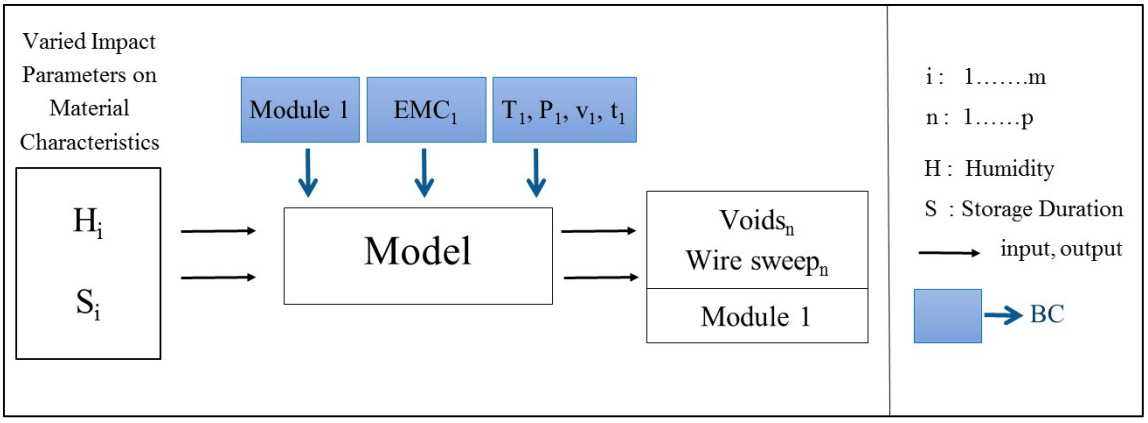

Figure 7.12: Schematic illustration of the material model

As input parameters in the material model, the humidity and the storage duration are selected. Those are the varied impact parameters on the material characteristics, whose influence is investigated on the output parameters. As output parameter, wire sweep and void formation are analyzed. The material model expresses the correlation between the input and the output parameters. The blue boxes in Figure 7.12 illustrate the boundary conditions for the model. Similar to the process model, the experimental investigations are performed with one certain package geometry, namely with selected test vehicle (see Chapter 3 for the dimensions of demonstrator). In addition, EMC 1 is used as main molding material, and impact of the variations in EMC 1 due to storage duration and humidity on the quality characteristics is investigated. Since EMC 1 has specific material characteristics (see Table 3.1 for the material properties) the material model involves those properties. Therefore, module 1 and EMC 1 are the boundary conditions of the model. In addition to that, as the variations in the material characteristics on the quality features are the focus in this model, the process parameters are kept constant and all the investigations in terms of material characteristics are performed with one predefined process parameter combination. Hence, the process parameters are the boundary conditions for the material model as well. All the investigations to establish a material model are performed with the central process parameter combinations of 175 °C molding temperature, 110 bar holding pressure, 4 mm/s transfer speed and 8 s preheat time.

For the generation of the material model, similar approach as in process model is applied as shown in Figure 7.3 only with slight variations. Firstly, the aim in the material model is to define the relationships between the variations in the material characteristics on the wire sweep and void formation. Thus, the variations in the material characteristics due to the humidity and the storage duration are the input of the material model. The pellets of EMC 1 are preconditioned for 8 h, 16 h, 24 h, 48 h and 72 h in humid environment in climate chamber at 30 °C and 90 % RH and in dry environment in vacuum oven at 30 °C and 0 % RH. The material investigations are constructed in a way to comprehend the influence of the dry and humid storage of EMC 1 pellets on the quality characteristics such as void formation and wire sweep directly. Thus, for material model the material investigations are performed to induce some changes in the material characteristics and the experiments are not constructed according to D-optimal design with a computer algorithm. Such kind of experimental approach can deliver only a linear model as opposite to the process model, where with D-optimal design quadratic model is generated. Nevertheless, except the difference in the experimental design construction, for the material model investigations, the similar approach as shown in Figure 7.3 is applied. The input parameters are selected whose impact on the output parameters in other words on quality characteristics are investigated. The influence of the storage duration and humidity on the void formation and wire sweep are already

discussed in Chapter 6, however, to find out the significant terms and the correlations between the input and output more precisely, regression analysis is necessary. Thus, regression analysis is carried out to determine the important terms for the material model, which is introduced in following section.

7.2.2 Evaluation of Material Parameter Correlations

Regression analysis is conducted to determine the influence of the storage duration of EMC 1 in humid and dry environment on the void formation and wire sweep. The adjusted response graphs are used to understand the impact of the storage duration at humid environment (30 °C / 90 % RH) and at dry environment (30 °C / 0 % RH) on the void formation and wire sweep. In addition, to describe the humidity effect on the void formation and wire sweep more precisely, the moisture contents of the preconditioned pellets, which are measured with Karl-Fischer titration, are also supplemented into the adjusted response graphs. Figure 7.13 represents the influence of the storage duration in humid and dry environment and the corresponding humidity level of the pellets on the area of voids and the number of voids. For regression analysis, the average values from the material investigations are used.

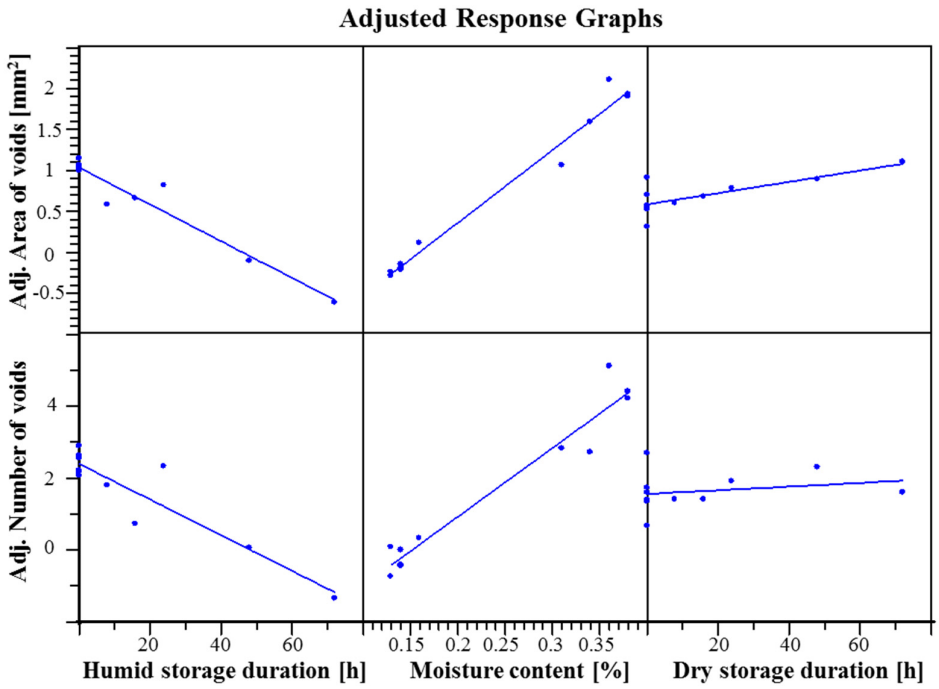

Figure 7.13: Influence of storage duration in humid environment at 30 °C / 90 % RH and in dry environment at 30 °C / 0 % RH as well as the humidity level of the pellets on the area of voids and the number of voids

In Figure 7.13, the influence of the humid and dry storage duration and the corresponding humidity level of EMC 1 pellets on area of voids and on the number of voids are illustrated on lower and upper part of the diagram respectively. As seen from the curves, the number of voids and the corresponding area of voids are only slightly influenced by the extended storage duration in dry environment. Since moisture content is very low almost around 0.13 % and kept constant during prolonged dry storage, no increase in the void formation is observed. On the other hand, the humid storage duration shows impact on the void formation. The number of voids as well as the corresponding area of voids decrease with increasing humid storage. It is important to emphasize that since the average values are used in the material model, the standard deviations are not considered in regression analysis. Although the variation in the void formation with extended humid storage duration stay constant after 24 h and lie within the standard deviation (see Figure 6.23), with regression analysis only the mean values are evaluated, which shows such decrease in void formation with increasing humid storage duration. Nevertheless, to analyze the effect of the humidity only regarding the humid storage duration can lead to false interpretation since

the humidity does not increase linearly with the extended humid storage duration. Therefore, the values of the moisture content, which are measured with Karl-Fischer titration for dry and humid storage durations from 0 h to 72 h are used to evaluate the impact of humidity on the void formation (see Figure 5.29 for Karl-Fischer titration results). As seen in Figure 7.13, the humidity shows remarkable impact on the void formation and the number of voids as well as the corresponding area of voids increase with increasing humidity content in the pellets. Therefore, to describe the humidity impact of the EMC 1 on the quality characteristics more precisely, in addition to the humidity storage time and the dry storage time, the moisture content measured in the pellets is also implemented as an input term into the material model. Figure 7.14 represents the impact of dry and humid storage duration as well as the moisture content of the pellets on the wire sweep for long wire bonds attached at 90° to the gate in near gate area. As the short wire bonds are also affected strongly by the variations in the material characteristics (see Figure 6.25), the short wire bond 2 attached at 45° and at 90° to the gate is also implemented in Figure 7.14.

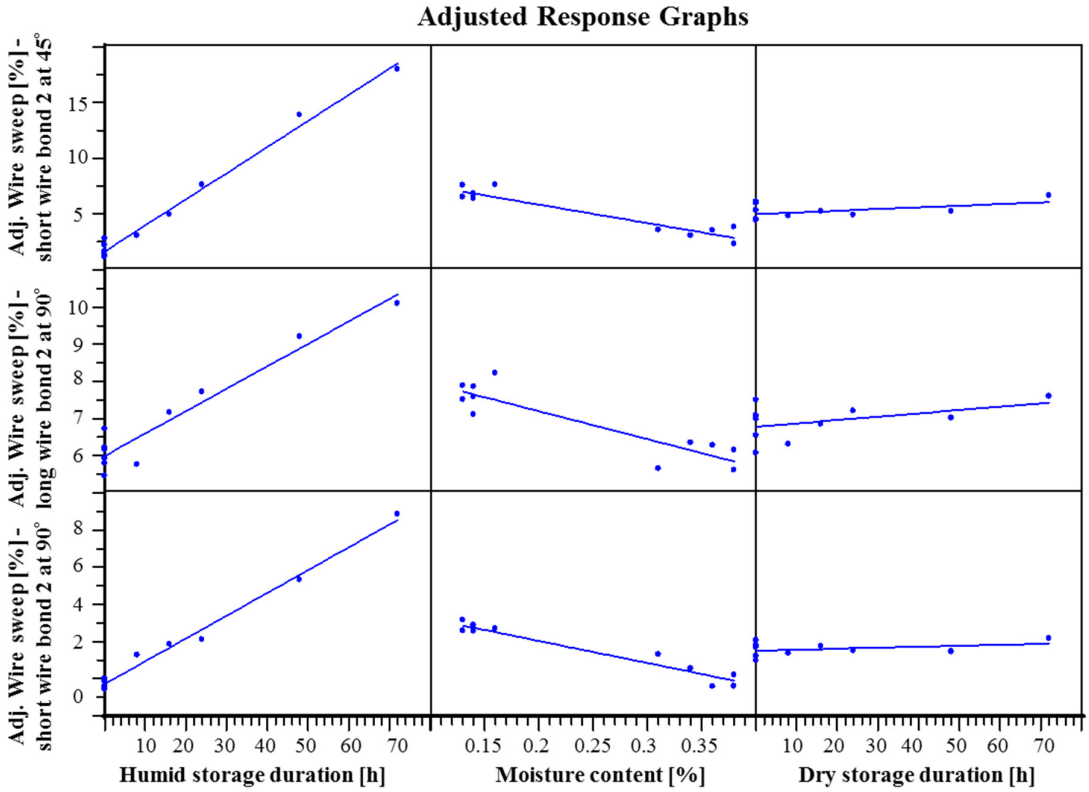

Figure 7.14: Influence of storage duration in humid environment at 30 °C / 90 % RH and in dry environment at 30 °C / 0 % RH as well as the humidity level of the pellets on the short wire bond 2 (s2) attached at 90° and 45° to gate and long wire bond 2 (l2) attached at 90° to the gate in near gate area

On the y-axis of Figure 7.14, the wire sweep of the long wire bond 2 and short wire bond 2 attached at 90° angle to the gate as well as short wire bond 2 attached at 45° to the gate in near gate area are represented. Dry storage duration shows slight influence on the wire sweep for long and short wire bonds and the wire sweep increases slightly with prolonged dry storage duration. On the other hand, the humid storage duration has a remarkable influence on all wire bonds illustrated in Figure 7.14. Increasing the storage duration in humid environment leads to a large increment in wire sweep. On the other hand, in contrary to the results seen in void formation in Figure 7.13, there is a slight decrease in the wire sweep with increasing moisture content. The reason for that although moisture content of EMC 1 almost reaches its saturation point after 48 h (0.38 %) and stays constant until 72 h of humid storage (0.38 %) (see Figure 5.29), the wire sweep continues to increase remarkably after 48 h storage. The most critical

wire sweep is observed after 72 h of humid storage for short wire bonds attached at 45° to the gate in spite of the fact that the moisture content in the molding compound does not change anymore. The reason for that, as shown in rheology results in Chapter 5, apart from the humidity influence on the viscosity, the viscosity of the molding compound also changes when the pellets stored for 48 h and 72 h in dry environment. Thus, the wire sweep is not only influenced by the existence of the humidity, but also by the variation in the viscosity raising with prolonged storage duration, which is not considered in the impact of moisture content shown in Figure 7.14. Therefore, the results in regression analysis are indeed due to a combined effect of the results observed in Chapter 5 and Chapter 6.
It is important to mention that in Chapter 6 the influence of the batch difference on the void formation and wire sweep is also investigated when examining the variations in the material characteristics on quality features. However, as seen in Figure 7.12, the batch variations are not included in the material model as input parameters. The reason for that is that the batch variation is difficult to quantify since it does not only involve the variation in the material properties due to manufacturing but also the alterations due to the storage duration of the molding compound. Yet, determining the differences between the batches are laborious. Furthermore, the aim is to generate a general material model, which can be applicable to other molding compounds as well. The measurable and easily applicable quantities are necessary to generalize and implement the models for other molding compounds. Therefore, the influence of batch variations on the void formation and wire sweep is investigated as discussed in Chapter 6 but it is not included as an input parameter in the material model.

7.2.3 Material Model Definition and Prediction Quality

After investigating the influence of the storage duration in humid and dry environment as well as the moisture content of the pellets on the wire sweep and void formation, the material model can be generated. However, before the material model is given, in order to determine whether a good correlation can be achieved with linear model between the material characteristics and the quality features, the correlation factor of those input parameters to the void formation and wire sweep are first evaluated. As already mentioned, no quadratic terms and no interactions between the parameters are considered with the conducted experimental plan, thus a linear model can be generated for the material model. Table 7.3 depicts the fitting quality of the regression model generated for the material models.

Table 7.3: Fitting quality of the material model

Quality characteristics	R^2	R^2_{adj}	RMS - Error
Number of voids	0.87	0.81	0.62
Area of voids	0.94	0.92	0.17 [mm^2]
Wire sweep of long wire bond 2 at 90° to gate near gate	0.83	0.76	0.49 [%]
Wire sweep of short wire bond 2 at 90° to gate near gate	0.97	0.96	0.40 [%]
Wire sweep of short wire bond 2 at 45° to gate near gate	0.98	0.97	0.75 [%]

As seen in Table 7.3, good fitting quality is observed in the material model for represented quality features due to the fact that the input parameters such as humidity and storage duration show a major impact on the void formation and wire sweep. Over 92 % of the area of voids can be explained by the variation in the material characteristics. As seen in adjusted response diagram in Figure 7.13, the voids are correlated very well with the moisture content, thus this high fitting quality indicates that close relationship. In addition, the wire sweep of the short wire bonds attached at 90° and 45° to the gate can be also correlated well with the variations in the material characteristics. Based on the fitting qualities over 96 % of variations measured in the wire sweep due to the variations in the material characteristics can be described with this material model. The fitting quality for the long wire bond 2 attached at 90° to gate is slightly lower and is found around 76 %. The reason for that is that the impacts originated due to the variation in the material characteristics on the wire sweep of long wire bonds and on the voids are

smaller in comparison to the process model. Furthermore, the relationship between the input and output parameters can only be correlated linearly and as a matter of fact it is not sufficient to describe the complex chemical mechanisms of the molding compound only with a linear model. Therefore, although good fitting quality is observed in the material model, more terms which are related to material characteristics such as the viscosity or the crosslinking degree should be considered in the material model in order to describe the alterations in the material characteristics due to humidity and prolonged storage duration thoroughly. Nevertheless, to give some representative example of models, which can be used to describe the impact of the variations in the material characteristics on the quality features, mathematical material models are generated. The material models for the area of voids, the wire sweep for long wire bond 2 attached at 90° to gate, short wire bond 2 attached at 90° to gate as well as short wire bond 2 attached at 45° to gate in near gate area are illustrated in Equation 10, 11, 12 and 13 respectively. In models equations H_t states for the humid storage duration, S_t states for the dry storage duration and h states for the moisture content of the pellets.

Material model for the area of voids [mm²]:

$$y_4 = -1.17608 + 0.006869\,\boldsymbol{S_t} - 0.0224\,\boldsymbol{H_t} + 8.87636\,\boldsymbol{h} \tag{10}$$

Material model for the wire sweep of long wire bond 2 attached at 90° to gate [%]:

$$y_5 = 7.63869 + 0.00902362\,\boldsymbol{S_t} + 0.0603\,\boldsymbol{H_t} - 7.50866\,\boldsymbol{h} \tag{11}$$

Material model for the wire sweep of short wire bond 2 attached at 90° to gate [%]:

$$y_6 = 2.4551 + 0.00519\,\boldsymbol{S_t} + 0.122672\,\boldsymbol{H_t} - 11.8723\,\boldsymbol{h} \tag{12}$$

Material model for the wire sweep for short wire bond 2 attached at 45° to gate [%]:

$$y_7 = 5.34796 + 0.0149640\,\boldsymbol{S_t} + 0.2343\,\boldsymbol{H_t} - 16.5804\,\boldsymbol{h} \tag{13}$$

As the material models are linear models with less input parameters, in contrary to the process models illustrated in Section 7.1, the material models do not include many terms. In fact, as mentioned previously such correlation about the variation in the characteristics in the molding compound which is directly combined with the chemical nature of the molding compound is difficult to describe mathematically with such less terms. However, the results of the experimental analysis can still be evaluated with regression analysis as previously shown to determine whether the input parameters have significant impact on the output parameters. Therefore, although the linear material model possibly is not suitable to describe the complex nature of the molding compound, the given approach of regression analysis can be applied to understand the relationship between input and output parameters and to define the processing limit of the preconditioned EMC.

7.3 Summary

In this chapter, the process model and material model are established based on the results of the main experiments given in Chapter 6. A systematic approach is evaluated, which helps to generate the models to describe the relationship between the input and output parameters. Firstly, process models are introduced, which deliver the relationship between the process parameters and the void formation and wire sweep. Regression analysis is performed to determine the correlations between the process parameters, void formation and wire sweep. Interactions between the process parameters are analyzed with regression analysis and high interactions between the process parameters for void formation are observed whereas for the wire sweep almost no significant interactions between the process parameters are determined. Based on regression analysis, the significant terms such as significant process

parameters and the interactions between the parameters are selected and corresponding coefficients are calculated. The process models are generated and the prediction quality of the process models are evaluated. The generated models show high fitting quality, which indicates that the void formation and wire sweep in the molded packages can be explained by the variations in the process parameters. Fitting quality of 94 % for void formation and 96 % for wire sweep are achieved with the established process models. After generating the process models, the optimum process parameters are determined. Optimum process parameters for the transfer molding process to reduce the area of voids as well as the wire sweep for long wire bond 2 attached at 90° to gate in near gate area are founds as:

- Temperature: 170 °C
- Transfer speed: 1.5 mm/s
- Holding pressure: 138 bar
- Preheat time: 16 seconds

With these optimum process parameter combinations, the area of voids can be reduced to almost 0 and the wire sweep for long wire bond 2 attached at 90° to gate can be reduced to 3.1 %. Thus, both selected defects in the molded package are diminished in a considerable degree with the help of the given approach, which allows to define the optimum process parameters of the transfer molding process. Therein, the target to decrease the wire sweep under 4 % for long wire bonds, and void formation to almost none in the package is achieved with the generated models.

In addition to that, the material models are also generated, which express the relationship between the variations in the material characteristics and the void formation as well as wire sweep. Similar approach as in the process model is applied as shown in Figure 7.3, where all required steps for generation of models are explained in detail. After evaluating the results of the material investigations, which are already given in Chapter 6, regression analysis is performed in this chapter to determine the significant input parameters in terms of variations in material characteristics on void formation and wire sweep. After determining the important terms, linear material models are generated by using regression analysis. Fitting quality of the material models is evaluated to observe whether the void formation and wire sweep can be correlated well with the variations in the material characteristics. Good fitting quality is observed for the material models. However, it is important to emphasize that as the humidity and storage duration influence the material characteristics for example the curing reaction, crosslinking degree as well as the viscosity of the EMC, to describe the correlation between the void formation and wire sweep thoroughly, more input parameters in terms of material characteristics should be added into the models. Nevertheless, the generated models represent a systematic approach to estimate the processing limitations of EMCs which are subjected to different preconditioning (storage duration and humidity) in order to achieve a predefined package quality. Thus, the given approach in this chapter can be applied for other package geometries and other molding compounds to describe the relationship between the material characteristics and the package quality.

8 Validation Experiments and Results

In Chapter 7 the process and material models are generated, which deliver correlations between process parameters, material characteristics and package quality. However, as emphasized previously, the process and the material models have boundary conditions, which are the molding compound and the lead frame geometry. Thus, in this chapter the models are calibrated to determine the limitations of the established models. One of the boundary conditions, namely the molding compound is chosen to calibrate the models and the models are applied to a second epoxy molding compound. The reason of the selection of the molding compound for calibration is explained in detail in Section 8.1. At first, the validation experiments of the process model are introduced in this chapter. The model is applied to a second epoxy molding compound, and void formation and wire sweep are predicted with the help of the process model for the second molding compound. After the experiments are conducted, the predicted values are compared with the results from the validation experiments. Moreover, the process model is verified additionally with an unknown process parameter set to determine the estimation quality of the process model. More details about the validation of the process model are given in Section 8.1. In addition to the process model, the material model is also calibrated with the second epoxy molding compound. The calibration approach and the results of the validation experiments for the material model are demonstrated in Section 8.2. The limitations and the potentials of the models are discussed. The results of the validation experiments for the process and material models are summarized in Section 8.3.

8.1 Validation of Process Model

Additional experiments are carried out to validate the process model. The validation experiments for the process model include two aspects. In first aspect, the prediction quality of the model is tested with unknown process parameters. The aim is to determine whether the process model delivers good estimation for void formation and wire sweep with the process parameter combinations that are not used to generate the process model. The second aspect is to calibrate the process model with other molding compound to determine the potentials of the process model and to verify boundary conditions. The schematic illustration of the process model with a model test is given in Figure 8.1.

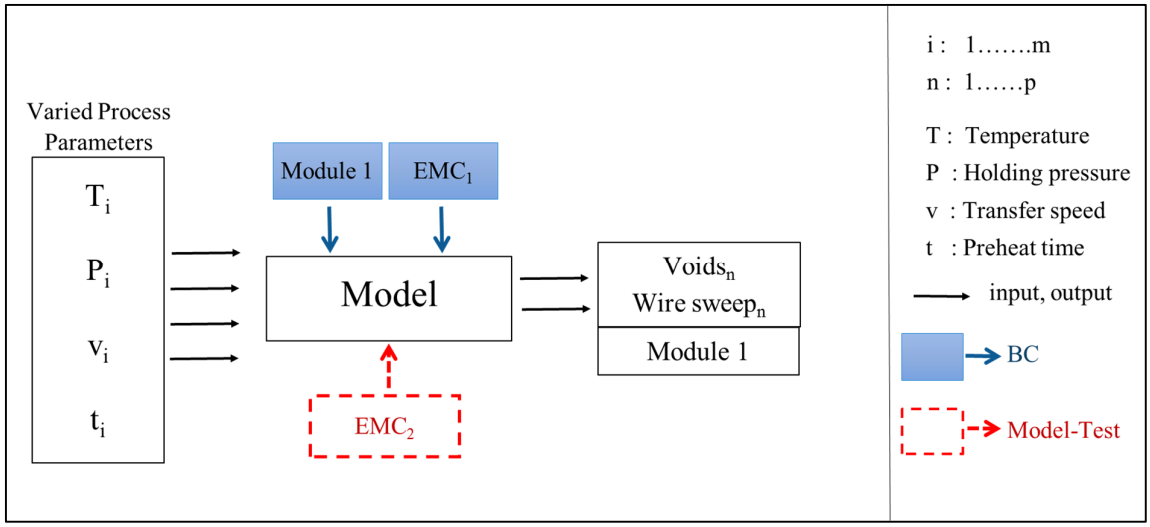

Figure 8.1: Schematic illustration of the calibration of process model with second epoxy molding compound

As shown in Figure 8.1, the process model has two boundary conditions. Module 1 states for the package geometry and EMC 1 implies that the main experiments are performed with one certain molding compound. To determine the potentials of the model and to verify the boundary conditions, it is important to calibrate the model with one of the boundary conditions. Variation of the package geometry

is very costly and time consuming, since a new mold tool is required to be built. In addition to the new molding tool, another fixing plate is necessary for the wire bond process of a new demonstrator. Moreover, a new program for the wire bond equipment as well as for the chip assembly equipment should be constructed for the positioning of the wire bonds as well as the dummy components on a new demonstrator. Thus, changing the lead frame geometry requires some elaborate revisions in the assembly process. Therefore, a second epoxy molding material, in other words EMC 2, is chosen to calibrate the model and test the limitations of the model as depicted in Figure 8.1. EMC 2 is selected for the calibration due to its different material characteristics in comparison to EMC 1 such as dissimilar epoxy systems and flow behavior (see Section 3.1.1 for the material properties of two molding compounds). The calibration of the process model with other molding compound is crucial due to the fact that the process model indeed includes the material characteristics information inside. Thus, EMC 2 is utilized to observe whether the process model can be applied for other molding compound, which has different properties, or whether the process model is restricted to a material type, which is used to generate the model. Therefore, an experimental design for the calibration of the process model is constructed and introduced in Section 8.1.1. The results of the validation experiments and the discussions about the limitations and the possibility of the process model are given in Section 8.1.2.

8.1.1 Experimental Design

Additional experiments are conducted to validate the process model. The aim is to determine whether the established process model delivers good estimation in terms of void formation and wire sweep with unknown process parameters. To ensure process stability and to compare the results, three known parameter combinations, which are already run in DoE with D-optimal plan, are repeated in the validation experiments. In addition, four new parameter combinations are integrated into the experimental plan to test the model with unknown process parameter combinations. Supplementation of the unknown parameters into the experimental is important to identify whether the established model delivers good results with unknown parameters as well. The experimental plan for the validation experiments is shown in Table 8.1.

Table 8.1: Experimental design of validation experiments

Parameter set no.	T [°C]	v [mm/s]	t [s]	P [bar]
1	165	6.5	0	80
2	168	2	2	80
3	168	5	4	100
4	175	4	8	110
5	177	2	12	85
6	182	1.5	0	140
7	185	1.5	16	80

The parameter set no. 2, 3, 5 and 6 are the unknown process parameters and indicated with red color in Table 8.1, whereas the parameter set no. 1, 4 and 7 are the process parameters which are already selected in DoE in main experiments. The reason for the selection of those process parameters from the main experiments is that parameter set no.1 causes large wire sweep, whereas parameter set no. 7 leads to a large amount of void formation in the package, which allows good comparison of the results of main experiments with validation experiments to prove the process stability. In addition to these process parameter combinations, the central parameter combination, parameter set no. 4, is included into the experimental plan for validation. Each parameter set no. is repeated five times to maintain reproducible results. Considering the left and right cavity, ten demonstrators are analyzed for each parameter set.

However, as the cavities are considered in process models separately, only the validation results of the left cavity are shown in this chapter.
As a second part of the validation experiments of the process model, the calibration of the process model is done. So far all the experiments for the process model are conducted with the same epoxy molding compound, EMC 1. However, to generalize the process model and to test the limits of the process model, the experiments are conducted with EMC 2. The experiments with the same parameter combinations, which are shown in Table 8.1, are performed with EMC 2 as well. The process model is utilized to estimate the wire sweep and the void formation of the packages, which are molded with EMC 2, and the predicted values from the process model are compared with the experimental results of EMC 2. The applicability of the process model to estimate the quality characteristics for the packages molded with another molding compound is evaluated. The results of the validation experiments for estimation quality of the process model for unknown process parameters are shown together with the calibration of the model with EMC 2 in the following section.

8.1.2 Quality Analysis Results

To determine the estimation quality of the process model for void formation and wire sweep, firstly the number of voids and wire sweep are estimated with generated process models. The process combinations for seven parameter set numbers are inserted in the Equation 7 and 9, and the number of voids and wire sweep are calculated respectively. Table 8.2 represents the predicted number of voids and the wire sweep. For the wire sweep determination, similar to Chapter 7 the long wire bond 2 attached at 90° to the gate in near gate area is used as representation.

Table 8.2: Predicted number of voids and wire sweep for long wire bond 2 attached at 90° to the gate in near gate area in left cavity with generated process models

Parameter set no.	Number of voids	Wire sweep [%]
1	1	7.4
2	3	4.2
3	0	6.9
4	1	6.0
5	6	3.8
6	1	3.0
7	11	2.7

After estimating the number of voids and wire sweep, the experiments are performed with seven process parameter combinations and the void formation as well as wire sweep are measured in the molded package. To assure the process stability, the results of void formation and wire sweep from the validation experiments are compared with the main experiments for those common process parameters: parameter set no. 1, 4 and 7. The results are depicted in Figure 8.2.

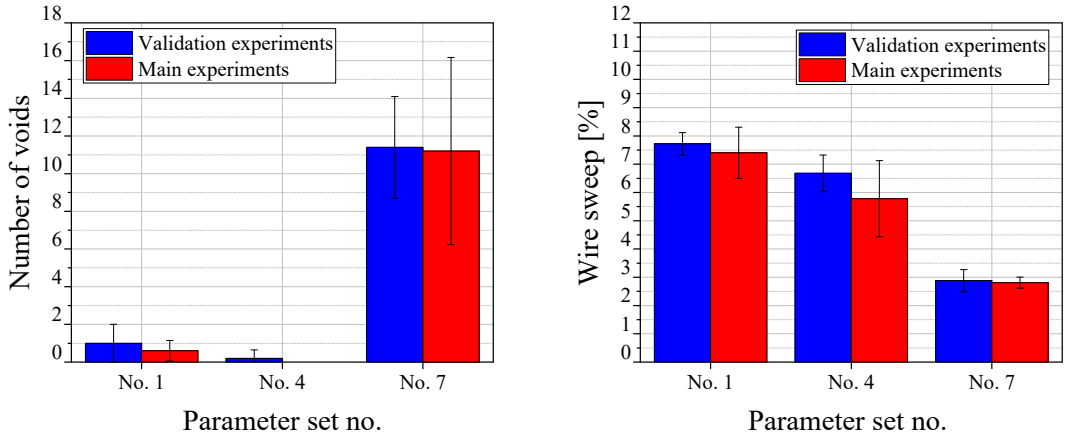

Figure 8.2: Comparison of the results from main experiments with the validation experiments with the common process parameters to ensure the process stability

The results show that the number of voids as well as the wire sweep measured with the same process parameter combination in validation experiments and main experiments are found close to each other. This assures that no big variations happen in the process and confirms the process stability. After ensuring the process stability in the validation experiments, the predicted number of voids are compared with the measured number of voids from the validation experiments. Figure 8.3 illustrates the comparison between the predicted number of voids and wire sweep for long wire bond 2 attached at 90° to gate and the results from the validation experiments.

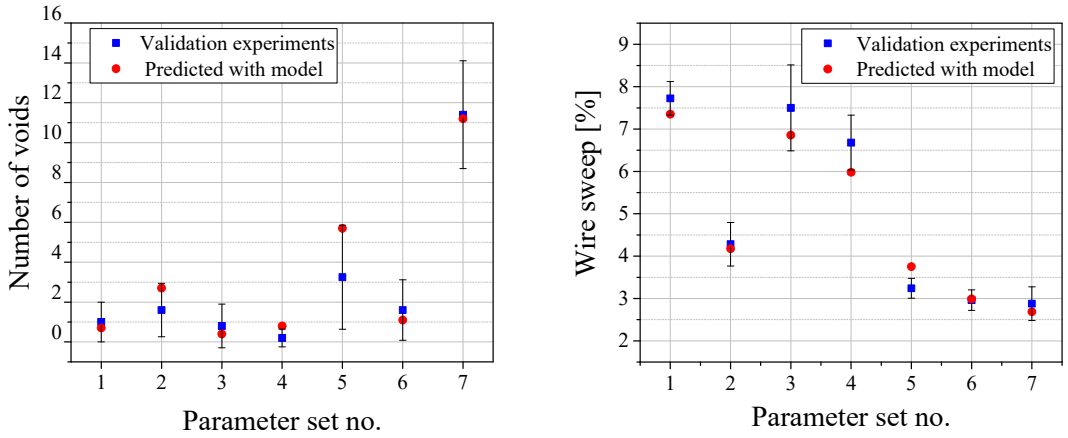

Figure 8.3: Comparison of the results predicted by using the process models with the results obtained from the validation experiments for number of voids (left), wire sweep for long wire bond 2 attached at 90° to the gate in near gate area (right)

The red points in the diagrams illustrate the predicted number of voids (Figure 8.3 left) and the predicted wire sweep (Figure 8.3 right) with the generated process models. The blue points depict the results obtained from the validation experiments. It is important to emphasize that the standard deviations shown in the diagrams are from the validation experiments. Since the average values are used to generate the models, it is important that the predicted values are close to the average values obtained from the validation experiments. As seen in Figure 8.3 (left), the number of voids estimated by using the process model matches very well with the results of the validation experiments. Additionally, the prediction quality for the wire sweep is found also very promising, where the predicted values for the wire sweep are very close to the experimental results. Most importantly, both models which are used to estimate the number of voids and wire sweep deliver very good prediction with unknown process parameters i.e. parameter set no. 2, 3, 5 and 6. Thus, with these generated process models, good estimation for void

formation as well as the wire sweep can be achieved for unknown process parameters within the selected process window.

In addition to the validation of the model with unknown process parameters, the process models are calibrated with EMC 2 to determine whether the process models also deliver good estimation for other molding compounds. Figure 8.4 depicts the comparison of the results of the experiments performed with EMC 2 and the estimated results from the models for number of voids and the wire sweep for long wire bond 2 attached at 90° in near gate area. The results of the validation experiments, which are carried out with EMC 1, are also supplemented into the diagram to compare the results.

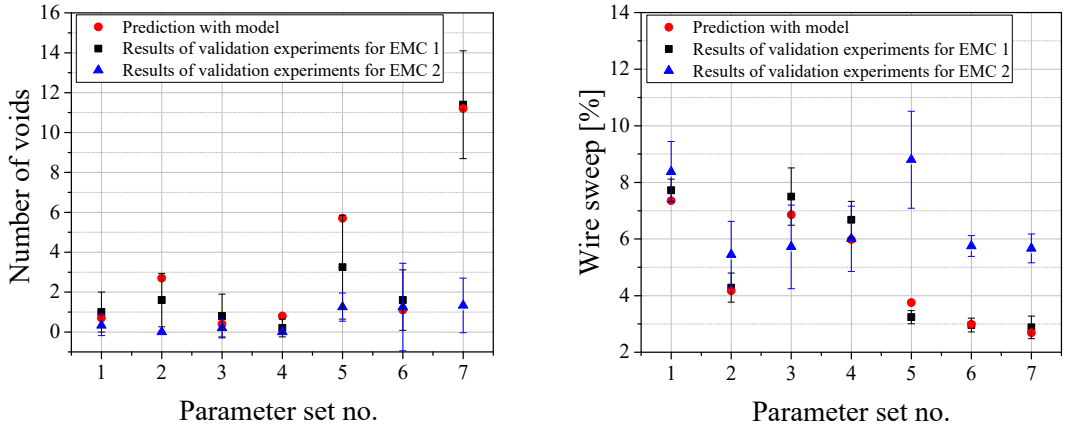

Figure 8.4: Calibration of the process models with EMC 2, comparison of the values predicted by using the process models with the results obtained from the validation experiment for number of voids (left) and wire sweep (right)

The black points in the diagrams demonstrate the results of the validation experiments for EMC 1, whereas the blue points illustrate the results of the validation experiments for EMC 2. The red points represent the predicted values with the process model. The predicted values for EMC 2 for number of voids match in almost all parameter set numbers (Figure 8.4 left). However, in parameter set no. 7 validation results for the number of voids of EMC 2 lie much lower than the predicted values with process model. For the wire sweep estimation, as seen in Figure 8.4 (right), for the parameter set no. 1, 2, 3, and 4 the predicted values correlate well with the validation results of EMC 2. On the other hand, for parameter set no. 5, 6, and 7, the results of wire sweep from the validation experiments of EMC 2 are found higher in comparison to the predicted values.

The obtained results, however, are not surprising. EMC 2, which is used to calibrate the model, has a different viscosity compared to EMC 1. As stressed frequently in this work, the wire sweep is influenced remarkably by the viscosity of the molding compound. Since the process models are generated with EMC 1, which has certain material properties such as viscosity, the generated models involve this information about the characteristics of the material ineluctably. To state the difference in the viscosity behavior of two molding compounds, the DEA and rotational rheometer results of EMC 1 and EMC 2 are depicted in Figure 8.5.

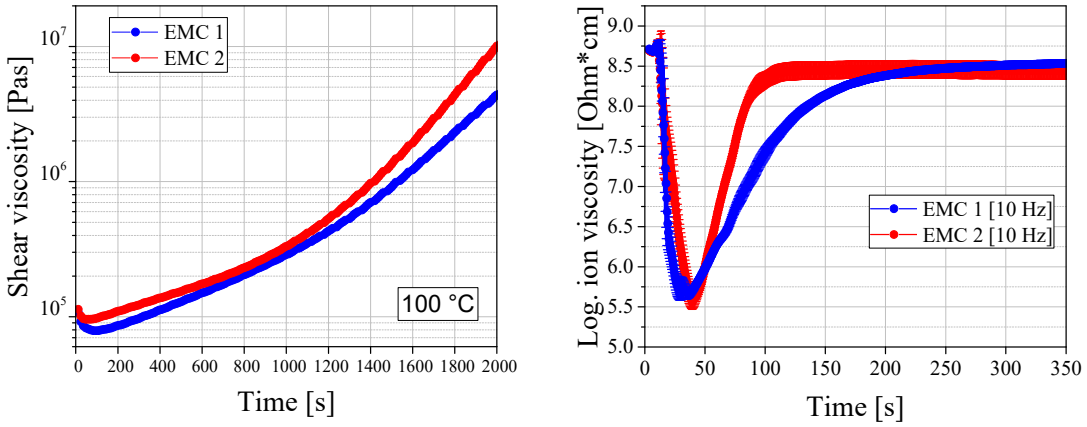

Figure 8.5: Comparison of the viscosity behavior of EMC 1 and EMC 2, shear viscosity measurement with rotational rheometer (left), ion viscosity measurement with DEA (right)

The cure reaction behavior of EMC 1 and EMC 2 differentiate remarkably from each other. According to the shear viscosity results in Figure 8.5 (left), the viscosity of EMC 2 is higher in comparison to the EMC 1. However, to acquire the best possible information about the viscosity during the molding process at 175 °C, ion viscosity curves should be compared. Ion viscosity curves in Figure 8.5 (right) demonstrate that EMC 2 has different cure reaction behavior under same processing conditions as EMC 1. The ion viscosity of EMC 2 at the same time point such as around 100 s is found higher than the ion viscosity of EMC 1. When comparing the slope of the ion viscosity curves, it is apparent that the cure reaction of EMC 2 propagates much faster. Yet, the maximum ion viscosity is achieved more quickly in ion viscosity curve of EMC 2 in comparison to EMC 1. As a matter of fact, by considering all seven process parameters for validation experiments in Table 8.2, cavity filling happens maximum within 28 s. The longest cavity filling of 28 s refers to the parameter set no. 7 which has the longest preheat time and slowest transfer speed. As the ion viscosity curves are recorded in-situ in transfer molding process, the direct comparison of the viscosities of two molding compounds can be done at certain time scale in the ion viscosity curves. Ion viscosity curves show that EMC 2 show higher viscosity also until 28 s, yet larger forces are exerted on the wire bonds during cavity filling. Thus, the rheology results can explain the higher wire sweep observed with EMC 2. In addition to the wire sweep, there is also some deviation observed between the results obtained from the validation experiments and predicted values for void formation. As shown in regression analysis for the void formation, the void formation is affected remarkably by the humidity such as the moisture content in the pellets. To understand the results depicted in Figure 8.4, the moisture content for the pellets of EMC 2 are measured with Karl-Fischer titration. The results of the moisture content for EMC 1 and EMC 2 are displayed together in Figure 8.6.

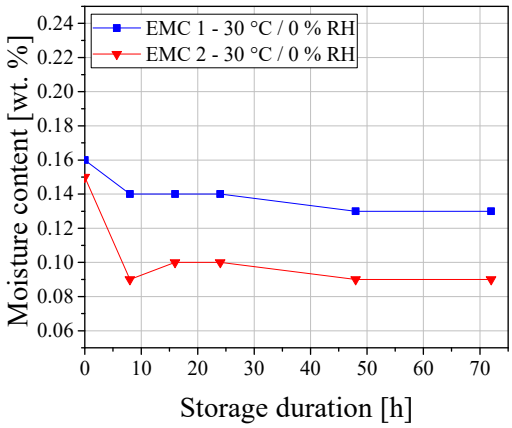

Figure 8.6: Comparison of the moisture content of EMC 1 and EMC 2

As seen in Figure 8.6, the moisture content of EMC 2 is found lower compared to EMC 1, which can explain the lower void formation observed in EMC 2. Besides, as explained in Chapter 2, the voids are not only formed due to the existing humidity in the pellets, but also due to the side products which are synthesized during cure reaction of molding compound. Two molding compounds have different epoxy systems and structures, thus have two different cure reaction mechanisms, which may also lead to variation in the void formation in the package.

8.2 Validation of Material Model

In addition to the process model, the material model is also validated with EMC 2. The main objective of the validation of the material model is to identify whether reaction behavior of EMC 2 is affected in similar extent as in EMC 1 when the pellets are subjected to the same preconditioning environments and whether those variations cause the likewise impact on the quality characteristics. The goal is to generalize the influences of alterations in the materials due to storage duration and humidity on the package quality. Figure 8.7 demonstrates the schematic illustration of the validation of the material model with EMC 2.

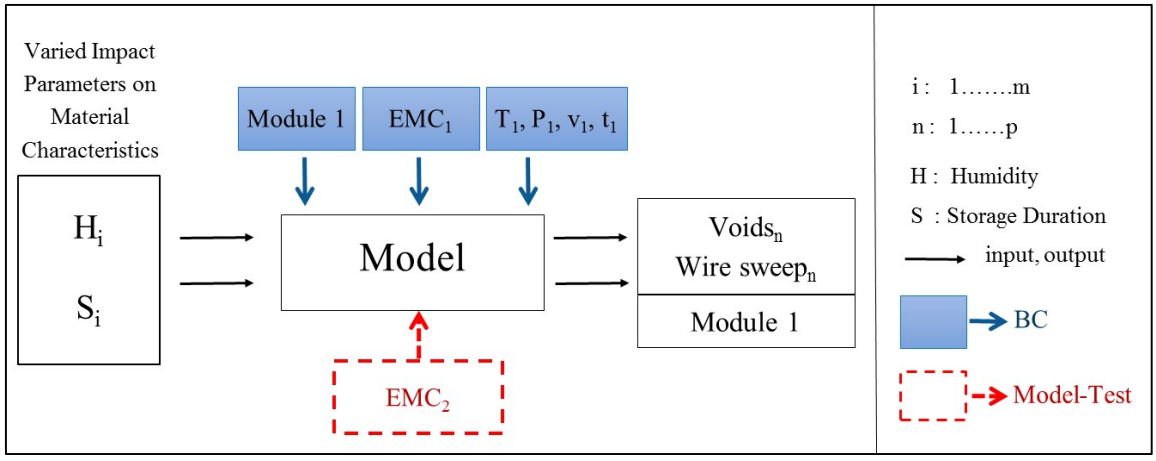

Figure 8.7: Schematic illustration of the validation of material model with second epoxy molding compound

As explained in Chapter 7, the material model has one extra boundary condition as in the process models namely the process parameters. However, this is only to note that the process parameters should be kept constant when investigating the variations in the material characteristics. Apart from that, similar boundary conditions as in the process model are also valid for the material model. Since the goal in the material model is to generalize the understanding gained with EMC 1 in terms of the impact of the

variations in the material characteristics on the quality features, EMC 2, which has different chemical structure in comparison to EMC 1, is selected for this purpose. The experimental approach applied to validate the material model is explained in following section.

8.2.1 Experimental Analysis

In the material model, two input parameters are selected, namely storage duration and humidity. The approaches applied to generalize the material model in terms of storage duration and humidity are explained in this section respectively.

Storage Duration

The obtained results with EMC 1 are validated by using EMC 2 to observe whether the prolonged storage duration has the same influence on void formation and wire sweep with other molding compound as well. For this reason, for EMC 2 similar storage duration approach is applied as in EMC 1. The pellets of EMC 2 are preconditioned for 0 h, 8 h, 16 h, 24 h, 48 h and 72 h in a vacuum oven at 0 % RH and 30 °C and molded in transfer molding process. Ion viscosity curves are recorded with DEA during the molding process. For each preconditioning trial five repetitions are done to evaluate the reproducibility of the results. The DEA signals shown in this chapter are the average values of these five repetitions. After the molding process, the packages are sent to PMC process, and subsequently analysis of void formation is executed. Afterwards, the molded packages are opened with laser etching process and the wire sweep is examined. To compare the viscosity behavior with EMC 1, the viscosity of the preconditioned EMC 2 pellets is measured with rotational rheometer as well as with squeeze flow rheometer. Moreover, the signals obtained from DEA for EMC 1 and EMC 2 and the results of quality characteristics of the package which are molded with EMC 1 and EMC 2 are compared with each other.

Humidity

To validate the results acquired with EMC 1 and to analyze whether the humidity shows similar impacts on void formation and wire sweep with other molding compounds, the same experimental approach as in EMC 1 is applied to EMC 2. EMC 2 pellets are preconditioned for 0 h, 8 h, 16 h, 24 h, 48 h and 72 h in a climate oven at 30 °C and 90 % RH. The demonstrator is encapsulated with the preconditioned EMC 2 pellets and the void formation and wire sweep are analyzed in a similar way described above in storage duration. The results obtained from EMC 2 in terms of void formation and wire sweep are compared with the results acquired from EMC 1. Furthermore, the viscosity behavior monitored with DEA for preconditioned EMC 2 is compared with the viscosity behavior of EMC 1. Each preconditioning trial is repeated five times to obtain maintainable results.
Besides, the water uptake of EMC 2 after the preconditioning is also measured with Karl-Fisher titration. The humidity contents of two molding compounds are compared. The experimental analysis conducted to validate the material model with EMC 2 is summed up in Table 8.3.

Table 8.3: The experimental analysis for validation of the material model with EMC 2

Fresh samples	Preconditioning at 30 °C / 0 % RH	Preconditioning at 30 °C / 90 % RH
0 h	8 h	8 h
	16 h	16 h
	24 h	24 h
	48 h	48 h
	72 h	72 h

8.2.2 Experimental Results

The aim of the experimental results is to determine whether other molding compounds behave similarly as EMC 1 when the pellets are preconditioned in dry environment and when they are exposed to

humidity. Thus, the viscosity behavior of EMC 2 is compared with the viscosity behavior of EMC 1 in this section. Additionally, DEA is proven as a suitable online monitoring method since the small variations in the characteristics of EMC 1 can be observed in-situ in transfer molding with DEA as shown in detail in Chapter 5. This allows to identify the variations in the characteristics of molding compound in-situ already during molding process, when the molding compound has humidity or prior curing. However, to generalize the effect which are observed in the ion viscosity curves of EMC 1, it is important to analyze whether other molding compounds behave in similar way when the pellets are preconditioned or have certain cross-linking degree prior to molding process. Thus, ion viscosity curves of EMC 1 and EMC 2 are compared and the variations in the ion viscosity curves due to the humid and dry storage duration are discussed.

In addition, in Chapter 7 the mathematical definition of the material model is given. As already mentioned in the previous chapter, the material model consists not enough terms to describe the complex alterations mechanisms in the epoxy molding compound commenced due to the humidity or prolonged storage duration. Although the application of the models to other molding compound is difficult due to the significant variations in the material characteristics, the calibration of the material model is also done with EMC 2 to determine the limitations of the material model. The results of the storage duration and the humidity of EMC 2 as well as the calibration of the model are shown in following.

Results of Storage Duration

The ion viscosity behaviors of EMC 1 and EMC 2 are compared to determine variations in the viscosity of the preconditioned molding compounds. Figure 8.8 illustrates the results obtained from the DEA which are taken in situ in transfer molding process.

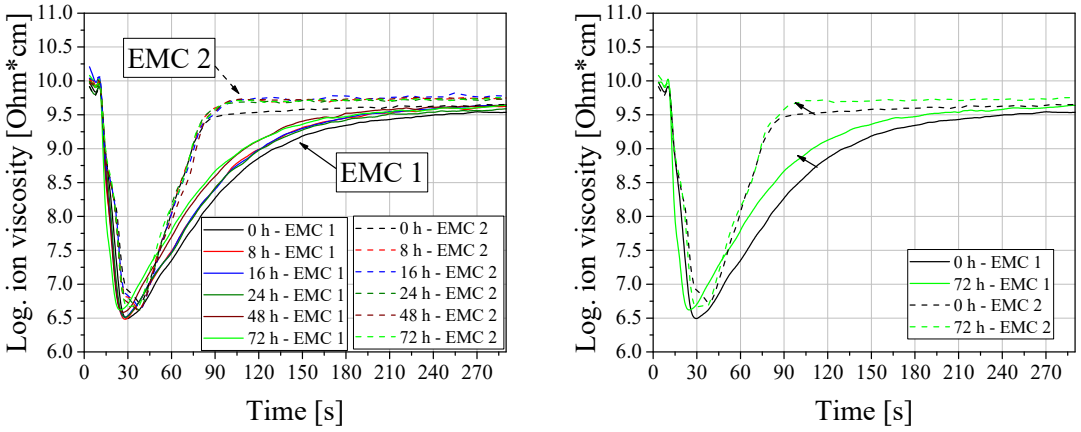

Figure 8.8: Ion viscosity curves for EMC 1 and EMC 2 pellets, which are preconditioned in dry environment at 30 °C and 0 % RH for a prolonged storage time

The ion viscosity curves of EMC 2 are also affected by the prolonged storage duration and the ion viscosity increases slightly when the pellets are preconditioned in dry environment. To visualize this alteration in the ion viscosity more clearly, in Figure 8.8 (right) only the 72 h preconditioned samples are illustrated. It can be seen that, although the cure reaction behavior of EMC 2 is different in comparison to EMC 1, the ion viscosity varies to similar extent when the pellets are preconditioned and the curves shift to higher ion viscosity level. The rheology measurements are also conducted to observe the possible variations in the viscosity of EMC 2 due to the prolonged storage duration in dry environment. Figure 8.9 depicts the results of rotational rheometer as well as the squeeze flow rheometer for preconditioned pellets of EMC 2.

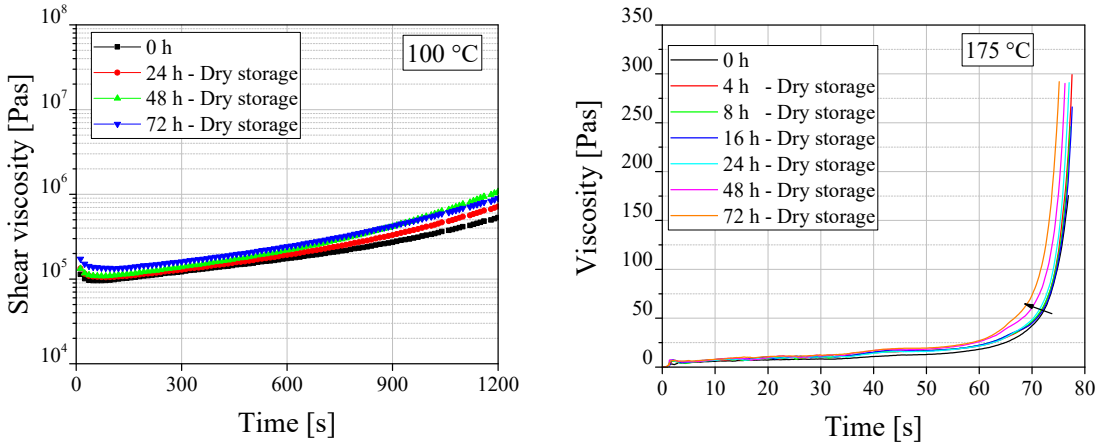

Figure 8.9: Results of rotational rheometer (left), and results of squeeze flow rheometer 2 (right) for EMC 2 pellets preconditioned in dry environment at 30 °C and 0 % RH for prolonged storage time

The viscosity of EMC 2 changes slightly with prolonging storage duration in dry environment. The rotational rheometer results show that the viscosity of the preconditioned pellets for 24 h, 48 h as well as 72 h are found higher in comparison to the fresh pellets. The squeeze flow rheometer results also confirm these findings (Figure 8.9 right). The viscosity curve shifts to the left gradually with increasing prolonged storage duration which indicates a decrease in the gel time of the molding compound. Thus, the DEA results and the rheology results for the preconditioned pellets of EMC 2 in dry environments are found very similar to the results obtained from EMC 1. Although EMC 2 has different chemical structure, the variations observed in the viscosities are very much alike as in EMC 1.
Subsequently, to determine the influence of such variations on the void formation and wire sweep, the packages are molded with the preconditioned pellets of EMC 2 and the number of voids and the corresponding area of the voids are measured which are shown in Figure 8.10.

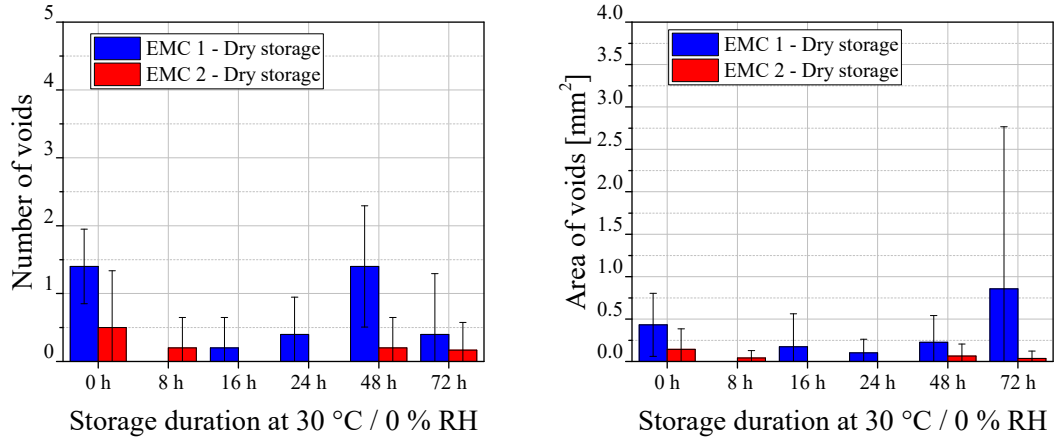

Figure 8.10: Number of voids (left) and corresponding area of voids (right) for the packages molded with EMC 1 and EMC 2 pellets, which are preconditioned in dry environment at 30 °C and 0 % RH for prolonged storage time

The number of voids and the corresponding area of voids stay almost constant with prolonged storage duration in the packages molded with preconditioned EMC 2 pellets. As a matter of fact, the void formation in the packages which are molded with preconditioned EMC 2 pellets are lower in comparison to the packages molded with preconditioned EMC 1 pellets for all storage durations. The reason for this difference is already explained in Section 8.1 with Karl-Fischer titration results, where EMC 2 pellets have generally less moisture content in comparison to EMC 1 pellets (see Figure 8.6). Figure 8.11 illustrates the comparison of the wire sweep measured in the packages molded with preconditioned

EMC 1 and EMC 2 pellets for the long wire bond 2 attached at 90° to the gate as well as for the short wire bond 2 attached at 45° to the gate.

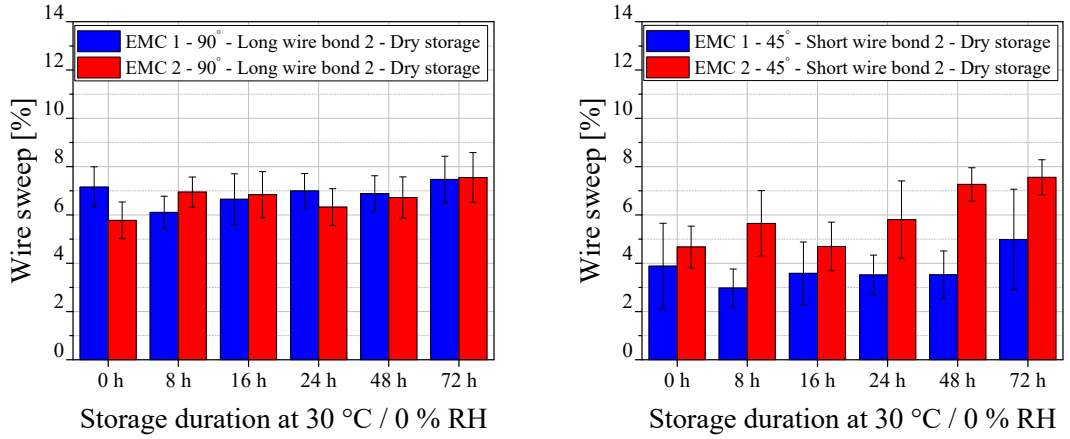

Figure 8.11: Comparison of wire sweep observed in the packages molded with pellets of EMC 1 and EMC 2 preconditioned in dry storage at 30 °C and 0 % RH for prolonged storage time; wire sweep for long wire bond 2 attached at 90° to gate (left) and wire sweep for the short wire bond 2 attached at 45° to gate (right)

Prolonged storage duration of the pellets of EMC 2 in dry environment shows slight influence on the wire sweep in the package which is similar to the results obtained from the packages molded with preconditioned EMC 1 pellets. In addition, for the short wire bonds, the wire sweep observed in EMC 2 packages increases with prolonged storage duration of the pellets. Indeed, for all storage durations, wire sweep is found larger in packages molded with EMC 2 in comparison to the packages molded with EMC 1.

To test the limitations of the material model, the area of the voids and the wire sweep for the packages molded with EMC 2 are estimated with the established material model. The comparison between the predicted values from the material model and the values measured in the validation experiments are shown in Figure 8.12.

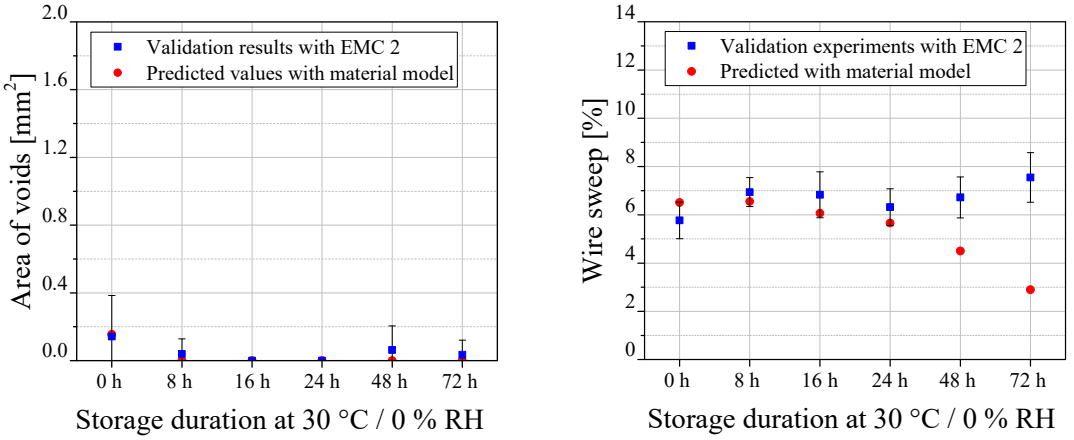

Figure 8.12: Comparison of the predicted values with the measured values from the validation experiments, area of voids (left), wire sweep for long wire bond 2 attached at 90° to the gate (right)

Predicted values for the number of voids are found to be very similar to the validation results for the packages molded with EMC 2. The wire sweep values predicted with material model match also good with the values measured in the validation experiments for EMC 2 packages. However, especially after 48 h of storage, the predicted values lie below the values obtained from the validation experiments. The larger wire sweep observed in EMC 2 packages in comparison to the wire sweep of EMC 1 packages can be attributed to the higher viscosity of EMC 2, which is already shown in Figure 8.5.

Results of Humidity

Ion viscosity curves of EMC 1 and EMC 2 are compared in Figure 8.13 for the pellets, which are preconditioned in humid environment at 30 °C and 90 % RH.

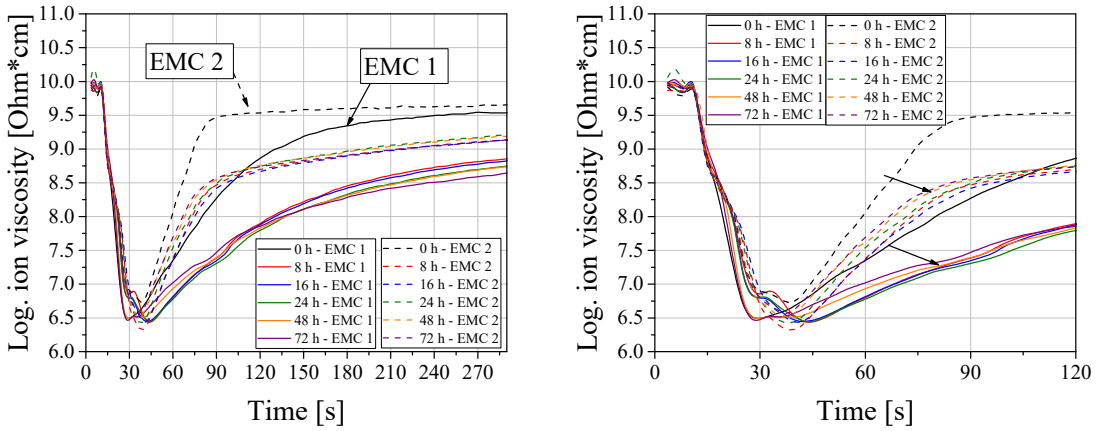

Figure 8.13: Ion viscosity curves of EMC 1 and EMC 2 pellets preconditioned in humid environment at 30 °C and 90 % RH for prolonged storage time

Ion viscosity curves for EMC 2 behaves similar as in EMC 1 when the pellets are exposed to the humidity. The existence of the humidity can be easily recognized from the ion viscosity curves for EMC 2 as well. All ion viscosity curves for different humid storage durations are shifted to right, the delta between the maximum and minimum ion viscosity becomes much smaller, when the pellets of EMC 2 are stored in humid environment. The propagation of the reaction varies significantly for the humid pellets of EMC 2 as well and the time required to reach the maximum ion viscosity becomes longer. Thus, two molding compounds illustrate similar variations when the pellets are stored in humidity. Therefore, such kind of variation in the ion viscosity curves can be considered as a typical signal for the humidity in the pellets.

In addition to the DEA measurements, the viscosity behavior of EMC 2 is also measured with rotational rheometer as well as with squeeze flow rheometer. The results of the rheology measurements are displayed in Figure 8.14.

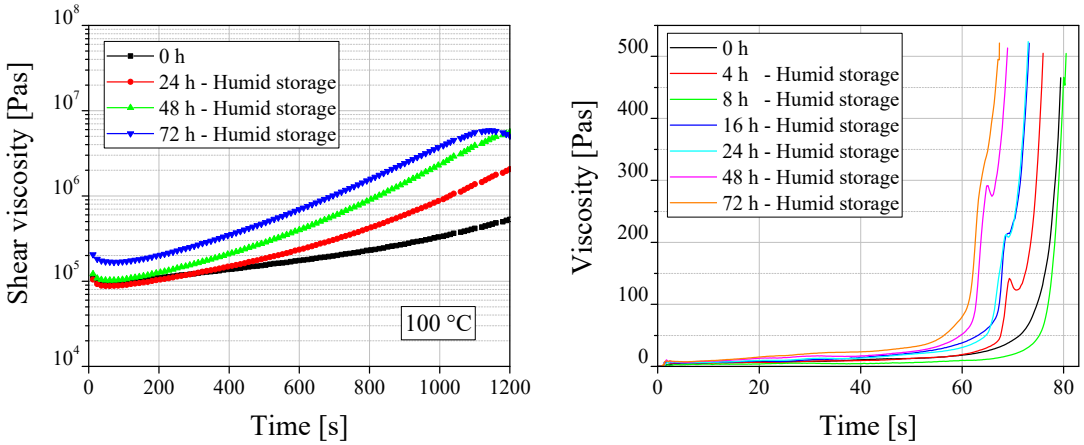

Figure 8.14: Results of rotational rheometer (left), and results of the squeeze flow rheometer (right) for EMC 2 pellets preconditioned in humid environment at 30 °C and 90 % RH for prolonged storage time

Humidity plays a significant role on the shear viscosity of EMC 2 as well. The viscosity increases with an increasing storage duration of the pellets in humid environment. Similar results can be also observed from the squeeze flow rheometer, where all storage durations in humid environment are illustrated together (Figure 8.14 right). The viscosity of the curves shifts with a large extent to the left to earlier

time by increasing storage duration in humid environment, which indicates a decrease in the gel time. To observe the water content of EMC 2 in humid environment with an extended storage duration, the pellets are measured with Karl-Fischer titration. The results Karl-Fischer titration for EMC 2 as well as for EMC 1 are depicted together in Figure 8.15.

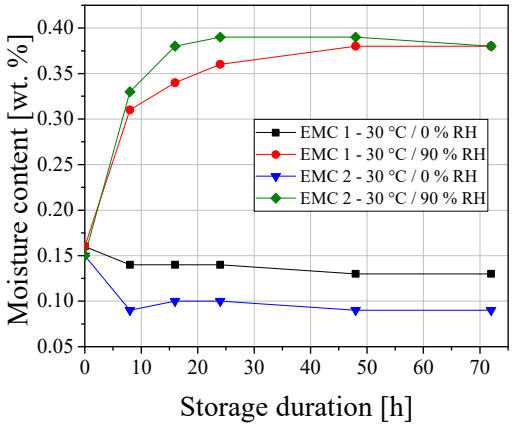

Figure 8.15: Comparison of the water uptake between EMC 1 and EMC 2 pellets preconditioned in dry (30 °C / 0 % RH) and humid (30 °C / 90 % RH) environment for storage time of 8 h, 16 h, 24 h, 48 h, 72 h as well as fresh pellets (0 h)

The water content of EMC 2 also increases significantly with extended storage duration in humid environment. In general, the moisture content measured in EMC 2 is also found high when the pellets are preconditioned in humid environment, which also confirms the big variations observed in viscosity behavior due to humidity shown in Figure 8.14. Nevertheless, EMC 1 and EMC 2 reach the same moisture content level after 72 h of humid storage.

The influence of the humid pellets of EMC 2 on the number of voids and the area of voids are also evaluated and the results are illustrated in Figure 8.16.

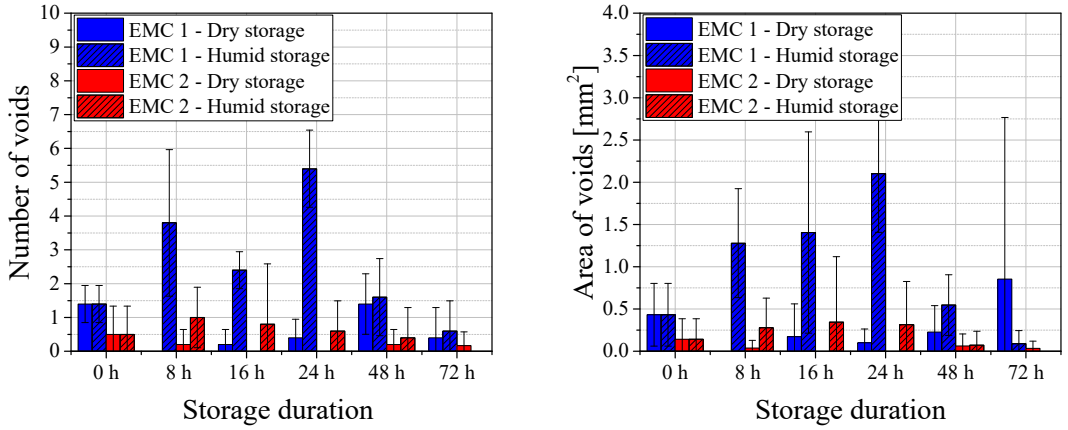

Figure 8.16: Number of voids (left) and corresponding area of voids (right) for packages which are molded with EMC 1 and EMC 2 pellets preconditioned in dry (30 °C / 0 % RH) and humid (30 °C / 90 % RH) storage

The number of voids and the area of voids are found much lower in the packages molded with EMC 2 in comparison to EMC 1 when the pellets are preconditioned in humid environment. As discussed in previous section, the dry pellets of EMC 2 cause in general less void formation in comparison to EMC 1. However, when EMC 2 pellets are exposed to humidity only a slight increase in the void formation in the packages can be inspected.

Figure 8.17 shows the comparison in the wire sweep of the packages molded with preconditioned pellets of EMC 2 and EMC 1 in dry and humid environment.

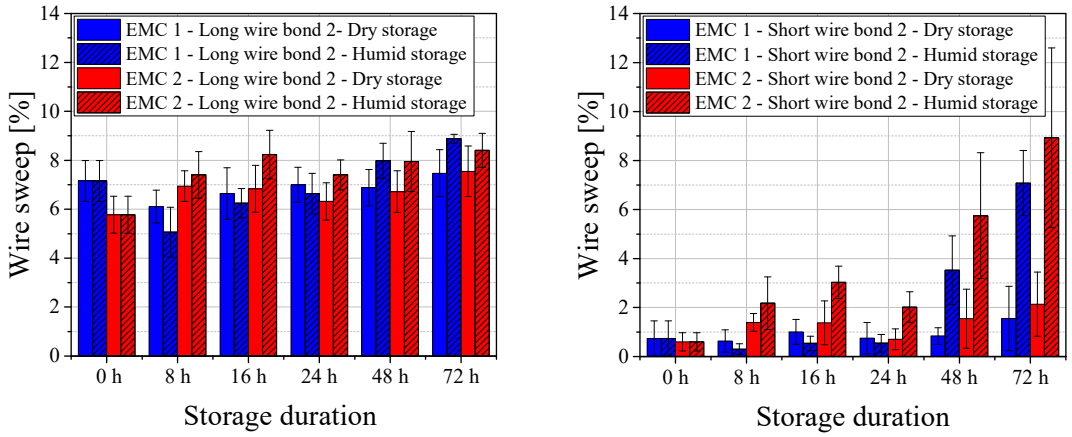

Figure 8.17: Comparison of wire sweep observed in packages molded with preconditioned pellets of EMC 1 and EMC 2 at dry environment of 30 °C / 0 % RH and at humid environment of 30 °C / 90 % RH; the wire sweep for long wire bond 2 attached at 90° angle to gate (left) and wire sweep for short wire bond 2 attached at 90° angle to gate (right) in near gate area

Wire sweep for the long wire bonds increases when the packages are molded with EMC 2 pellets preconditioned for extended storage duration in humid environment. The results and the extent of increment observed in the long wire bonds are similar to the results obtained in the packages molded with preconditioned EMC 1 pellets. The pronounced impact of the humidity on the wire sweep can be seen more obviously in the short wire bonds shown in Figure 8.17 (right). With increasing humid storage of pellets, the wire sweep in the package molded with EMC 2 increases remarkably. The increase in the wire sweep for EMC 2 packages due to the humidity is much larger in comparison to EMC 1 packages. It is evident that, the humidity shows also pronounced impact on the wire sweep of the EMC 2 packages. The material model for the humidity is also validated with EMC 2. As input parameters, dry storage duration, humid storage duration as well as the water content of EMC 2 pellets, which are measured with Karl-Fischer titration, are given into the material model, and the predictions for the void formation and the wire sweep are done. The prediction values are compared with the results obtained from the validation experiments with EMC 2. Figure 8.18 illustrates the comparison between the predicted values and results of the validation experiments.

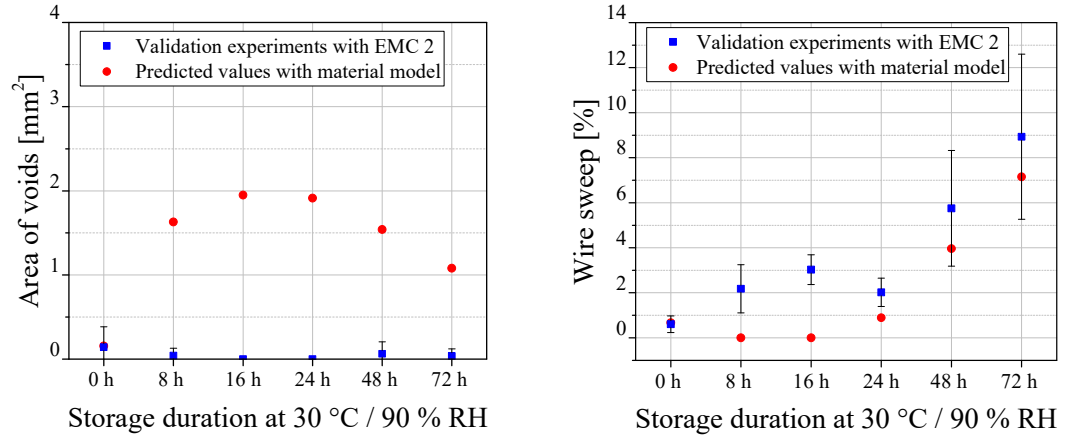

Figure 8.18: Comparison of the predicted values with the measured values from the validation experiments, area of voids (left), wire sweep for short bond 2 attached at 45° to the gate (right)

As seen from the diagrams in Figure 8.18 the values estimated with material model show higher void formation for EMC 2 packages in comparison to the experimental results. This difference can be attributed to the fact that void formation for the packages molded with EMC 1 is found larger in

comparison to the packages molded with EMC 2 under same humidity preconditioning. Figure 8.18 (right) illustrates the wire sweep observed for the short wire bond 2 at 90° angle to the gate which demonstrates usually larger wire sweep. As seen from the diagram, no perfect match is found between the predicted values and the results of validation experiments. The wire sweep values measured with the validation experiments are found to be higher in comparison to the predicted values. As already discussed in validation of the process model, the material model also involves the material characteristic information inside such as viscosity, which is very crucial in terms of wire sweep. Moreover, as shown previously, EMC 2 viscosity is found to be higher in comparison to EMC 1, which can induce therefore larger wire sweep. When the same model is applied to the other molding compound, deviations occur between predicted values and the real results due to the differences in the material properties, such as viscosity. Thus, as in the process model, material model has also limitations and the boundary conditions. Nevertheless, the results observed in the validation show that although EMC 2 has different material characteristics as in EMC 1, the variations in the ion viscosity signal due to the dry and humid storage are very similar to the ion viscosity of EMC 1. Thus, such alterations in the DEA curves can be attributed to the humidity and the results can be widened and applied for other molding compounds as well. When such changes are observed in the DEA signal in-situ in transfer molding process, the effect can be distinguished and can be attributed to the existence of the humidity in the EMC pellets.

8.3 Summary

Chapter 8 is dedicated to the validation experiments for the process and material models to determine the applicability and the limitation of the models. Firstly, the estimation quality of the process model is evaluated by conducting the experiments with unknown process parameters. The void formation and wire sweep are estimated for the unknown process parameter combinations with the process model and the predicted values are compared with the results from the validation experiments. Good prediction quality of the process model is found for the unknown process parameters. Additionally, as explained in Chapter 7, the process and material models have two major boundary conditions, which are the geometry of the demonstrator and the utilized epoxy molding compound (EMC 1). Thus, to determine the limitations of the models, one of the boundary conditions, namely EMC 1 is selected and the validation experiments are conducted with EMC 2. The process model is used to estimate the void formation and wire sweep for EMC 2, and the results of the validation experiments, which are conducted with EMC 2, are compared with the predicted values. The results show that there are some alterations between the predicted values and the validation experimental results, which implies that the process model has some limitations when used for other materials. Since the process models are generated with one certain molding compound with given properties (EMC 1), the properties of the molding compound have a direct influence on void formation and wire sweep. The model involves those properties automatically inside. When the process model is used for other molding compound with different viscosity behavior, the model considers still the output values in accordance to the results obtained from EMC 1. Thus, the utilized molding compound is the boundary conditions for the process models. To use the same process model such as for other molding compounds additional calibration of the models are necessary. Nonetheless, it is evident that the process models can make very precise prediction on the void formation and wire sweep even with some unknown process parameter combinations. Hence, the generated models can be used to predict the void formation and wire sweep with all possible parameter combination within the selected process window. Therefore, with an introduced approach, the process models with high prediction quality can be generated to define the relationship between the process parameters and the quality features as well as to make an estimation on the quality characteristics of the electronic packages.

As a second part of the validation experiments, the material model is validated with EMC 2 to generalize the effect observed with EMC 1 in terms of the variations in the cure behavior of material under different preconditioning. The similar variations in the cure behavior of EMC 2 as in EMC 1 are observed when the pellets are preconditioned under dry and humid environment. Additionally, the material models are

validated with EMC 2 and the predicted values from the models are compared with the results of validation experiments. Similar deviations as in the process models are observed between the predicted values and the validation results. It is evident that the material model also involves material characteristics information inside, and application of the same material model to other molding compound requires additional calibration. In addition to that, the same alterations in the DEA signal are observed when the pellets of different compounds are exposed to humidity or preconditioned in dry environment. Therein, the effects examined in the variations of DEA signal can be broadened to other molding compounds and DEA can be used as a suitable online monitoring method to detect the processing limitations of the EMC in-situ in transfer molding process.

9 Conclusions and Outlook

In this work a conceptual understanding of the influence of the process parameters and variations in the material characteristics of EMC on the package quality is provided in order to minimize the defects in the electronic packages which arise during transfer molding process. Detailed process and material analyses are conducted to understand the relationship between process parameters, material characteristics and package quality. To have a better process control in transfer molding process, online monitoring method, DEA, is introduced and developed as an in-situ cure monitoring technique in transfer molding process. The correlations between process parameters, material characteristics and package quality are generated by using DoE methods to design and evaluate the experiments systematically. The experimental analysis is divided into three parts: preliminary experiments, main experiments and validation experiments.

In preliminary experiments, an extensive process study is conducted to determine the dominant process parameters of the transfer molding process on the selected quality characteristics: wire sweep, void formation and warpage. It is found that among the four process parameters: molding temperature, preheat time, holding pressure and transfer speed, transfer speed and holding pressure are two dominant process parameters on wire sweep and void formation. Detailed wire sweep analysis demonstrates that wire sweep is influenced by angle of the wire bonds with respect to the gate, position of the wire bonds on test vehicle as well as length of the wire bonds. Wire bonds attached in near gate area illustrate more wire sweep in comparison to the wire bonds attached in far from the gate area for the selected package geometry. The angle of the wire bonds with respect to gate show also an impact on the wire sweep. Comprehensive void analysis is conducted to analyze number of voids, area of voids as well as positions of the voids in regard of process parameters. The results demonstrate that the voids have a tendency to form in far from the gate area in the cavity. Among investigated quality characteristics, it is found that void formation and wire sweep are strongly affected by the process parameters, whereas warpage of the selected demonstrator does not differ significantly with variations in the process parameters in the evaluated parameter field. This warpage result is attributed to the stable thickness and the small surface area of the test vehicle. Furthermore, in the preliminary experiments, basic characterization of the EMC 1 in regard to alterations in material properties due to prolonged storage duration, humidity and batch variations are done. It is observed that the cure behavior of EMC 1 is impacted by prolonged storage duration, batch variations and heavily by the humidity. Those variations can be also observed and monitored with DEA in-situ during transfer molding process. Moreover, DEA signals are validated and compared with the results obtained from DSC, DMA, rotational rheology as well as squeeze flow rheometer measurements and good correlation is found between the methods. The feasibility analysis of DEA as an online monitoring method in transfer molding demonstrates that DEA delivers relevant information about the cure reaction of the EMC from cavity and is a suitable method to determine the alterations in the cure behavior of the EMC in-situ in transfer molding process.

After the preliminary experiments, the main experiments are performed to establish process and material models. By using these results, a systematic approach is introduced to generate process and material models, which describe the relationships between process parameters, material characteristics and package quality. Process models are developed and hereby the correlations between the process parameters, void formation and wire sweep are expressed mathematically. High correlation quality is obtained, where over 94 % area of voids and 96 % of wire sweep are predicted with the model. Based on the generated process models, the optimum process parameters of the transfer molding process are determined. As optimum process parameters, temperature of 170 °C, transfer speed of 1.5 mm/s, holding pressure of 138 bar and preheat time of 16 seconds are suggested which lead to a reduction in the area of voids to $3.88 \times 10^{-5} \pm 1.73$ mm^2 and the wire sweep of long wire bond to 3.13 ± 1.08 %. Thus, with the given approach, the optimum process parameters of transfer molding process are determined and the

target to obtain the wire sweep under 4 % for the long wire bonds and to acquire the packages without any void formation is successfully achieved.

Furthermore, the correlations between the variations in the material characteristics of EMC 1 due to prolonged storage duration, humidity and batch variations and the quality characteristics, wire sweep and voids are identified. Storage duration shows only slight impact on void formation in the package, whereas wire sweep is affected by the prolonged storage duration of EMC 1. Especially after 48 h of dry storage, wire sweep of the long wire bonds and short wire bonds in the near gate area increases. Moreover, pronounced impact of the humidity on void formation and wire sweep is determined. Void formation and wire sweep are increased dramatically when the pellets are preconditioned in humid environment for extended storage time. Therefore, it can be concluded that the alterations in the material characteristics of the EMC due to prolonged storage duration and humidity have a direct impact on void formation and wire sweep, and hence the processing limitations of the EMC should be taken into account to prevent possible defects which may arise in the transfer molding process.

In addition to the process model, a material model is also generated. The correlations between the alterations in material characteristics and the package quality is obtained by applying regression analysis. This statistical material model is illustrated mainly to show how such variations in the high complex EMC characteristics, where the exact formulations are not known, can be correlated with the package quality in a regression model without applying any detailed physical material models. Nevertheless, for more precise correlations, more terms can be included into the models, which describe the variations in the complicated chemical nature of the EMC such as viscosity change or alterations in reaction mechanisms under humidity and storage duration.

After the generation of the models, the validation experiments are conducted to determine the possibility and the limitations of the models. The process model is tested with unknown process parameters to ascertain whether the process model delivers precise estimation on void formation and wire sweep with unknown process parameters. The validation results show that a very good prediction of the void formation and wire sweep is found with the process model. The predicted values with the process model match very well with the results from the validation experiments. Therein, the generated process model can be used to estimate void formation and wire sweep for all possible parameter combinations within the selected process window.

Afterwards, validation of the models is extended to one further step, a second molding compound is chosen, which has substantially different flow characteristics and rheological behavior to determine whether the same model can be applied to other molding compounds having different chemical formulations. The predicted values from the process model are compared with the experimental results of EMC 2, and it is found that the predicted values and the experimental results show some deviations. This result delivers the fact that generated models involve the information on molding compound characteristics inside. As the EMC properties have a direct impact on the quality features, the crucial material characteristics influencing flow behavior in the cavity such as viscosity, spiral flow and gel time, which are most relevant properties on the quality characteristics, are considered already in the models. Thus, to apply the same model to other molding compounds which have profoundly different flow behavior and viscosity as shown in DEA and rheology measurements for EMC 2, new models should be generated by applying the same approach given in this work. Therefore, application of the same model to other molding compounds with different flow characteristics requires additional calibration, however when the process models are generated for one certain EMC, it delivers precise estimation on void formation and wire sweep for the unknown process parameters within the selected process window.

In addition to the process model, the material model is also validated with EMC 2 to determine the boundary conditions of the validity of the material model. It is observed that the storage duration and humidity show similar effect on the cure behavior of EMC 2 as well. The representative material models are validated with EMC 2, and the results of the validation are compared with the predicted values from the models. The results show that there are some deviations between the predicted values and the

validation experiments. Hence, similar to the process model, to apply the same material model to other molding compounds, which have substantial differences, a new calibration has to be done, which should also, in best case, involve more information concerning the alterations in chemical reaction of the material under humidity and storage duration. However, it is observed that although both molding compounds have different viscosities and chemical formulations, the ion viscosity behaviors of the preconditioned molding compounds are varied in a similar extent in DEA signal. Hence, the inspected alteration mechanisms in the EMC characteristics due to prolonged storage duration and humidity in DEA signal can be expanded and applied to other molding compounds as well.

Therefore, based on the given results, the systematic approaches described in this work deliver good correlations between process parameters, material characteristics and package quality. With a given process model, the mathematical relationship between process parameters, void formation and wire sweep is defined and good estimation quality can be determined. The approach given in this work enables to describe the complex relationships which involves multi-objective molding process optimization and highly complex material properties within a process model. Additionally, the model represents an approach to identify the process parameters which allow to determine the optimum process parameters to reduce the defects in the molded packages, yet the failure costs. Thus, the methodology given in this work can be implemented for other packages to define the mathematical correlations between the process parameters and the package quality, and to estimate the quality features with unknown process parameters without conducting large efforts of experiments. In addition, the impact of variations in the material characteristics on void formation and wire sweep is defined in material model. The model represents a systematic approach to estimate the processing limitations of the EMC which are subjected to the different preconditioning such as storage duration and humidity in order to achieve a predefined package quality. These systematic approaches described above, which are used to generate these models can also be applied for other molded packages and for different EMCs to define the relationships between the input and the output parameters and to generate different models for such systems. Additionally, DEA method is shown as a promising online monitoring method to monitor the variations in the EMC characteristics in transfer molding process. This work introduced the crucial characteristics information for EMC, which can be derived from DEA method and calibrated the signal alterations with respect to the variations in the EMC properties. Hence, this characteristic information gathered on DEA method in this work provide an elaborate basis and can be further applied for other molding compounds and other molded packages, where the process control is challenging. Therein, DEA method can be implemented in the production lines of the industries to monitor the cure behavior of the EMC which is especially valuable for large power modules in order to decrease the yield loss due to the problems caused by variations in the EMC characteristics.

It is worth noting that such process models which deliver good predictions on the package quality can be very helpful in the production processes to forecast possible defects in order to reduce the failure rate. Currently machine learning methods and artificial intelligence are tried to be established to improve the available processes and to decrease the yield loss. It could be an aspect to consider in future work, whether the process models based on real experiments could be implemented into the algorithms of the neuronal networks which is one example of an artificial intelligence method. In addition to that, as the variations in EMC properties have also an impact on the package quality, the information delivered from the in-situ cure monitoring can be given as an input into the algorithm as well. Thus, with the machine learning, the new set of optimum process parameters can be calculated by considering the actual properties of the EMC together with the process parameters, and the algorithms can calculate the new optimum process parameters. Subsequently, with the approach describe above, a machine could regulate itself to set those parameters in-line to obtain the best package quality and to decrease the failure rate.

List of Figures

List of Tables

Bibliography

[1] H. Ardebili and M. G. Pecht, *Encapsulation technologies for electronic applications*. Burlington, MA: William Andrew, 2009.

[2] S. Komori and Y. Sakamoto, "Development trend of epoxy molding compound for encapsulating semiconductor chips," in *Materials for Advanced Packaging*, D. Lu and C. P. Wong, Eds. Boston, MA: Springer US, 2009, pp. 339–363.

[3] M. G. Pecht, L. T. Nguyen, and E. B. Hakim, *Plastic-Encapsulated Microelectronics - Materials, Processes, Quality, Reliability, and Applications*. New York: John Wiley & Sons, Inc., 1995.

[4] K. W. Tong, C. K. Kwong, and K. M. Yu, "Process optimisation of transfer moulding for electronic packages using artificial neural networks and multiobjective optimisation techniques," *Int. J. Adv. Manuf. Technol.*, vol. 24, no. 9–10, pp. 675–685, Nov. 2004.

[5] L. T. Nguyen, "Reactive flow simulation in transfer molding of IC packages," in *Electronic Components and Technology Conference*, 1993, pp. 375–390.

[6] K. W. Tong, C. K. Kwong, and C. Y. Chan, "Initial process-parameters setting of transfer moulding in microchip encapsulation: a case-based reasoning approach," *J. Mater. Process. Technol.*, vol. 113, pp. 432–438, 2001.

[7] R. R. Tummala, E. J. Rymaszewski, and A. G. Klopfenstein, *Microelectronics Packaging Handbook: Technology Drivers, Part 1*, Second Edition. Springer, 1997.

[8] J. H. Lupinski, *Polymer materials for electronics packaging and interconnection*. Washington, DC: American Chemical Society, 1989.

[9] N. L. Dias Filho, H. A. de Aquino, G. Pires, and L. Caetano, "Relationship between the dielectric and mechanical properties and the ratio of epoxy resin to hardener of the hybrid thermosetting polymers," *J. Braz. Chem. Soc.*, vol. 17, no. 3, pp. 533–541, 2006.

[10] C. A. Kovac, "Plastic Package Fabrication," in *Electronic Materials Handbook - Volume 1 Packaging*, M. L. Minges, Ed. ASM International, 1989, pp. 470–482.

[11] M. H. Shirangi, "Simulation-based Investigation of Interface Delamination of Plastic IC Packages under Temperature and Moisture Loading," PhD Thesis, Technical University of Berlin, Berlin, 2010.

[12] N. Kinjo, M. Ogata, K. Nishi, A. Kaneda, and K. Dušek, "Epoxy molding compounds as encapsulation materials for microelectronic devices," in *Speciality Polymers/Polymer Physics*, Springer, 1989, pp. 1–48.

[13] J. Han, H. Chen, F. Wong, K. Leung, I. Shiu, and J. Wu, "Effects of package and mold cavity structures on the wire sweep behavior during package array transfer molding," in *Electronics Packaging Technology Conference*, 2011, pp. 667–673.

[14] K. W. Tong, C. K. Kwong, and K. W. Ip, "Optimization of process conditions for the transfer molding of electronic packages," *J. Mater. Process. Technol.*, vol. 138, no. 1–3, pp. 361–365, Jul. 2003.

[15] W. D. van Driel *et al.*, "Prediction and verification of process induced warpage of electronic packages," *Microelectron. Reliab.*, vol. 43, no. 5, pp. 765–774, May 2003.

[16] Y. Liu, Y. Liu, Z. Yuan, T. Chen, K. Lee, and S. Belani, "Warpage analysis and improvement for a power module," in *Electronic Components and Technology Conference*, 2013, pp. 475–480.

[17] D. G. Yang *et al.*, "Prediction of process-induced warpage of IC packages encapsulated with thermosetting polymers," in *Electronic Components and Technology Conference*, 2004, vol. 1, pp. 98–105.

[18] P. Sun, V. C.-K. Leung, B. Xie, V. W. Ma, and D. X.-Q. Shi, "Warpage reduction of package-on-package (PoP) module by material selection & process optimization," in *International Conference on Electronic Packaging Technology & High Density Packaging*, 2008, pp. 1–6.

[19] W. L. Hunter, "Association of bonding-wire displacement with gas bubbles in plastic-encapsulated integrated circuits," in *IBBB Transactions on Components, Hybrids and Manufacturing Technology*, 1987, pp. 327–331.

[20] L. T. Nguyen and F. J. Lim, "Wire sweep during molding of integrated circuits," in *Electronic Components and Technology Conference*, 1990, pp. 777–785.

[21] A. Tanaka, T. Asano, S. Oizumi, K. Niwa, and T. Nishioka, “Flow analysis of semiconductor encapsulating material,” in *Electronic Components and Technology Conference*, 1994, pp. 134–140.

[22] S. Ichimura, K. Kinashi, and T. Urano, “Relation between inner voids of plastic IC packages and non-Newtonian flow characteristics of resin encapsulant,” in *Electronic Components and Technology Conference*, 1990, pp. 641–645.

[23] L. T. Nguyen, R. L. Walberg, C. Chua, and A. Danker, “Voids in IC packages from molding,” in *Proceedings of ASME/JSME Conference Electronic Packaging*, 1992, pp. 751–762.

[24] L. T. Manzione, *Plastic Packaging of Microelectronic Devices*. New York: Van Nostrand Reinhold, 1990.

[25] S. Noijen, R. Engelen, J. Martens, A. Opran, O. van der Sluis, and R. van Silfhout, “Prediction of the epoxy moulding compound aging effect on package reliability,” *Microelectron. Reliab.*, vol. 50, no. 7, pp. 917–922, Jul. 2010.

[26] S. Abdullah, Z. A. Aziz, I. Ahmad, A. Jalar, and M. F. Abdullah, “Wire sweep issue in a newly developed Quad Flat No-Lead (QFN) semiconductor package,” in *International Conference on Microelectronics, Nanoelectronics, Optoelectronics*, Istanbul, Turkey, 2008, pp. 40–44.

[27] L. Nguyen *et al.*, “Wire sweep control with mold compound formulations,” in *Electronic Components and Technology Conference*, 1997, pp. 60–71.

[28] C. Chiang, “Wire sweep improvement in low cost manner,” in *International Conference on Solid-State and Integrated-Circuit Technology*, 2008, pp. 1192–1194.

[29] J. H. Wu, A. A. O. Tay, K. S. Yeo, and T.-B. Lim, “A three-dimensional modeling of wire sweep incorporating resin cure,” *IEEE Trans. Compon. Packag. Manuf. Technol. Part B*, vol. 21, no. 1, pp. 65–72, 1998.

[30] S. K. Prasad, *Advanced Wirebond Interconnection Technology*. United States: Kluwer Academic Publishers, 2004.

[31] P. Seeger, “Einfluss der Prozessparameter Im Transfer Molding Verfahren auf den Fehlermechanismus der Bauteile,” Masterarbeit, Hochschule Darmstadt, Darmstadt, 2015.

[32] K.-F. Becker *et al.*, “Transfer molding technology for smart power electronics modules: Materials and processes,” *J. Microelectron. Electron. Packag.*, vol. 9, pp. 78–86, 2012.

[33] A. B. Spoelstra, “Transfer Moulding of Reactive Materials: Application to Encapsulation of Integrated Circuits,” Eindhoven University of Technology, Eindhoven, Holland, 1992.

[34] M. M. Prasad, “Design of experiments case study of a transfer molding process,” *Soc. Manuf. Eng.*, pp. 1–14, 2008.

[35] K. Chai, L. Vicky, Y. P. Wang, and T. D. Her, “The Application of Mold Flow Simulation in Electronic Package,” in *International Symposium on Electronic Materials & Packaging*, Hong Kong, China, 2000, pp. 330–334.

[36] C. D. Rudd, A. C. Long, K. N. Kendall, and C. G. E. Mangin, *Liquid Moulding Technologies-Resin Transfer Moulding, Structural Reaction Injection Moulding and Related Processing Techniques*. Cambridge England: Woodhead Publishing Limited, 1997.

[37] J. de Vreugd *et al.*, “Effect of postcure and thermal aging on molding compound properties,” in *Electronics Packaging Technology Conference*, 2009, pp. 342–347.

[38] W. Michaeli, *Einführung in die Kunststoffverarbeitung*, 4th ed. Munich: Hanser Fachbuch, 1999.

[39] A. A. O. Tay, K. S. Yeo, and J. H. Wu, “The effect of wirebond geometry and die setting on wire sweep,” *IEEE Trans. Compon. Packag. Manuf. Technol. Part B*, vol. 18, no. 1, pp. 201–209, 1995.

[40] T. Yeung and M. Yuen, “Implementation study of intelligent system for IC transfer molding process,” in *Proceedings of SPIE- The International Society for Optical Engineering*, 1996, vol. 2644, pp. 471–476.

[41] K.-F. Becker, T. Braun, M. Koch, F. Ansorge, R. Aschenbrenner, and H. Reichl, “Advanced flip chip encapsulation: Transfer molding process for simultaneous underfilling and postencapsulation,” in *Polymers and Adhesives in Microelectronics and Photonics*, 2001, pp. 130–139.

[42] S. L. Liu, G. Chen, and M. S. Yong, “EMC characterization and process study for electronics p ackaging,” *Thin Solid Films*, vol. 462, pp. 454–458, 2004.

[43] H. Q. Yang, S. A. Bayyuk, and L. T. Nguyen, "Time-accurate, 3-D computation of wire sweep during plastic encapsulation of IC components," in *Electronic Components and Technology Conference*, 1997, pp. 158–167.

[44] D. Ramdan, C. Y. Khor, A. Mujeebu, Z. Abdullah, W. K. Loh, and C. K. Ooi, "FSI analysis of wire sweep in encapsulation process of plastic ball grid array packaging," *J. Therm. Sci. Technol.*, vol. 33, no. 1, pp. 101–109, 2013.

[45] J. Tamil *et al.*, "Molding flow modeling and experimental study on void control for flip chip package panel molding with molded underfill technology," *J. Microelectron. Electron. Packag.*, vol. 9, no. 1, pp. 19–30, 2012.

[46] M. S. Bhatnagar, "Epoxy Resins (Overview)," in *Polymeric Materials Encyclopedia*, J. C. Salomone, Ed. FL, USA: CRC Pres, 1996, pp. 1–11.

[47] R. B. Prime, "Thermosets," in *Thermal characterization of polymeric materials*, 2nd Edition., E. Turi, Ed. San Diego: Academic Press, 1981.

[48] K. Jinhwan, Y. Seokyoon, B. Jin-Young, Y. Hyo-Chang, H. Jwangwon, and K. Byung-Seon, "Thermal stabilities and mechanical properties of epoxy molding compounds (EMC) containing encapsulated red phosphorous," *Polymer Degradation and Stability*, vol. 81, pp. 207–213, 2003.

[49] L. P. Rector, S. Gong, and K. Gaffney, "On the performance of epoxy molding compounds for flip chip transfer molding encapsulation," in *Electronic Components and Technology Conference*, 2001, pp. 293–297.

[50] A. K. Knudsen, K. E. Howard, J. Braley, D. Magley, and H. Yoshida, "Reliability, performance and economics of thermally enhanced plastic packages," in *IEMT/IMC Symposium*, 1998, pp. 374–379.

[51] J. D. Vreugd, "The Effect of Aging on Molding Compound Properties," PhD Thesis, Technical University Delft, Netherlands, 2011.

[52] T. S. Kiong, I. Ruzaini, and F. C. Seng, "Package warpage challenges for LQFP 144 lead CMOS 90 device and it's impact to lead coplanarity," in *Electronic Manufacturing Technology Symposium*, 2010, pp. 1–6.

[53] W. G. Kim and J. Y. Lee, "Curing characteristics of epoxy resin systems that include a biphenyl moiety," *J. Appl. Polym. Sci.*, vol. 86, pp. 1942–1952, 2002.

[54] P. Procter and J. Solc, "Improved thermal conductivity in microelectronic encapsulants," in *Electronic Components and Technology Conference*, 1991, pp. 835–842.

[55] M. Ko, M. Kim, D. Shin, I. Lim, M. Moon, and Y. Park, "The effect of filler on the properties of molding compounds and their moldability," in *Electronic Components and Technology Conference*, 1997, pp. 108–113.

[56] U. Mokhtar, R. Rasid, S. Ahmad, A. E. Said, F. L. A. Latip, and C. C. Ng, "Effect of molding compound and die attach adhesive material on QFN package delamination and warpage issue," *Solid State Technol.*, vol. 16, no. 2, pp. 83–91, 2008.

[57] H. Liu, W. Tan, L. Li, C. Qiu, X. Cheng, and J. Han, "Influence of coupling agent on the performance of epoxy molding compound," *Electrochem. Soc.*, vol. 60, no. 1, pp. 781–786, 2014.

[58] L. T. Nguyen, R. H. Y. Lo, A. S. Chen, and J. G. Belani, "Molding compound trends in a denser packaging world: Qualification tests and reliability concerns," *IEEE Trans. Reliab.*, vol. 42, no. 4, pp. 518–535, 1993.

[59] N. Y. A. Shammas, "Present problems of power module packaging technology," *Microelectron. Reliab.*, vol. 43, no. 4, pp. 519–527, Apr. 2003.

[60] T. Thomas, K.-F. Becker, M. V. Dijk, O. Wittler, J. Bauer, and K.-D. Lang, "Reliability assessment of molded smart power modules," in *International Conference on Integrated Power Electronics Systems*, Nuremberg/Germany, 2014, pp. 55–62.

[61] T. Braun, K.-F. Becker, M. Koch, V. Bader, R. Aschenbrenner, and H. Reichl, "Reliability potential of epoxy based encapsulants for automotive applications," *Microelectron. Reliab.*, vol. 45, no. 9–11, pp. 1672–1675, Sep. 2005.

[62] Y. Liu and D. Kinzer, "Challenges of power electronic packaging and modeling," in *Thermal, Mechanical and Multi-Physics Simulation and Experiments in Microelectronics and Microsystems*, 2011, pp. 1–9.

[63] S. J. Dodd, N. Chalashkanov, L. A. Dissado, and J. C. Fothergill, "Influence of absorbed moisture on the dielectric properties of epoxy resins," in *Annual Report Conference on Electrical Insulation and Dielectric Phenomena*, 2010, pp. 1–4.

[64] X. Fan and V. Nagaraj, “In-situ moisture desorption characterization of epoxy mold compound,” in *Thermal, Mechanical and Multi-Physics Simulation Experiments in Microelectronics and Micro-Systems*, 2012, pp. 1–6.

[65] X. Fan, G. Q. Zhang, W. D. van Driel, and L. J. Ernst, “Analytical solution for moisture-induced interface delamination in electronic packaging,” in *Electronic components and technology conference*, 2003, pp. 733–738.

[66] M. K. Yeh and K. C. Chang, “Failure Prediction of Plastic Ball Grid Array Electronic Packaging,” in *Proceedings of the Pacific Rim/ASME International Intersociety Electronic and Photonic Packaging Conference (InterPACK1999)*, Hawai, USA, 1999, pp. 469–476.

[67] M. G. Lu, M. J. Shim, and S. W. Kim, “Effects of moisture on properties of epoxy molding compounds,” *J. Appl. Polym. Sci.*, vol. 81, no. 9, pp. 2253–2259, Aug. 2001.

[68] E. Dermitzaki, J. Bauer, H. Walter, B. Wunderle, B. Michel, and H. Reichl, “Molecular dynamics simulation for the diffusion of water in amorphous polymers examined at different temperatures,” in *Thermal, Mechanical and Multi-Physics Simulation Experiments in Microelectronics and Micro-Systems*, 2007, pp. 1–9.

[69] H. Walter, J. Bauer, T. Braun, O. Hölck, B. Wunderle, and O. Wittler, “In-situ-characterization of moisture induced swelling behaviour of microelectronic relevant polymers,” in *Thermal, Mechanical and Multi-Physics Simulation Experiments in Microelectronics and Micro-Systems*, 2012, pp. 1–6.

[70] H. Shirangi, J. Auersperg, M. Koyuncu, H. Walter, W. H. Müller, and B. Michel, “Characterization of Dual-Stage moisture diffusion, residual moisture content and hygroscopic swelling of epoxy molding compounds,” in *Thermal, Mechanical and Multi-physics Simulation and Experiments in Micro-Electronics and Micro-Systems*, 2008, pp. 1–8.

[71] J. Sheirs, *Compositional and Failure Analysis of Polymers. A Practical Approach*. Wiley, 2000.

[72] S. Luo, C. P. Wong, and J. Leisen, “Fundamental study on moisture absorption in epoxy for electronic application,” in *International Symposium on Advanced Packaging Materials: Processes, Properties and Interfaces*, 2001, pp. 293–298.

[73] A. A. O. Tay and T. Y. Lin, “Moisture-induced interfacial delamination growth in plastic IC packages during solder reflow,” in *Electronic Components & Technology Conference*, 1998, pp. 371–378.

[74] H. Ardebili, E. H. Wong, and M. Pecht, “Hygroscopic swelling and sorption characteristics of epoxy molding compounds used in electronic packaging,” *IEEE Trans. Compon. Packag. Technol.*, vol. 26, no. 1, pp. 206–214, Mar. 2003.

[75] B. Njoman, “A study on the effects of moisture exposure on the mold compound,” Agere systems internal report, 2002.

[76] M. R. Vanlandingham and J. J. W. Gillespie, “Moisture diffusion in epoxy systems,” *J. Appl. Polym. Sci.*, vol. 71, pp. 781–798, 1999.

[77] R. Buchhold *et al.*, “Influence of moisture uptake on mechanical properties of polymers used in microelectronics,” *Material*, vol. 511, pp. 359–364, 1998.

[78] M. Uschitsky and E. Suhir, “Moisture diffusion in epoxy molding compounds filled with particles,” *J. Electron. Packag.*, vol. 123, pp. 47–51, 2001.

[79] A. A. Gallo and R. Munamarty, “Popcorning: a failure mechanism in plastic-encapsulated microcircuits,” *IEEE Trans. Reliab.*, vol. 44, no. 3, pp. 362–367, 1995.

[80] R. C. J. Vogels, M. Huang, D. G. Yang, W. D. Van Driel, and G. Q. Zhang, “Fast Characterization for Moisture Properties of Moulding Compounds: Influence of Temperature and Humidity,” in *International Conference on Electronic Packaging Technology*, 2005, pp. 185–190.

[81] K. S. Chian, S. H. Lim, S. Yi, and W. T. Chen, “Effect of moisture on the curing behaviour of underfills,” in *International Symposium on Electronic Materials and Packaging*, 2000, pp. 289–296.

[82] J. Lin, A. Teng, and M. M. Yuen, “A fast, low cost method to check for moisture in epoxy molding compound,” in *Electronics Packaging Technology Conference*, 1998, pp. 359–361.

[83] T. Y. Lin and C. M. Fang, “Mold void evaluation for TQFP package,” Lucent internal reports, 2001.

[84] T. Y. Lin, B. Njoman, D. Crouthamel, K. H. Chua, S. Y. Teo, and Y. Y. Ma, “The impact of moisture in mold compound preforms on the warpage of PBGA packages,” *Microelectron. Reliab.*, vol. 44, no. 4, pp. 603–609, Apr. 2004.

[85] U. Penapunga, K. Ugsornrat, P. Thorlor, C. Sumithpibul, and A. Phoawongsa, “Effect of epoxy molding compound floor life to reliability performance for integrated circuit (IC) package,” in *Slam Physics Congress*, 2016, pp. 1–5.

[86] R. E. Wright, *Injection/Transfer Molding of Thermosetting Plastics*. Hanser/Gardner Publications, Inc., Cincinnati, 1995.

[87] M. Yoshii, Y. Mizukami, and H. Shoji, “Rheological properties and moldability of epoxy molding compound for IC encapsulation,” in *Asian Workshop on Polymer Processing*, Singapore, 2002.

[88] TA Instruments, “Thermal Solutions - Storage Effects on Tg for Epoxy Molding Compound.” [Online]. Available: http://www.tainstruments.com/pdf/literature/TS1.pdf. [Accessed: 18-Nov-2017].

[89] S. Han, K. K. Wang, and C. A. Hieber, “Characterization of the rheological properties of a fast-curing epoxy-molding compound,” *J. Rheol.*, vol. 41, no. 2, pp. 177–195, Jun. 1997.

[90] C. Garschke, P. P. Parlevliet, C. Weimer, and B. L. Fox, “Cure kinetics and viscosity modelling of a high-performance epoxy resin film,” *Polym. Test.*, vol. 32, no. 1, pp. 150–157, Feb. 2013.

[91] N. Kiuna, C. J. Lawrence, P. D. Lee, T. Selerland, and P. D. M. Spelt, “A model for resin viscosity during cure in the resin transfer moulding process,” *Compos. Part Appl. Sci. Manuf.*, vol. 33, pp. 1497–1503, 2002.

[92] Q. P. V. Fontana, “Viscosity: thermal history treatment in resin transfer moulding process modelling,” *Compos. Part A*, vol. 29A, pp. 153–158, 1997.

[93] S. Han, K. K. Wang, and C. A. Hieber, “Characterization of the rheological properties of a fast-curing epoxy-molding compound,” *J. Rheol.*, vol. 41, no. 2, pp. 177–195, Jun. 1997.

[94] N. Sbirrazzuoli and S. Vyazovkin, “Learning about epoxy cure mechanisms from isoconversional analysis of DSC data,” *Thermochim. Acta*, vol. 388, pp. 289–298, 2002.

[95] S. Vyazovkin and C. A. Wight, “Isothermal and non-isothermal kinetics of thermally stimulated reactions of solids,” *Int. Rev. Phys. Chem.*, vol. 17, pp. 407–433, 1998.

[96] B. Bilyeu, W. Brostow, and K. P. Menard, “Epoxy thermosets and their applications II. Thermal analysis,” *J. Mater. Educ.*, vol. 22, no. 4/6, pp. 107–130, 2000.

[97] L. Merad *et al.*, “In-situ monitoring of the curing of epoxy resins by Raman spectroscopy,” *Polym. Test.*, vol. 28, no. 1, pp. 42–45, Feb. 2009.

[98] M. A. Druy, P. J. Glatkowski, and W. A. Stevenson, “Mid-IR tapered chalcogenide fiber optic attenuated total reflectance sensors for monitoring epoxy resin chemistry,” in *Optical Tools for Manufacturing and Advanced Automation*, 1993, pp. 113–120.

[99] F. Fouchal, J. A. G. Knight, P. Dickens, and N. Garrington, “On-line monitoring of epoxy resin cure using infrared spectroscopy,” in *Solid Freeform Fabrication Proceedings*, Austin, 2001, pp. 441–451.

[100] M. G. González, J. Baselga, and J. C. Cabanelas, “Applications of FTIR on epoxy resins-identification, monitoring the curing process, phase separation and water uptake,” in *Infrared Spectroscopy - Materials Science, Engineering and Technology*, T. Theophanides, Ed. INTECH Open Access Publisher, 2012.

[101] S. Cholake *et al.*, “Quantitative analysis of curing mechanisms of epoxy resin by Mid- and Near-Fourier Transform Infra Red Spectroscopy,” *Def. Sci. J.*, vol. 64, no. 3, pp. 314–321, May 2014.

[102] M. Lodeiro and D. Mulligan, “Cure Monitoring Techniques for Polymer Composites, Adhesives and Coatings - Good Practice Guide to Cure Monitoring,” Engineering and Process Control Division, National Physical Laboratory, Teddington, Middlesex, United Kingdom, No 75, 2005.

[103] R. Hardis, J. L. P. Jessop, F. E. Peters, and M. R. Kessler, “Cure kinetics characterization and monitoring of an epoxy resin using DSC, Raman spectroscopy, and DEA,” *Compos. Part Appl. Sci. Manuf.*, vol. 49, pp. 100–108, Jun. 2013.

[104] D. Kranbuehl, D. Hood, J. Rogozinski, A. Meyer, and M. Neag, “Monitoring the changing state of a polymeric coating resin during synthesis, cure and use,” *Prog. Org. Coat.*, vol. 35, no. 1, pp. 101–107, 1999.

[105] S. T. Lim and W. I. Lee, “An analysis of the three-dimensional resin-transfer mold filling process,” *Compos. Sci. Technol.*, vol. 60, pp. 961–975, 2000.

[106] J. P. Dunkers, J. L. Lenhart, S. R. Kueh, J. H. van Zanten, S. G. Advani, and R. S. Parnas, “Fiber optic flow and cure sensing for liquid composite molding,” *Opt. Lasers Eng.*, vol. 35, pp. 91–104, 2001.

[107] G. R. Powell, P. A. Crosby, D. N. Waters, C. M. France, R. C. Spooncer, and G. F. Fernando, "In-situ cure monitoring using optical fibre sensors-a comparative study," *Smart Mater. Struct.*, vol. 7, no. 4, pp. 557–568, 1998.

[108] G. Tuncol, M. Danisman, A. Kaynar, and E. M. Sozer, "Constraints on monitoring resin flow in the resin transfer molding (RTM) process by using thermocouple sensors," *Compos. Part Appl. Sci. Manuf.*, vol. 38, no. 5, pp. 1363–1386, May 2007.

[109] D. Heider, D. Roderick, E. T. Thostensen, K. Tackitt, J. H. Belk, and T. Munns, "ASM handbook - Composites," *Cure Monitoring and Control*, vol. 21, pp. 692–698, 2001.

[110] E. Schmachtenberg, J. Schulte zur Heide, and J. Töpker, "Application of ultrasonics for the process control of Resin Transfer Moulding (RTM)," *Polym. Test.*, vol. 24, no. 3, pp. 330–338, May 2005.

[111] F. Lionetto, R. Rizzo, V. A. M. Luprano, and A. Maffezzoli, "Phase transformations during the cure of unsaturated polyester resins," *Mater. Sci. Eng. A*, vol. 370, no. 1–2, pp. 284–287, Apr. 2004.

[112] F. Stephan, X. Duteurtre, and A. Fit, "In-process control of epoxy composite by microdielectrometric analysis. Part II: On-line real-time dielectric measurements during a compression molding process," *Polym. Eng. Sci.*, vol. 38, no. 9, pp. 1566–1571, Sep. 1998.

[113] M. Rosentritt, A. C. Shortall, and W. M. Palin, "Dynamic monitoring of curing photoactive resins: A methods comparison," *Dent. Mater.*, vol. 26, no. 6, pp. 565–570, Jun. 2010.

[114] C. Y. Shigue, R. G. S. dos Santos, C. A. Baldan, and E. Ruppert-Filho, "Monitoring the epoxy curing by the dielectric thermal analysis method," *IEEE Trans. Appl. Supercond.*, vol. 14, no. 2, pp. 1173–1176, Jun. 2004.

[115] G. M. Maistros and I. K. Partridge, "Autoclave cure of composites: validation of models using dynamic dielectric analysis," in *International Conference on Flow Processes in Composite Materials*, 1996.

[116] D. J. Melotik, M. Czaplicki, T. J. Whalen, and D. R. Day, "Analysis of the resin transfer molding process using in-mold dielectric sensors," *Thermochim. Acta*, vol. 217, pp. 251–262, Apr. 1993.

[117] M. Danisman, G. Tuncol, A. Kaynar, and E. M. Sozer, "Monitoring of resin flow in the resin transfer molding (RTM) process using point-voltage sensors," *Compos. Sci. Technol.*, vol. 67, no. 3–4, pp. 367–379, Mar. 2007.

[118] H. G. Kim and others, "Dielectric cure monitoring for glass/polyester prepreg composites," *Compos. Struct.*, vol. 57, no. 1, pp. 91–99, 2002.

[119] D. Shepard and K. Smith, "A new ultrasonic measurement system for the cure monitoring of thermosetting resins and composites," *J. Therm. Anal. Calorim.*, vol. 49, no. 1, pp. 95–100, 1997.

[120] D. D. Shepard and K. R. Smith, "Ultrasonic cure monitoring of advanced composites," *Sens. Rev.*, vol. 19, no. 3, pp. 187–194, 1999.

[121] M. Rath, J. Döring, W. Stark, and G. Hinrichsen, "Process monitoring of moulding compounds by ultrasonic measurements in a compression mould," *Ndt E Int.*, vol. 33, no. 2, pp. 123–130, 2000.

[122] A. McIlhagger, D. Brown, and B. Hill, "The development of a dielectric system for the on-line cure monitoring of the resin transfer moulding process," *Compos. Part Appl. Sci. Manuf.*, vol. 31, no. 12, pp. 1373–1381, 2000.

[123] M. Sernek and F. A. Kamke, "Application of dielectric analysis for monitoring the cure process of phenol formaldehyde adhesive," *Int. J. Adhes. Adhes.*, vol. 27, no. 7, pp. 562–567, Oct. 2007.

[124] A. Maffezzoli, A. Trivisano, M. Opalicki, J. Mijovic, and J. M. Kenny, "Correlation between dielectric and chemorheological properties during cure of epoxy-based composites," *J. Mater. Sci.*, vol. 29, no. 3, pp. 800–808, Jan. 1994.

[125] J. Steinhaus, B. Hausnerova, T. Haenel, D. Selig, F. Duvenbeck, and B. Moerginger, "Correlation of shear and dielectric ion viscosity of dental resins - Influence of composition, temperature and filler content," *Dent. Mater.*, vol. 32, no. 7, pp. 899–907, 2016.

[126] D. Shepard, K. R. Smith, and D. C. Maurer, "A comparison of dielectric and ultrasonic cure monitoring of advanced composites," in *Nondestructive Characterization of Material VIII*, R. E. Green, Ed. Boston, MA: Springer, 1998, pp. 383–392.

[127] F. Lionetto and A. Maffezzoli, "Monitoring the cure state of thermosetting resins by ultrasound," *Materials*, vol. 6, no. 9, pp. 3783–3804, 2013.

[128] L. Núñez, S. Gómez-Barreiro, C. A. Gracia-Fernández, and M. R. Núñez, "Use of the dielectric analysis to complement previous thermoanalytical studies on the system diglycidyl ether of bisphenol A/1,2 diamine cyclohexane," *Polymer*, vol. 45, no. 4, pp. 1167–1175, Feb. 2004.
[129] A. Vassilikou-Dova and I. M. Kalogeras, "Dielectric analysis (DEA)," in *Thermal Analysis of Polymers, Fundamentals and Applications*, J. D. Menczel and R. B. Prime, Eds. New Jersey: Wiley, 2009.
[130] K. Zahouily, C. Decker, E. Kaisersberger, and M. Gruener, "Real-time UV cure monitoring," *Eur. Coat. J.*, no. 11, pp. 14–34, 2003.
[131] D. D. Shepard and B. Twombly, "Simultaneous dynamic mechanical analysis and dielectric analysis of polymers," *Thermochim. Acta*, vol. 272, pp. 125–129, 1996.
[132] D. R. Day, D. D. Shepard, and K. J. Craven, "In-process endpoint determination of epoxy resin cure," in *International Society for the Advancement of Material and Process Engineering*, 1990, pp. 724–732.
[133] J. P. Runt and J. J. Fitzgerald, *Dielectric Spectroscopy of Polymeric Materials, Fundamentals and Applications*. Washington, DC: American Chemical Society, 1997.
[134] R. Hardis, "Cure kinetics characterization and monitoring of an epoxy resin for thick composite structures," Master Thesis, Iowa State University, United States, 2012.
[135] Y. He, "DSC and DEA studies of underfill curing kinetics," *Thermochim. Acta*, no. 367–368, pp. 101–106, 2001.
[136] J. S. Kim and D. G. Lee, "Measurement of the degree of cure of carbon fiber epoxy composite materials," *J. Compos. Mater.*, vol. 30, no. 13, pp. 1436–1457, 1996.
[137] J. Steinhaus, B. Moeginger, M. Großgarten, and B. Hausnerova, "Evaluation of dielectric curing monitoring investigating light-curing dental filling composites," *Mater. Eng.*, vol. 18, pp. 28–33, 2011.
[138] J. Chen, M. A. Octeau, and M. Hojjati, "Resin flow front and cure monitoring in resin transfer molding (RTM) process using a dielectric sensor," in *Proceeding of International Conference on Flow Processes in Composite Materials*, 2008, pp. 1–9.
[139] S. D. Senturia and N. F. Sheppard, "Dielectric analysis of thermoset cure," in *Epoxy Resins and Composites IV - Advances in Polymer Science*, vol. 80, K. Dušek, Ed. Berlin, Heidelberg: Springer, 1986, pp. 1–47.
[140] A. R. Blythe, *Electrical properties of polymers*. Cambridge: Cambridge University Press, 1979.
[141] S. A. Bidstrup and D. R. Day, "Assignment of the glass transition temperature using dielectric analysis," in *ASTM Special Technical Publication*, 1994, pp. 104–117.
[142] W. W. Wright, "Characterisation of a bisphenol a epoxy resin," *Polym. Int.*, vol. 15, no. 4, 1983.
[143] Netzsch-Gerätebau GmbH, "Operating Instructions, DEA 288 Series, Epsilon," 2014.
[144] ASTM International E 2039 - 04, "Standard Test Method for Determining and Reporting Dynamic Dielectric Properties." Beutch Verlag, Mar-2004.
[145] C. A. May *et al.*, "Process Automation: A Rheological and Chemical Overview of Thermoset Curing," in *Chemorheology of Thermosetting Polymers*, vol. 227, C. A. May, Ed. Washington, D.C.: American Chemical Society, 1982, pp. 1–24.
[146] T. Jianmao and L. Kuiyang, "Cure behavior of epoxy amine-resin system by rheometric techniques," in *International SAMPE Symposium*, 1997, pp. 189–96.
[147] N. F. Sheppard, "Dielectric Analysis of the Cure of Thermosetting Epoxy/Amine Systems," PhD Thesis, Department of Electrical Engineering and Computer Science, Massachusetts Institute of Technology, Cambridge, 1986.
[148] G. M. Maistros and I. K. Partridge, "Dielectric monitoring of cure in a commercial carbon-fibre composite," *Compos. Sci. Technol.*, vol. 53, no. 4, pp. 355–359, 1995.
[149] G. M. Maistros and I. K. Partridge, "Monitoring autoclave cure in commercial carbon fibre/epoxy composites," *Compos. Part B Eng.*, vol. 29, no. 3, pp. 245–250, 1998.
[150] J.-P. Pascault, H. Sautereau, J. Verdu, and R. J. J. Williams, *Thermosetting Polymers*. New York: Marcel Dekker Inc., 2002.
[151] C. Y. Shigue, R. G. S. dos Santos, M. M. S. P. De Abreu, C. A. Baldan, A. L. M. Robin, and E. Ruppert-Filho, "Dielectric thermal analysis as a tool for quantitative evaluation of the viscosity and the kinetics of epoxy resin cure," *IEEE Trans. Appl. Supercond.*, vol. 16, no. 2, pp. 1786–1789, Jun. 2006.
[152] Z. N. Sanjana and R. L. Selby, "The use of dielectric analysis to study the cure of a filled epoxy resin," *IEEE Trans. Electr. Insul.*, no. 6, pp. 496–501, 1981.

[153] A. J. Mackinnon, S. D. Jenkins, P. T. McGrail, and R. A. Pethrick, “A dielectric, mechanical, rheological and electron microscopy study of cure and properties of a thermoplastic-modified epoxy resin,” *Macromolecules*, vol. 25, no. 13, pp. 3492–3499, 1992.

[154] D. Lairez, J. R. Emery, D. Durrand, D. Hayward, and R. A. Pethrick, “Real time dielectric measurements of network formation in a crosslinked epoxy resin system,” *Plast. Rubber Compos. Process. Appl.*, vol. 16, no. 4, pp. 231–238, 1991.

[155] L. Núñez-Regueira, C. A. Gracia-Fernández, and S. Gómez-Barreiro, “Use of rheology, dielectric analysis and differential scanning calorimetry for gel time determination of a thermoset,” *Polymer*, vol. 46, no. 16, pp. 5979–5985, Jul. 2005.

[156] Lambient Technologies, “Dielectric Measurements and Viscosity - Application Note 6.” [Online]. Available: http://lambient.com/docs/App%20Note%206.pdf. [Accessed: 10-Nov-2015].

[157] D. Abraham and R. McIlhagger, “Glass fibre epoxy composite cure monitoring using parallel plate dielectric analysis in comparison with thermal and mechanical testing techniques,” *Compos. Part Appl. Sci. Manuf.*, vol. 29, no. 7, pp. 811–819, 1998.

[158] J. Gillham, “A generalised time-temperature-transformation phase diagram for thermosetting systems,” in *Society Plastics Engineering Proceedings Annual Technical Conference*, 1980, vol. 38, pp. 268–271.

[159] J. Steinhaus, B. Hausnerova, T. Haenel, M. Großgarten, and B. Möginger, “Curing kinetics of visible light curing dental resin composites investigated by dielectric analysis (DEA),” *Dent. Mater.*, vol. 30, no. 3, pp. 372–380, Mar. 2014.

[160] M. Rosentritt, M. Behr, S. Knappe, and G. Handel, “Dielectric analysis of light-curing dental restorative materials—a pilot study,” *J. Mater. Sci.*, vol. 41, no. 10, pp. 2805–2810, May 2006.

[161] A. A. Skordos, P. I. Karkanas, and I. K. Partridge, “A dielectric sensor for measuring flow in resin transfer moulding,” *Meas. Sci. Technol.*, vol. 11, pp. 25–31, 2000.

[162] J. Steinhaus, B. Moeginger, M. Großgarten, M. Rosentritt, and B. Hausnerova, “Dielectric analysis of depth dependent curing behavior of dental resin composites,” *Dent. Mater.*, vol. 30, no. 6, pp. 679–687, Jun. 2014.

[163] J. Mijovic and B. D. Fitz, “Dielectric spectroscopy of reactive polymers. Novocontrol application note dielectrics 2.,” 1998. [Online]. Available: https://www.novocontrol.de/pdf_s/APND2.PDF. [Accessed: 08-May-2016].

[164] M. Henkel, “Untersuchung des Aushärteverhaltens lichthärtender Füllungskomposite mittels dielektrischer Analyse (DEA),” Dissertation, Friedrich-Alexander-Universität Erlangen-Nürnberg, 2012.

[165] “Netzsch Product Brochure: Dielectric Cure Monitoring; Method, Technique, Applications,” 2013. [Online]. Available: https://www.netzsch-thermal-analysis.com/en/products-solutions/dielectric-analysis/dea-288-epsilon/#!/tabs/literature. [Accessed: 10-Dec-2015].

[166] S. C. Chen, T. E. Skogland, M. A. White, B. Crowell, and D. D. Shepard, “Investigation of the in-mold viscosity characteristics of electronics packaging polymers during transfer molding using dielectric analysis.” [Online]. Available: https://www.netzsch-thermal-analysis.com. [Accessed: 06-Feb-2015].

[167] G.-J. Park, *Analytic methods for design practice*. London: Springer, 2007.

[168] T. Wember, *Technische Statistik und Statistische Versuchsplanung: Einführung in Statistische Methoden mit Anwendungsschwerpunkt in der Analyse technischer Daten für Techniker, Ingenieure und Naturwissenschaftler*. P & P Informationstechnologie GmbH, 1999.

[169] K. Siebertz, D. van Bebber, and T. Hochkirchen, *Statistische Versuchsplanung*. Berlin, Heidelberg: Springer Berlin Heidelberg, 2010.

[170] J. Zimmer, “Analyse und Optimierung des flüssigkeitsgestützten Streckblasformens,” Dissertation, Technische Universität Dortmund, Dortmund, 2015.

[171] W. Kleppmann, *Taschenbuch Versuchsplanung: Produkte und Prozesse optimieren*, 4., Überarb. Aufl. München: Hanser, 2006.

[172] A. Frank, “Einführung in die Statistische Versuchsplanung, HS Vorlesung Quality Engineering.” [Online]. Available: http://www.tqu-group.com/we-dokumente/Downloads/Vorlesung/DoEPhilosophie.pdf. [Accessed: 06-Oct-2017].

[173] H. Petersen, *Grundlagen der Statistik und der statistischen Versuchsplanung*. Ecomed, 1991.

[174] F. Triefenbach, “Design of Experiments: The D-optimal approach and its implementation as a computer algorithm,” Bachelor Thesis, Umea University, Sweden, 2008.
[175] M. Knaak, “Steuerung und Regelung von KFZ-Antriebssträngen - Desing of Experiments & Modellbildung,” Vorlesungsmanuskript:7, TU Berlin, 2013.
[176] G. Bandow and H. H. Holzmüller, Eds., *“Das ist gar kein Modell!”: unterschiedliche Modelle und Modellierungen in Betriebswirtschaftslehre und Ingenieurwissenschaften*, 1. Auflage. Wiesbaden: Gabler Research, 2010.
[177] C. Weihs and J. Jessenberger, *Statistische Methoden zur Qualitätssicherung und -optimierung in der Industrie*. Wiley, Weinheim, 1999.
[178] G. W. Ehrenstein, G. Riedel, and P. Trawiel, *Thermal Analysis of Plastics: Theory and Practice*. Carl Hanser Verlag GmbH & Co. KG, 2004.
[179] “TA- Instruments - Thermal Solutions - Measurement of the glass transition temperature using dynamic mechanical analysis.” [Online]. Available: http://www.tainstruments.com/pdf/literature/TS1.pdf. [Accessed: 09-Sep-2017].
[180] M. Sadeghinia, K. M. B. Jansen, and L. J. Ernst, “Characterization of the viscoelastic properties of an epoxy molding compound during cure,” *Microelectron. Reliab.*, vol. 52, pp. 1711–1718, 2012.
[181] ASTM International, “ASTM E473 Standard terminology relating to thermal analysis and rheology,” 2016.
[182] J. M. Barton, “The application of differential scanning calorimetry (DSC) to the study of epoxy resin curing reactions,” *Epoxy Resins Compos. Adv. Polym. Sci.*, vol. 72, pp. 111–154, 2005.
[183] J. D. Menczel, L. Judovits, R. B. Prime, H. E. Bair, M. Reading, and S. Swier, “Differential Scanning Calorimetry (DSC),” in *Thermal Analysis of Polymers: Fundamentals and Applications*, J. D. Menczel and R. B. Prime, Eds. New Jersey, USA: John Wiley & Sons, Inc., 2009.
[184] G. W. Ehrenstein and E. Bittmann, *Duroplaste Aushärtung - Prüfung - Eigenschaften*. Carl Hanser Verlag Münschen Wien, 1997.
[185] H. Zhao, J. Gao, Y. Li, and S. Shen, “Curing kinetics and thermal property characterization of Bisphenol-F epoxy resin and MeTHPA system,” *J. Therm. Anal. Calorim.*, vol. 74, pp. 227–236, 2003.
[186] http://www.tainstruments.com/pdf/brochure/2012%20DSC%20Brochure%20r1.pdf. [Accessed: 08-Jun-2017].
[187] S. Mutlur, “Thermal analysis of composites using DSC,” in *Advanced Topics in Characterization of Composites*, M. R. Kessler, Ed. Canada: Trafford Publishing, 2004, pp. 11–33.
[188] Bosch Norm, “PVA 7855, Viscosity measurement for epoxy resin transfer molding compounds.”
[189] “DIN EN ISO 15512 Plastics - Determination of water content,” 2014.
[190] http://www.ndk.com/catalog/AN-CU_PFU_e.pdf. [Accessed: 27-May-2017]
[191] H. K. Charles, “Advanced Wire Bonding Technology: Materials, Methods, and Testing,” in *Materials for Advanced Packaging*, D. Lu and C. P. Wong, Eds. Boston, MA: Springer US, 2009, pp. 339–363.
[192] G. Harman, *Wire Bonding in Microelectronics - Materials, Processes, Reliability and Yield*, Second Edition. New York, 1997.

Appendix

Table A. 1: Experimental plan for evaluation of the suitable process window for complete filling of demonstrator

Parameter set no.	T [°C]	v [mm/s]	P [bar]	t [s]	Quality of cavity filling
1	155	6.5	80	0	Complete filling – Strong cull sticking
2	155	6.5	140	0	Complete filling - Strong cull sticking
3	155	6.5	80	15	Complete filling - Very strong cull sticking
4	160	6.5	140	15	Complete filling- Moderate cull sticking
5	185	1.5	80	15	Complete filling
6	185	1	80	15	Incomplete filling
7	185	1	140	15	Incomplete filling
8	185	0.5	140	15	Incomplete filling
9	185	1.5	160	15	Complete filling
10	185	1.5	180	15	Complete filling
11	185	1.5	140	20	Complete filling
12	185	1.2	140	15	Complete filling
13	185	1.1	140	15	Complete filling

Table A.2: Experimental plan on evaluation of the influence of process parameters and the vacuum on void formation

Parameter set no.	**T [°C]**	**v [mm/s]**	**P [bar]**	**t [s]**	**Vacuum**	**Average number of voids**
1	165	4	80	0	on	4
2	165	4	80	0	off	10
3	165	4	140	0	on	1
4	165	4	140	0	off	2
5	175	4	110	7.5	on	6
6	175	1.5	80	10	on	33
7	175	2.8	110	7.5	on	10
8	185	1.5	140	15	on	11
9	185	1.5	80	15	on	30